



University
of Glasgow

White, Kevin (2011) *The serotonin transporter, gender and 17 beta estradiol in pulmonary arterial hypertension*. PhD thesis

<http://theses.gla.ac.uk/2582/>

Copyright and moral rights for this thesis are retained by the author

A copy can be downloaded for personal non-commercial research or study, without prior permission or charge

This thesis cannot be reproduced or quoted extensively from without first obtaining permission in writing from the Author

The content must not be changed in any way or sold commercially in any format or medium without the formal permission of the Author

When referring to this work, full bibliographic details including the author, title, awarding institution and date of the thesis must be given.

Serotonin, Gender and 17 β Estradiol in Pulmonary Arterial Hypertension

**Kevin White
BSc. (Hons)**

Submitted in fulfilment of the requirements for the
Degree of Doctor of Philosophy, Institute of
Cardiovascular and Medical Sciences, University of
Glasgow

Institute of Cardiovascular and Medical Sciences
College of Medical, Veterinary and Life Sciences
University of Glasgow



University
of Glasgow

May 2011

© Kevin White

Author Declaration

In declaration, the entire contents of this thesis have been solely written by me. All experimental data has been self-generated with the exception of quantitative real-time PCR data, which was performed in collaboration with Dr. Zakia Maqbool. No contents of this thesis have been previously submitted for a Higher Degree. All research was performed at the Institute of Cardiovascular and Medical Sciences, College of Medical, Veterinary and Life Sciences, University of Glasgow under the supervision of Professor Margaret R. MacLean.

Kevin White

May 2011

Acknowledgments

Firstly, I thank my supervisor Prof. Mandy MacLean for the excellent support, guidance and advice over the last three years. My PhD has been a really good experience. I would like to acknowledge the Integrative Mammalian Biology Initiative Award funded by the Biotechnology and Biological Sciences Research Council, British Pharmacological Society, Knowledge Transfer Network, Medical Research Council and Scottish Funding Council for financial support of this research.

Thanks to everyone in the MacLean Research Group. Especially to Dr. Yvonne Dempsie and Lynn Loughlin who have helped with just about everything since I've been in the lab. Thanks also to Margaret Nilsen, who always manages to find time to help me out at the last minute. Also, thanks to Dr. Ian Morecroft and Dr. Kirsty Mair for their help around the lab.

Also, thanks to my family who have always encouraged me, despite having no idea what it is I actually do. And finally thanks to Laura, who not only always supports me with everything but sometimes even listens to my Science chat.

All the help was really appreciated.

Table of Contents

Author Declaration.....	II
Acknowledgments.....	III
List of Figures	VII
List of Tables	X
List of Publications	XI
List of Abbreviations	XII
Abstract	XVIII
Chapter 1	1
Introduction.....	1
1.1 The Pulmonary Circulation.....	2
1.1.1 Structural Organisation	2
1.1.2 Functional Organisation.....	2
1.1.3 Structure of the Pulmonary Vascular Wall	4
1.1.4 Function of the Pulmonary Circulation.....	6
1.1.5 Control of the Pulmonary Circulation.....	7
1.1.6 Pulmonary Vascular Resistance.....	7
1.1.7 Passive Regulation and Distribution of Blood Flow.....	8
1.1.8 Active Distribution and Regulation of Blood Flow	9
1.1.9 Pulmonary Vascular Contraction	11
1.1.10 Hypoxic Pulmonary Vasoconstriction	12
1.2 Pulmonary Arterial Hypertension	16
1.2.1 Classification.....	16
1.2.2 Current Therapeutic Strategies in PAH	19
1.2.3 Future Perspectives in the Treatment of PAH	24
1.2.4 Pathobiology of PAH	25
1.2.5 Genetic Basis of Pulmonary Arterial Hypertension.....	30
1.3 Serotonin Biosynthesis and Metabolism.....	34
1.4 Serotonin Signalling.....	36
1.4.1 Tryptophan Hydroxylase.....	36
1.4.2 5-HT Receptors	37
1.4.3 5-HT Receptor and Serotonin Transporter Interactions	44
1.4.4 Serotonin Transporter	45
1.5 Serotonin Hypothesis of PAH.....	48
1.6 The Serotonin Transporter in PAH	51
1.7 Gender Differences in Cardiovascular Disease	53
1.8 Estrogen	55
1.8.1 Synthesis and Metabolism	55
1.8.2 Estrogen Receptors	58
1.8.3 17 β Estradiol Effects in the Systemic Circulation	61
1.8.4 17 β Estradiol Metabolite Effects in the Systemic Circulation.....	63
1.8.5 17 β Estradiol Effects in the Pulmonary Circulation	65
1.8.6 17 β Estradiol Metabolite Effects in the Pulmonary Circulation.....	67
1.9 Estrogen and Serotonin Interactions	68
1.10 Aim.....	69
Chapter 2	70
Materials and Methods.....	70
Materials.....	71
2.1.1 Chemicals and Reagents	71
Methods.....	71
2.1.1 SERT+ Mice	71

2.1.2	Bilateral Ovariectomy	72
2.1.3	17 β Estradiol Administration	73
2.1.4	Chronic Hypoxia	73
2.2	Assessment of PAH	75
2.2.1	Haemodynamic Measurements	75
2.2.2	Right Ventricular Pressure	75
2.2.3	Systemic Arterial Pressure	76
2.2.4	Right Ventricular Hypertrophy	77
2.2.5	Pulmonary Vascular Remodelling	78
2.3	Pulmonary Vascular Reactivity	78
2.3.1	Dissection	78
2.3.2	Small Vessel Wire Myography	78
2.3.3	Application of Tension	79
2.3.4	Cumulative Concentration Response Curve	80
2.3.5	Analysis	80
2.4	Histology	80
2.4.1	Fixation	80
2.4.2	Immunohistochemistry	81
2.5	Tissue Culture	82
2.5.1	Human Pulmonary Artery Smooth Muscle Cells	83
2.5.2	Proliferation Assays	84
2.6	Western Blotting	86
2.6.1	PASMCs	86
2.6.2	Pulmonary Arteries	86
2.6.3	SDS-PAGE	87
2.6.4	Immunoblotting	87
2.6.5	Quantitative Expression of Protein	88
2.7	RNA Extraction	90
2.7.1	Pulmonary Arteries	90
2.7.2	PASMCs	91
2.7.3	DNase Treatment of RNA	91
2.7.4	cRNA Synthesis	91
2.8	Microarray Analysis	92
2.8.1	cRNA Direct Hybridization Assay	92
2.8.2	Statistical Analysis	93
2.9	Quantitative Real-time PCR	93
2.10	Statistical Analysis	94
Chapter 3		95
The Serotonin Transporter, Gender and 17 β Estradiol in the Development of Pulmonary Arterial Hypertension		95
3.1	Introduction	96
3.2	Results	98
3.2.1	Male SERT+ Mice Do Not Develop Spontaneous PAH or Exaggerated Hypoxia-induced PAH Compared to Wildtype Mice ...	98
3.2.2	Female SERT+ Mice Develop Spontaneous PAH and Exaggerated Hypoxia-Induced PAH via the Effects of 17 β Estradiol	98
3.2.3	Ovariectomized Wildtype Mice Develop PAH	109
3.2.4	Ovariectomy Increases Body Weight and Decreases Uterine Weight	112
3.2.5	Male SERT+ Mice Do Not Develop PAH Following 17 β Estradiol Administration	112
3.2.6	17 β Estradiol Prevents Hypoxia-Induced PAH in Male Wildtype Mice	116

3.2.7	Effects of Ovariectomy and 17 β Estradiol on Serotonin Induced Pulmonary Vascular Contraction	119
3.2.8	Effects of 17 β Estradiol, Estrone, Estriol and Progesterone in PASMCs.....	122
3.2.9	17 β Estradiol Has No Effect on Serotonin Induced Proliferation in PASMCs.....	127
3.2.10	17 β Estradiol Increases Tryptophan Hydroxylase-1, 5-HT _{1B} Receptor and Serotonin Transporter Expression in PASMCs.....	129
3.2.11	Serotonin Pathway Inhibitors Prevent 17 β Estradiol Induced Proliferation in PASMCs	133
3.3	Discussion	135
Chapter 4	142
The Serotonin Transporter, Gender and Hypoxia: Microarray Analysis in the Pulmonary Arteries of Mice Identifies Genes with Relevance to Human PAH		
4.1	Introduction.....	143
4.2	Results	145
4.2.1	Female SERT+ Mice Exhibit Right Ventricular Hypertrophy in Chronic Hypoxia at 2 Months and PAH at 5 Months	145
4.2.2	Genotypic Differences in SERT+ Mice	152
4.2.3	Genotypic Differences in Hypoxic SERT+ Mice	153
4.2.4	qRT-PCR Analysis in the Pulmonary Arteries of SERT+ Mice.....	171
4.2.5	C/EBP β , CYP1B1 and c-FOS Protein Expression is Increased in Female SERT+ Mice.....	176
4.2.6	Serotonin and 17 β Estradiol Stimulate C/EBP β , CYP1B1 and c-FOS Expression in PASMCs.....	180
4.2.7	C/EBP β , CYP1B1 and c-FOS mRNA and Protein Expression is Increased in PASMCs Derived From IPAH Patients.....	184
4.3	Discussion	189
Chapter 5	195
General Discussion		
Future Perspective.....		
Reference List	204
Appendices	259

List of Figures

Figure 1.1	Musculature in the pulmonary arteries.	4
Figure 1.2	Vascular cell types which compose the pulmonary vascular wall.	5
Figure 1.3	Passive distribution of blood flow throughout the lung.....	9
Figure 1.4	The mechanism underlying pulmonary vascular smooth muscle contraction.	14
Figure 1.5	Proposed mechanism of hypoxic pulmonary vasoconstriction (HPV)....	15
Figure 1.6	Current therapeutic targets in PAH.....	21
Figure 1.7	Histopathological changes associated with human and experimental PAH.	27
Figure 1.8	Bone morphogenetic protein receptor-2 signalling in PAH.	33
Figure 1.9	Serotonin biosynthesis and metabolism.....	35
Figure 1.10	Classification of the 14 structurally distinct 5-HT receptor subtypes.	38
Figure 1.11	Representative structure of a G-protein coupled receptor (GPCR).	39
Figure 1.12	5-HT receptor subtype signalling pathways.	39
Figure 1.13	Structure of the serotonin transporter.	48
Figure 1.14	Serotonin signalling in the pulmonary vasculature.	54
Figure 1.15	Estrogen biosynthesis and metabolism.....	57
Figure 1.16	Estrogen receptor structure.	61
Figure 1.17	17 β estradiol signalling.....	64
Figure 2.1	In vivo study design.....	74
Figure 2.2	Representative recording of right ventricular pressure.....	76
Figure 2.3	Representative recording of systemic arterial pressure.	77
Figure 2.4	Equation to calculate transmural pressure.	79
Figure 2.5	Typical morphology of human pulmonary artery smooth muscle cells..	84
Figure 3.1	Male SERT+ mice do not exhibit spontaneous PAH or exaggerated hypoxia-induced PAH compared to male WT mice.....	100
Figure 3.2	Male SERT+ mice exhibit similar systemic arterial pressure to male WT mice.....	101
Figure 3.3	Male SERT+ mice exhibit a similar heart rate to male WT mice.	101
Figure 3.4	Female SERT+ mice exhibit increased RVSP in normoxia and chronic hypoxia, via the effects of 17 β estradiol.....	102
Figure 3.5	Female SERT+ mice exhibit increased pulmonary vascular remodelling in normoxia and chronic hypoxia, via the effects of 17 β estradiol.....	103
Figure 3.6	Photomicrographs of representative resistance pulmonary arteries in SERT+ mice.....	104
Figure 3.7	Female ovariectomized SERT+ mice exhibit reduced right ventricular hypertrophy in normoxia and chronic hypoxia, via the effects of 17 β estradiol.....	105
Figure 3.8	Female SERT+ mice exhibit no change in systemic arterial pressure compared to female wildtype mice, and this is further unaffected by ovariectomy or 17 β estradiol.	106
Figure 3.9	Female SERT+ mice exhibit no change in heart rate compared to female wildtype mice, and this is further unaffected by ovariectomy or 17 β estradiol.....	106
Figure 3.10	Ovariectomized wildtype mice exhibit PAH.	110
Figure 3.11	Ovariectomy has no effect on systemic arterial pressure in either normoxic or chronically hypoxic wildtype mice.	111
Figure 3.12	Ovariectomy has no effect on heart rate in either normoxic or chronically hypoxic wildtype mice.....	111
Figure 3.13	Body weight is increased in wildtype mice following ovariectomy.....	113

Figure 3.14	Uterine weight is decreased in normoxic and chronically hypoxic ovariectomized wildtype and SERT+ mice.	113
Figure 3.15	17 β estradiol has no effect on PAH phenotype in male SERT+ mice. ...	114
Figure 3.16	17 β estradiol has no effect on systemic arterial pressure in male SERT+ mice.	115
Figure 3.17	17 β estradiol has no effect on heart rate in male SERT+ mice.	115
Figure 3.18	17 β estradiol attenuates hypoxia-induced PAH in male wildtype mice.	117
Figure 3.19	17 β estradiol has no effect on systemic arterial pressure in normoxic and chronically hypoxic male wildtype mice.	118
Figure 3.20	17 β estradiol has no effect on heart rate in normoxic and chronically hypoxic male wildtype mice.	118
Figure 3.21	Serotonin-induced pulmonary arterial contraction is unaffected following ovariectomy in both normoxic wildtype and SERT+ mice.	120
Figure 3.22	Serotonin-induced pulmonary arterial contraction is unaffected following ovariectomy in chronically hypoxic wildtype and SERT+ mice.	120
Figure 3.23	Serotonin-induced pulmonary arterial contraction is unaffected following 17 β estradiol administration in ovariectomized SERT+ mice.	121
Figure 3.24	Serotonin-induced pulmonary arterial contraction is unaffected following 17 β estradiol administration in chronically hypoxic ovariectomized SERT+ mice.	121
Figure 3.25	17 β estradiol stimulates human pulmonary artery smooth muscle cell proliferation.	123
Figure 3.26	Estrone has no effect on human pulmonary artery smooth muscle cell proliferation.	124
Figure 3.27	Estriol has no effect on human pulmonary artery smooth muscle cell proliferation.	125
Figure 3.28	Progesterone has no effect on human pulmonary artery smooth muscle cell proliferation.	126
Figure 3.29	17 β estradiol has no effect on serotonin-induced proliferation in human pulmonary artery smooth muscle cells.	128
Figure 3.30	17 β estradiol increases tryptophan hydroxylase-1 expression in human pulmonary artery smooth muscle cells.	130
Figure 3.31	17 β estradiol increases 5-HT _{1B} receptor expression in human pulmonary artery smooth muscle cells.	131
Figure 3.32	17 β estradiol increases serotonin transporter expression in human pulmonary artery smooth muscle cells.	132
Figure 3.33	Effects of inhibitors for serotonin synthesis, 5-HT receptors and serotonin transporter on 17 β estradiol-stimulated proliferation.	134
Figure 4.1	Male SERT+ mice do not exhibit increased right ventricular systolic pressure in normoxia or chronic hypoxia.	146
Figure 4.2	Male SERT+ mice do not exhibit increased pulmonary vascular remodelling.	147
Figure 4.3	Male SERT+ mice do not exhibit increased right ventricular hypertrophy.	148
Figure 4.4	Female SERT+ mice exhibit increased right ventricular systolic pressure in normoxia and chronic hypoxia at 5 months of age.	149
Figure 4.5	Female SERT+ mice exhibit increased pulmonary vascular remodelling in normoxia and chronic hypoxia at 5 months of age.	150
Figure 4.6	Female SERT+ mice exhibit increased right ventricular hypertrophy in chronic hypoxia at both 2 and 5 months of age.	151

Figure 4.7	Representation of differentially expressed genes in normoxic female and male wildtype and SERT+ mice by hierarchical cluster analysis and gene ontology.	169
Figure 4.8	Representation of differentially expressed genes in chronically hypoxic female and male wildtype and SERT+ mice by hierarchical cluster analysis and gene ontology.	170
Figure 4.9	FOS, CEBPB and CYP1B1 mRNA expression in the pulmonary arteries of normoxic female wildtype and SERT+ mice.	172
Figure 4.10	MYL3, HAMP2 and CEBPB mRNA expression in the pulmonary arteries of chronically hypoxic female wildtype and SERT+ mice.	173
Figure 4.11	LTF, PLN and NPPA mRNA expression in the pulmonary arteries of normoxic male wildtype and SERT+ mice.	174
Figure 4.12	UCP1, LTF and C1S mRNA expression in the pulmonary arteries of chronically hypoxic male wildtype and SERT+ mice.	175
Figure 4.13	C/EBP β expression in the pulmonary arteries of female wildtype and SERT+ mice.	177
Figure 4.14	CYP1B1 expression in the pulmonary arteries of female wildtype and SERT+ mice.	178
Figure 4.15	c-FOS expression in the pulmonary arteries of female wildtype and SERT+ mice.	179
Figure 4.16	C/EBP β expression in human PASMCs following serotonin and 17 β estradiol stimulation.	181
Figure 4.17	CYP1B1 expression in human PASMCs following serotonin and 17 β estradiol stimulation.	182
Figure 4.18	c-FOS expression in human PASMCs following serotonin and 17 β estradiol stimulation.	183
Figure 4.19	CEBPB, CYP1B1 and FOS mRNA expression in PASMCs derived from control and IPAH patients.	185
Figure 4.20	C/EBP β expression is increased in PASMCs derived from IPAH patients.	186
Figure 4.21	CYP1B1 expression is increased in PASMCs derived from IPAH patients.	187
Figure 4.22	c-FOS expression is increased in PASMCs derived from IPAH patient.	188

List of Tables

Table 1.1	Current WHO clinical classification of pulmonary hypertension.....	17
Table 1.2	Current World Health Organisation/ New York Heart association Classification of functional status in patients with pulmonary hypertension.	18
Table 2.1	Immunoblotting antibody table.....	89
Table 3.1	Ventricle and body weight in WT and SERT+ mice	107
Table 3.2	Haemodynamics in WT and SERT+ mice.	108
Table 4.1	List of genes up-regulated in the pulmonary arteries of 2 month female SERT+ mice	154
Table 4.2	List of genes down-regulated in the pulmonary arteries of 2 month female SERT+ mice	155
Table 4.3	List of genes up-regulated in the pulmonary arteries of 2 month hypoxic female SERT+ mice	157
Table 4.4	List of genes down-regulated in the pulmonary arteries of 2 month hypoxic female SERT+ mice	161
Table 4.5	List of genes up-regulated in the pulmonary arteries of 2 month male SERT+ mice	163
Table 4.6	List of genes down-regulated in the pulmonary arteries of 2 month male SERT+ mice	164
Table 4.7	List of genes up-regulated in the pulmonary arteries of 2 month hypoxic male SERT+ mice	165
Table 4.8	List of genes down-regulated in the pulmonary arteries of 2 month hypoxic male SERT+ mice	167
Table 4.9	Primer pairs used for PCR analysis.....	168

List of Publications

K. White, Y. Dempsie, M. Nilsen, A.F. Wright, L. Loughlin & M.R. MacLean. The Serotonin Transporter, Gender and 17β Estradiol in the Development of Pulmonary Arterial Hypertension. *Cardiovascular Research* 1;90(2):373-382, 2011.

K. White, L. Loughlin, Z. Maqbool, M. Nilsen, J. McClure, Y. Dempsie, A.H. Baker & M.R. MacLean. The Serotonin Transporter, Gender and Hypoxia: Microarray Analysis in the Pulmonary Arteries of Mice Identifies Genes with Relevance to Human PAH. *Physiological Genomics* 43: 417–437, 2011.

Abstract:

K. White, M. Baranowska, L. Loughlin, Y. Dempsie & M.R. MacLean. Effects of Hypoxia on Serotonin Induced Pulmonary Arterial Vasoconstriction in Mice Over-Expressing the Serotonin Transporter: Role of the 5-HT_{1B} Receptor and Rho-Kinase. *American Journal of Respiratory and Critical Care Medicine*. 2009; 179:A6250.

K. White, Y. Dempsie, M. Nilsen, L. Loughlin & M.R. MacLean. Female Gender is a Risk Factor in Experimental PAH When the Serotonin Transporter is Over-Expressed. *American Journal of Respiratory and Critical Care Medicine*. 2010; 81:A4026.

List of Abbreviations

16-OHE1	16 α -hydroxyestrone
2-OHE	2-hydroxyestradiol
2-ME	2-methoxyestradiol
5-HIAA	5-hydroxyindole acetic acid
5-HT	5-hydroxytryptamine
5-HTP	5- hydroxytryptophan
5-HTT	5-hydroxytryptamine transporter
AC	Adenylate cyclase
ACh	Acetylcholine
ADP	Adenosine 5' diphosphate
AF	Activation function
AF-1	Activation function 1
AF-2	Activation function 2
ALK-1	Activin receptor-like kinase 1
Ang-1	Angiopoietin 1
ApoE	Apolipoprotein E
ANOVA	One-way analysis of variance
ATP	Adenosine 5' triphosphate
BMPR-II	Bone morphogenetic protein type 2 receptor
BSA	Bovine serum albumin
Ca ²⁺	Calcium ion
[Ca ²⁺] _i	Intracellular calcium
CaM	Calmodulin
cAMP	Cyclic 3', 5' adenosine monophosphate

CCB	Calcium channel blocker
C/EBP β	CCAAT enhancer binding protein beta
cGMP	Guanosine 3', 5' monophosphate
Cl ⁻	Chloride ion
CO	Cardiac output
CO ₂	Carbon dioxide
COMT	Catechol-O-methyltransferase
cRNA	Complimentary RNA
CTEPH	Chronic thromboembolic pulmonary hypertension
CYP1B1	Cytochrome P450 1B1
CYP450	Cytochrome P450
DAG	1,2-Diacylglycerol
DMEM	Dulbeccos modified Eagle medium
EDTA	Ethylenediaminetetraacetic acid
eNOS	Endothelial nitric oxide synthase
E ₂	17 β estradiol
ESR1	Estrogen receptor 1
ESR2	Estrogen receptor 2
ER	Estrogen receptor
ER α	Estrogen receptor alpha
ER β	Estrogen receptor beta
ERE	Estrogen response element
ERK	Extracellular signal-regulated protein kinase
ET-1	Endothelin-1
ETA	Endothelin A receptor
ETB	Endothelin B receptor
FBS	Fetal bovine serum

HPAH	Heritable pulmonary arterial hypertension
GPCR	G-protein-coupled receptor
GPR30	G-protein coupled receptor 30
GDP	Guanosine 5' diphosphate
GTP	Guanosine 5' triphosphate
HAPE	High altitude pulmonary oedema
HIV	Human immunodeficiency virus
HHT	Hereditary hemorrhagic telangiectasia
hPASMC	Human pulmonary artery smooth muscle cell
HPV	Hypoxic pulmonary vasoconstriction
HR	Heart rate
ID	Internal diameter
IP3	Inositol 1,4,5 trisphosphate
IPAH	Idiopathic pulmonary arterial hypertension
K ⁺	Potassium ion
[K ⁺] _i	Intracellular potassium
KCNQ	Voltage gated potassium- 7 subfamily channel
K _v	Voltage gated potassium channel
LV	Left ventricle
LV+S	Left ventricle plus septum
M	Muscarinic
MAO	Monoamine oxidase
MAO-A	Monoamine oxidase A
MAP	Mean systemic arterial pressure
MAPK	Mitogen activated protein kinase
MLC	Myosin light chain
MLCK	Myosin light chain kinase

MLCP	Myosin light chain phosphatase
mPAP	Mean pulmonary arterial pressure
mRNA	Messenger RNA
Mts1	Calcium binding protein S100A4
NA	Noradrenaline
Na ⁺	Sodium ion
NANC	Non-adrenergic non-cholinergic system
NBF	Neutral-buffered formalin
NH ₂	Amine group
NO	Nitric oxide
NYHA	New York Heart Association Classification
O ₂	Oxygen molecule
OH	Hydroxyl group
OVX	Ovariectomy
P13K	Phosphatidylinositol-3-kinase
P _A	Alveolar pressure
P _a	Arterial pressure
P _v	Venous pressure
PAEC	Pulmonary artery endothelial cell
PAF	Pulmonary artery fibroblast
PAH	Pulmonary arterial hypertension
PAP	Pulmonary artery pressure
PASMC	Pulmonary artery smooth muscle cell
PBS	Phosphate-buffered saline
PCH	Pulmonary capillary hemangiomatosis
pCO ₂	Partial pressure of carbon dioxide
pO ₂	Partial pressure of oxygen

PCPA	P-chlorophenylalanine
PDE	Phosphodiesterase
PDE-5	Phosphodiesterase 5
PDGF	Platelet derived growth factor
PDGFR	Platelet derived growth factor receptor
PDGFR α	Platelet derived growth factor receptor alpha
PDGFR β	Platelet derived growth factor receptor beta
PE	Phenylephrine
PGI ₂	Prostacyclin
PH	Pulmonary hypertension
PKA	Protein kinase A
PKB	Protein kinase B
PKC	Protein kinase C
PKG	Protein kinase G
PLC	Phospholipase C
PP2A	Protein phosphatase 2A
PPHN	Persistent pulmonary hypertension of the newborn
PSS	Physiological saline solution
PVDF	Polyvinylidene difluoride
PVOD	Pulmonary veno-occlusive disease
PVR	Pulmonary vascular resistance
PVR	Pulmonary vascular remodelling
RAGE	Receptor for advanced glycosylation end products
ROC	Receptor operated calcium channel
ROCK	Rho-kinase
RV	Right ventricle
RV/LV+S	Ratio of right ventricle to left ventricle plus septum

RIN	RNA integrity number
ROS	Reactive oxygen species
RVH	Right ventricular hypertrophy
RVP	Right ventricular pressure
RVSP	Right ventricular systolic pressure
SAP	Systemic arterial pressure
SHAM	Sham-operated
SEM	Standard error of mean
SERM	Selective estrogen receptor modulator
SERT	Serotonin transporter
SERTLPR	Serotonin transporter gene LL allele polymorphism
SLC6A4	Serotonin transporter gene
SMC	Smooth muscle cell
SNP	Single-nucleotide polymorphism
SOCC	Store operated calcium channel
TGF- β	Transforming growth factor beta
Tie2	Angiopoietin receptor
TMD	Transmembrane domain
TPH	Tryptophan hydroxylase
TPH1	Tryptophan hydroxylase 1
TPH2	Tryptophan hydroxylase 2
TRPC6	Transient receptor potential cation channel, subfamily C, member 6
VEGF	Vascular endothelial growth factor
VIP	Vasoactive intestinal peptide
VMAT	Vesicular monoamine transporter
WT	Wildtype

Abstract

Pulmonary arterial hypertension (PAH) is a progressive disease characterised by vasoconstriction and remodelling of the pulmonary vasculature. The consequence of this is increased pulmonary arterial pressure, right heart failure and eventual death if left untreated. Even in those patients receiving advanced PAH therapy, mortality rates remain high. Therefore, the development of novel therapeutic approaches in the treatment of PAH is urgently required. A better understanding of PAH pathogenesis is critical to achieving this. Gender differences exist in human PAH, with females up to three-fold more likely to present with disease than males. Limited evidence suggests that estrogens may be accountable for these differences. For example, the use of oral contraceptives has been associated with the development of PAH. Paradoxical to this however, experimental models of PAH exhibit male susceptibility which has limited research into the role of estrogens in the pathogenesis of PAH.

Serotonin is implicated in both experimental and human PAH. Activity of the serotonin transporter (SERT) modulates the development of PAH and mice over-expressing SERT (SERT+ mice) exhibit PAH and exaggerated hypoxia-induced PAH. In the central nervous system, estrogens regulate expression of several serotonin signalling components including tryptophan hydroxylase (TPH), the 5-HT receptors and SERT. One hypothesis is that similar estrogen effects on serotonin signalling may also be apparent in the pulmonary vasculature, and this is one hypothesis for the increased female susceptibility observed in PAH. To examine this, the influence of gender and estrogen on the development of PAH in SERT+ mice was investigated. This was repeated following exposure to chronic hypoxia. Pulmonary vascular reactivity was determined using small vessel myography. The genotypic differences in SERT+ mice were also assessed via microarray analysis. Genes of interest were validated by qRT-PCR analysis and immunoblotting. To translate

clinical relevance to any findings, the effects of female hormones were also investigated in human pulmonary artery smooth muscle cells (PASMCs) derived from both non-PAH (control) and idiopathic pulmonary arterial hypertension (IPAH) patients.

PAH was assessed via measurement of right ventricular systolic pressure (RVSP), pulmonary vascular remodelling and right ventricular hypertrophy (RVH). Male SERT⁺ mice do not develop PAH. Female SERT⁺ mice exhibited increased RVSP and pulmonary vascular remodelling. This increased RVSP and pulmonary vascular remodelling were completely prevented following ovariectomy in SERT⁺ mice. The chronic administration of 17 β estradiol (1.5mg/kg/day), which is the pre-dominant circulating female hormone in pre-menopausal women, fully re-established PAH as assessed by increased RVSP and pulmonary vascular remodelling. Pulmonary vascular reactivity to serotonin was unaffected in these mice. In chronic hypoxia, female SERT⁺ mice exhibited exaggerated hypoxia-induced PAH whereas male SERT⁺ mice remained unchanged compared to their respective wildtype (WT) controls. This exaggerated hypoxia-induced PAH phenotype was attenuated in SERT⁺ mice following ovariectomy, as assessed by a reduction in RVSP and pulmonary vascular remodelling. The chronic administration of 17 β estradiol completely re-established exaggerated hypoxia-induced PAH in ovariectomized SERT⁺ mice. Similar to normoxia, serotonin-induced pulmonary vascular contraction was also unaffected in these mice. The stimulation of PASMCs with 17 β estradiol increased tryptophan hydroxylase-1, SERT and 5-HT_{1B} receptor expression. Consistent with our in vivo findings, physiological concentrations of 17 β estradiol (1nmol/L) stimulated PASMC proliferation whereas estrone, estriol and progesterone had no effect. This proliferation was successfully blocked by both the tryptophan hydroxylase inhibitor para-chlorophenylalanine and the 5-HT_{1B} receptor antagonist SB224289.

Microarray analysis in the pulmonary arteries of female SERT⁺ mice confirmed the dysregulation of multiple pathways with relevance to PAH including those associated with metabolism, cell differentiation and contraction. A large number of PAH-related pathways were also dysregulated in female SERT⁺ mice exposed to chronic hypoxia. In contrast, pathways were altered in normoxic and chronically hypoxic male SERT⁺ mice to a much lesser extent. For microarray validation, qRT-PCR analysis was performed in ten selected genes (FOS, CEBPB, CYP1B1, MYL3, HAMP2, LTF, PLN, NPPA, UCP1 and C1S) and 100% concordance was reported. Three genes were selected for further investigation (FOS, CEBPB and CYP1B1). Immunoblotting confirmed that protein expression of c-FOS, C/EBP β and CYP1B1 was increased in the pulmonary arteries of female SERT⁺ mice compared against female WT mice. With relevance to human PAH, we also confirmed that mRNA expression of FOS, CEBPB and CYP1B1 was increased in PASMCs derived from IPAH patients. Protein validation with immunoblotting confirmed that c-FOS, C/EBP β and CYP1B1 expression was also increased in IPAH PASMCs.

In summary of these findings, we have identified that females may be at an increased risk to the development of PAH via the effects of 17 β estradiol. Specifically, 17 β estradiol appears to increase expression of several key serotonin pathway mediators including tryptophan hydroxylase-1 (the rate-limiting enzyme in serotonin synthesis), SERT and the 5-HT_{1B} receptors, all of which have been previously implicated in the pathogenesis of PAH. Our results suggest that 17 β estradiol stimulates PASMC proliferation via activation of the serotonin pathway. Microarray analysis in the pulmonary arteries of SERT⁺ mice confirmed that a large number of genes associated with PAH-related pathways were differentially expressed in females. RNA and protein validation further confirmed these differences in selected genes (CEBPB, CYP1B1 and FOS). With relevance to human PAH, we also confirmed the dysregulation of several key genes at both mRNA and protein level in PASMCs derived from IPAH patients. Taken together, these findings describe the

critical role of 17β estradiol in PAH, and this may offer an explanation for the increased susceptibility observed in females.

Chapter 1

Introduction

1.1 The Pulmonary Circulation

1.1.1 Structural Organisation

The pulmonary circulation constitutes the entire cardiac output from the right ventricle, which receives mixed venous blood draining into the right atria from the systemic circulation via the superior and inferior vena cava. The pulmonary artery originates at the anterior base of the right ventricle where it bifurcates to become the *left* and *right* pulmonary artery, both of which extend into the hilum of their corresponding lungs. The left lung is divided into the superior and inferior lobe, separated by the oblique fissure and each receives an arterial branch from the *left* pulmonary artery. In contrast, the right lung is divided into three lobes (superior, middle and inferior) separated by interlobular fissures and each is supplied with a branch resulting from bifurcation of the *right* pulmonary artery, one entering the superior lobe and the other supplying the middle and inferior lobes. Each of the five lobes can be further subdivided into distinct anatomical compartments termed bronchopulmonary segments (Sealy et al., 1993). Each of these contains segmental bronchi and its accompanying (tertiary) pulmonary artery. Subsequent distal branching of the pulmonary arterial circulation continues irregularly but in parallel series with the bronchial tree until the terminal alveoli are reached, which is equivalent to fifteen orders of branching.

1.1.2 Functional Organisation

This order of branching can be numerically categorised by function using the *convergent* approach (Huang et al., 1996). In convergence, the most peripheral pulmonary arteries (the pre-capillary arteries) are termed order 1 and this numbering continues with each proximal branch-point until the main pulmonary artery (order 15) is reached. The proximal elastic arteries (orders 15-13) are highly compliant and typically have an internal

diameter greater than 1mm and also have increased elastic laminae in the tunica media to facilitate compliance. The more distal muscular arteries (orders 13-4) progressively lose their compliance with continual branching, as a direct consequence of increased smooth muscle and decreased elastic laminae in the tunica media. These pulmonary arteries can be phenotypically characterised by the increased presence of medial smooth muscle relative to the rest of the vasculature (Heath and Edwards, 1958), and are important in blood pressure regulation. Medial smooth muscle is completely diminished in the non-muscular pre-capillary arteries (orders 4-1) (Meyrick and Reid, 1983; deMello et al., 1997), which exist as extremely thin-walled vessels composed of endothelial cells and pericytes (undifferentiated smooth muscle cells) to facilitate blood-gas exchange (Figure 1.1).

The network of pulmonary pre-capillary arteries contains more than 300 million vessels over 15 orders of branching. This ultimately becomes the pulmonary capillary network, which serves as an extremely distensible complex arrangement of almost 280 billion capillaries. Each capillary has an internal diameter less than 10 μ m and supplies blood to several alveoli. Together, the capillaries form a large surface area (125m²) to efficiently facilitate blood oxygenation, and this is the primary function of the lung. Following completion of circulation through the pulmonary capillaries, the re-oxygenated blood enters the pulmonary venous circulation via the venules and convergent branching of the pulmonary veins continue until the left and right pulmonary veins are formed from their corresponding lungs, and these enter into the left atria.

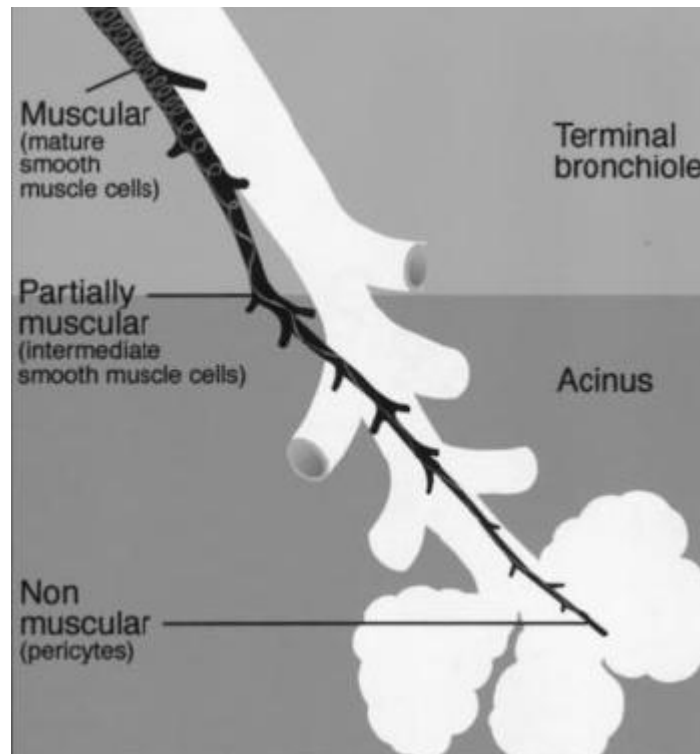


Figure 1.1 Musculature in the pulmonary arteries. The absence of mature smooth muscle cells is apparent in distal pulmonary arteries and typically replaced with immature non-muscular pericytes. Adapted from (MacLean et al., 2000).

1.1.3 Structure of the Pulmonary Vascular Wall

The transverse section of a normal pulmonary artery reveals that the vessel wall typically consists of three concentric layers or ‘tunics’ termed the *tunica intima*, *tunica media* and *tunica adventitia* (Figure 1.2). In addition, each tunic is composed of a population of phenotypically distinct cells. The (innermost) tunica intima exists as a monocellular endothelial cell layer attached to an underlying connective tissue matrix, termed the basement membrane. The pulmonary artery endothelial cells (PAECs) compose the lumen, and are unique to the vascular wall in that they are the only cells in constant

physical contact with blood flow. PAECs are proposed to continually monitor and regulate the luminal environment via the release of various factors (Liu et al., 1994; Aaronson et al., 2002). The tunica media is typically the predominant of the three tunics and is composed of a conserved longitudinal arrangement of smooth muscle cells with an underlying elastic layer. Pulmonary artery smooth muscle cells (PASMCs), of which several heterogeneous populations exist (Frid et al., 1997; Stenmark and Frid, 1998), are the only cell type in the vascular wall capable of producing a contractile response following their stimulation, and therefore are commonly referred to as the ‘effectors’ in determining arterial tone and blood pressure. The outermost tunica adventitia exists as a collagen matrix and helps maintain the structural integrity of the vessel wall. In addition, pulmonary artery fibroblasts (PAFs) also exist in the adventitia, and have been identified to play an important role in response to environmental stimuli (Stenmark et al., 2006).

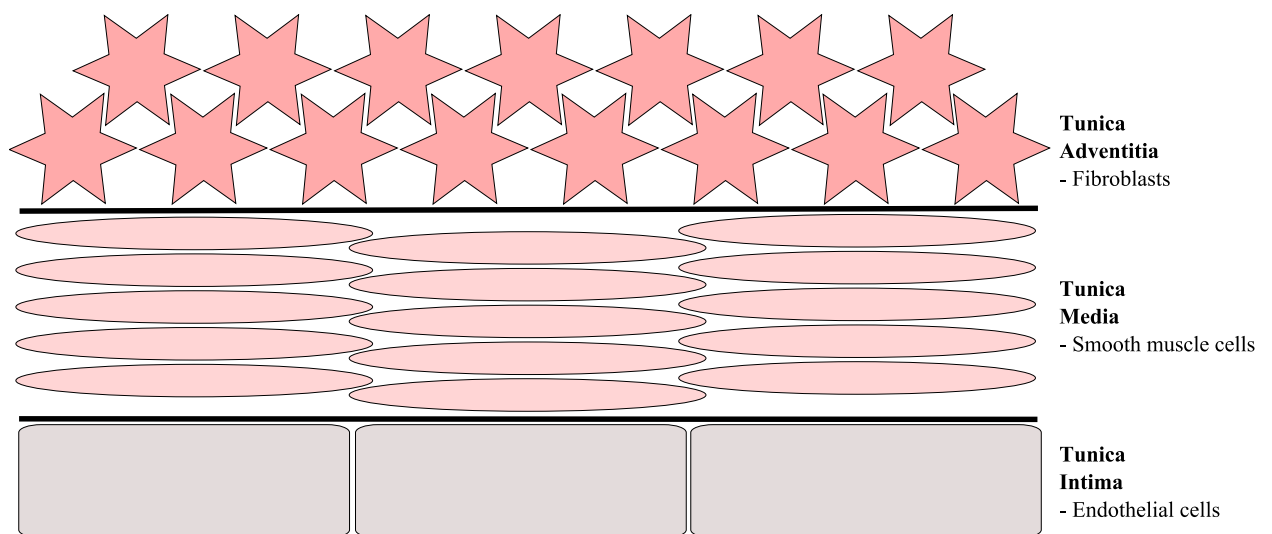


Figure 1.2 Vascular cell types which compose the pulmonary vascular wall. Endothelial cells, smooth muscle cells and fibroblasts primarily compose the pulmonary vascular wall.

1.1.4 Function of the Pulmonary Circulation

In the adult circulation both the left and right ventricles are arranged in parallel series. Therefore, pulmonary blood flow is exactly equal to that of the left ventricular cardiac output, which typically equates to 5 litres per minute at rest and up to 25 litres per minutes during exercise. The most essential function of the pulmonary circulation is to facilitate the oxygenation of deoxygenated blood arriving from the systemic circulation, via a blood-gas interface (Comroe, Jr., 1966). This continuously occurs by the rapid unloading of CO₂ molecules and subsequent binding of O₂ molecules to haemoglobin, which resides within red blood cells, and this is vital to supply and maintain the metabolic processes throughout the body.

In addition to gas exchange, the pulmonary circulation is required to perform additional functions. For example, the pulmonary circulation acts as a physical barrier, by filtering and preventing the passage of inhaled foreign bodies from the respiratory system to the cardiovascular system (Comroe, Jr., 1966). Within the cardiovascular system, it also acts as a physical barrier to prevent the passage of potentially lethal thrombi, which are typically formed in the systemic venous circulation, to the systemic arterial circulation. In addition, thrombolytic mediators synthesised and released from PAECs, including prostacyclin (Gryglewski et al., 1988) and nitric oxide (Nong et al., 1997), act to dissolve lodged thrombi via a process termed fibrinolysis. Similarly, air and lipid emboli are rapidly absorbed and removed during their passage through the pulmonary capillaries. Together, the blood filtration function of the pulmonary circulation acts to prevent the thrombotic or embolic occlusion of essential arterial beds which may otherwise lead to infarction. The pulmonary circulation may also function as a blood reservoir (Comroe, Jr., 1966). Under physiological conditions, about 40% of the total lung weight is blood and this equates to a total pulmonary blood volume of 500ml, or 10% of the total circulating blood volume. Moreover, this blood volume can be rapidly mobilized back into the

circulation during periods of trauma or haemorrhagic shock to significantly improve short-term cardiac output (Shoemaker, 1974).

1.1.5 Control of the Pulmonary Circulation

The pulmonary circulation is a high-flow, low-resistance, low-pressure system. In contrast to the arteries which comprise the systemic circulation, the pulmonary arteries contain less medial smooth muscle and elastin, and therefore thinner walled allowing for greater distensibility (Kilner, 2004). As a consequence, pulmonary arterial pressure (PAP) is typically 24/9mmHg and significantly lower than systemic arterial pressure (SAP), which is typically 120/80mmHg (Morgan et al., 2004). As a result, the mean PAP (mPAP) is roughly 1/8th of the mean SAP (~15mmHg cf. ~93mmHg). Similarly, the pressure gradient throughout the pulmonary circulation is 7 to 9mmHg, and up to ten-fold lower than those which exist in the systemic circulation (Mandegar et al., 2004).

1.1.6 Pulmonary Vascular Resistance

Pulmonary vascular resistance (PVR) is defined as the total peripheral resistance which must be overcome to maintain continuous blood flow through the pulmonary arteries. According to Poiseuille's law, the diameter (D) is to the fourth power and therefore even small changes in this are likely to significantly affect flow and thus PVR (Krenz et al., 1994). For example, a 50% reduction in vessel diameter would result in a 16-fold increase in PVR. Physiologically, blood vessel diameter is regulated via changes in basal tone of the smaller muscular pulmonary arteries (100µm - 500µm ID), with vasoconstriction decreasing this, whereas the opposite effect would occur during vasodilatation. This would result in an increase/decrease of PVR, and as a consequence cause a reflective change in PAP. The relationship between lumen diameter, PVR and PAP is also essential in the pathobiology of pulmonary vascular disease states where elevated PAP is apparent, such as

pulmonary hypertension. Intimal thickening of the pulmonary vascular wall, arising from vascular remodelling, results in an irreversible reduction of lumen diameter and as a consequence leads to a sustained increase in PAP.

1.1.7 Passive Regulation and Distribution of Blood Flow

The relatively low pulmonary pressures combined with the mid-entry point of the artery into the lung results in the uneven distribution of blood flow throughout the pulmonary circulation. When upright, pulmonary blood flow through the apex of the lung is extremely low. However, towards the base of the lung blood flow is greatly increased (Lee, 1971). To explain, the lung is divided into three zones as determined by the relative values of the pulmonary arterial (P_a), pulmonary venous (P_v) and alveolar (P_A) pressure (Figure 1.3). Zone 1 describes the upper portion of the lung where blood flow is extremely low, and this can be explained because the apex alveolar pressure is greater than both the arterial and venous pressures ($P_A > P_a > P_v$), resulting in collapse of the highly compliant vasculature. Zone 2 exists in the mid-portion where arterial pressure is greatest, however alveolar pressure still exceeds venous pressure ($P_a > P_A > P_v$) and therefore blood flow remains impaired. In this portion of lung, a modest increase in arterial pressure is sufficient to functionally recruit the vessels back into the pulmonary circulation. Zone 3 is the most inferior and below-heart level. At rest, this is the area of the lung where vessel recruitment for the pulmonary circulation is greatest (Hughes, 1975). Both the arterial and venous pressures are greater than the alveolar pressure ($P_a > P_v > P_A$) which allows the vessels to be maximally distended at all times. During periods of increased blood flow (e.g. stress, exercise), there is substantial recruitment of the pulmonary vasculature which exist in zone 1 and zone 2, resulting in an even blood flow distribution throughout the lung (Harf et al., 1978).

1.1.8 Active Distribution and Regulation of Blood Flow

In addition to the passive distribution of blood flow, the active regulation of blood flow is also a major determinant of pulmonary arterial pressure (Barnes and Liu, 1995). Active factors include sympathetic nerves, humoral mechanisms and respiratory gases. All of these influence PVR via the regulation of pulmonary artery smooth muscle contraction.

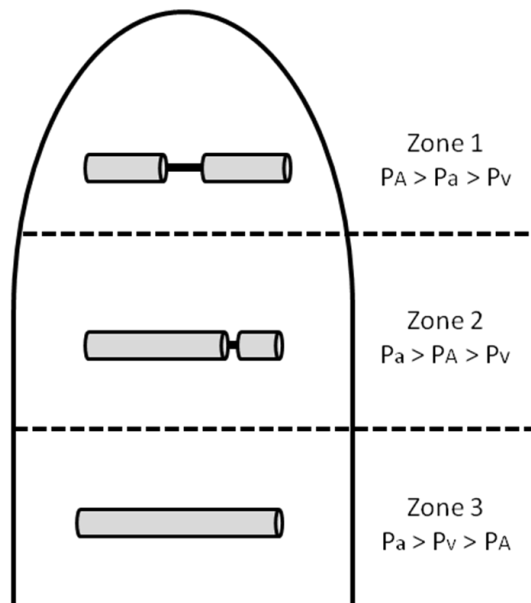


Figure 1.3 Passive distribution of blood flow throughout the lung. Each lung is divided into three zones as determined by the pulmonary arterial pressure (P_a), pulmonary venous pressure (P_v) and alveolar (P_A) pressure. These are important determinants of passive blood flow through the lung.

1.1.8.1 Neural Mechanisms

The pulmonary circulation is innervated by both the sympathetic (adrenergic) and parasympathetic (cholinergic) branches of the autonomic nervous system (Dawson, 1984). In addition, a third neural mechanism comprised of nonadrenergic noncholinergic (NANC) nerves, also regulates pulmonary vascular tone (Kubota et al., 1988). All innervating nerves terminate in the perivasculature and release vasoactive neurotransmitters following stimulation. Vasomotor regulation is an essential component in maintaining the vasoconstrictor-vasodilator balance in the pulmonary vasculature.

Stimulation of the sympathetic nervous system results in increased neuron firing, increased pulmonary vascular resistance, and as a consequence increased PAP (Kadowitz et al., 1974). Vasoconstriction is primarily mediated via the α adrenoceptors, which are predominantly expressed in PSMCs (Hyman et al., 1986). These receptors are stimulated following release of their endogenous ligand noradrenaline from stimulated sympathetic post-ganglionic nerves (Tong et al., 1978). Although all α_1 adrenoceptor subtypes are expressed in the pulmonary arteries (Xu et al., 1997), the α_{1D} adrenoceptors appear to predominantly mediate vasoconstriction (Hussain and Marshall, 1997). The α_2 adrenoceptors are not expressed in pulmonary arteries, but are thought to play an important role in pulmonary venous constriction (Ohlstein et al., 1989). In addition, both the β_1 and β_2 adrenoceptor subtypes are expressed in the pulmonary circulation, and mediate vasodilatation following their stimulation by noradrenaline (Hyman et al., 1981; Hyman et al., 1990).

The parasympathetic branch of the autonomic nervous system appears much less dense in the pulmonary arteries compared to sympathetic innervation (Downing and Lee, 1980). In addition, this also appears less important in the regulation of pulmonary vascular tone, as its pharmacological blockade does not influence pulmonary vascular resistance or

pulmonary arterial pressure (Murray et al., 1986). However, exogenous administration of the parasympathetic post-ganglionic neurotransmitter acetylcholine (ACh) relaxes endothelium-intact human pulmonary arteries (Greenberg et al., 1987) via stimulation of the endothelial muscarinic (M) receptors (McCormack et al., 1988).

Functional NANC nerves have also been identified in the pulmonary arteries, as observed by frequency dependent nitric oxide mediated relaxations which are completely unaffected by adrenergic or cholinergic blockade in isolated pulmonary arteries (Scott and McCormack, 1999). Multiple NANC neurotransmitters have been described as important in this, including substance P, ATP, calcitonin-gene related peptide and adenosine (Kobayashi and Amenta, 1994). The effect of NANC nerves in the regulation of pulmonary vascular tone remains to be described *in vivo*.

1.1.9 Pulmonary Vascular Contraction

Increased intracellular $[Ca^{2+}]$ is the major determinant in vasoconstriction, and plays an essential role in the mechanism of smooth muscle cell contraction (Figure 1.4). The calcium-binding protein calmodulin (CaM) forms a complex with Ca^{2+} and this construct binds to and activates myosin light chain kinase (MLCK). When activated, MLCK phosphorylates myosin light chain (MLC) in an adenosine 5' triphosphate (ATP) driven process, resulting in a conformational change which allows the interaction of myosin with actin filaments (Kuriyama et al., 1982). These interactions are collectively termed cross-bridge cycling and it is this mechanism which forms the basis of smooth muscle contraction (Gunst and Fredberg, 2003). Contraction is terminated via the dephosphorylation of MLC by myosin light chain phosphatase (MLCP).

1.1.10 Hypoxic Pulmonary Vasoconstriction

The pulmonary arteries are unique from those which comprise the systemic circulation in that they constrict in response to hypoxia (Fishman, 1961). Hypoxic pulmonary vasoconstriction (HPV) is an intrinsic adaptive response to alveolar hypoxia (Madden et al., 1992), which results in the redistribution of blood flow throughout the lung to segments with greater oxygen supply. The small resistance arteries (~200µm ID) are the primary site of HPV (McCulloch et al., 2000). This regulative shunting mechanism ensures optimal ventilation-perfusion matching, and as a consequence more efficient blood re-oxygenation. Several observations in the systemic circulation have identified that they dilate in response to hypoxia (Gregor and Janig, 1977), confirming that HPV is intrinsic to the pulmonary vasculature. PSMCs are proposed to be the cell type which monitors the hypoxic environment in the vasculature. This is supported by evidence which shows that HPV still occurs in endothelium-denuded pulmonary arteries (Marshall and Marshall, 1992). Additionally, a contractile response is also observed in cultured PSMCs derived from pulmonary resistance arteries following their exposure to hypoxia (Zhang et al., 1997). In opposition to this others have proposed that, although not essential to HPV, the endothelium must be present and functional for a prolonged contractile response following sustained hypoxia (Holden and McCall, 1984; Archer et al., 2004). This suggests the existence of both endothelium-dependent and endothelium-independent components in HPV.

HPV is likely initiated by the inhibition of redox-sensitive membrane K_v channels via adaptive changes in mitochondria derived reactive oxygen species (ROS) generation. In turn, this leads to cell depolarisation and the opening of L-type Ca^{2+} channels, resulting in pulmonary vascular contraction. However at present, several detailed mechanisms have been proposed for HPV (Aaronson et al., 2006). There is general agreement that all classical vasoactive mediators which mediate constriction in both the pulmonary and

systemic arteries (e.g. 5-HT, endothelin-1) are unlikely to be involved. On this basis, the initial mediator of HPV must be uniquely expressed in the pulmonary vasculature, however this component remains to be unanimously identified (Figure 1.5). Downstream, rho-kinase mediated Ca^{2+} sensitization of the smooth muscle contractile apparatus is an important regulatory component of HPV (Robertson et al., 2000). The mitochondrial-derived generation of reactive oxygen species (ROS) is also considered pivotal although their exact role still remains unclear as both an increase and decrease of ROS generation have been reported in hypoxia (Archer et al., 1989; Archer et al., 1989; Archer et al., 1989; Michelakis et al., 2002; Killilea et al., 2000). The involvement of both $\text{K}_v1.5$ channels and L-type Ca^{2+} channels has also been described. In PASMCs, hypoxia leads to decreased $\text{K}_v1.5$ and $\text{K}_v2.1$ expression (Wang et al., 1997; Wang et al., 2005), resulting in the net reduction of tonic K^+ cellular efflux and as a consequence depolarisation and the opening of the L-type Ca^{2+} channels. If hypoxia is adequately sustained for a prolonged period, this increase in intracellular Ca^{2+} not only results in vasoconstriction but also stimulates expression of several pro-proliferative target genes resulting in hypoxia-induced PASMC proliferation (Platoshyn et al., 2007).

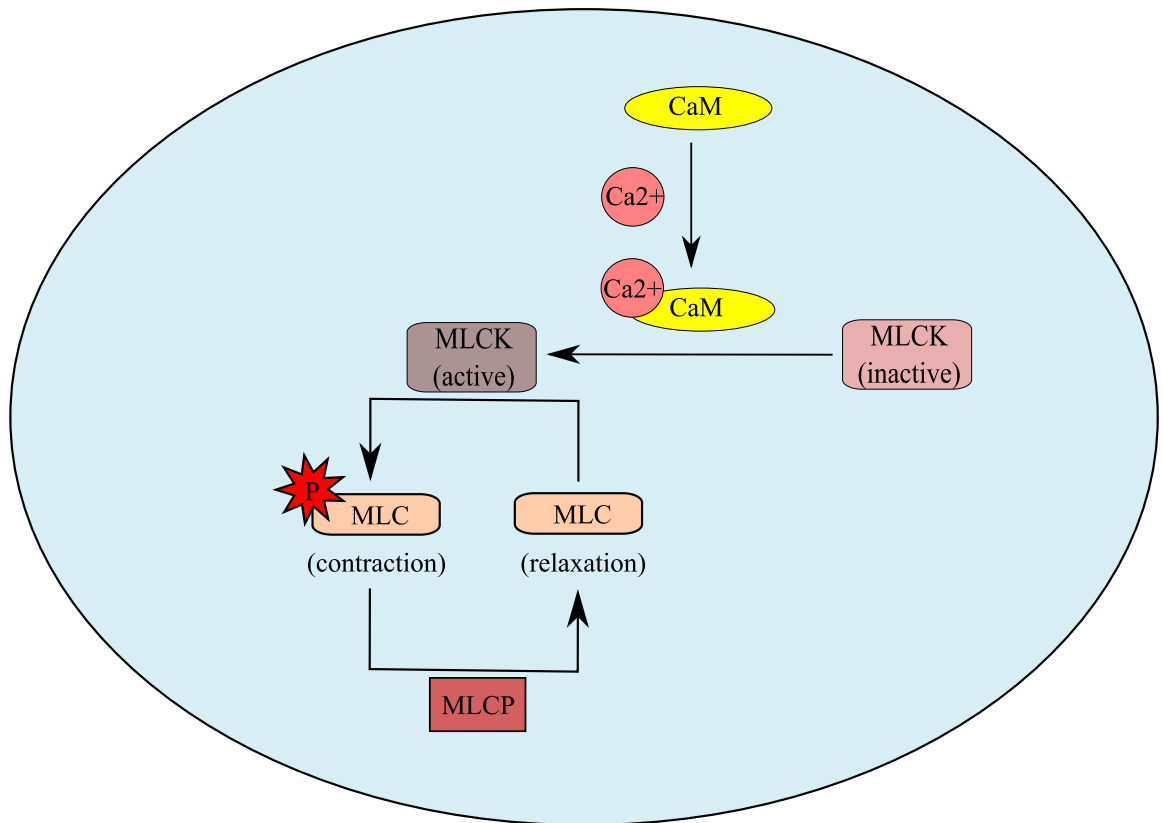


Figure 1.4 The mechanism underlying pulmonary vascular smooth muscle contraction. Intracellular $[Ca^{2+}]$ is the major determinant of smooth muscle tone. The formation of a Ca^{2+} -calmodulin (CaM) complex activates myosin light-chain kinase (MLCK), which subsequently phosphorylates myosin light-chain (MCL) to facilitate actin and myosin interaction to promote contraction. Contraction is terminated via the dephosphorylation of MLC by myosin light chain phosphatase (MLCP).

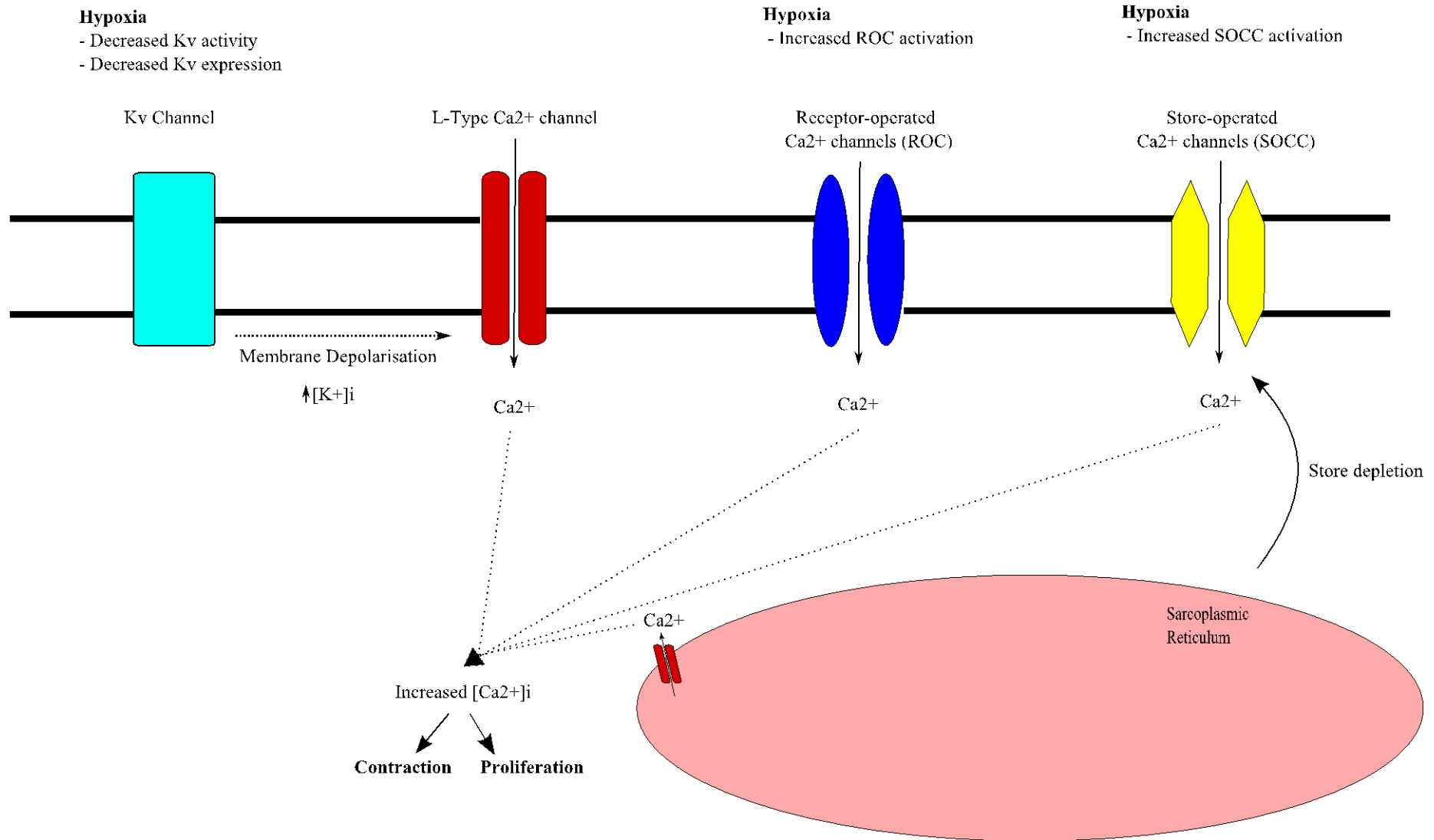


Figure 1.5 Proposed mechanism of hypoxic pulmonary vasoconstriction (HPV). Hypoxia results in decreased K_v channel function, increased intracellular K^+ and membrane depolarisation. Increased Ca^{2+} influx occurs via the depolarisation-activated L-type Ca^{2+} channels. Hypoxia also activates the receptor-operated Ca^{2+} channels (ROCs) and store-operated calcium channels (SOCCs), further increasing intracellular Ca^{2+} . As a consequence, the increased cytosolic Ca^{2+} promotes smooth muscle contraction, and if sustained will stimulate proliferation.

1.2 Pulmonary Arterial Hypertension

1.2.1 Classification

Pulmonary arterial hypertension (PAH) is a progressive disease characterised by vasoconstriction and remodelling of the pulmonary vasculature, resulting in right heart failure and eventual death. According to the latest clinical classification, PAH is diagnosed if mean pulmonary arterial pressure (mPAP) is greater than 25mmHg at rest (Simonneau et al., 2009). This is typically confirmed following right heart catheterization (Barst et al., 2004). Further clinical assessment is also performed to confirm PAH aetiology, as multiple diseases not directly associated with the pulmonary circulation (e.g. left heart failure) can indirectly influence PAP (Oudiz, 2007). Patients with mild or moderate PAH typically present asymptomatic at both rest and during physical activity (Simonneau et al., 2009). Only in late-stage/severe PAH, are clinical symptoms apparent and include dyspnoea, syncope, chest pain and fatigue.

The mean age of PAH diagnosis is 56 years of age (NCASP Pulmonary Hypertension Audit 2010), and patients have a median survival time of 2.8 years if left untreated (Gaine and Rubin, 1998). Although the development of PAH can arise from multiple aetiologies, all share a common phenotypic pathobiology (Voelkel and Cool, 2004). According to the World Health Organisation (Rosenkranz and Erdmann, 2008), PAH is subcategorized into the following clinical classification (Table 1.1): idiopathic (IPAH), heritable (HPAH), drug & toxin induced, associated with chronic haemolytic anaemia, schistosomiasis, congenital heart diseases, portal hypertension, HIV infection or connective tissue diseases, and persistent pulmonary hypertension of the newborn (PPHN). Non-arterial pulmonary hypertension can also occur and is classified into the following categories; pulmonary hypertension with unclear multifactorial mechanisms; chronic thromboembolic pulmonary hypertension (CTEPH), pulmonary hypertension owing to lung diseases and/or hypoxia,

pulmonary hypertension owing to left heart disease and pulmonary veno-occlusive disease (PVOD) and/or pulmonary capillary hemangiomatosis (PCH).

**Clinical Classification of Pulmonary Hypertension
4th World Health Organisation Symposium on Pulmonary Hypertension, Dana Point
2008**

1. Pulmonary arterial hypertension (PAH)

- 1.1. Idiopathic PAH
- 1.2. Heritable
 - 1.2.1. BMPR2
 - 1.2.2. ALK1, endoglin (with or without hereditary hemorrhagic telangiectasia)
 - 1.2.3. Unknown
- 1.3. Drug- and toxin-induced
- 1.4. Associated with:
 - 1.4.1. Connective tissue diseases
 - 1.4.2. HIV infection
 - 1.4.3. Portal hypertension
 - 1.4.4. Congenital heart diseases
 - 1.4.5. Schistosomiasis
 - 1.4.6. Chronic hemolytic anemia
- 1.5 Persistent pulmonary hypertension of the newborn

1. Pulmonary veno-occlusive disease (PVOD) and/or pulmonary capillary hemangiomatosis (PCH)

2. Pulmonary hypertension owing to left heart disease

- 2.1. Systolic dysfunction
- 2.2. Diastolic dysfunction
- 2.3. Valvular disease

3. Pulmonary hypertension owing to lung diseases and/or hypoxia

- 3.1. Chronic obstructive pulmonary disease
- 3.2. Interstitial lung disease
- 3.3. Other pulmonary diseases with mixed restrictive and obstructive pattern
- 3.4. Sleep-disordered breathing
- 3.5. Alveolar hypoventilation disorders
- 3.6. Chronic exposure to high altitude
- 3.7. Developmental abnormalities

4. Chronic thromboembolic pulmonary hypertension (CTEPH)

5. Pulmonary hypertension with unclear multifactorial mechanisms

- 5.1. Hematologic disorders: myeloproliferative disorders, splenectomy
- 5.2. Systemic disorders: sarcoidosis, pulmonary Langerhans cell histiocytosis: lymphangioleiomyomatosis, neurofibromatosis, vasculitis
- 5.3. Metabolic disorders: glycogen storage disease, Gaucher disease, thyroid disorders
- 5.4. Others: tumoral obstruction, fibrosing mediastinitis, chronic renal failure on dialysis

Table 1.1 Current WHO clinical classification of pulmonary hypertension. Dana

Point 2008. BMPR2, bone morphogenetic protein receptor type 2; ALK1, activin receptor like kinase-1, HIV, human immunodeficiency virus.

Current World Health Organization/ New York Heart Association Classification of Functional Status of Patients with Pulmonary Hypertension

Class I:	Patients with PH without limitation of usual activity. Ordinary physical activity does not cause increased dyspnoea, fatigue, chest pain or pre-syncope.
Class II:	Patients with PH with slight limitation of usual physical activity. There is no discomfort at rest, but normal physical activity causes increased dyspnoea, fatigue, chest pain or pre-syncope.
Class III:	Patients with PH with marked limitation of usual physical activity. There is no discomfort at rest, but less than ordinary activity causes increased dyspnoea, fatigue, chest pain or pre-syncope.
Class IV:	Patients with PH with inability to perform any physical activity without symptoms and who may have signs of right ventricular failure. Dyspnoea and/or fatigue may be present at rest and symptoms are increased by almost any physical activity.

Table 1.2 Current World Health Organisation/ New York Heart association Classification of functional status in patients with pulmonary hypertension.

The severity of PAH in patients can be categorized using the NYHA (class I – IV) functional classification system (Table 1.2). It is the physical limitations imposed on the patient by the disease which determines the functional classification. For example, asymptomatic patients with early-stage PAH reside within class I and those most affected (late-stage PAH with right heart failure) are class IV. The NYHA (class I – IV) system is an important factor in both the choice of PAH therapy and is also an accurate predictor of patient mortality.

1.2.2 Current Therapeutic Strategies in PAH

PAH results in an elevation of PVR, and as a consequence increased PAP. To date, all current therapeutic strategies act to decrease PVR via the promotion of vasodilatation or the inhibition of vasoconstriction. To date, none of these treatments have proven effective in the prevention and/or regression of remodelling in PAH. These PAH drug therapies can be broadly categorised into the following four groups; prostanoids, calcium channel blockers, endothelin receptor antagonists and phosphodiesterase-5 (PDE-5) inhibitors (Figure 1.6). These are typically prescribed in combination as the most effective treatment of PAH.

1.2.2.1 Prostanoids

The prostanoid analogue epoprostenol was the first FDA-approved drug used in the treatment of PAH, and is still prescribed for severe PAH (NYHA class III and class IV). Prostacyclin (PGI_2), an endogenous prostanoid synthesised in PAECs, is a potent vasodilator in the pulmonary circulation and also exhibits anti-mitogenic and anti-thrombotic properties in experimental PAH (Hoshikawa et al., 2001; Geraci et al., 1999). Previously, it has been reported that a deficiency in circulating PGI_2 , via decreased lung expression of PGI_2 synthase, contributes to the pathogenesis of PAH (Christman et al., 1992). Data generated from clinical trials confirm that the chronic administration of exogenous epoprostenol demonstrate a marked improvement in haemodynamic function, exercise capacity and survival time in NYHA class III and class IV PAH patients (Barst et al., 1996; Sitbon et al., 2002; Badesch et al., 2000; McLaughlin et al., 2002). However, the chronic intra-venous infusion and short half-life (<6mins) of epoprostenol are the major limitations of its use. Common side effects include flushing, jaw pain, headache and sepsis, with the latter resulting from intra-venous catheter complications. Treprostinil is a modern generation prostanoid analogue with similar beneficial haemodynamic effects to

epoprostenol, but has the advantage of an improved half-life (~3 hours), and can also be administered subcutaneously. Recently, the inhaled prostanoid iloprost has also been FDA approved for therapeutic use, and this improved route of administration will bypass the side effects associated with other prostacyclin-based treatments.

1.2.2.2 *Calcium Channel Blockers*

Calcium channel blockers (CCBs) comprise a class of drugs which act to functionally alter calcium channel Ca^{2+} conductance. In PASMCs, the consequence is a net decrease in $[\text{Ca}^{2+}]_i$ and cellular hyperpolarisation, resulting in pulmonary vascular smooth muscle relaxation. Clinical trials involving the use of CCBs in PAH have shown their beneficial therapeutic effects, with a marked improvement in survival rate observed (Rich et al., 1992). However, this was only apparent in a subset of patients. Subsequently, it was identified that CCB therapy is only an effective treatment in patients who are vasoreactive (the pulmonary vasculature still responds to local mediators via relaxation or contraction) (Sitbon et al., 2005). Only a reported 5-10% of PAH patients exhibit vasoreactivity, and therefore CCBs have limited therapeutic use. Significant adverse events including the increased risk of fatality can also occur as side-effects of CCB administration. This is typically observed in NYHA class IV PAH patients with right ventricular failure, and is a likely consequence of their pronounced negative inotropic effects.

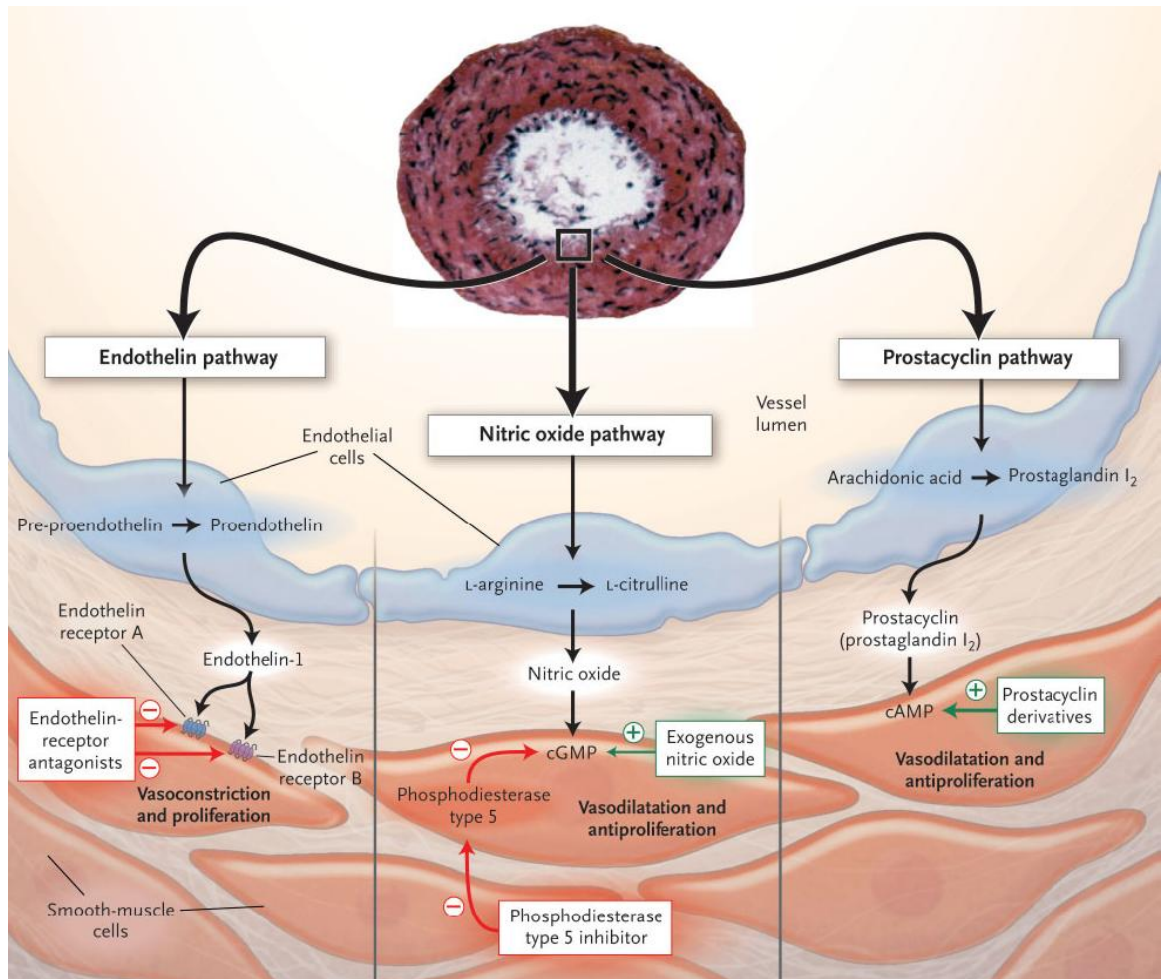


Figure 1.6 Current therapeutic targets in PAH. Current PAH therapies (endothelin receptor antagonists, phosphodiesterase type 5 inhibitors, inhaled nitric oxide and prostacyclin derivatives) act to promote vasodilatation and inhibit proliferation. Adapted from (Humbert et al., 2004).

1.2.2.3 Endothelin Receptor Antagonists

Endothelins are a class of vasoactive peptides which are synthesised and released from both systemic and pulmonary artery endothelial cells. Endothelin-1 (ET-1) is the predominant isoform within the pulmonary circulation, and circulating levels are reported to be increased in at least two different forms of PAH (Giaid et al., 1993; Galie et al., 2004). ET-1 is a potent vasoconstrictor in pulmonary arteries and also stimulates proliferation in PASMCs (McCulloch et al., 1998). Currently, two endothelin receptor isoforms (ET_A and ET_B) have been identified, both of which are G-coupled protein receptors (GPCRs). Endothelin receptor A (ET_A) is primarily expressed in the PASMCs and mediates both vasoconstriction and smooth muscle cell proliferation following stimulation (Zamora et al., 1993). In comparison, endothelin receptor B (ET_B) is predominantly expressed in the PAECs and to a lesser extent in PASMCs (Hori et al., 1992). In the lung, ET_B stimulation appears to promote pulmonary artery vasodilatation via both NO and PGI₂ mediated release, which would decrease pulmonary vascular tone (Fukuroda et al., 1992). Therefore on this basis, selective ET_A inhibitors would prove most effective for endothelin-based therapy in PAH.

Sitaxsentan and ambrisentan, both which are ET_A selective antagonists, are currently under clinical investigation for their potential use in PAH (Benza et al., 2007; Benza et al., 2008; Galie et al., 2008; Galie et al., 2005). To date, the non-selective endothelin receptor antagonist bosentan is the only FDA-approved drug for treatment in its class (Sitbon et al., 2003; Channick et al., 2001; Channick et al., 2001). Clinical trials have reported an improvement in pulmonary haemodynamics, exercise capacity and functional class following its use. Bosentan is generally well-tolerated, but hepatic toxicity and a prolonged time period (~12 weeks) from the start of treatment to clinical improvement are the major disadvantages to this therapy.

1.2.2.4 Phosphodiesterase Type 5 Inhibitors

NO released from PAECs acts paracrinally on the underlying PASMCs to activate the NO/cGMP pathway, resulting in increased levels of the second messenger cyclic guanosine monophosphate (cGMP). Activation of this pathway results in cGMP-mediated protein kinase G (PKG) activation, decreased $[Ca^{2+}]_i$ and vasodilatation. Phosphodiesterases (PDEs) are a class of enzymes which mediate the hydrolysis of cGMP. Phosphodiesterase-5 (PDE-5) is the most abundantly expressed PDE-isoform within the lung, and its activity and expression is also reported to be further increased in PAH (Black et al., 2001). The highly selective PDE-5 inhibitor sildenafil acts to inhibit the hydrolysis of cGMP, therefore prolonging its half-life. As a consequence, this leads to improved vasodilatation. PDE-5 inhibition is reported to inhibit PASMC proliferation (Wharton et al., 2005) and attenuate hypoxia-induced PAH (Zhao et al., 2001). Indeed, improvements in both NYHA functional class and exercise capacity have been reported in PAH patients when administered sildenafil treatment (Galie et al., 2005). Although randomized clinical trials remain to be carried out, PDE-5 inhibitors have thus far proven to be an effective PAH treatment. However, minor side effects are reported (headache, indigestion, muscle aches) and in rare cases ventricular arrhythmia, stroke and hearing loss have also been described.

1.2.2.5 Combination Therapy

It is generally considered that the simultaneous targeting of multiple pathways is the most effective treatment strategy in PAH (Benza et al., 2007). This is achieved via adjunctive or combinational therapy. Multiple clinical trials involving the use of multiple treatments have been described, and results appear promising with improvements in both haemodynamics and exercise capacity being reported (Benza et al., 2008).

1.2.3 Future Perspectives in the Treatment of PAH

Although recent advances in PAH therapy have led to significant improvements in survival rate, prognosis still remains relatively poor in patients. A 15% mortality rate is still reported at 2 years even in those undergoing advanced PAH therapy. For this reason, an improvement in current therapies and the discovery of novel treatments is urgently required. This has led to the research-led discovery of multiple novel drugs which may be beneficial for the treatment of PAH.

1.2.3.1 Tyrosine Kinase Inhibitors

Platelet-derived growth factor (PDGF) signalling is one potential target in the treatment of PAH (Grimminger and Schermuly, 2010). The family of PDGF ligands, which exist as PDGF A-D and form homodimers or heterodimers, bind to and activate PDGF receptors (PDGFRs). To date, two PDGFR isoforms have been identified, and are termed PDGFR- α and PDGFR- β . The stimulation of PDGFR- α and PDGFR- β activates multiple signal transduction pathways, resulting in the phosphorylation of various mitogen-activating protein kinases (MAPKs) including ERK and P38. As a consequence, these undergo nuclear translocation and regulate expression of multiple immediate early-response target genes (e.g. c-fos). These genes directly regulate proliferation, migration, differentiation and apoptosis, all of which are essential cellular components in pulmonary vascular remodelling. Indeed, PDGF stimulation of PASMCs results in increased proliferation (Yu et al., 2003). *In vivo*, the PDGF receptor inhibitor STI571 (Imatinib) reverses established disease in at least two experimental models of PAH (Schermuly et al., 2005). In human PAH, PDGF is also important (Perros et al., 2008) and several clinical studies have demonstrated the beneficial effects of Imatinib in the treatment of PAH (Ghofrani et al., 2005). Imatinib has been recently investigated in a phase II clinical trial (Ghofrani et al., 2010), which demonstrated that NYHA functional class III-IV showed a marked

improvement following treatment highlighting its potential therapeutic benefits in severe PAH.

1.2.3.2 Statin Therapy

Another novel approach in the treatment of PAH is statin therapy. Statins act to reduce isoprenoid synthesis via HMG-CoA reductase inhibition (Goldstein and Brown, 1990). Cholesterol is the most widely recognised isoprenoid. Statins are involved in the post-translational modification of rho and ras GTPases, and their use have been reported to decrease reactive-oxygen species (ROS) generation, inflammation and proliferation. This may be mediated in part via the upregulation of endothelial nitric oxide synthase (eNOS) (Laufs et al., 1998). Experimentally, simvastatin treatment successfully prevents (Nishimura et al., 2002) and reverses (Nishimura et al., 2003) monocrotaline-induced PAH. Similar results have also been observed in hypoxia-induced PAH (Girgis et al., 2003; Girgis et al., 2007). The inhibition of rho-kinase appears important to this (Girgis et al., 2007). In human PAH, a moderate improvement is observed in patients prescribed simvastatin (Wilkins et al., 2010). However, this effect appears transient and lasts less than 12 months. An improvement in drug design and/or drug delivery may result in a more sustained beneficial effect for this therapy.

In addition to PDGF inhibition and statin therapy, a number of potentially beneficial PAH treatments are also under investigation. In combination with current PAH therapies, these may be effective in the treatment of PAH.

1.2.4 Pathobiology of PAH

PAH is a disease with a multifactorial pathobiology. Vasoconstriction, thrombosis and vascular remodelling all contribute to increased pulmonary vascular resistance observed in

PAH (Tuder et al., 2009). Within the vasculature, increased vasoconstriction is recognized as the initiating factor which promotes disease progression (Mandegar et al., 2004). This sustained elevation in vasoconstriction consequently results in an elevation of pulmonary vascular resistance. If this persists, the activation of multiple stress-related pathways occur within pulmonary vascular cells (endothelial cell, smooth muscle cell, fibroblast), resulting in vascular remodelling. Currently, pulmonary vascular remodelling is an irreversible component of PAH, and is considered the hallmark of disease pathogenesis (Hassoun et al., 2009). As a consequence of this, the pressure-intolerant right ventricle is subjected to increased after-load and subsequently right ventricular hypertrophy. Although initially compensatory, this eventually leads to right ventricular failure, and this is the primary cause of mortality in PAH patients (Klepetko et al., 2004). The identification and pharmacological targeting of signalling pathways which promote pulmonary vascular remodelling is considered the best treatment approach in the regression of PAH. Currently, several aberrant signalling pathways have been identified, which are stimulated by their respective pathway mediators. These include serotonin, endothelin-1, prostacyclin, nitric oxide, angiotensin-1, cytokines, chemokines and TGF- β .

1.2.4.1 Vasoconstriction

Excessive vasoconstriction is considered an essential initiating factor in the development of PAH (Mandegar et al., 2004). If sustained, this leads to endothelial cell dysfunction and the impaired production of vasodilators such as nitric oxide and prostacyclin. This in combination with the increased synthesis of several vasoconstrictors (e.g. serotonin, endothelin-1) results in a marked elevation of pulmonary vascular resistance. This sustained elevation of pulmonary arterial pressure is considered the 'pre-cursor' resulting in pulmonary vascular remodelling.

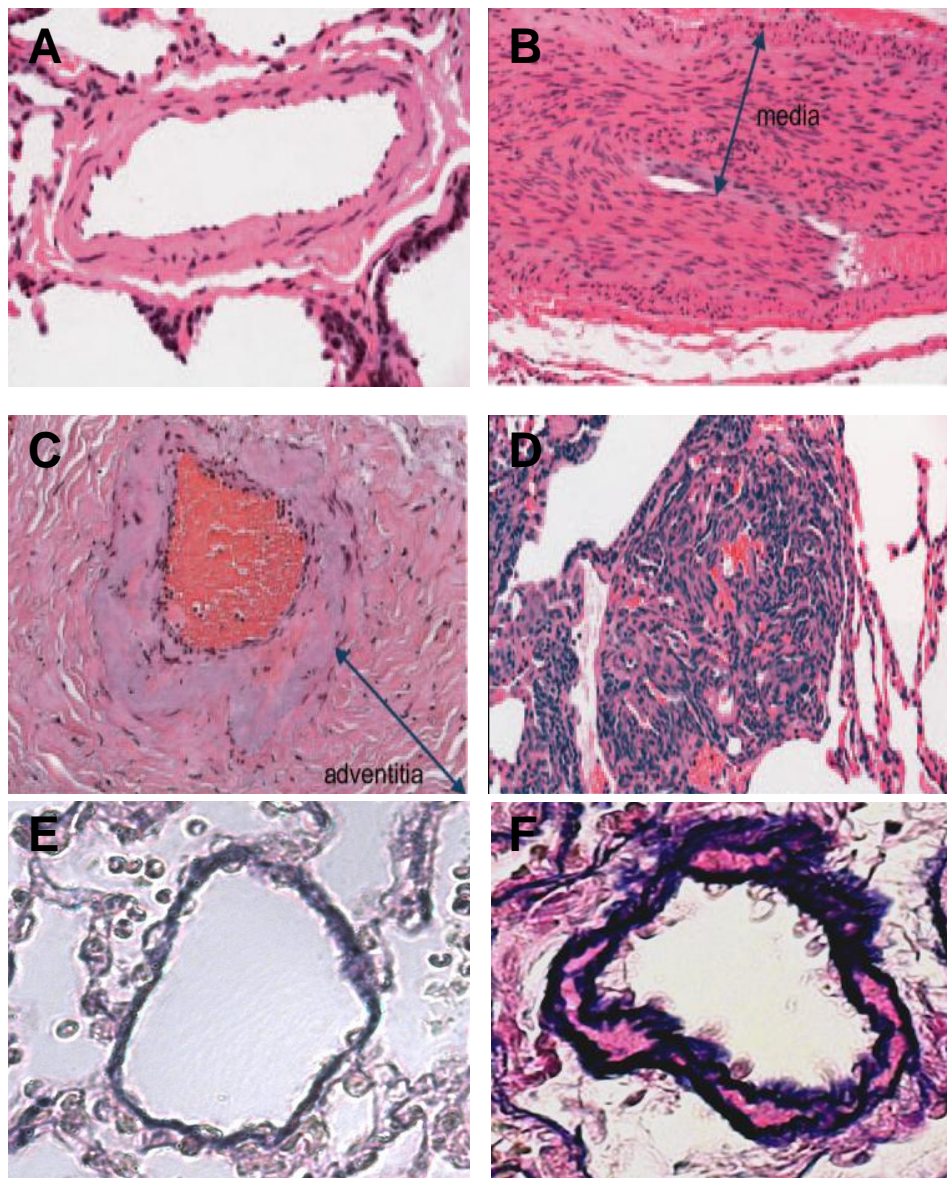


Figure 1.7 Histopathological changes associated with human and experimental PAH.

Top Left, A: A normal human pulmonary artery. *Top Right, B:* Smooth muscle hypertrophy leading to medial hyperplasia typically observed in mild/moderate human PAH. *Middle Left, C:* Adventitial fibrosis typically observed in moderate human PAH. *Middle Right, D:* Plexiform lesion characterised by lumen obliteration observed in severe/end-stage human PAH. *Bottom Left, E:* Normal mouse pulmonary artery, *Bottom Right, F:* Medial hypertrophy observed in a mouse pulmonary artery following exposure to chronic hypoxia, note the failure to recapitulate plexiform lesion formation. A-D adapted from (Cool et al., 2005).

1.2.4.2 Pulmonary Vascular Remodelling

PAH is characterised by intimal thickening of the pulmonary vascular wall, resulting in the impairment of blood flow through the lumen. This disease component arises from a process termed pulmonary vascular remodelling, and is considered the hallmark in PAH pathogenesis (Tuder et al., 2009). PAH is associated with increased proliferation combined with suppression of apoptosis, and this is the primary cause of pulmonary vascular remodelling. Each of the three predominating cell types (endothelial, smooth muscle, fibroblast) contributes to this. Typically, a transverse section of a remodelled pulmonary artery reveals neointimal thickening and fibrosis, smooth muscle hypertrophy arising from PASMC hyperplasia and adventitial thickening and/or fibrosis (Figure 1.7).

There are several histopathological subtypes of pulmonary vascular remodelling which exist in human PAH (Cool et al., 2005). Smooth muscle hyperplasia and thickening is widely apparent and typically observed in mild/early-stage PAH. Patients with moderate/mid-stage PAH also exhibit marked adventitial fibrosis in addition to increased medial thickness (Humbert et al., 2004). In severe/end-stage PAH, plexiform lesions are usually present and represent the most severe subtype of pulmonary vascular remodelling. These are most commonly observed at bifurcation points in smaller resistance arteries (<200µm external diameter) and exist as an accumulation of disarranged proliferative endothelial cells which result in pronounced neointimal formation and marked intimal thickening (Cool et al., 2005). The consequence of plexiform lesion development is complete obliteration of the artery, resulting in the severe impairment and cessation of blood flow through the lumen (Tuder et al., 1994). The pathological process leading to their formation remains an area of intense investigation. Neoplasia likely contributes to plexiform lesion formation. For example, loss of the tumour suppressor gene peroxisome proliferator-activated receptor- γ (PPAR- γ), is reported in plexiform lesions of PAH patients (Ameshima et al., 2003). PPAR- γ is antiproliferative and anti-inflammatory

(Jiang et al., 1998) and has been previously shown to mediate an important protective role in experimental PAH (Hansmann et al., 2008). Restoring function of such apoptotic pathways would result in inhibition of progressive pulmonary vascular remodelling, and considered the most effective therapeutic strategy in PAH.

Established models of PAH (e.g. hypoxia, monocrotaline) fail to recapitulate severe plexiform lesion histopathology. Recently, several experimental models which exhibit a similar lung pathobiology have been recently generated for study into their progressive pathobiology. These include the S100A4/mts1 over-expressing murine model (Greenway et al., 2004; Spiekerkoetter et al., 2008), schistosomiasis murine model (Crosby et al., 2010), and vascular endothelial growth factor (VEGF) antagonist Sugeng 5416 + hypoxia rat model (Abe et al., 2010).

The exact stimulus leading to abnormal endothelial cell proliferation remains unknown but may include shear stress, hypoxia, drugs/toxins and/or genetic susceptibility (Humbert et al., 2004). Initial endothelial apoptosis is considered important to this, which results in both a vasoconstrictor/vasodilator imbalance whilst also exposing the PASMCs to circulating mitogenic factors. For example, BMPR-II signalling promotes survival in PAECs (Teichert-Kuliszewska et al., 2006). Therefore, an overall reduction in this signalling pathway (i.e. as observed in BMPR-II loss of function mutation carriers) may instead promote endothelial cell apoptosis (Teichert-Kuliszewska et al., 2006). As a consequence, loss of functional endothelium may promote the stimulation of PASMCs via their exposure to circulating mitogenic factors.

One feature common to PAH is the distal progression of smooth muscle into the normally non-muscular small peripheral pulmonary arteries. This results in pronounced muscularisation of the terminal portion of the pulmonary arterial circulation (MacLean et

al., 2000). Neointimal formation is also a common feature in severe PAH, as discussed previously. The neointima is composed of a pronounced extracellular matrix surrounded with a layer of myofibroblasts, and is situated between the endothelium and internal elastic laminae. Regardless of the histopathologic subtype, pulmonary vascular remodelling always results in increased obstruction of the lumen and the impairment of blood flow.

1.2.5 Genetic Basis of Pulmonary Arterial Hypertension

1.2.5.1 Bone Morphogenetic Protein Type 2 Receptor

PAH is a disease with underlying genetic susceptibility. That is, those individuals who inherit specific genotypes are more likely to develop PAH. This is termed heritable PAH (HPAH). The inheritance pattern for HPAH is autosomal dominant (Thompson and McRae, 1970). Therefore, each child of an affected individual is at a 50% risk of inheriting the mutant allele. Both genetic anticipation and female bias exists in HPAH (female 3:1 male). Therefore, it is predicted that younger females are the risk category most susceptible to the development of HPAH. Initially, the first identified disease locus was mapped to chromosome 2q31-32, and was termed *PPH1* (Morse et al., 1998). Subsequently, this gene was identified as the bone-morphogenetic protein receptor-2 (BMPR-II) (Lane et al., 2000). BMPR-II mutations are widely recognized as the most common cause of HPAH, with mutation carriers up to ~100,000 times more likely to develop HPAH. These individuals are also accountable for up to 80% of HPAH cases (Morrell, 2010). Despite this, penetrance for the gene remains relatively low as only ~20% of mutation carriers actually develop HPAH (Newman et al., 2004). Therefore, it is assumed that other genetic and/or modifying risk factors contribute to this disease pathogenesis.

BMPR-II mediated dysfunction of transforming growth factor β (TGF- β) signalling is the pre-dominant genetic cause of PAH (Figure 1.8). However in addition to BMPR-II mutations, alternative members of the TGF- β family may also render those affected individuals susceptible to the development of PAH. Activin receptor-like kinase 1 (ALK-1) receptor mutations are associated with hereditary hemorrhagic telangiectasia (HHT), but may also render those individuals susceptible to the development of PAH (Trembath et al., 2001; Harrison et al., 2003). This mutation, which results in defective SMAD signalling, leads to both an earlier-age of PAH onset and poorer prognosis in carriers when compared to those without the mutation.

1.2.5.2 Serotonin Transporter

Another genetic risk factor is the serotonin transporter (SERT). SERT is encoded by the solute carrier family 6 member 4 (SLC6A4) gene located on chromosome 17 position 17q11.2. The SERT promoter region (*SERTPR*) contains a polymorphism which exists as short (S) or long (L) repeats in the region, the S allele has 14 repeats of a sequence, whilst the L allele has 16 repeats. The S allele results in reduced SLC6A4 transcription and therefore reduced SERT protein expression. SERT is an integral membrane protein that facilitates the transport of serotonin across the membrane in a Na⁺ dependant manner. SERT is implicated in the pathogenesis of both experimental and human PAH. Mice over-expressing the human SERT gene construct (SERT⁺ mice) develop PAH and severe hypoxia-induced PAH (MacLean et al., 2004). Similarly, mice with targeted SERT over-expression in the PSMCs develop PAH (Guignabert et al., 2006), whilst mice devoid of the SERT gene are protected against the development of hypoxia-induced PAH (Eddahibi et al., 2000). SERT expression is also increased in PSMCs derived from idiopathic PAH (IPAH) patients and these proliferate to a greater extent than those from controls following serotonin stimulation, which is dependent on SERT activity (Eddahibi et al., 2006).

Indeed, the LL allele *SERTPR* polymorphism, which leads to increased activity/expression of SERT, has been associated with the increased development of PAH in a small cohort of patients (Eddahibi et al., 2001). Subsequent studies in larger patient studies have failed to support these findings, although patients with the SERT polymorphism may present at an earlier age than those without (Willers et al., 2006).

1.2.5.3 *Transient Receptor Potential Channel 6*

Recently, a single-nucleotide polymorphism (SNP) in the transient receptor potential cation channel, subfamily C, member 6 (TRPC6) has been identified which may predispose those individuals to the development of PAH (Yu et al., 2009). Increased frequency of the -254 (C→G) SNP in the TRPC6 gene is associated with increased incidence of PAH. It is assumed that this SNP leads to both increased transcription and function of TRPC6, and as a consequence defective cytosolic Ca²⁺ handling in the PSMCs, leading to increased vasoconstriction and proliferation.

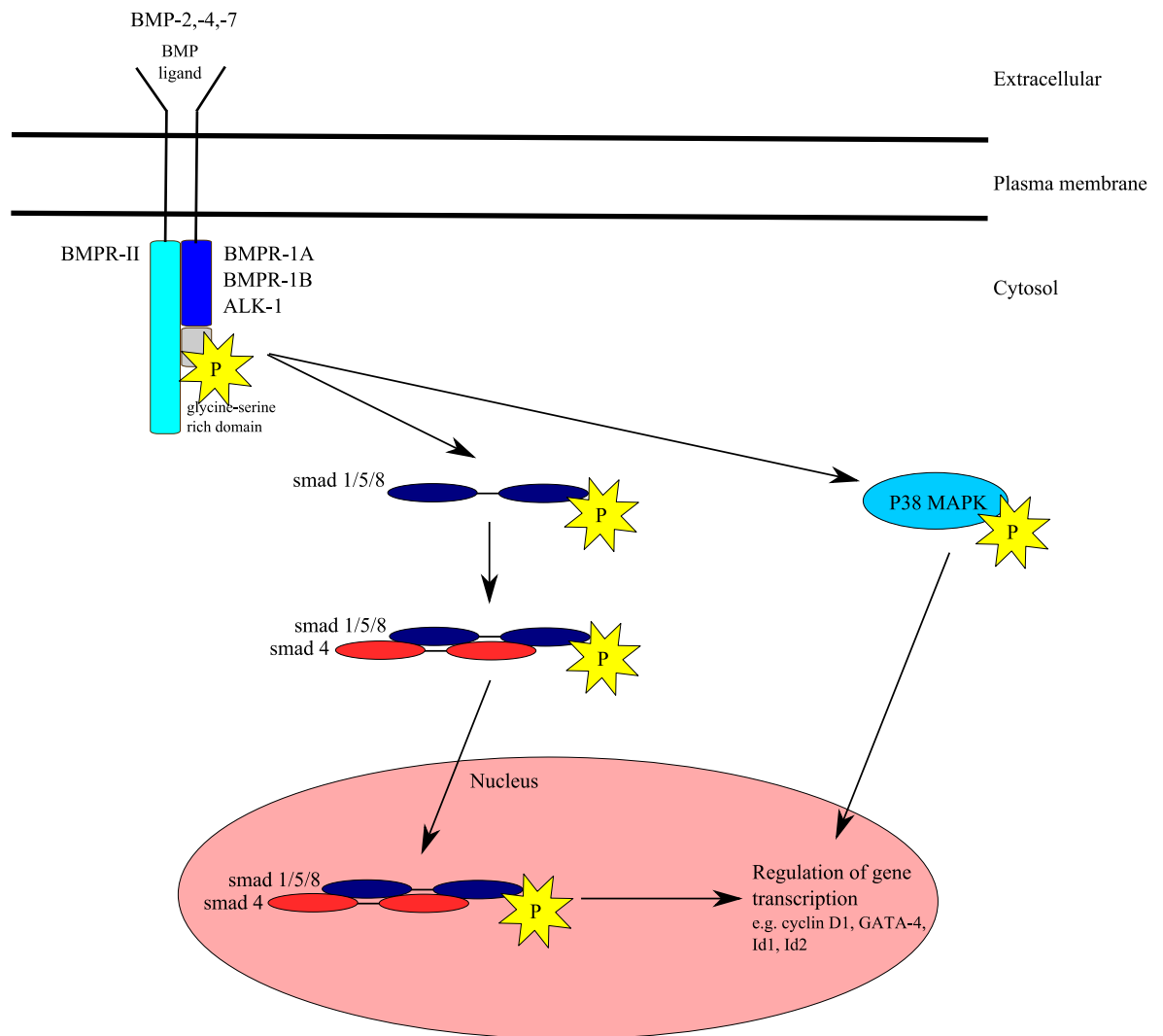


Figure 1.8 Bone morphogenetic protein receptor-2 signalling in PAH. Following ligand binding (BMP-2,-4,-7), BMPR-II heterodimerizes with a type-I receptor (BMPR1A, 1B, ALK-1) and phosphorylates the type-I glycine-serine rich tail domain. Heterodimerization initiates nuclear translocation of PSmad1/5/8 via co-Smad 4, or alternatively initiates smad independent P38MAPK signalling. As a consequence, these pathways regulate transcription of several target genes (e.g cyclin D1, GATA-4, Id1, Id2) which regulate transcription and proliferation.

1.3 Serotonin Biosynthesis and Metabolism

Serotonin (5-hydroxytryptamine; 5-HT) was first described following its isolation from serum (Rapport et al., 1948). Physiologically, serotonin circulates at very low concentrations (<1nmol/L) and is maintained via SERT-mediated uptake into platelets, which act as a store for up to 99% of total peripheral serotonin. Over 80% of peripheral serotonin synthesis occurs in the intestinal enterochromaffin cells, with the remaining 20% synthesised in other cell types including serotonergic neurons and PAECs (Hoyer et al., 2002). Serotonin controls many physiological functions in the cardiovascular system, including heart rate and vascular tone (Berger et al., 2009). In addition to this, serotonin regulates the function of multiple other organs including the brain (e.g. the control of respiration, memory, nociception) and intestine (Hoyer et al., 2002).

Serotonin is synthesised via the hydroxylation and subsequent decarboxylation of its biochemical pre-cursor tryptophan (Figure 1.9). This two-step biosynthetic pathway is catalysed by tryptophan hydroxylase (TPH) and the aromatic L-amino acid decarboxylase, respectively. TPH is the rate-limiting enzyme involved in serotonin synthesis, and specifically catalyses the hydroxylation of tryptophan via the addition of a hydroxyl group (–OH) to the 5 position, resulting in the formation of 5-hydroxytryptophan (5-HTP). Currently, two genes have been identified which encode for TPH, and are termed *tph1* and *tph2* (Walther et al., 2003). These *tph* isoforms share 71% sequence homology. Although both are functionally identical, TPH1 mediates peripheral serotonin synthesis whereas TPH2 mediates central serotonin synthesis.

Serotonin inactivation occurs via its rapid metabolism in the liver and lung (Hart and Block, 1989). Monoamine oxidase-A (MAO-A) initiates this metabolism via oxidative deamination (removal of –NH₂ group) of the amino chain. The product, 5-hydroxyindol-acetaldehyde, is subsequently oxidised to 5-hydroxyindole acetic acid (5-HIAA) by

aldehyde dehydrogenase. 5-HTIAA is the primary serotonin metabolite produced and is excreted in the urine following conjugation.

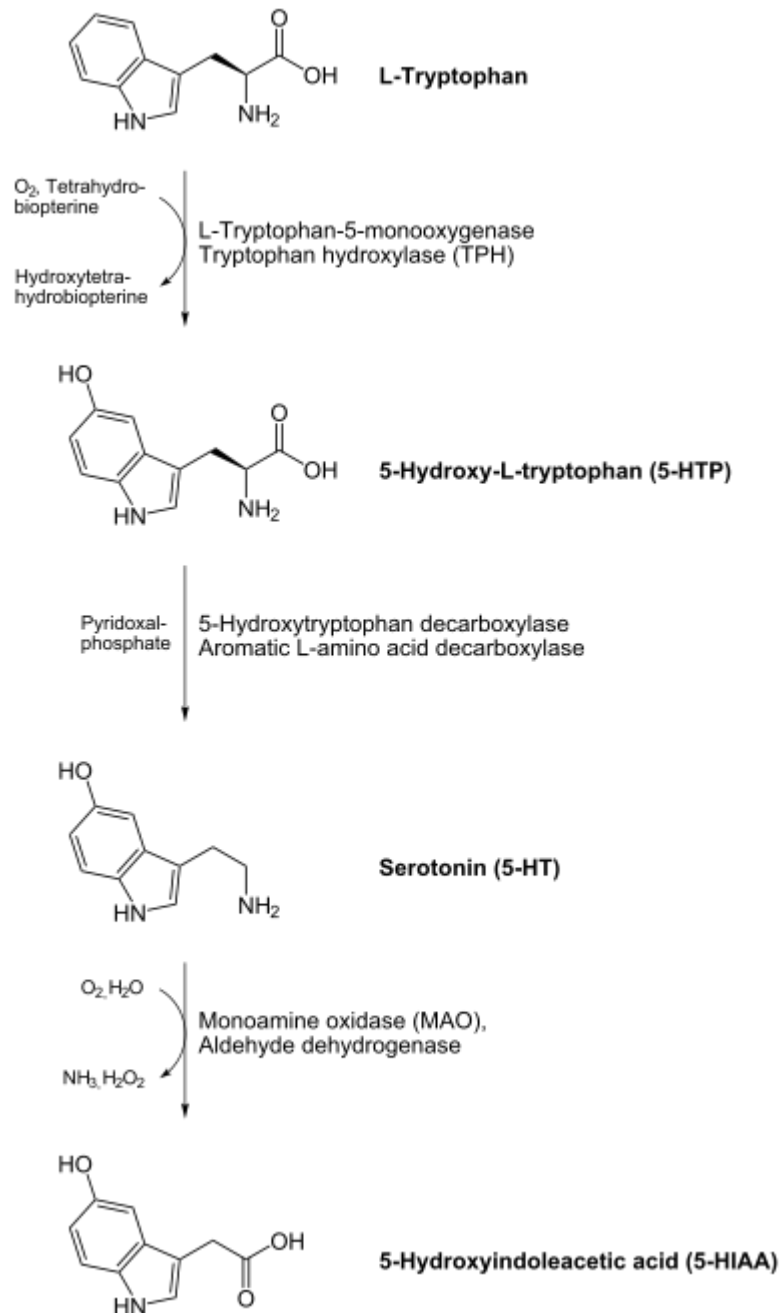


Figure 1.9 Serotonin biosynthesis and metabolism. The amino acid tryptophan is converted to 5-hydroxy-L-tryptophan/5-HTP via tryptophan hydroxylase. This is the rate-limiting enzyme in serotonin synthesis. Subsequently, non-specific decarboxylase enzymes convert 5-HTP to serotonin. Serotonin metabolism to 5-hydroxyindoleacetic acid occurs via both monoamine oxidase and aldehyde dehydrogenase. Adapted from (Druce et al., 2009).

1.4 Serotonin Signalling

A wealth of evidence exists which suggests that the serotonin system facilitates the development of human and experimental PAH (MacLean and Dempsie, 2010). Elevated levels of circulating serotonin have also been reported in PAH (Herve et al., 1995). The exogenous administration of serotonin promotes the development of PAH in rats and also uncovers a PAH phenotype in *BMPR-II*^{-/-} mice (Long et al., 2006). Within the pulmonary circulation, serotonin signalling is mediated via three distinct pathway components. These are TPH1, SERT and the 5-HT receptors. In addition, stimulation of SERT and/or the 5-HT receptors initiates multiple downstream signalling pathways which are essential to serotonin signalling.

1.4.1 Tryptophan Hydroxylase

Tryptophan hydroxylase (TPH) catalyses the rate-limiting step involved in serotonin synthesis. Currently, two TPH isoforms have been described (Walther et al., 2003), and are termed TPH1 and TPH2. These are distinguishable by sequence heterology and their location of expression. TPH2 is exclusively expressed in the central nervous system, and completely absent in the periphery. In contrast, TPH1 mediates peripheral serotonin synthesis and is predominantly expressed in the intestinal enterochromaffin, and to a lesser extent in PAECs. Although the enterochromaffin cells synthesise up to 80% of total peripheral serotonin, local serotonin synthesis within the PAECs is also considered important. This local synthesis is thought to facilitate a 'serotonin micro-environment' which promotes the vasoconstrictive and mitogenic effects of serotonin on the underlying PSMCs. Indeed, this appears to play a role in the pathogenesis of PAH as TPH1 expression is increased in both the lungs and PAECs derived from IPAH patients (Eddahibi et al., 2006).

TPH1 expression is influenced by a number of physical, environmental and humoral factors. As a consequence, this affects serotonin synthesis. For example, TPH1 expression is increased in pulmonary neuroendocrine cells following stimulation by mechanical stretch (Pan et al., 2006). Also, stimulation of the Tie-2 receptor via the growth factor angiopoietin-1 (Ang-1) stimulates serotonin synthesis in PAECs via increased TPH1 expression (Dewachter et al., 2006).

Previously, we have made unpublished observations that TPH1 is abundantly expressed in the pulmonary arteries of mice following exposure to chronic hypoxia. Specifically, TPH1 appears to be localised to the pulmonary endothelium. Indeed, mice deficient of the *tph1* gene (*tph1*^{-/-} mice) do not develop hypoxia-induced PAH (Morecroft et al., 2007), suggesting the importance of peripheral serotonin synthesis in its development.

1.4.2 5-HT Receptors

There are a total of 14 structurally distinct 5-HT receptor types (Figure 1.10). These are divided into seven classes (5-HT₁₋₇), defined by their structure and downstream coupling to signal transduction pathways (Alexander et al., 2006). In addition, several isoforms can exist for the same 5-HT receptor subtype (e.g. 5-HT₁ receptors comprise the 5-HT_{1A}, 5-HT_{1B} and 5-HT_{1D}) as a result of alternative splicing and RNA editing. All of the 5-HT receptors exist as membrane-bound G protein coupled receptors (GPCRs), with the exception of the 5-HT₃ receptor which operates as a ligand-gated ion channel (Hoyer et al., 2002).

The 5-HT GPCRs all share similar structural homology. They contain an extracellular N terminus domain, seven transmembrane α -helices and an intracellular C terminal domain (Figure 1.11). Following ligand binding at the extracellular portion of the receptor, this

initiates activation of the associated (or ‘coupled’) G-protein. G-proteins exist as heterotrimeric structures composed of α , β and γ subunits. These are typically classified by their α -subunit type, of which four exist; G_s , G_i , G_q and $G_{12/13}$ (Figure 1.12). Each respective G-protein initiates its own unique downstream signalling transduction pathways, and therefore the cellular function of a GPCR will be ultimately determined by the G-protein it is coupled with. For example, the G_s subunit increases adenylyl cyclase (AC) whereas the G_i subunit inhibits AC. Also, the G_q and $G_{12/13}$ subunits activate phospholipase C (PLC) and small G-proteins, respectively. In addition, five β subunits and twelve γ subunits have also been described (Milligan and Kostenis, 2006). G-proteins are typically coupled to their respective GPCR via a direct interaction with the second or third intracellular loop (Hoyer et al., 2002). Specifically, the binding of a ligand to its receptor initiates a conformational change which promotes the exchange of guanosine 5'-diphosphate (GDP) for guanosine 5'-triphosphate (GTP) at the guanosine nucleotide binding site within the G_α subunit (Hamm, 1998). In turn, G-protein activation results in dissociation of the G_α subunit from the $G_{\beta\gamma}$ complex, and both entities activate downstream signalling pathways.

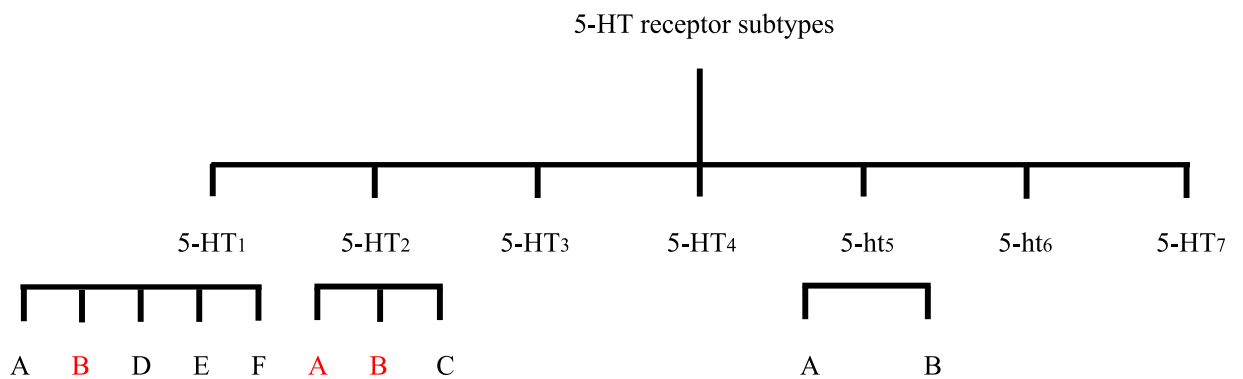


Figure 1.10 Classification of the 14 structurally distinct 5-HT receptor subtypes. Those highlighted in red have been previously shown to mediate serotonin effects in PAH. 5-HT receptor subtypes denoted in lower case indicate that their physiological role remain to be described

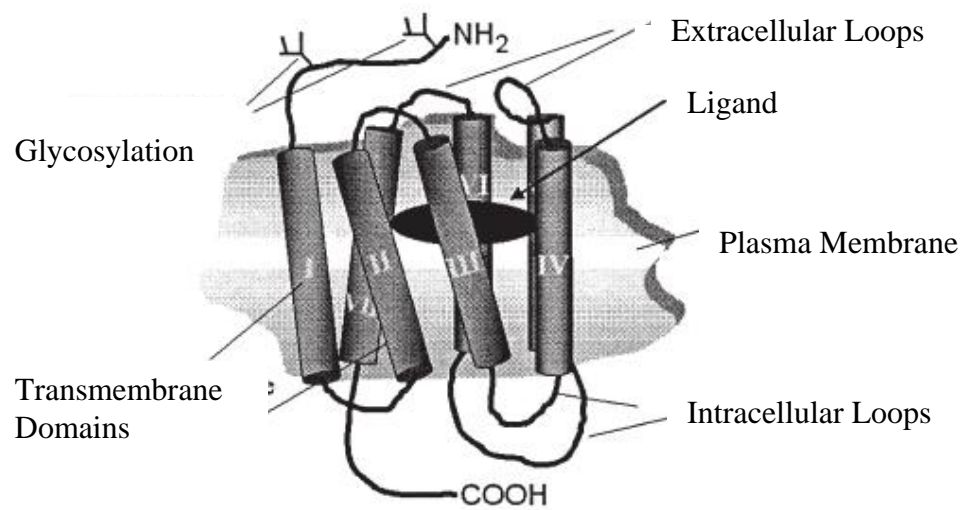


Figure 1.11 Representative structure of a G-protein coupled receptor (GPCR).

GPCRs typically exist of an extracellular N-terminus domain, seven transmembrane alpha-helices and an intracellular C-terminus domain. The ligand binds directly to the GPCR, and glycosylation of the N-terminus domain is involved in cell trafficking.

Receptor	Type	Mechanism
5-HT ₁	G _i /G _o	Decreased cAMP
5-HT ₂	G _q /G ₁₁	Increased IP3 and DAG
5-HT ₃	Ligand-gated Na ⁺ and K ⁺ cation channel.	Depolarisation
5-HT ₄	G _s	Increased cAMP
5-HT ₅	G _i /G _o	Decreased cAMP
5-HT ₆	G _s	Increased cAMP
5-HT ₇	G _s	Increased cAMP

Figure 1.12 5-HT receptor subtype signalling pathways. All 5-HT receptor subtypes act via an intracellular second messenger, with the exception of 5-HT₃, which is a ligand-gated ion channel.

1.4.2.1 5-HT₁ Receptor Subtypes

The 5-HT₁ class of receptors comprise five subtypes (5-HT_{1A}, 5-HT_{1B}, 5-HT_{1D}, 5-ht_{1E} and 5-ht_{1F}), and these share 40-63% sequence homology. Both the 5-ht_{1E} and 5-ht_{1F} receptors are represented in lower case to denote that their physiological role remains to be determined. All 5-HT₁ receptors are coupled to the G_i protein. Therefore, stimulation of the receptor and G-protein activation results in the inhibition of AC and cAMP production. All 5-HT₁ receptor subtypes are expressed in both the CNS and periphery. Specifically, it is the 5-HT_{1B} and 5-HT_{1D} receptors which predominantly mediate serotonin effects in the cardiovascular system. Although 5-HT_{1D} receptor expression is relatively low in comparison to the 5-HT_{1B} receptor, it has been shown to evoke serotonin release from cardiomyocytes in humans, and is also important in inflammation (Hoyer et al., 2002). Indeed, 5-HT_{1D} receptor antagonists are currently prescribed in the treatment of migraine (Cutrer et al., 1999).

The 5-HT_{1B} receptors are expressed in nerve terminals where they act as auto-receptors in the release of several neurotransmitters including noradrenaline and acetylcholine (Hoyer et al., 2002). In the cardiovascular system, it mediates serotonin-induced vasoconstriction in both cerebral (van den Broek et al., 2002) and pulmonary (Morecroft et al., 1999) arteries. With respect to the pulmonary circulation in humans, the 5-HT_{1B} subtype is the primary 5-HT receptor which mediates receptor-driven serotonin signalling. For example, it is implicated in both serotonin-induced pulmonary arterial vasoconstriction and proliferation, both of which are hallmarks of PAH. Indeed, up-regulation of the 5-HT_{1B} receptor has already been described in experimental PAH (Rondelet et al., 2003). A functional role for the 5-HT_{1B} receptor was initially described following the observation that sumatriptan (5-HT_{1B/1D} receptor agonist) stimulated contraction of human small muscular pulmonary arteries (MacLean et al., 1996). In support of this, serotonin-induced vasoconstriction was also successfully inhibited with the 5-HT_{1B/1D} receptor antagonist

GR55562. Subsequently, the role of the 5-HT_{1B} receptor was confirmed by the observation that the selective 5-HT_{1B} receptor antagonist SB224289 abolished sumatriptan-mediated vasoconstriction whereas BRL15572 (a selective 5-HT_{1D} receptor antagonist) had no effect (Morecroft et al., 1999). The 5-HT_{1B} receptor is also involved in the contraction of non-human pulmonary arteries. Although, sumatriptan does not stimulate contraction of bovine pulmonary arteries in basal conditions, it promotes vasoconstriction in the presence of U44619 tone (MacLean et al., 1994). This is an example of pharmacological synergism. Additional factors often described in PAH (e.g. decreased NOS expression leading to reduced NO bioavailability) have also been found to potentiate 5-HT_{1B} receptor-mediated contraction (Dempsie and MacLean, 2008). In non-human pulmonary arteries, it is typically assumed that serotonin-induced vasoconstriction is via the 5-HT_{2A} receptor in the absence of tone, whilst via the 5-HT_{1B} receptor in the presence of tone.

Animal models of PAH have also described a role for the 5-HT_{1B} receptor in disease pathogenesis. In rats, the 5-HT_{1B} receptor antagonist GR127935 attenuates the severity of hypoxia-induced PAH (Marcos et al., 2003). In addition, 5-HT_{1B} receptor knockout mice exhibit a reduction in RVSP and pulmonary vascular remodelling following exposure to hypoxia (Keegan et al., 2001). Indeed, increased 5-HT_{1B} receptor expression is also reported in an overcirculation-induced model of PAH in piglets (Rondelet et al., 2003). Fawn-hooded rats, which exhibit altered serotonergic function and develop exaggerated hypoxia-induced PAH, also show increased 5-HT_{1B} receptor mediated contraction in the pulmonary arteries (Morecroft et al., 2005).

1.4.2.2 5-HT₂ Receptor Subtypes

Serotonin exerts multiple physiological effects via the activation of multiple 5-HT receptor subtypes. In the cardiovascular system, the 5-HT₁ and 5-HT₂ receptor subtypes mediate

most of the serotonin effects (Hoyer et al., 2002). The 5-HT₂ subtypes include the 5-HT_{2A}, 5-HT_{2B} and 5-HT_{2C} receptors, which share 46-50% of overall sequence homology. The majority of these receptors are coupled to the G_q protein, which signals via the activation of PLC to form inositol 1,4,5 trisphosphate (IP3) and 1,2-diacylglycerol (DAG). In turn, these second messengers increase [Ca²⁺]_i. The 5-HT_{2A} receptor is widely expressed in both the central nervous system and periphery, and mediates many physiological functions. In the cardiovascular system, this receptor promotes vasoconstriction in both the systemic and pulmonary arteries. Indeed, the 5-HT_{2A} receptor antagonist ketanserin is a proven therapeutic treatment for systemic hypertension in humans. In contrast, its use in the treatment of PAH is much less effective (Domenighetti et al., 1997). In one study involving a cohort of PAH patients, ketanserin had no effect on pulmonary vascular resistance until extremely high doses were administered, and this effect was minimal compared to those observed on systemic vascular resistance. Therefore, expression of the 5-HT_{2A} receptor in both the systemic and pulmonary arteries has limited its effectiveness as a therapeutic target in the treatment of PAH. Multiple serotonin effects mediated via the 5-HT_{2A} receptor have also been described in animal models of PAH. For example, serotonin promotes vasoconstriction in mouse, rat, dog and cow pulmonary arteries predominantly via the 5-HT_{2A} receptors (MacLean and Dempsie, 2010). This is in contrast to human pulmonary arteries, where both the 5-HT_{2A} and 5-HT_{1B} receptors mediate serotonin-induced vasoconstriction. In isolated rat PSMCs, the 5-HT_{2A} receptor has also been shown to directly inhibit K_v channels, which results in decreased K⁺ cellular efflux and depolarisation (Varghese et al., 2006).

The 5-HT_{2A} receptor is also involved in the proliferation of pulmonary vascular cells. It has been shown to mediate the exaggerated serotonin-induced proliferative response of PAFs in chronic hypoxia (Welsh et al., 2004). In bovine PSMCs, this receptor may also stimulate serotonin-induced proliferation via the phosphatidylinositol-3-kinase/protein

kinase B (PI3K/PKB) pathway (Liu and Fanburg, 2006). In addition, this subtype promotes platelet aggregation and thrombosis (Nagatomo et al., 2004), which is a common feature in PAH.

The 5-HT_{2B} receptor has also been shown to mediate multiple serotonin effects in the pulmonary vasculature. Nordexfenfluramine, which is an active metabolite of dexfenfluramine and potent 5-HT_{2B} receptor agonist, stimulates the contraction of pulmonary arteries (Ni et al., 2004). This 5-HT_{2B} agonist also activates MAPK signalling in cells expressing the recombinant 5-HT_{2B} receptor (Fitzgerald et al., 2000). This pathway has previously been shown to stimulate the proliferation of both PASMCs (Liu and Fanburg, 2006) and PAFs (Welsh et al., 2001). *In vivo*, the development of hypoxia-induced PAH is completely ablated in 5-HT_{2B} receptor knockout mice, and is also similarly ablated in mice treated with the 5-HT_{2B} receptor antagonist RS-127445 (Launay et al., 2002). In addition, evidence which suggests that the 5-HT_{2B} receptor is involved in the regulation of plasma serotonin levels has also been described in mice (Callebert et al., 2006). The 5-HT_{2B} receptor is also essential in heart development during embryogenesis (Nebigil et al., 2000). It appears to promote the survival of adult cardiomyocytes (Nebigil et al., 2003), which may be a feature of serotonin-induced right ventricular hypertrophy. However its therapeutic target in the treatment of PAH is limited, as loss of 5-HT_{2B} receptor function may actually predispose to the development of dexfenfluramine-induced PAH in humans (Blanpain et al., 2003).

1.4.2.3 Additional 5-HT Receptor Subtypes

In addition to the 5-HT₁ and 5-HT₂ receptors previously discussed, the expression of additional 5-HT receptors has also been described in the pulmonary circulation. mRNA transcripts for the 5-HT_{1A}, 5-HT_{1D}, 5-HT_{3A}, 5-HT_{3B}, 5-HT₄, 5-HT₆ and 5-HT₇ receptors

have been identified in rabbit pulmonary arteries (Molderings et al., 2006), whilst 5-HT_{1B/1D}, 5-HT_{2A}, 5-HT_{2B}, 5-HT₄ and 5-HT₇ receptor transcripts have been found in porcine pulmonary arteries. In the latter, this is an identical receptor expression profile to that observed in human PSMCs with the exception of the 5-HT₄ receptor, which appears to be absent in humans (Ullmer et al., 1995). Multiple physiological functions have been described for the majority of these 5-HT receptor subtypes, however these appear to play a minor role in the receptor-dependent effects of serotonin in the pulmonary circulation. Therefore, it is assumed that the 5-HT_{1B}, 5-HT_{2A} and 5-HT_{2B} receptors mediate receptor driven serotonin signalling in PAH.

1.4.3 5-HT Receptor and Serotonin Transporter Interactions

Functional interactions between the 5-HT_{1B} receptors and SERT have also been described. In the pulmonary circulation, this results in increased vasoconstriction and proliferation. In rat pulmonary arteries, synergy between the inhibitory effects of 5-HT_{1B} receptor antagonism and SERT inhibition on serotonin-induced contraction have been reported (Morecroft et al., 2005). Similar interactions have also been described in mouse pulmonary arteries (Morecroft et al., 2010). Indeed, dual inhibition of both the 5-HT_{1B} receptors and SERT is more effective in preventing hypoxia-induced PAH in mice than inhibition of SERT alone (Morecroft et al., 2010). SERT is considered to mediate serotonin-induced proliferation in cells, however involvement of the 5-HT_{1B} receptor is also considered important. In bovine PSMCs, stimulation of the 5-HT_{1B} receptor results in activation of rho small G protein and its downstream mediator rho-kinase (ROCK), and in turn facilitates the nuclear translocation of SERT-induced phosphorylated ERK1/2 (Liu et al., 2004). This interaction between SERT and the 5-HT_{1B} receptors stimulates proliferation via the transcriptional regulation of multiple proliferative genes including GATA-4 and cyclin D1. In human PSMCs, stimulation of the 5-HT_{1B} receptor promotes

ERK1/2 phosphorylation and proliferation in a RAGE dependent manner (Lawrie et al., 2005). 5-HT_{1B} receptor stimulation results in the phosphorylation of ERK1/2, and via a mechanism involving serotonin metabolism, generated reactive oxygen species (ROS) facilitated nuclear translocation occurs. Inside the nucleus, target genes are activated (e.g. GATA-4) resulting in increased mts1 synthesis and release. As a consequence, Mts1 activates membrane-bound RAGE receptors to stimulate proliferation (Lawrie et al., 2005). Dual blockade of both the 5-HT_{1B} receptors and SERT is also more effective than singular SERT blockade at inhibiting serotonin-induced proliferation in both non-IPAH and IPAH PASMCs (Morecroft et al., 2010). 5-HT_{1B} receptor expression appears confined to the pulmonary circulation and mediates both serotonin-induced vasoconstriction and proliferation. On this evidence, the 5-HT_{1B} receptor is one viable future therapeutic target in the treatment of PAH.

1.4.4 Serotonin Transporter

1.4.4.1 Structure

A single gene encodes for the serotonin transporter (SERT; 5-HTT), which is located on chromosome 17q11.2, and its transcriptional regulation and function is controlled by the repetitive sequence of varying length in the promoter region of the gene (Ramamoorthy et al., 1993). The alleles are composed of either fourteen (short; S) or sixteen (long; L) repeated sequences. The L allele promotes a higher rate of SERT gene transcription than the S allele, and is also associated with increased mRNA expression, protein expression and functional activity (Lesch et al., 1996). The SERT protein is a ~630 amino acid sequence (molecular weight 70kDa) which consists of an intracellular N-terminus, 12 transmembrane spanning domains (6 extracellular and 5 cytoplasmic loops) and an intracellular C-terminus (Figure 1.13).

1.4.4.2 *Function*

SERT expression is reported in multiple cell types across both the central nervous system and cardiovascular system. Specifically, it is abundantly expressed in both the platelets (Talvenheimo and Rudnick, 1980) and PASMCs (Eddahibi et al., 2001), and these cell types have been described in the pathobiology of PAH. SERT operates as a Na⁺-dependant transporter, utilising the Na⁺ concentration gradient to facilitate serotonin transport across the membrane (Torres et al., 2003). It is assumed that serotonin flux only occurs when the transporter simultaneously binds Na⁺, Cl⁻ and serotonin. Specifically, the aspartic acid residue (D98) situated at transmembrane domain 1 (TMD1) is essential for serotonin recognition via charge interactions with the negatively charged serotonin amine group (Nelson, 1998). This interaction induces a conformational change to facilitate the transport of serotonin, in accompaniment with Na⁺ and Cl⁻, across the membrane. The SERT must also bind an intracellular K⁺, via an active cysteine residue located on TMD3, which is consequently transported outside the cell. This allows the inactivation of SERT back to its native/resting state. Typically, serotonin is transported into the cell via SERT and this direction of transport is energetically unfavourable (net loss of K⁺). To compensate, the Na⁺/K⁺ ATPase-mediated continuous influx of K⁺ coupled with the continuous efflux of Na⁺ acts as an equilibrators to maintain the transmembrane concentration gradient.

1.4.4.3 *Pre and Post Translational Modifications*

SERT activity is regulated via pre- and post-translational modifications. As discussed earlier, the allelic variation of the SERT gene leading to altered expression and activity, is the primary determinant of pre-translational function. However, SERT activity is also regulated to a large extent via post-translational modifications. The phosphorylation levels of SERT, which are regulated via protein kinase C (PKC), protein phosphatase 2A (PP2A)

and P38, are important in modulating SERT function (Ramamoorthy et al., 1998). There are multiple serine and threonine binding sites located on the transmembrane domain cytoplasmic loops and these are the target-site of phosphorylation for these kinase pathways. The functional consequence of SERT phosphorylation is the regulation of SERT expression via trafficking from the cell membrane. For example, the activation of PKC has been shown to phosphorylate SERT resulting in increased sequestration from the membrane. In contrast, PPA2 appears to maintain higher levels of membrane expression, as its inhibition results in increased SERT membrane sequestration. The activation of P38 is also associated with increased SERT activity. P38 inhibition reduces serotonin uptake via reduction in SERT membrane expression (Samuvel et al., 2005). Indeed, receptor-mediated P38 activation can also increase SERT function itself independent of expression levels (Zhu et al., 2005). Moreover, it is observed that serotonin can also directly decrease SERT phosphorylation. This negative feedback mechanism may act to prevent the internalisation of SERT in circumstances where extracellular serotonin levels are higher than normal. Combined, the regulation of SERT expression and activity via these pre- and post-translational modifications are important in SERT function.

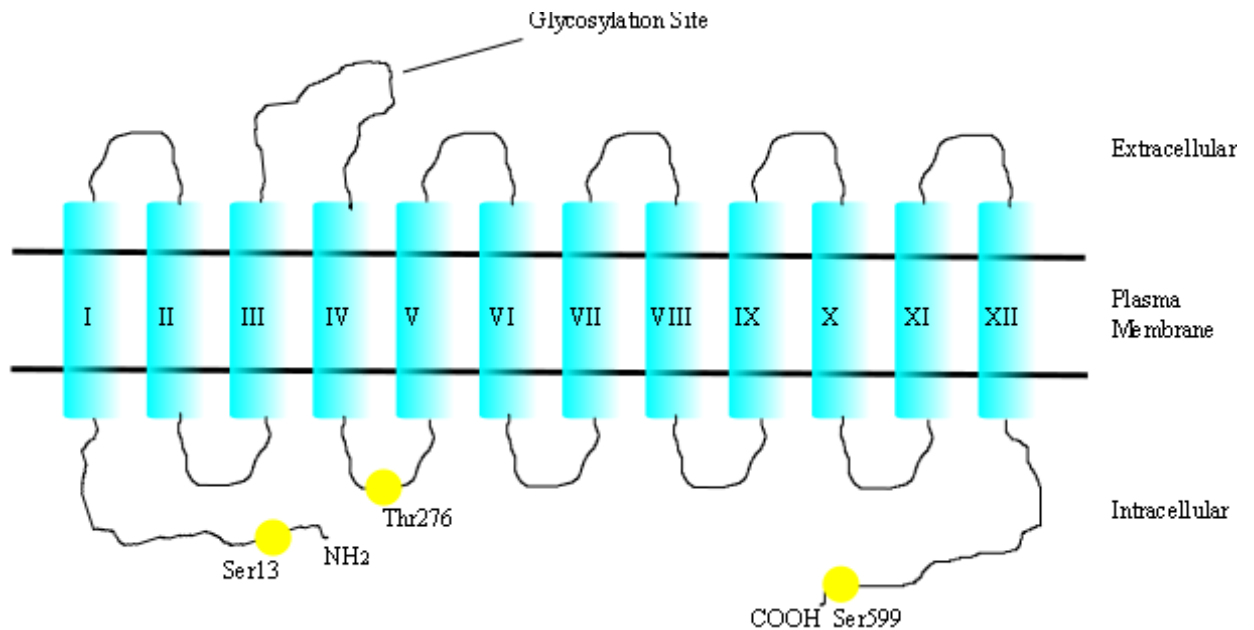


Figure 1.13 Structure of the serotonin transporter. The serotonin transporter exists as an intracellular N-terminus, twelve transmembrane domains and an intracellular C-terminus. The serotonin transporter also contains several sites which can undergo post-translational modification to affect its function.

1.5 Serotonin Hypothesis of PAH

Serotonin is a potent mitogen and vasoconstrictor in the pulmonary vasculature (Figure 1.14). Serotonin was first implicated in the pathogenesis of PAH following introduction of the ‘serotonin hypothesis’ of anorexigen-induced PAH. These appetite suppressant drugs act to inhibit SERT-mediated serotonin uptake whilst also increasing serotonin release. In the 1960’s, use of the indirect serotonergic agonist aminorex, which is an appetite-suppressant drug, was associated with >30 fold increased incidence of PAH (Abenham et al., 1996; Kramer and Lane, 1998). The subsequent generation of anorexigens, termed fenfluramines, were introduced in the 1980’s, and also found to be associated with an increased risk of PAH. Following a multicentre study investigation, it was observed that

use of these anorexigens for a period greater than three months, was associated with a >30 fold increased risk of developing PAH. This discovery resulted in the complete withdrawal of all aminorex/fenfluramine-based anorexigens for clinical use in the treatment of obesity.

Both aminorex and fenfluramine are amphetamine-like compounds which act to influence serotonin signalling. Specifically, both are SERT substrates which results in their uptake into cells. Inside the cell, both aminorex and fenfluramine compete with monoamines at the vesicular monoamine transporter (VMAT) for entry into storage vesicles. Once inside they disrupt monoamine storage, resulting in the reversal of normal serotonin flux to instead promote serotonin release. Indeed, fenfluramine has been shown to increase plasma serotonin concentrations by evoking its release from platelets and neurons (Rothman et al., 1999). Fenfluramines were often prescribed in combination with phentermine (fen-phen), which is also a SERT substrate and MAO inhibitor, resulting in the further potentiation of plasma serotonin levels via increased serotonin release and decreased metabolism. These observations formed the basis of the 'serotonin hypothesis' in PAH.

It was initially proposed that the anorexigen-mediated release of serotonin from platelets, leading to the accumulation of plasma serotonin, resulted in the development of anorexigen-induced PAH. Consistent with this, elevated circulating levels were observed in PAH patients and individuals affected with platelet storage disorders also appear susceptible to the development of PAH (Herve et al., 1995; Herve et al., 1990). Normal circulating levels of serotonin reside at ~1nmol/L, but have been reported to increase up to 30-fold (~30nmol/L) in PAH patients. However in fenfluramine-induced PAH, it was observed that serotonin levels were minimally elevated and still within normal physiological range (Kawut et al., 2006). Of further interest, fenfluramine administration

leading to decreased plasma serotonin levels, has also been described (Stubbs et al., 1986). This converging evidence suggests that elevated plasma serotonin levels are not essential in the development of anorexigen-induced PAH.

In humans, fenfluramines promote the development of PAH, and these effects have also been investigated in experimental PAH. For example, dexfenfluramine promotes the development of PAH in both mice (Dempsey et al., 2008) and rats (Eddahibi et al., 1998). However the exact role of this drug remains controversial, as it has been shown to protect against the development of both hypoxia-induced PAH (Rochefort et al., 2006) and monocrotaline-induced PAH (Mitani et al., 2002).

Non-serotonin mediated mechanisms have also been described for fenfluramines in PAH. For example, it can both directly inhibit potassium channels and increase intracellular $[Ca^{2+}]$, which act to promote vasoconstriction and proliferation (Weir et al., 1996). In addition, fenfluramine metabolism results in formation of the active fenfluramine-derivative nordexfenfluramine, which has been shown to mediate pulmonary arterial vasoconstriction via activation of the 5-HT_{2B} receptors (Hong et al., 2004). Indeed, this receptor may be involved in disease pathogenesis as 5-HT_{2B} receptor knockout mice do not develop hypoxia-induced PAH (Launay et al., 2002).

However, it is considered that serotonin effects of fenfluramines, as opposed to the non-serotonin effects, promote the development of anorexigen-induced PAH. Indeed, this has been confirmed experimentally as mice deficient of peripheral serotonin (tph1^{-/-} mice) do not develop dexfenfluramine-induced PAH (Dempsey et al., 2008).

1.6 The Serotonin Transporter in PAH

The SERT is highly expressed in both the platelets and lungs. These play an important role in the regulation of plasma serotonin concentrations, and are thought to store or inactivate up to 95% of total circulating levels, therefore reducing serotonin effects in pulmonary vascular cells. However, serotonin is implicated in the pathogenesis of PAH, and this is mediated in part via SERT. One study in a small cohort of IPAH patients identified that 65% of those were homozygous for the SERT L-allele variant (LL), which is associated with increased SERT expression and activity, compared to only 27% of non-PAH controls (Eddahibi et al., 2001). Although subsequent studies in larger patient cohorts have failed to support these findings (Machado et al., 2006), patients with the LL allele polymorphism may still present at an earlier age than those without (Willers et al., 2006). Irrespective of genotype, SERT expression is increased in the lungs of IPAH patients (Eddahibi et al., 2001). In addition, PSMCs derived from IPAH patients also exhibit increased SERT expression and these proliferate to a greater extent than those from controls following serotonin stimulation, and this is dependent on SERT activity (Eddahibi et al., 2006). The SERT-mediated uptake of serotonin has been shown to activate multiple signalling pathways relevant to PAH, and this activation of has been reported in several pulmonary vascular cell types. For instance, the role of SERT is implicated in increased Mts1 synthesis and release from PSMCs, which in turn stimulates proliferation via the RAGE pathway (Spiekerkoetter et al., 2005). In bovine PSMCs, ROS derived from serotonin metabolism results in the phosphorylation and nuclear translocation of ERK1/2, and this is dependent on SERT function (Liu et al., 2004). Once inside the nucleus, pERK1/2 can itself then phosphorylate multiple nuclear factors including elk-1, erg-1, GATA-4 and cyclin D1, all of which stimulate proliferation. The serotonin-induced proliferation of PAFs is also mediated via SERT, as citalopram can successfully block these effects (Welsh et al., 2004). Alternatively, intracellular serotonin can directly bind to and activate small GTPases which also reside within the cytoplasm in a process termed

serotonylation (Liu et al., 2010). This further promotes the mitogenic effects of serotonin. Independent of serotonin, the SERT itself has also been shown to directly transactivate the PDGF receptors (Liu et al., 2007).

Animal models of PAH have also implicated SERT in the development of PAH. For example, mice over-expressing SERT (SERT+ mice) exhibit increased RVSP and pulmonary vascular remodelling, and also develop exaggerated hypoxia-induced PAH (MacLean et al., 2004). Similarly, mice with targeted SERT over-expression in the PASMCs (under the guidance of its own SM22 promoter) develop PAH (Guignabert et al., 2006). Conversely, mice devoid of the SERT gene are less susceptible to the development of hypoxia-induced PAH (Eddahibi et al., 2000). Also, the SERT inhibitor citalopram attenuates the severity of hypoxia-induced PAH in both wildtype and SERT+ mice (Morecroft et al., 2010), and prevents hypoxia-induced PAH in rats (Marcos et al., 2003). Hypoxia also appears to regulate SERT expression, as its expression is decreased in the lungs of hypoxic mice (MacLean et al., 2004).

SERT is also a target for many drugs/toxins which promote the development of PAH. The SERT substrate dexfenfluramine is one such example. Dexfenfluramine enters the cell through SERT and then subsequently enters the storage vesicles via the VMAT. Once inside these vesicles, dexfenfluramine acts to evoke serotonin release. The consequence of this is increased circulating serotonin levels. Methamphetamines also act to release serotonin via a similar mechanism, and have also been associated with the development of PAH (Rothman and Baumann, 2007; Zolkowska et al., 2006).

A wealth of evidence exists which implicates the serotonin system in the pathogenesis of PAH. Serotonin appears to act via the 5-HT receptors and the SERT to promote both

vasoconstriction and proliferation in the pulmonary vasculature. The pharmacological target of these serotonin pathway mediators is one viable option in the treatment of PAH.

1.7 Gender Differences in Cardiovascular Disease

Gender differences exist in cardiovascular disease. Although mortality rates are equally prevalent in both males and females, the age of disease onset is typically later in women. Also, pre-menopausal females are at a reduced risk of cardiovascular disease compared to males. The beneficial effects of estrogens in the cardiovascular circulation are likely related to these differences (Mendelsohn and Karas, 1999). This is further supported by the increased incidence of cardiovascular disease in women following surgically-induced or natural menopause. Similarly, incidence is also decreased in those undergoing hormone replacement therapy (Bush et al., 1987; Stampfer et al., 1991) (estrogen and/or progestin). Experimentally, a wealth of evidence highlights the protective effects of estrogens, and particularly 17β estradiol in cardiovascular disease.

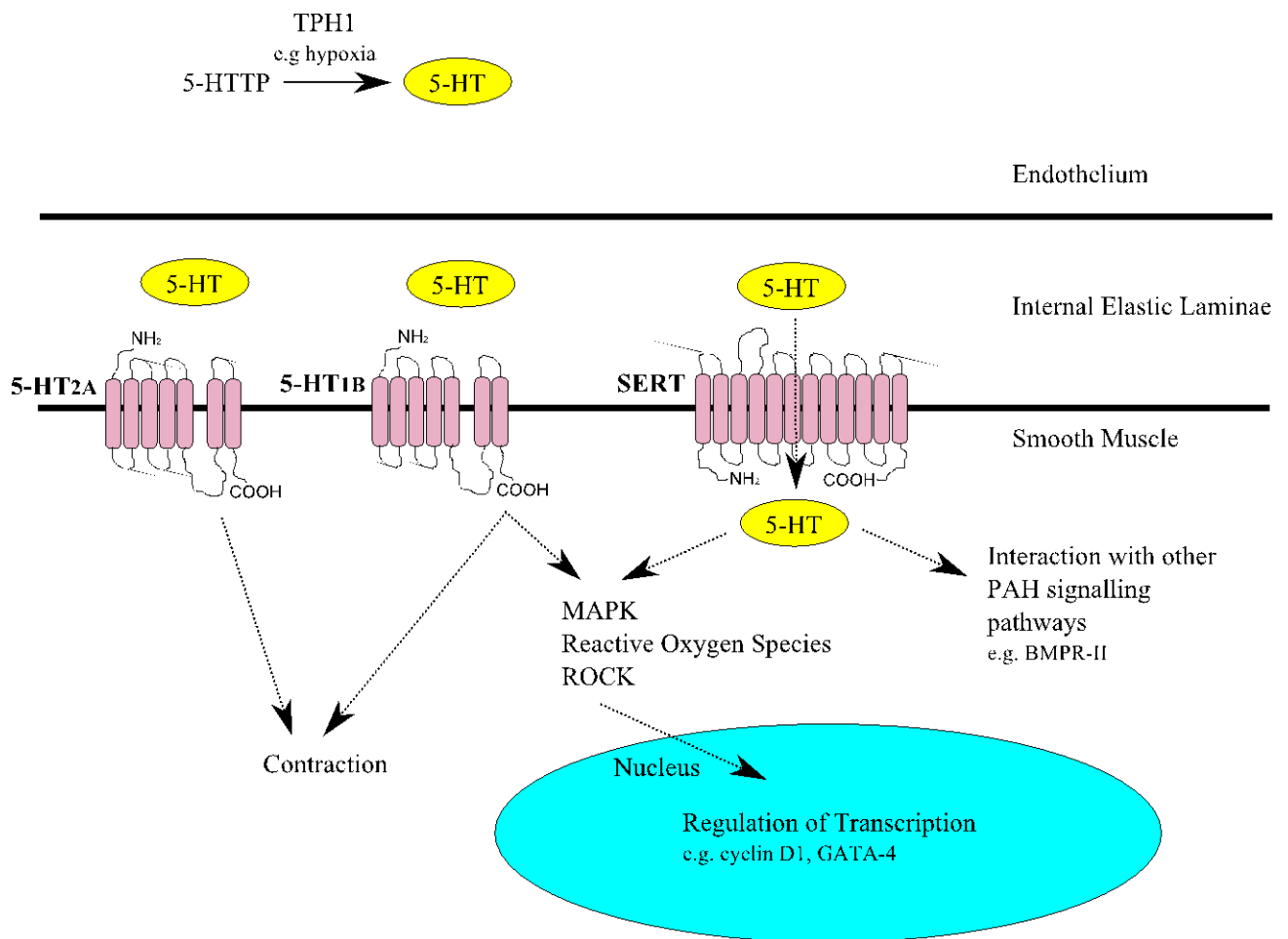


Figure 1.14 Serotonin signalling in the pulmonary vasculature. Tryptophan hydroxylase-1 (TPH1) mediates serotonin synthesis in pulmonary artery endothelial cells. Serotonin is then released where it acts on the underlying pulmonary artery smooth muscle cells. Specifically, serotonin can stimulate contraction via the 5-HT_{2A} and 5-HT_{1B} receptors, or alternatively enter the cell via the serotonin transporter (SERT) to stimulate proliferation. Additionally, stimulation of the 5-HT_{1B} receptor also promotes proliferation.

1.8 Estrogen

1.8.1 *Synthesis and Metabolism*

Female steroid hormones (female sex hormones) comprise both estrogens and progesterone. The majority of estrogen synthesis occurs in both the ovarian follicles and corpus luteum and to a lesser extent the liver, adipose tissue and skin. In addition, estrogen-synthesising enzymes are also expressed in both the endothelial and smooth muscle cells within the vasculature, suggesting the importance of 'local' estrogen synthesis within the cardiovascular system. In humans, estrogen synthesis is continuously modulated by the influence of various endocrine hormones, which are typically secreted from the brain. For example, the release of pituitary-derived luteinising hormone stimulates the estrogen synthesis. This continuous modulation of estrogen is the basis of both the menstrual (in humans) and estrous (in mammals) cycle. Estrogens exist as a family of steroid compounds which include three major subtypes; estrone, 17β estradiol and estriol. 17β estradiol is the pre-dominant circulating hormone in pre-menopausal women, whereas estrone and estriol circulate at lower concentrations and have little contribution. Estrone appears important only in post-menopausal women, whilst increased circulating levels of estriol are reported during pregnancy (Goodwin, 1999).

The biosynthesis of 17β estradiol is well-described (Payne and Hales, 2004). Cholesterol, which is the common pre-cursor in steroidogenesis, is converted to pregnenolone (Figure 1.15). The synthesis of androstenedione then acts as an intermediate step in estrogen synthesis. 17β estradiol is derived from androstenedione via two distinct biosynthetic pathways. The enzyme aromatase converts androstenedione to estrone, which in turn is converted to 17β estradiol via 17β hydroxysteroid dehydrogenase. Alternatively, 17β estradiol can be directly derived from aromatase-mediated testosterone metabolism. In pre-menopausal females, circulating levels of 17β estradiol typically range between 0.1-

1nmol/L (Rosselli et al., 1994), and this is influenced to a large extent on the menstrual cycle stage.

Following its synthesis, 17β estradiol is rapidly metabolized. There are multiple pathways which are involved in this (Zhu and Conney, 1998). All convert 17β estradiol to various hormonally inactive non-estrogenic metabolites ready for elimination from the body. The first-step of 17β estradiol metabolism is oxidative metabolism (hydroxylation) which occurs in the liver, and to a lesser extent in several extrahepatic tissues including the brain and vasculature. Several members of the cytochrome P450 (CYP450) family are essential in mediating this NADPH-dependent oxidative metabolism of 17β estradiol. Specifically, CYP1A1, CYP1A2, CYP1B1 and CYP3A4 appear critical to this (Martucci and Fishman, 1993). In the liver, around 80% of 17β estradiol is metabolized to 2-hydroxyestradiol via CYP1A1, CYP1A2 and CYP3A4, whereas the remaining 20% is metabolized to 4-hydroxyestradiol via CYP1B1. In extrahepatic tissues 2-hydroxyestradiol formation is predominantly via CYP1B1. In addition to this, several other CYP isoforms (CYP2A6, CYP2C8, CYP3A5 and CYP3A7) also play a minor role in 17β estradiol metabolism, resulting in the formation of multiple other metabolites including 6α , 6β , 7α , 12β , 15α , 15β , 16α and 16β hydroxyestradiol (Martucci and Fishman, 1993). All of these water-soluble catechol metabolites are readily eliminated by the kidneys via urine excretion. Alternatively, these hydroxyestradiol metabolites can themselves undergo metabolism via their COMT mediated O-methylation conversion to monomethoxyestradiols (e.g. 2-methoxyestradiol, 4-methoxyestradiol) before excretion from the body.

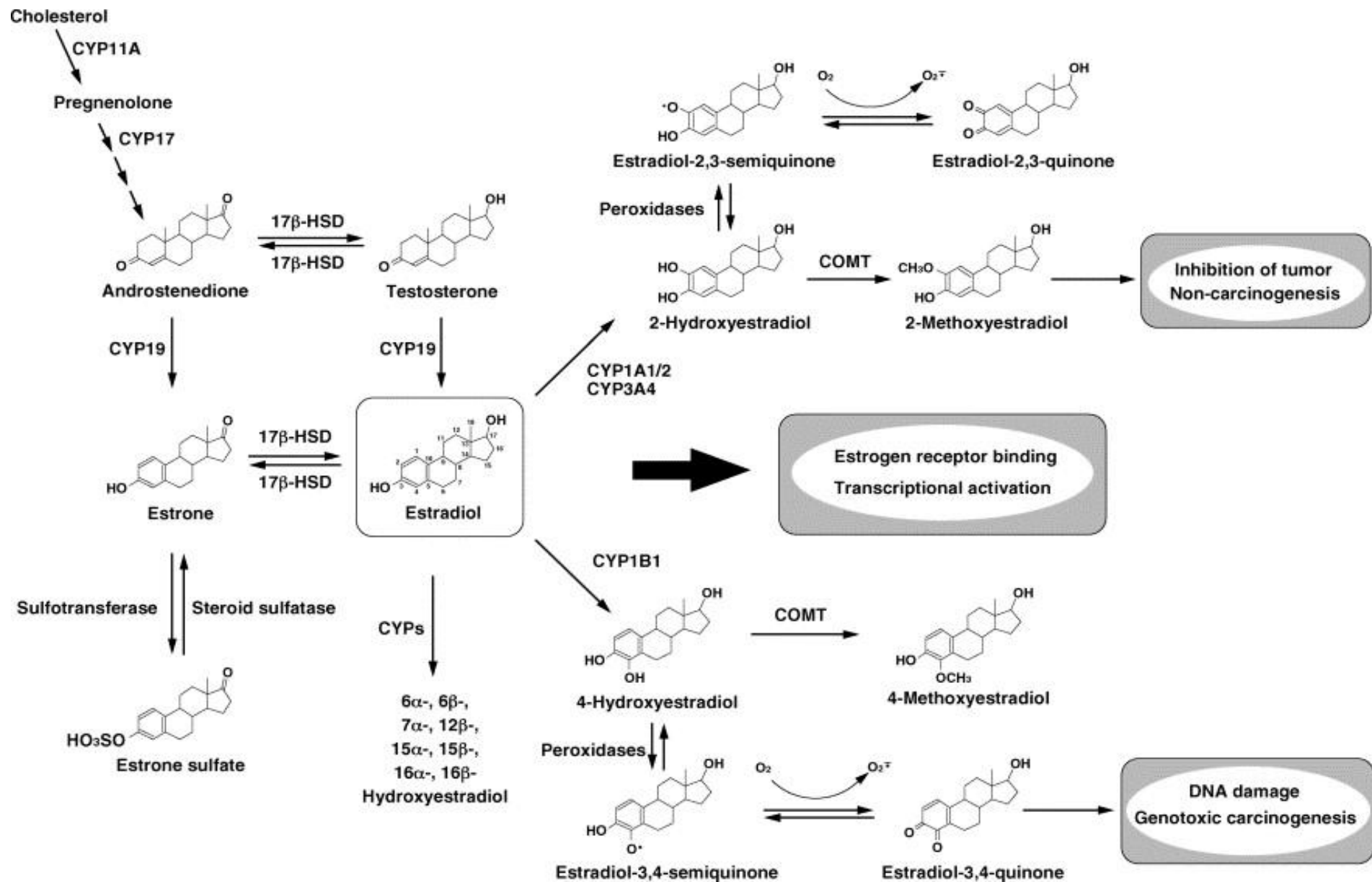


Figure 1.15 Estrogen biosynthesis and metabolism. Androstenedione is derived from the steroid hormone pre-cursor cholesterol via cytochrome P450-11A (CYP11A) and CYP17. (17 β) estradiol is derived from testosterone or estrone via CYP19 or 17 β hydroxysteroid dehydrogenase (17 β -HSD), respectively. (17 β) estradiol is metabolised to 2- and 4-hydroxyestradiol via CYP1A1, CYP1A2, CYP3A4 and CYP1B1. Subsequently, the hydroxyestradiol compounds are metabolised to mono-methoxyestradiol compounds via catechol-O-methyltransferase (COMT). Adapted from (Tsuchiya et al., 2005).

1.8.2 Estrogen Receptors

Both non-rapid and rapid 17β estradiol effects have been described and these are typically referred to as ‘genomic’ and ‘nongenomic’ effects, respectively (Mendelsohn, 2002). The genomic effects of 17β estradiol are well-described, and involves ligand-binding to intracellular estrogen receptors to directly regulate transcription of a target gene. In contrast, nongenomic effects do not require the regulation of gene transcription but instead act through signal transduction. Recent evidence, through the use of cell-impermeable BSA conjugated 17β estradiol, suggests that these rapid nongenomic effects are mediated via the stimulation of estrogen receptors expressed in the plasma membrane (Pietras and Szego, 1977; Aronica et al., 1994). Indeed, these observations are further supported by the observation that 17β estradiol stimulates responses in non-nuclear cells (e.g. platelets) which are not capable of gene transcription (Moro et al., 2005; Jayachandran et al., 2005; Jayachandran et al., 2010). It is this activation of both intracellular and membrane estrogen receptors which mediate the effects of 17β estradiol.

1.8.2.1 Estrogen Receptor α and β

Intracellular estrogen receptors are ligand-activated transcription factors which typically exist as nuclear hormones receptors. Similar to all steroid hormone receptors, estrogen receptors share a common structure of four functionally active units or ‘domains’ (Katzenellenbogen et al., 2000; Katzenellenbogen et al., 2000). These include the variable domain, which is typically the most heterologous domain between receptors, the DNA-binding domain, the hinge domain and the ligand-binding domain (Figure 1.16). Currently, two intracellular estrogen receptor (ER) isoforms have been identified and referred to as ER α and ER β (Kuiper et al., 1996). Each receptor is encoded by a separate gene (ESR1 and ESR2 respectively). Both ER subtypes share an equal affinity for 17β estradiol, although estrone selectively binds ER α , whereas estriol selectively binds ER β .

Both ER α and ER β are expressed in a variety of tissues including the uterus, testes, prostate, ovaries, bone, breast, liver and brain (Heldring et al., 2007). With respect to the cardiovascular system, ER β predominates and is expressed in the cardiomyocytes, endothelial and vascular smooth muscle cells (Imamov et al., 2005).

Although both ER α and ER β share 97% sequence homology for the DNA-binding domain and 56% for the ligand-binding domain, the N terminus shares relatively poor homology at 24%, which impacts their function. ERs must co-operate as dimers in order to translocate from the cytosol to the nucleus. Following this, the transcriptional activation of both ERs is mediated via two distinct activation functions (AFs) termed AF-1 and AF-2, which are located in the ligand-binding domain. AF-1 is constitutively active and resides at the N-terminus domain (Kushner et al., 2000), while AF-2 is located at the C-terminus and typically requires ligand-dependent activation for transcriptional activation. With respect to both ER isoforms, ER α mediates transcriptional activation via AF-1 to a much greater extent than ER β , which instead appears to regulate transcription via AF-2 function. This balance of AF-1 and AF-2 is critical to the nuclear receptor-dependent cellular effects of 17 β estradiol. Both AF-1 and AF-2 signal via the recruitment of co-regulator complexes (either co-activators or co-repressors) to activate or suppress gene expression. Specifically, the binding of the ERs to specific DNA sequences (estrogen response elements, EREs) are responsible for regulating the transcription of genes (Kushner et al., 2000). As a consequence, this regulates protein translation which consequently will affect cell function. Alternatively, ER dimers can recognize and bind non-ERE DNA sequences which are primarily a target for other transcription factors. This commonly includes cAMP-responsive elements (Sabbah et al., 1999). Collectively, ER α /ER β transcriptional regulation is the basis of the 'genomic' effects of 17 β estradiol (Figure 1.17).

The ERs are themselves also subject to pre- and post-translational modification which can influence their expression and/or function. For example, estrogen receptors are subject to phosphorylation, acetylation, ubiquitination and SUMOlation (Mendelsohn and Karas, 2010). Numerous promoters have also been identified for both ER α and ER β , which directly regulate their expression. Also, a number of ER α gene polymorphisms have been identified, which most commonly exist as a variable number of tandem repeats within the promoter region. These are associated with the increased development of multiple diseases including breast cancer (Dunning et al., 2009), prostate cancer (Tanaka et al., 2003), osteoporosis (Styrkarsdottir et al., 2008) and cardiovascular disease (Lu et al., 2002). ER β polymorphisms have also been associated with the increased incidence of cardiovascular disease in women (Rexrode et al., 2007). Specifically, the rs1271572 polymorphism variant A allele (A \rightarrow C transposition in the promoter region) is associated with increased incidence of cardiovascular disease and myocardial infarction in women (Rexrode et al., 2007). Whether ER polymorphisms contribute to the development of PAH remains to be investigated.

1.8.2.2 G-Protein Coupled Receptor 30

17 β estradiol also mediates its effects via ligand-binding to a third receptor, termed the G-protein coupled receptor 30 (GPR30, GPER, mER) (Filardo et al., 2007). GPR30 is described to act via both transcriptional regulation and activation of signal transduction pathways. These signalling pathways include those associated with Ca²⁺ mobilization, ERK1/2 MAPK activation and NO production. At the cellular level, GPR30 expression is localised at both the plasma membrane and endoplasmic reticulum, and has been identified in the stomach, pancreas, duodenum and the endothelial and smooth muscle cells of the vasculature. Indeed, GPR30 is an important regulator of 17 β estradiol effects in the cardiovascular system (Olde and Leeb-Lundberg, 2009). GPR30 activation mediates

endothelial dependent NO-derived relaxation in isolated carotid arteries from both male and female rats (Broughton et al., 2010). In addition, 17 β estradiol-induced apoptosis of vascular SMCs requires ERK phosphorylation, and this appears dependent on GPR30 (Ding et al., 2009). Deletion of the GPR30 gene *in vivo* (GPR30^{-/-} mice) results in the elevation of systemic blood pressure, and impaired glucose tolerance (Haas et al., 2009). In the pulmonary vasculature, the role of GPR30 remains poorly defined.

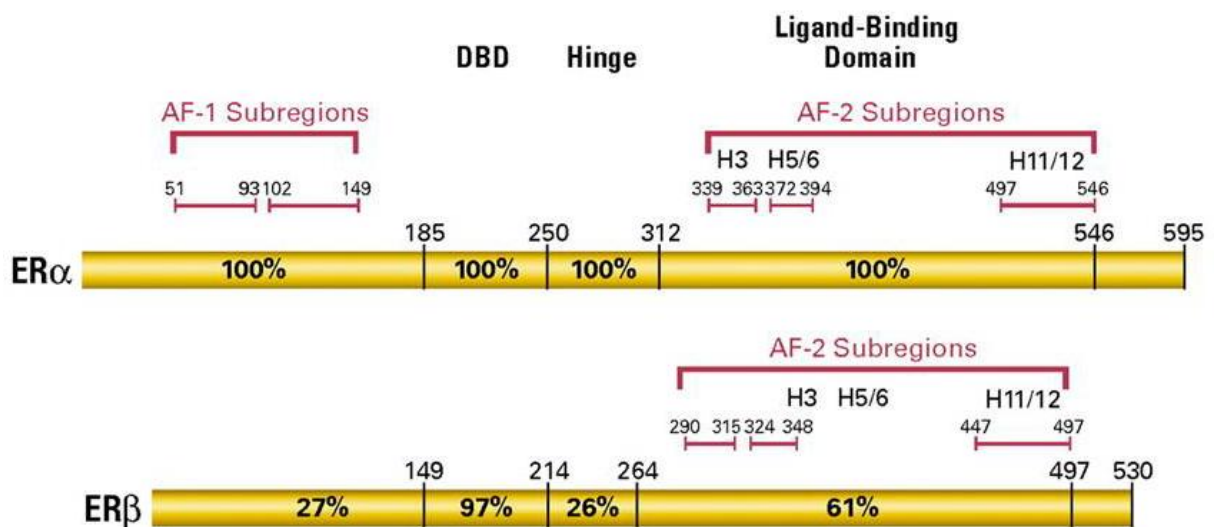


Figure 1.16 Estrogen receptor structure. Estrogen receptors (ERs) exist as a four domain structure. The N-terminal variable domain, which is the most heterologous part of the receptor, is essential for receptor transactivation. Both the DNA binding domain (DBD) and hinge domain are important in DNA binding receptor activity. The ligand-binding domain, which is located at the C-terminus, directly interacts with the ligand and is also important in nuclear translocation. Adapted from (Jordan and O'Malley, 2007).

1.8.3 17 β Estradiol Effects in the Systemic Circulation

17 β estradiol has multiple physiological effects in multiple target organs including bone, breast, prostate, heart and the vasculature (Vitale et al., 2009). In the cardiovascular

system, a wealth of evidence highlights a cardio-protective and vaso-protective role for 17β estradiol in cardiovascular disease. In women, the incidence of cardiovascular disease is negatively correlated with circulating estrogen levels, which are modulated by a number of factors including menopause and hormone replacement therapy. For example, women are at an increased risk of cardiovascular disease following menopause (Rosano et al., 2003).

17β estradiol stimulates both NO-mediated (Caulin-Glaser et al., 1997) and prostacyclin-mediated (Mikkola et al., 1995) vasodilatation. In addition, this hormone limits the progression of atherosclerosis by reducing low-density lipoprotein and also reduces vascular inflammation, coagulation and fibrinolysis. Indeed, 17β estradiol attenuates the development of atherosclerosis in apolipoprotein E (ApoE) deficient (ApoE^{-/-}) mice (Bourassa et al., 1996). A wealth of evidence highlights the specific vaso-protective role of ER α in the vasculature. In endothelial cells, ER α stimulation activates multiple kinases including P38 to promote eNOS-derived NO production, thereby promoting vasodilatation (Anter et al., 2005). *In vivo*, ER α appears to mediate the protective effects of 17β estradiol following vascular injury, as ER α knockout mice do not show vascular recovery following treatment with 17β estradiol compared to wildtype mice (Brouchet et al., 2001). In contrast, ER β ^{-/-} mice fully recover from vascular injury following 17β estradiol treatment, providing further evidence that this vascular response is ER α -mediated. Instead, ER β appears important in other forms of cardiovascular disease. For example, the development of age-related systolic and diastolic hypertension is reported in ER β ^{-/-} mice (Zhu et al., 2002). This phenotype is not observed in ER α ^{-/-} mice. Vasodilatation appears to be mediated via ER α (Darblade et al., 2002; Pendaries et al., 2002). Disruption of ion channel function is also apparent in vascular SMCs derived from ER β ^{-/-} mice (Zhu et al., 2002). These mice also develop systemic hypoxia arising from lung dysfunction, and as a result develop systemic hypertension and left ventricular hypertrophy (Morani et al., 2006).

Taken together, a wealth of evidence supports a vasoprotective role for both ER α and ER β in systemic vascular function and regulation of blood pressure.

However, under certain circumstances estrogen exposure may conversely lead to an increased incidence of cardiovascular disease. In one study cohort, the Women's Health Initiative reported that those prescribed estrogen for hormone replacement therapy were at an increased risk of cardiovascular events (Anderson et al., 2004). This appeared most significant during the initial 12 months of therapy. This is also termed the 'timing' hypothesis. The mechanisms underlying this pathophysiology of estrogens are unclear. Increased expression of both ER α and ER β is reported in both cardiac hypertrophy and heart failure in humans (Mahmoodzadeh et al., 2006; Nordmeyer et al., 2004). However, this must be further investigated as a wealth of evidence has shown that both ER α and ER β protect against the development of cardiovascular disease.

1.8.4 17 β Estradiol Metabolite Effects in the Systemic Circulation

17 β estradiol metabolites are also vasoactive in the systemic circulation. 2-hydroxyestradiol, 2-methoxyestradiol and 4-methoxyestradiol all inhibit the migration and proliferation of human and rat vascular SMCs. Moreover, these metabolites do not appear to be ER α /ER β dependent as the non-selective ER antagonist ICI-182,780 does not exert any inhibitory effects (Dubey et al., 2005). *In vivo*, the metabolite 2-methoxyestradiol prevents the elevation of systemic arterial blood pressure associated with chronic NOS inhibition and also reduces inflammation, collagen synthesis and proliferation in the heart (Tofovic et al., 2005). 2-methoxyestradiol appears most potent in the prevention and regression of systemic cardiovascular disease. Specifically, it is proposed to act via the inhibition of tubulin polymerization, which is an important component of the cytoskeleton and involved in cell growth.

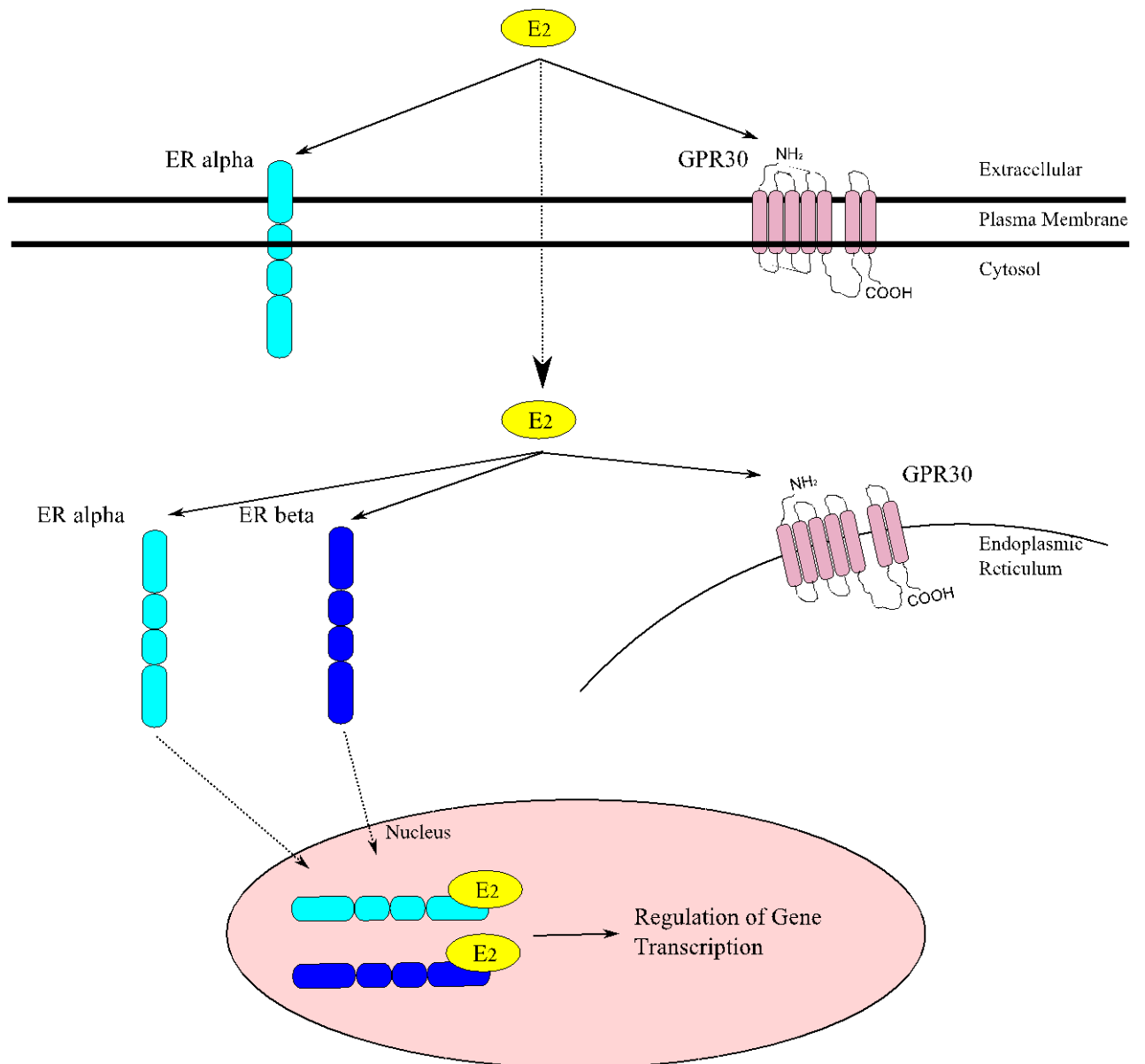


Figure 1.17 17β estradiol signalling. 17β estradiol (E₂) mediates both nongenomic and genomic effects. E₂ enters the cell where it can act on ER alpha and ER beta to regulate the transcription of target genes (genomic effects). Alternatively, E₂ can act on GPR30 to stimulate a more rapid mechanism of action (nongenomic effects). Membrane-bound estrogen receptors are also proposed to exist, however their precise function remains to be determined.

1.8.5 17β Estradiol Effects in the Pulmonary Circulation

In both idiopathic and heritable forms of PAH there is a gender bias, with females up to three fold more likely to present with disease (Peacock et al., 2007; Humbert et al., 2006; Thenappan et al., 2007). Currently, BMPR-II mutations are not considered pivotal to this, confirmed by one study which showed no influence of gender in BMPR-II affected PAH patients (Girerd et al., 2010). Therefore, the mechanisms attributing to these gender differences remain obscure. Estrogen is one risk factor in PAH. For example, the use of oral contraceptives have previously been associated with PAH (Masi, 1976) and female PAH patients exhibit increased expression of ESR1, which is the gene encoding for ER α , compared to unaffected (non-PAH) females (Rajkumar et al., 2010). Decreased expression of the estrogen-metabolising enzyme cytochrome P450 1B1 (CYP1B1), leading to alterations in estrogen metabolism, has also been identified in female PAH patients harbouring a BMPR-II mutation compared to unaffected female carriers (West et al., 2008; Austin et al., 2009).

In contrast, experimental models of PAH have repeatedly shown that females exhibit moderate PAH compared to males. For example, male rats develop increased RVSP, pulmonary vascular remodelling and RVH compared to female rats following exposure to hypoxia (Rabinovitch et al., 1981). Similar observations are also reported in mice (Stupfel et al., 1984). In support of this, male swine and chicken also exhibit an exaggerated hypoxia-induced PAH phenotype compared to females. These protective effects appear to be mediated via female hormones, as ovariectomy can increase the severity of hypoxia-induced PAH (Resta et al., 2001). Specifically, 17β estradiol appears to mediate these effects as its exogenous administration can attenuate increased RVSP and pulmonary vascular remodelling in ovariectomized females (Resta et al., 2001). In transgenic models, male ApoE $-/-$ mice subjected to a high-fat diet develop increased RVSP and pulmonary vascular remodelling compared against high-fat treated ApoE $-/-$ female mice (Hansmann

et al., 2007). Also, male VIP^{-/-} mice are more susceptible to PAH than female VIP^{-/-} mice (Said et al., 2007). The loss of ER β function, as is observed in ER β ^{-/-} mice, also results in the development of right ventricular hypertrophy (Morani et al., 2006). Estrogens appear to promote both NO-mediated (Gonzales et al., 2001) and prostacyclin-mediated (Sherman et al., 2002) endothelium-dependent vasodilatation in the pulmonary circulation. For example, 17 β estradiol has been shown to promote vasodilatation in the pulmonary vasculature. In pulmonary arteries isolated from proestrus rats (highest circulating levels of 17 β estradiol in the menstrual cycle), both phenylephrine and hypoxia-induced vasoconstriction is markedly attenuated compared to those responses observed in pulmonary arteries isolated from estrus, diestrus and male rats (Lahm et al., 2007). In support of this, hypoxic pulmonary vasoconstriction is reduced in female sheep compared to males, and 17 β estradiol attenuates this response. Hypoxic pulmonary vasoconstriction is also reduced in the pulmonary arteries of dogs and rats during pregnancy, when circulating levels of estrogen are elevated. 17 β estradiol has also been reported to increase endothelial nitric oxide synthase (eNOS) mRNA expression and activity in PAECs via an estrogen receptor-dependant mechanism (MacRitchie et al., 1997). In addition, 17 β estradiol also inhibits hypoxia-induced endothelin-1 gene expression (Earley and Resta, 2002).

Taken together, these findings indicate a protective role for female gender in experiment PAH. This may not be entirely unexpected, as estrogens are beneficial in several forms of human PAH distinct from IPAH and HPAH. For example, estrogens may protect against the development of PAH in high-altitude natives. The incidence of high altitude pulmonary edema (HAPE), which occurs as a result of pronounced hypoxic pulmonary vasoconstriction, is also higher in males than females. There is also an increased incidence of sclerosis-related PAH in post-menopausal females, and its risk of development is reduced in those prescribed hormone replacement therapy. To date, the absence of a

suitable experimental model of PAH which replicates the female susceptibility observed in IPAH and HPAH has limited research into the role of estrogens in the pathogenesis of PAH.

1.8.6 17β Estradiol Metabolite Effects in the Pulmonary Circulation

Non-estrogenic 17β estradiol metabolites also mediate protective effects within the pulmonary circulation. Those most extensively studied are the hydroxyestradiol and methoxyestradiol compounds. 2-hydroxyestradiol, which is derived from the CYP1A1-mediated hydroxylation of 17β estradiol (and to a lesser extent CYP1B1), attenuates increased RVSP, pulmonary vascular remodelling and RVH associated with monocrotaline-induced PAH in rats (Tofovic et al., 2005). The administration of this metabolite also successfully prevents isoproterenol-induced RVH and cardiac fibrosis in rats (Tofovic et al., 2008). In support of this, 2-hydroxyestradiol successfully inhibits serum-induced proliferation of cardiac fibroblasts (Dubey et al., 2005).

The subsequent O-methylation of 2-hydroxyestradiol, which is derived via COMT, results in the formation of 2-methoxyestradiol. The anti-mitogenic effects of this metabolite are well-described in PAH. For example, 2-methoxyestradiol attenuates the development of monocrotaline-induced PAH (Tofovic et al., 2004) and hypoxia-induced PAH (Zhang et al., 2005). Pharmacological concentrations of this metabolite also inhibit serum-induced proliferation in PAECs, PASMCs and PAFs (Tofovic et al., 2008). 2-ethoxyestradiol, which is a potent synthetic analogue of 2-methoxyestradiol, also successfully inhibits the proliferation of PAECs, PASMCs and PAFs. *In vivo*, 2-EE successfully prevents the elevation of RVSP and pulmonary vascular remodelling in monocrotaline-induced PAH.

1.9 Estrogen and Serotonin Interactions

Interactions between estrogen and serotonin are widely investigated in the central nervous system. In most cases, estrogens are reported to increase expression of multiple serotonin pathway mediators, which as a consequence would likely promote serotonin signalling. In the dorsal raphe nucleus, 17β estradiol increases both SERT expression and function in acutely ovariectomized mice (Bertrand et al., 2005). Increased SERT binding is also reported in the basolateral amygdala and lateral septum of these mice. Similar observations are also reported in rats (McQueen et al., 1997). These 17β estradiol effects can be successfully blocked with the selective estrogen receptor modulators (SERMs) tamoxifen and raloxifene, suggesting the involvement of estrogen receptors in this induction (Sumner et al., 2007). In addition, 17β estradiol is also reported to increase 5-HT_{2A} receptor expression in rats (Sumner et al., 2007). Increased expression and/or function in the dorsal raphe nucleus and cerebral cortex is similarly reported in acutely ovariectomized mice subjected to 17β estradiol administration, and an increase is also observed in chronically ovariectomized rats and macaques following chronic 17β estradiol administration (Chavez et al., 2010; Rivera et al., 2009). Similar to SERT, 17β estradiol-induced expression of the 5-HT_{2A} receptor is also proposed to act via an ER-dependent mechanism as both tamoxifen and raloxifene can block this effect (Sumner et al., 2007).

The synthesis and metabolism of serotonin is also influenced via 17β estradiol in the central nervous system. Both mRNA and protein expression of TPH (the rate-limiting enzyme involved in serotonin synthesis) is increased in the brain of 17β estradiol-treated animals following ovariectomy (Pecins-Thompson et al., 1996), and its induction is similarly blocked in the presence of tamoxifen. In addition, dorsal raphe expression of the serotonin-metabolizing enzyme MAO-A is decreased following 17β estradiol administration (Smith et al., 2004). In combination, these likely facilitate increased

serotonin bioavailability. Overall, 17β estradiol appears to increase expression of TPH, SERT and the 5-HT receptors in the central nervous system.

Although estrogen-serotonin interactions are widely reported in the central nervous system, these remain poorly defined in the cardiovascular system. Only functional interactions have been described. A reported increase in serotonin-induced contraction is observed in the mesentery vascular bed of 17β estradiol-treated rats compared to vehicle controls (Mark et al., 2007). To date, this study is the only to report the potentiated response of serotonin in the presence of 17β estradiol in the cardiovascular system. Therefore, interactions between estrogen and serotonin remain to be investigated in the pulmonary circulation.

1.10 Aim

The principle research aim was to investigate the influence of gender in the development of PAH. This may offer insight into the increased incidence of PAH in women. This was evaluated through investigation of the following experimental study aims:

- *In vivo* characterisation of gender and estrogen via assessment of PAH phenotype in a transgenic model of PAH (SERT⁺ mouse model).
- Determine genotypic differences in the pulmonary arteries of female and male SERT⁺ mice.
- *In vitro* characterisation of female hormones in pulmonary artery smooth muscle cells.
- Influence of estrogen on serotonin signalling in pulmonary artery smooth muscle cells.
- Identify novel genes in important in SERT⁺ PAH and human PAH.

Chapter 2

Materials and Methods

Materials

2.1.1 Chemicals and Reagents

All chemicals and reagents were of the highest grade obtainable and supplied by Sigma-Aldrich (Poole, UK), Invitrogen (Paisley, UK), Fisher Scientific (Loughborough, UK), Tocris Bioscience (Bristol, UK), Roche Diagnostics (West Sussex, UK) or BDH Prolabo (West Sussex, UK), as stated. All cell culture reagents were supplied by Sigma-Aldrich (Poole, UK) or Gibco (Paisley, UK), unless otherwise stated. Fetal bovine serum (FBS) was supplied by Sera Laboratories International (West Sussex, UK).

Methods

All experimental procedures conform with the United Kingdom Animal Procedures Act (1986) and with the 'Guide for the Care and Use of Laboratory Animals' published by the US National Institutes of Health (NIH publication No. 85-23, revised 1996). All *in vivo* procedures were performed under the project license 60/3773 held by Professor M.R MacLean (University of Glasgow, UK).

2.1.1 SERT+ Mice

Mice over-expressing the serotonin transporter (SERT+ mice) were generated and supplied by Professor Tony Harmer, University of Edinburgh, UK. The generation SERT+ mice was achieved using the C57BL/6xCBA background strain. The transgene introduced was a 500kb yeast artificial chromosome (YAC35D8) containing the human SERT gene flanked by 150 kb of 5' and 300 kb of 3' sequence, with the short (S) allele of the *SERTLPR* in the promoter region and the 10-repeat allele of the variable number tandem repeat in intron 2. Previously, *in situ* hybridization analysis has shown that human SERT

mRNA is similarly expressed in a manner which resembles that of the endogenous mouse SERT gene. Genotyping was performed to confirm the presence of the human SERT transgene. Mice were housed with littermates in the central biological services research facility at the University of Glasgow. All mice were subject to a continuous 12hour light/dark cycle with access to food and water *ad libitum*. PAH phenotype was assessed in female and male SERT+ mice at both 8 and 20 weeks of age (Figure 2.1), and C57BL/6xCBA littermate mice studied as controls.

2.1.2 Bilateral Ovariectomy

For pre-operative care, mice were administered 0.1mg/kg buprenorphine (an analgesic) and 4ml/kg sterile saline via intra-peritoneal injection. Surgical removal of the *left* and *right* ovaries (bilateral ovariectomy) was performed under general anaesthesia (1%-3% (v/v) isoflurane supplemented with O₂) in 8 week old female mice. This is a commonly used surgical technique used to deplete circulating ovarian hormone levels. Briefly, a dorsal midline skin incision was performed to expose the dorsal back. This was followed by incision through the muscle caudal to the posterior border of the ribs, and lateral blunt dissection was performed to advance into the abdominal cavity through the muscles of the abdominal posterior wall. The ovary (including periovarian fat) was located underneath the muscle, and removed via cauterization through the distal uterine tube. 1-2 simple interrupted sutures were performed to repair incision through the muscle. This surgical procedure was repeated to excise the remaining ovary. 2-3 surgical staples were used to close the dorsal midline skin incision. For post-operative care, 2.5mg/kg carprofen (a non-steroidal anti-inflammatory drug) and 4ml/kg sterile saline were administered via intra-peritoneal injection. Successful removal of the ovaries was confirmed at necropsy via weight measurement of the uterus. The assessment of PAH was carried out 12 weeks following surgery (20 week old mice). Sham-operated mice were studied as controls.

2.1.3 17β Estradiol Administration

17β estradiol containing pellets (0.1mg/21 day pellet, Innovative Research of America, Florida, USA) or vehicle pellets were subcutaneously implanted into the dorsal neck. This was performed under general anaesthesia (1%-3% (v/v) isoflurane supplemented with O₂) using a sterile 12-gauge hypodermic needle. These pellets have been previously shown to have a constant rate of drug release (Karas et al., 2001), and therefore an effective dosing method. The selected dose of 17β estradiol has been previously shown to produce physiologically relevant (~1nmol/L) concentrations of circulating 17β estradiol. Following completion of the 21 day dosing regime, the assessment of PAH was carried out.

2.1.4 Chronic Hypoxia

The development of hypoxia-induced PAH was achieved in mice using a hypobaric hypoxic chamber. Following acclimatization, mice were exposed to 550mbar for a continuous period of 14 days. As a consequence of atmospheric depressurization from ~1000mbar (ambient room pressure) to 550mbar, oxygen availability is decreased from 21% O₂ to 10% O₂, resulting in sustained HPV and the development of PAH. Temperature (21°C-23 °C) and relative humidity (30-50%) were maintained within a normal range and mice were re-housed with clean bedding and food/water every five days.

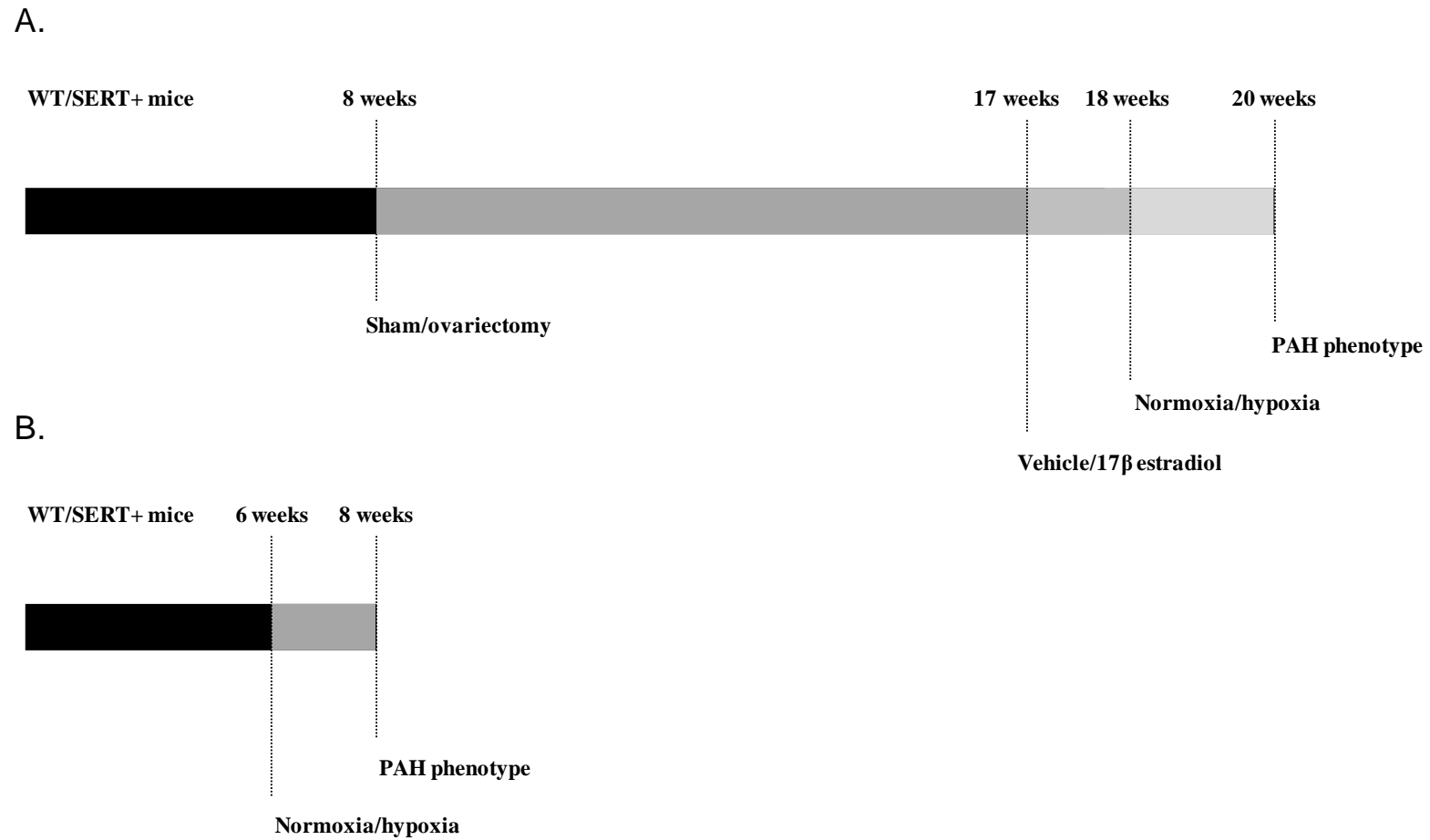


Figure 2.1 In vivo study design. Chapter 3 - Female SERT+ mice were subject to sham/ovariectomy (at 8 weeks of age), vehicle/17 β estradiol administration (at 17 weeks of age) and normoxia/ hypoxia (at 18 weeks of age) and PAH phenotype assessed at 20 weeks of age (A). Chapter 4 - Female and male SERT+ mice were exposed to hypoxia (at 6 weeks of age) and PAH phenotype assessed at 8 weeks of age. WT mice were studied as control (B).

2.2 Assessment of PAH

2.2.1 Haemodynamic Measurements

The induction of general anaesthesia was performed via exposure to 3% (v/v) isoflurane supplemented with O₂. Mice were immediately weighed and 1-2% (v/v) isoflurane continuously administered via a facemask to maintain general anaesthesia. General anaesthesia was confirmed by the absence of a hind-limb and tail reflex. These reflexes were also routinely assessed throughout surgery. Following confirmation of general anaesthesia, both right ventricular pressure (RVP) and systemic arterial pressure (SAP) were measured.

2.2.2 Right Ventricular Pressure

Right ventricular pressure (RVP) was measured via a transdiaphragmatic approach. The continuous measurement of RVP was assessed via a heparinised saline-filled calibrated 25-gauge needle attached to an Elcomatic E751A pressure transducer connected to a MP100 data acquisition system (BIOPAC Systems Inc, Santa Barbra, USA). Briefly, a portion of skin was removed from the ventral chest to expose the anterior sternum. The 25-gauge needle was then advanced through the mid-portion of the sternum, into the abdomen. Following entry into the diaphragm (confirmed by a negative pressure reading), the needle was advanced directly into the right ventricle via puncture through the right ventricular free wall. This was confirmed by the characteristic pressure waveform typically observed inside the right ventricle (Figure 2.2). From this recording, right ventricular systolic pressure (RVSP) was deduced and used as an index of PAH. Following RVP measurement, two additional controls were performed to confirm successful right ventricular catheterisation. This was achieved by further advancing the needle into the left ventricle to measure left ventricular pressure, which is typically positioned inferior to the

right ventricle *in situ*. At necropsy, the heart was also microscopically assessed to confirm the presence of a puncture in the right ventricular free wall.

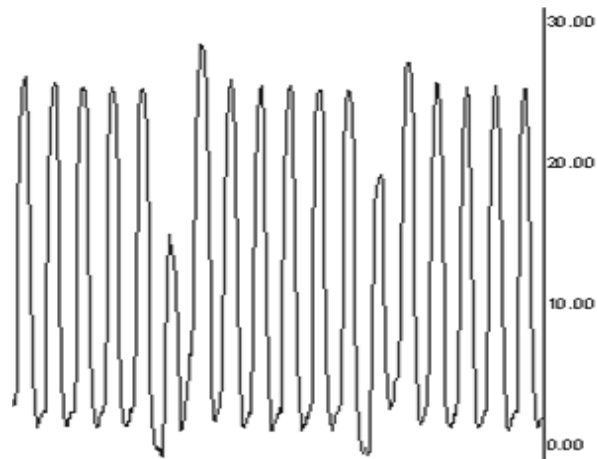


Figure 2.2 Representative recording of right ventricular pressure. Three second representative measurement of right ventricular pressure in mice. Y-axis expressed in mmHg.

2.2.3 Systemic Arterial Pressure

Systemic Arterial Pressure (SAP) was measured via cannulation of the left common carotid artery (Figure 2.3). Briefly, this was approached via skin incision through the ventral neck to expose the trachea. Lateral blunt dissection was performed through the muscle lying inferior to the trachea. The left common carotid artery is typically positioned ~2mm lateral (left) and less than 1mm posterior to the trachea. Precision dissection was performed to separate the artery from both the vagus nerve and the recurrent laryngeal nerve. Distal suture (7-0 silk non-braided) was used for isolation of the artery and an arterial clip positioned at the most proximal arterial segment to temporarily occlude blood flow through the lumen. Following incision through the arterial wall, a heparinised saline-filled polypropylene cannula (Harvard Apparatus, Boston, USA) was proximally inserted 4-5mm into the lumen and secured using suture. Similar to the technique used for RVP

measurement, the systemic arterial cannula was also attached to an Elcomatic E751A pressure transducer connected to a MP100 data acquisition system (BIOPAC Systems Inc, Santa Barbra, USA).

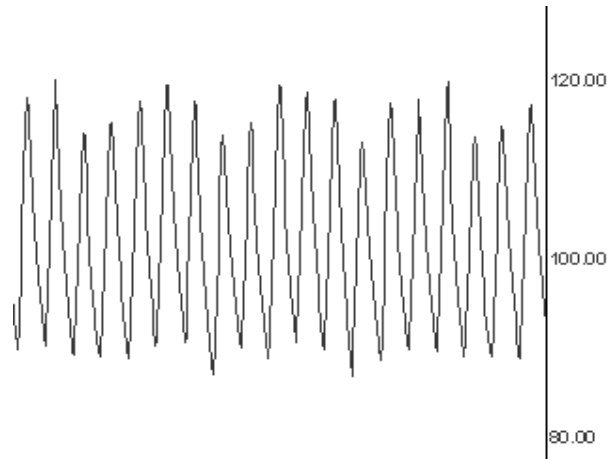


Figure 2.3 Representative recording of systemic arterial pressure. Three second representative measurement of systemic arterial pressure in mice. Y-axis expressed in mmHg.

Following measurement of RVP and SAP, mice were killed by cervical dislocation. The heart and lungs were dissected *en bloc* and placed in ice-cold physiological saline solution (PSS; pH 7.4; mmol/L, NaCl 119, NaHCO₃ 25, KCl 4.7, KH₂PO₄ 1.2, MgSO₄ 0.6, CaCl₂ 2.5, C₆H₁₂O₆ 11.1). Where appropriate, the uterus was also removed for weight measurement in female mice.

2.2.4 Right Ventricular Hypertrophy

The atria, large blood vessels and pericardial fat were dissected free from the ventricles. The right ventricular free wall (RV) was dissected from the left ventricle plus septum (LV+S) and both were dry blotted. Right ventricular hypertrophy (RVH) was assessed by weight measurement of the RV and LV+S. The ratio expressed is RV/LV+S, and used as an index of PAH.

2.2.5 Pulmonary Vascular Remodelling

Three 5µm sagittal sections of lung were elastica-Van Gieson stained and microscopically assessed for the muscularisation of pulmonary arteries (<80µm external diameter) in a blinded fashion. Remodelled arteries were confirmed by the presence of a double elastic laminae. Lung sections from 4 to 6 mice for each group were studied. Approximately 150 arteries from each sagittal lung section were assessed (~450 vessels from each animal in total). This was expressed as a percentage of pulmonary vascular remodelling (remodelled vessels/total pulmonary vessels x 100 = % pulmonary vascular remodelling).

2.3 Pulmonary Vascular Reactivity

2.3.1 Dissection

The intralobar pulmonary artery (internal diameter 200µm-250µm) from the superior (large) lobe of the left lung was studied for pulmonary vascular reactivity. Dissection was approached from the visceral surface of the lung, and the artery was positioned laterally and posterior to the secondary bronchi. Once isolated, the surrounding parenchyma and airway smooth muscle was carefully dissected free from the pulmonary artery and suspended in ice-cold PSS until use.

2.3.2 Small Vessel Wire Myography

Small vessel wire myography was performed to investigate pulmonary vascular reactivity in mice. In preparation of mounting the arteries, each organ bath chamber was filled with 5ml PSS heated to 37°C ± 0.5°C and continuously bubbled with 16% O₂, 5 % CO₂ and 79% N₂. This gas composition was used to replicate the partial pressure of O₂ (pO₂) typically observed within the lung *in vivo*. Following dissection from the lung, the intralobar pulmonary artery (~5mm length) was divided into 2mm segments. Two sections

of stainless steel wire (40µm diameter, 3cm length) were passed through the lumen and tied to their respective myograph clamp to securely position the artery. Once achieved, the artery was equilibrated for at least 20 minutes under resting/zero tension.

2.3.3 Application of Tension

The pulmonary circulation operates as a high flow, low pressure circuit. In control (non-PAH) mice, the mean PAP typically resides at 15mmHg, whilst in mice exposed to chronic hypoxia this is increased to ~30mmHg. Therefore to replicate similar conditions *in vitro*, a transmural pressure of 12-16mmHg (normoxia) or 27-32mmHg (hypoxia) was applied to the artery. Isometric tension was applied to the artery to replicate transmural pressure. Pressure was then deduced from the force of tension (Figure 2.4). For these, resting/zero tension (X_0), active tension (X_i) and passive force (F) values were required. In addition, the constant value of 2 (mm) was used for vessel length (L).

$$P_i = (2\pi) \times F/2 \times L (205.6 + (X_i - X_0))$$

Figure 2.4 Equation to calculate transmural pressure. The given value (P_i) must be divided by 0.133 in order for successful conversion to mmHg.

Tension was incrementally applied to the artery until the appropriate transmural pressure was achieved. Following this, the artery was again equilibrated under active tension for at least 20 minutes prior to the addition of 50mmol/L KCl for a 30 minute period. KCl-induced contraction was used to confirm both a contractile response is apparent, and also to normalise this contraction. This step was subsequently repeated, and a contractile response of ≥ 1 millinewton (mN) in the artery was considered sufficient to perform a cumulative concentration response curve.

2.3.4 Cumulative Concentration Response Curve

Prior to the construction of a serotonin concentration response curve, a baseline tension was established for at least 30 minutes. Serotonin (serotonin hydrochloride, Sigma-Aldrich, Poole, UK) was initially added at 1×10^{-9} mol/L and increased in 0.5 log increments until a final concentration of 1×10^{-4} mol/L was achieved. To maintain consistency between the addition of each drug concentration, the subsequent concentration was added once the vascular response had reached a plateau which was typically every three minutes. Where appropriate, all antagonists and inhibitors were added to the organ bath at least 30 minutes prior to the addition of the initial drug concentration.

2.3.5 Analysis

The contractile response to an agonist was normalised against the maximum contractile response to 50mmol/L KCl and expressed as a percentage. For comparison, the $\log EC_{50}$ (defined as the agonist concentration required to produce 50% of the maximal contraction) was generated and used as an index to describe serotonin potency. This was calculated using the 'log [Agonist] Variable Slope - Best Fit' function (Graphpad 5.0, CA, USA), which assumes baseline is 0% response and maximal contraction is 100% response. The E_{max} value, defined as the maximum contractile response generated by an agonist, was used as an index of efficacy. Where appropriate, this was used to compare the maximum contractile responses across groups.

2.4 Histology

2.4.1 Fixation

Following death, the *inferior* and *middle* lobes of the right lung were dissected free and fixed in 10% (v/v) neutral-buffered formalin (NBF; 90% dH₂O, 10% formalin, 33mmol/L

NaH₂PO₄, 45mmol/L Na₂HPO₄) for three days, under gentle agitation. Formalin-fixed lungs were then paraffin-embedded and 5µm sagittal sections cut and mounted onto salinized glass microscope slides.

2.4.2 Immunohistochemistry

5µm sagittal lung sections were deparaffinized and re-hydrated through a xylene-ethanol gradient (100% xylene > 100% ethanol > 90% ethanol > 70% ethanol; 10 minutes each step) and washed in deionised water for 10 minutes. Following hydration, heat-induced epitope retrieval (HIER/antigen retrieval) was performed by the incubation of lung sections in 10mmol/L citric acid (pH 6.0) at 90°C-100°C for 20 minutes, which was then cooled to room temperature. Lung sections were then rinsed in deionised water for 10 minutes, before endogenous peroxidase activity was blocked via incubation in methanol containing 3% (v/v) hydrogen peroxide (Sigma-Aldrich, Poole, UK) for 30 minutes at room temperature. After this, sections were washed in deionised water for 10 minutes and further PBS washed for 10 minutes. Non-specific blocking was carried out using 10% (v/v) goat serum and 5% (w/v) BSA in 0.01mol/L PBS, and incubation performed in a humidified chamber for 1 hour at room temperature. The next step was to block endogenous biotin, which was performed in a two-step process. Initially, lung sections were incubated in avidin D blocking solution for 15 minutes followed by a PBS wash, then subject to an additional incubation in biotin blocking solution for 15 minutes followed by 2 x 10 minute PBS washes. The lung sections were then incubated in a humidified chamber at 4°C overnight with primary antibody diluted in 15% (v/v) primary antiserum and 10% (w/v) BSA in PBS. The negative control slide was incubated in identical diluent, with the only exception the absence of primary antibody. Subsequent to this, sections were washed in PBS for 2 x 10 minutes at room temperature prior to the biotinylated-conjugated secondary antibody incubation. The purpose of the biotinylated-conjugated secondary

antibody was to selectively bind the primary antibody. To perform this, lung sections were incubated in a humidified chamber for 1 hour at room temperature with the appropriate secondary antibody diluted in 0.01mol/L PBS. Sections were then 3 x 10 minute PBS washed, and incubated with avidin-biotin complex (ABC) solution (Vector Laboratories, Peterborough, UK) for 1 hour at room temperature. To stop this reaction, sections were rinsed with PBS and then subjected to a further 2 x 10 minute PBS wash. For immunoperoxidase staining, the DAB Substrate kit (3,3-diaminobenzidine, hydrogen peroxide and nickel solution; Vector Laboratories, Peterborough, UK) was used and the solution was incubated with lung sections until dark brown staining was apparent, which was typically 2-5 minutes. To stop the immunoperoxidase staining reaction, sections were placed in deionised water. The lung sections were further washed in deionised water for 10 minutes before ethanol-xylene dehydration (70% ethanol > 90% ethanol > 100% ethanol > 100% xylene; 10 minutes each step). Finally, glass coverslips were mounted onto each slide using Tissue-Mount (Sakura Finetek, Alphen aan den Rijn, Netherlands). Immunostaining was visualised using a light microscope and positive protein-staining was brown/dark-brown in appearance. Where appropriate, adjacent sagittal lung sections were counter-stained with hematoxylin and eosin (H&E), which stain for the nucleus and cytoplasm respectively.

2.5 Tissue Culture

Tissue culture was performed in sterile conditions using a Biological Safety Class II vertical laminar flow cabinet. Tissue explants and cells were incubated at 37°C and maintained in 5% CO₂, 95% air. Human pulmonary artery smooth muscle cells (PASMCs) were the cellular model studied.

2.5.1 Human Pulmonary Artery Smooth Muscle Cells

Human pulmonary artery smooth muscle cells (PASMCs) were provided by Prof N.W Morrell, University of Cambridge, UK. Briefly, PASMCs were derived from the pulmonary arteries (1-3mm internal diameter) of three non-heritable idiopathic PAH (IPAH) patients. PASMCs derived from macroscopically normal lung biopsies (pulmonary arteries; 1-3mm internal diameter) excised from non-PAH donors were studied as control. The homogeneity of PASMCs was confirmed via cell morphology (Figure 2.5) and positive staining for α -smooth muscle actin. PASMCs were incubated in a 75cm² culture flask and media was aspirated and replenished every 48 hours. These were cultured in Dulbecco's Modified Eagle Medium (DMEM; Gibco, Paisley, UK) supplemented with 2mmol/L L-glutamine, antibiotic antimycotic solution (contains 100U/ml penicillin, 100 μ g/ml streptomycin, 0.25 μ g/ml amphotericin B; Sigma-Aldrich, Poole, UK) and 10% (v/v) fetal bovine serum (Sera Laboratories International, West Sussex, UK). Cells were routinely passaged when monolayer cell growth reached 95% confluency, to prevent cell growth arrest via contact inhibition. For passaging, cells were phosphate-buffered saline (PBS; 2.7mmol/L KCl, 0.137mol/L NaCl, pH 7.4) washed and twice rinsed with 0.06% (v/v) trypsin-ethylenediamine tetra-acetic acid (trypsin-EDTA; Gibco, Paisley, UK) suspended in 0.01mol/L PBS and incubated at 37°C until detached from the flask, which was typically less than 5 minutes. Trypsinization of the cells was immediately stopped following the addition of 10ml 10% (v/v) FBS DMEM which acts to neutralize trypsin, and the cell-suspension used for sub-culturing. Where appropriate, cell density was assessed via cell counts using a haemocytometer.

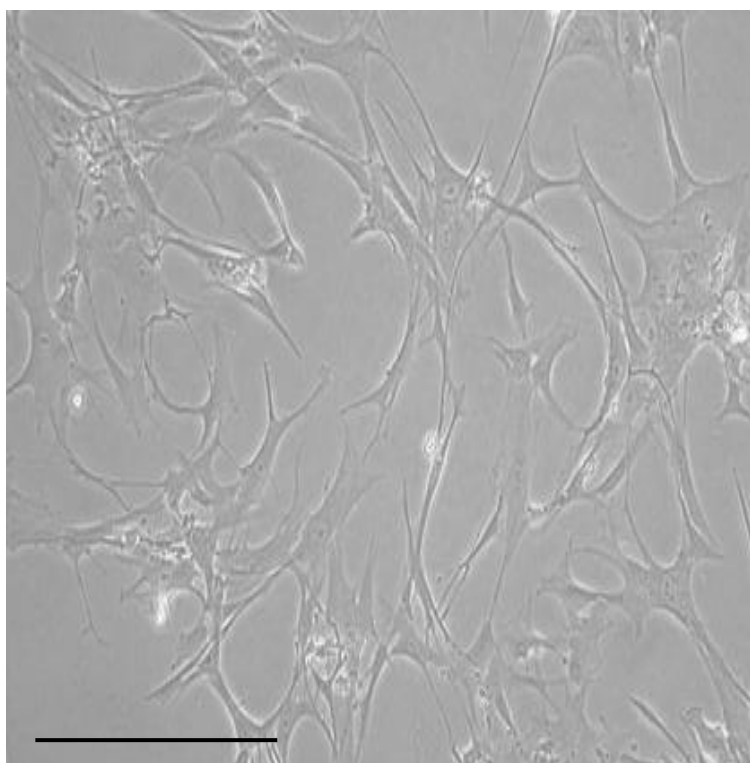


Figure 2.5 Typical morphology of human pulmonary artery smooth muscle cells.

Scale bar 100 μ m.

2.5.2 Proliferation Assays

2.5.2.1 Cell Counting

Cell counts were performed to identify total cell number. PASMCs (passage 3-7) were seeded in 24-well plates at a density of 20,000 per/well and grown to 60% confluency in 10% FBS DMEM before quiescence in 0.2% (v/v) FBS DMEM for 24 hours. PASMCs were then exposed to the required agonist (in the presence of 2.5% (v/v) FBS) and proliferation assessed at 4-5 days. Where appropriate, cells were stimulated with steroid hormone-depleted FBS for throughout experiments. For the cell counting proliferation assay, media was aspirated and 70 μ l 0.06% (v/v) trypsin-EDTA added. This was immediately aspirated and 150 μ l trypsin-EDTA added to each well and incubated at 37°C until the cells were free-suspended, which was typically 5-10 minutes. To inhibit

trypsinization, 400µl 10% FBS DMEM was simultaneously added to each well and gently mixed. The total volume of each well (550µl) was then transferred to 1.5ml tubes and centrifuged (10,000rpm) at 4°C for 10 minutes. Following this, the supernatant was carefully aspirated and the remaining cell pellet re-suspended via vortex in 200µl 10% FBS DMEM. Cell counts were performed using a haemocytometer and the mean value used to calculate the total cell number per well (mean x 2000 = cells per well). Data are expressed as total cell number.

2.5.2.2 [³H] Thymidine Incorporation

The [³H] thymidine proliferation assay is based on the use of a radioactive nucleoside ([³H] thymidine) which is incorporated into chromosomal DNA during mitosis. This is an accurate method to determine the rate of proliferation, as previously shown. PASMCS were seeded in 24-well plates at a density of 20,000 per/well and grown to 60% confluency in 10% FBS DMEM before quiescence for 24 hours. Following this, cells were then exposed to the agonist of interest for the required time. Where appropriate, all antagonists/inhibitors were added at least 30 minutes prior to the addition of agonist. For the last 24 hours, 0.2µCi [³H] thymidine was added to each well. The experiment was stopped by twice rinsing each well with 0.01mol/L PBS. Protein was precipitated by three-times washing each well with 5% (w/v) trichloroacetic acid, which was performed immediately prior to the addition of 0.3mol/L NaOH for 30 minutes. The total volume of each well (500µl) was then transferred to 1.5ml tubes and 1ml Ecoscint A scintillation fluid (Ecoscint, Atlanta, USA) added. The radioactivity level of [³H] thymidine was an index of DNA synthesis and measured using a Wallac scintillation counter (PerkinElmer, Cambridgeshire, UK). Data are expressed as percentage change compared to 2.5% FBS-induced proliferation.

2.6 Western Blotting

2.6.1 PASMCs

Human PASMCs (passage 3-7) were seeded in 6-well plates at a density of 25,000 per/well and grown to 80% confluency in 10% FBS DMEM before quiescence for 24 hours. Following agonist stimulation for the required time, experiments were stopped by 6-well plate incubation on ice. Immediately, the media was aspirated and each well PBS-rinsed three times. Ice-cold RIPA buffer (50mmol/L HEPES pH 7.5, 150mmol/L NaCl, 1% (v/v) Triton X-100, 0.5% (v/v) sodium deoxycholate, 0.1% (v/v) SDS, 0.01M sodium phosphate, 5mmol/L EDTA, 0.1mmol/L PMSF, 1µg/ml soybean trypsin inhibitor, 1µg/ml benzamidine) was then added to each well for 15 minutes, under gentle agitation. Following this, cell lysates were collected by scraping. Whole cell lysates were stored at -80°C for Western blot analysis.

2.6.2 Pulmonary Arteries

The *main*, *left* and *right* pulmonary arteries were studied for Western blot analysis. Proximal pulmonary arteries were investigated as these were the smallest that could be practically dissected from mice, and more representative of the pulmonary vasculature than whole lung analysis. Immediately following death, the arteries were dissociated free from the heart and lungs, snap-frozen in liquid N₂ and stored at -80°C until use. In order to obtain a sufficient concentration of protein for analysis, arteries from 4 mice were suspended in 250µl lysis buffer (50mmol/L tris pH 7.4, 1mmol/L DTT, 1x complete-protease inhibitor tablet; Roche Diagnostics, West Sussex, UK) and homogenised using a micro-rotary blade. Protein samples were aliquoted as required, and stored at -80°C for Western blot analysis. For protein validation of novel genes, pulmonary arteries were

isolated and prepared from age-matched littermate mice to those studied for microarray analysis.

2.6.3 SDS-PAGE

Protein was separated on the basis of their molecular weight by performing SDS-PAGE using NuPage Gel Electrophoresis system (Invitrogen, Paisley, UK) as per manufacturer's instructions. Briefly, protein samples were subjected to reducing conditions in the presence of 10 μ l 4x NuPage (lithium dodecyl sulfate) LDS sample buffer and 10x NuPage sample reducing agent (10mmol/L dithiothreitol), and heated to 70°C for 10 minutes. Samples were loaded into NuPage Novex 4%-12% Bis-Tris Mini Gels (Bis-Tris-HCl buffer pH 6.4, 4%-12% acrylamide, bis-acrylamide, 0.1% ammonium persulfate) and subjected to 150V constant in the presence of NuPage MES or MOPS running buffer. SeeBlue Plus2 pre-stained size standard was used as a surrogate for protein molecular weight. Once SDS-PAGE fractionation was complete, protein and size standard was then transferred to a polyvinylidene difluoride (PVDF) membrane (Millipore, County Durham, UK) at 30V constant for 1 hour. The protein-loaded PVDF membrane was then three-times 15 minutes washed with Tris-buffered saline (20mmol/L Tris pH 7.5, 150mmol/L NaCl) containing 0.1% (v/v) Tween-20 (TBST; Sigma-Aldrich, Poole, UK).

2.6.4 Immunoblotting

Immunoblotting was performed for protein expression analysis. Briefly, membranes were blocked for 1 hour in 5% (w/v) dried milk suspended in tris-buffered saline supplemented with 0.2% (v/v) Tween (TBST) at room temperature under gentle agitation. Following this, membranes were TBST-washed and incubated overnight at 4°C with primary antibody diluted in 5% (w/v) bovine serum albumin (BSA; Sigma-Aldrich, Poole, UK) suspended in TBST. Optimized antibody dilutions are summarized in Table 2.1.

Subsequently, membranes were TBST-washed prior to 1 hour room temperature incubation with horse-radish peroxidase (HRP) conjugated-secondary antibody diluted in 5% dried milk-TBST. Following secondary antibody incubation, membranes were TBST-washed. Protein visualisation was performed using the enhanced luminol-based chemiluminescence detection system (ECL-detection system, Amersham Bioscience UK Ltd, Buckingham, UK). To perform this, membranes were exposed to 1:1 dilution of ECL solution mix for 60 seconds, dry blotted and placed in a light-sensitive cassette. General purpose Kodak X-ray film was used for the chemiluminescent visualisation of proteins.

2.6.5 Quantitative Expression of Protein

α tubulin was used as the protein loading control, which did not overlap with the molecular weight of any protein(s) which had been previously probed on the PVDF membrane. To confirm equal protein loading, densitometry was employed. Densitometrical analysis was performed in scanned X-ray film visualised protein using TotalLab TL100 software, via calculation of the protein: α tubulin ratio. To maintain ratio consistency across biological experimental replicates, multiple α tubulin time points were assessed and analysed.

Reactive Protein	Molecular Weight	Supplier and Order Number	Antibody Description	1° Dilution	2° Dilution
TPH1	55kDa	Chemicon AB15570	Rabbit polyclonal to TPH1	1:250	Anti-rabbit HRP 1:1000
5-HT _{1B} Receptor	47kDa	Abcam AB85937	Rabbit polyclonal to 5-HT _{1B} Receptor	1:250	Anti-rabbit HRP 1:1000
SERT	70kDa	Abcam AB36127	Goat polyclonal to SERT	1:500	Anti-goat HRP 1:1000
C/EBP β	32kDa	Abcam AB32358	Rabbit polyclonal to C/EBP β	1:1000	Anti-rabbit HRP 1:1000
CYP1B1	70kDa	Abcam AB33586	Rabbit polyclonal to CYP1B1	1:500	Anti-rabbit HRP 1:1000
c-FOS	60kDa	Abcam AB7963	Rabbit polyclonal to c-FOS	1:1000	Anti-rabbit HRP 1:2000
α tubulin	50kDa	Abcam AB7291	Mouse monoclonal to α -tubulin	1:5000	Anti-mouse HRP 1:5000

Table 2.1 Immunoblotting antibody table. List of antibodies used for immunoblotting.

Primary (1°) antibodies were incubated overnight at 4°C in 5% (w/v) BSA-TBST. Secondary

(2°) antibodies were incubated for 1 hour at room temperature in 5% (w/v) dried milk-TBST.

2.7 RNA Extraction

2.7.1 Pulmonary Arteries

The *main*, *left* and *right* pulmonary arteries were studied for RNA expression analysis. Immediately following death, the arteries were dissociated free from the heart and lungs, snap-frozen in liquid N₂ and stored at -80°C in nuclease-free conditions until use. Total RNA extraction was performed in the pulmonary arteries of mice using the RNeasy Mini-Kit (Qiagen, Crawley, UK) as per manufacturer's instructions. Briefly, 400µl of buffer RLT was added to each pulmonary artery and subsequently homogenised (2 x 20Hz for 2 minutes) using the TissueLyser II (Qiagen, Crawley, UK). Buffer RLT contains guanidine isothiocyanate which immediately inactivates nucleases to ensure the isolation of intact total RNA. Samples were then incubated for 10 minutes at 55°C in proteinase K solution (10µl:590µl dilution in nuclease free water) to ensure the optimal lysis and maximum total RNA yield from the fibrous tissue. Subsequent to this, each sample was centrifuged (10,000rpm, 3 minutes, room temperature), the supernatant transferred to a 1.5ml tube and 400µl ethanol added to promote ideal binding conditions. The samples were then loaded and centrifuged (10,000rpm, 15 seconds, room temperature) into RNeasy spin columns, which results in the binding of total RNA to the silica-membrane component of the column. The spin column was then washed three times with buffer RWT before RNA elution in 30µl RNase-free water (10,000rpm, 1 minute, room temperature). To further increase total RNA yield, the 30µl volume was again centrifuged through the spin column. RNA integrity and quantification was assessed using the NanoDrop ND-1000 Spectrophotometer (Nano-Drop Technologies, Delaware, USA) and Agilent 2100 Bioanalyzer system (Agilent Technologies, Berkshire, UK). Absorbance of the RNA samples was quantified at 260 and 280 nm, and the 260/280 ratio was calculated. All samples showed a 260/280 ratio ≥ 1.9 and RNA Integrity Number (RIN) ≥ 8.0 , which was indicative of RNA purity.

2.7.2 PSMCs

RNA was extracted from PSMCs derived from IPAH patients and control using the RNeasy Mini-Kit (Qiagen, Crawley, UK). PSMCs (passage 3-5) were seeded in 6 well plates at 25,000 per well and grown to 95% confluency. Following trypsinization, PSMCs were centrifuged (10,000rpm, 10 minutes, 4°C), the media aspirated and cells re-suspended in ice cold PBS. Subsequent to this, centrifuge and aspiration was repeated and PSMCs snap-frozen in liquid N₂ and stored at -80°C in nuclease-free conditions until use.

2.7.3 DNase Treatment of RNA

Currently, no RNA extraction method is sufficient at completely eliminating DNA contamination. Therefore, DNase digestion is typically performed in RNA samples prior to microarray or qRT-PCR analysis. To perform this, DNase treatment of RNA was performed using TURBO DNA-free kit (Ambion, Texas, USA) according to manufacturer's instructions. Briefly, 10% (v/v) of TURBO DNase buffer and 1µl TURBO DNase was added to each RNA sample and incubated at 37°C for 30 minutes. To terminate this reaction, 10% (v/v) DNase Inactivation Reagent was added to each sample and incubated for 3 minutes at room temperature. The DNase free RNA samples were then centrifuged (12,000rpm, 2 minutes, room temperature) and the supernatant stored at -80°C until use.

2.7.4 cRNA Synthesis

cRNA synthesis and amplification was achieved using the Illumina TotalPrep RNA Amplification Kit (Ambion, Texas, USA) according to manufacturer's instructions. Briefly, reverse transcription with an oligo(dT) primer containing a T7 promoter (a genetically engineered reverse transcriptase which generates higher yields than wild type

reverse transcriptase enzymes) was performed in 200ng total RNA for first-strand cDNA synthesis. To do this, 9µl Reverse Transcription Master Mix was added to each sample and incubated at 42°C for 2 hours. Second-strand cDNA synthesis was then performed by adding 80µl Second Strand Master Mix to each sample and incubating at 16°C for 2 hours. Following purification, the cDNA is used as a template for in-vitro transcription (IVT) with T7 RNA polymerase. The synthesis of biotinylated cRNA was performed in the presence of 7.5µl IVT and incubated at 37°C for 14 hours, and the reaction stopped by adding 75µl RNase-free water. This biotin-labelling of cRNA is essential for streptavidin-cy3 staining following array hybridization. Following cRNA purification, which removes unincorporated nucleotide triphosphates (NTPs), enzymes and reagents, the samples were analysed for integrity using the Agilent Bioanalyzer system (Agilent Technologies, Berkshire, UK). To determine cRNA concentration (µg/ml), we used the NanoDrop ND-1000 (Nano-Drop Technologies, Delaware, USA) to obtain the A_{260} reading, which was then multiplied by 40-fold the elute volume ($A_{260} \times \text{elute volume} \times 40 = \text{cRNA } \mu\text{g/ml}$).

2.8 Microarray Analysis

Microarray analysis was used to investigate the genotypic changes associated with the development of PAH (Available online: Accession number E-MTAB-455). To perform this, microarray analysis was performed in the pulmonary arteries of normoxic and chronically hypoxic male and female SERT⁺ mice (8-10 weeks of age). Age-matched C57BL/6xCBA littermate mice were studied as controls.

2.8.1 cRNA Direct Hybridization Assay

Genome-wide cRNA microarray analysis was performed using the MouseRef-8 v1.1 Expression BeadChip (Illumina, Essex, UK) according to manufacturer's instructions.

Briefly, 750ng cRNA was loaded into each BeadChip array and incubated at 58°C for 16 hours under gentle agitation. Once cRNA direct hybridization was complete, the Beadchips were washed in 1x High-Temp Wash buffer at 55°C for 10 minutes, then subject to a series of further washes in 0.06% (v/v) E1BC buffer and nuclease free ethanol prior to incubation in Block E1 buffer for 10 minutes at room temperature, under medium agitation. Subsequent to this, each BeadChip was transferred into 2ml Block E1 buffer containing 1µg/ml streptavidin-Cy3 and incubated at room temperature for 10 minutes, under medium agitation. A third room temperature wash was then performed in 0.06% (v/v) E1BC buffer for 5 minutes. BeadChips were then dried by centrifuge (350rpm) at 25°C for 4 minutes, and immediately scanned with a BeadStation 500GX (Illumina, Essex, UK). Each beadchip contained approximately 25,600 probe sets which represented a total of ~19,100 unique genes. The direct hybridization signal strength of a gene was indicative of its expression.

2.8.2 Statistical Analysis

Microarray data was analysed with BeadStudio software (Illumina). Hybridisation signal strength was normalised to the median array and expression levels determined using the Average Normalisation Beadstudio algorithm. For identifying differentially expressed genes, the following parameters (as recommended by Illumina) were used: P value <0.05, Diff Score >15, Average Signal >100.

2.9 Quantitative Real-time PCR

Quantitative real-time PCR (RT-PCR) was employed to validate results obtained from microarray analysis. For validation, RNA extracted from mice studied for microarray was pooled into comparative groups (n=4, repeated in triplicate) and analysis performed.

Gene-specific primers corresponding to the PCR targets were designed based on published sequences in GenBank using the primer 3 program and synthesised by IDT (Integrated DNA Technologies, Belgium). We confirmed the absence of nonspecific amplification by examining PCR products by agarose gel electrophoresis ensuring amplification of single discrete bands with no primer-dimers. Real-time PCR was carried out in a DNA Engine OPTICON2 (MJ Research). Each reaction was performed according to the Brilliant II SYBRGreen PCR Master Mix (Agilent Technologies, Berkshire, UK) protocol, using 10ng of RNA. Three replicates were performed for each sample plus template-free samples as negative controls. Cycling parameters consisted of an initial reverse transcription step for 40 minutes at 50°C, followed by a 10 minute incubation at 95°C to fully activate the DNA polymerase and 40 amplification cycles at 95°C for 30 seconds, 56°C - 58°C for 30 or 40 seconds, and 72°C for 30 seconds. Fluorescence measurements were assessed at the end of the annealing phase at 78°C, 82°C, and 86°C. The CT values were determined using the Opticon2 software, and the total amount of RNA was normalised against β actin.

2.10 Statistical Analysis

Data were analyzed using a two-way ANOVA followed by Bonferroni's post-hoc test, one-way ANOVA followed by Dunnett's post-hoc test or unpaired t-test as appropriate, and described in figure legend. Data are expressed as mean \pm SEM.

Chapter 3

The Serotonin Transporter, Gender and 17 β Estradiol in the Development of Pulmonary Arterial Hypertension

3.1 Introduction

Pulmonary arterial hypertension (PAH) is characterised by both remodelling and vasoconstriction of the pulmonary vasculature. Mutations in the gene encoding for the bone morphogenetic protein receptor-2 (BMPR-II) are accountable for ~80% of heritable PAH cases, however penetrance for this gene is incomplete as only 20% of BMPR-II mutation carriers develop PAH (Newman et al., 2004). Therefore, it is assumed that other genetic or environmental risk factors are involved. This is the basis of the ‘multiple hits’ hypothesis in PAH.

In both idiopathic and heritable forms of PAH there is a gender bias, with females up to three-fold more likely to present with disease (Peacock et al., 2007; Humbert et al., 2006; Thenappan et al., 2007). Despite this, the reasons underlying this female susceptibility remain unknown. Estrogens are one possible risk factor in PAH. The ingestion of oral contraceptives have previously been associated with PAH (Masi, 1976; Morse et al., 1999) and female PAH patients show increased expression levels of ESR1 (estrogen receptor 1), the gene encoding for ER α , compared to unaffected females (Rajkumar et al., 2010). Decreased expression of the estrogen-metabolising enzyme cytochrome P450 1B1 (CYP1B1) leading to altered estrogen metabolism has also been identified in female PAH patients harbouring a BMPR-II mutation compared to unaffected female carriers (Austin et al., 2009).

In contrast, experimental models of PAH have repeatedly shown that female rodents exhibit less severe PAH compared to males. For example, female rats exposed to chronic hypoxia develop moderate PAH compared with severe PAH in males (Rabinovitch et al., 1981). Ovariectomized rats exhibit severe PAH following hypoxic insult and this is attenuated with 17 β estradiol treatment (Resta et al., 2001). In addition, male ApoE -/-

mice prescribed a high-fat diet develop a more established PAH phenotype compared against high-fat treated ApoE ^{-/-} females (Hansmann et al., 2007). This absence of a suitable animal model which replicates the female bias observed in human PAH has limited experimental research to date.

Multiple studies have implicated serotonin, the serotonin transporter (SERT) and 5-HT_{1B} receptors in the pathobiology of PAH. In mice the development of hypoxia-induced PAH and dexfenfluramine-induced PAH are dependent on peripheral serotonin synthesis (Morecroft et al., 2007; Dempsey et al., 2008). SERT expression is increased in human pulmonary artery smooth muscle cells (PASMCs) derived from idiopathic PAH (IPAH) patients and this is responsible for increased serotonin-induced proliferation in these cells (Eddahibi et al., 2001). The 5-HT_{1B} receptor mediates human pulmonary arterial vasoconstriction (Morecroft et al., 1999) and is also involved in PASMC proliferation (Morecroft et al., 2010).

In the central nervous system, estrogens regulate expression of multiple serotonin pathway mediators including tryptophan hydroxylase (Pecins-Thompson et al., 1996) (TPH; the rate-limiting enzyme in serotonin synthesis) and SERT (Lu et al., 2003). We have previously shown that mice over-expressing the SERT (SERT⁺ mice) develop PAH and severe hypoxia-induced PAH (MacLean et al., 2004). Here, we investigated the possible interactions between serotonin and estrogens in human PASMCs and SERT⁺ mice.

3.2 Results

3.2.1 Male SERT+ Mice Do Not Develop Spontaneous PAH or

Exaggerated Hypoxia-induced PAH Compared to Wildtype Mice

We investigated the effects of gender on the development of PAH in SERT+ mice. Firstly, we assessed right ventricular systolic pressure (RVSP), pulmonary vascular remodelling and right ventricular hypertrophy (RVH) in male SERT+ mice. This was also investigated in male SERT+ mice following exposure to chronic hypoxia. Male SERT+ mice did not develop PAH or exaggerated hypoxia-induced PAH compared to male WT mice, as indicated by no differences in RVSP, pulmonary vascular remodelling or RVH (Figure 3.1). Similarly, no changes in mean systemic arterial pressure (MAP; Figure 3.2) or heart rate (HR; Figure 3.3) were reported. To further investigate, PAH was assessed in female SERT+ mice.

3.2.2 Female SERT+ Mice Develop Spontaneous PAH and Exaggerated

Hypoxia-Induced PAH via the Effects of 17 β Estradiol

The effects of gender, ovariectomy, SERT and 17 β estradiol were investigated in the development of PAH in SERT+ mice. In normoxia, sham-operated female SERT+ mice demonstrated increased RVSP (Figure 3.4) and pulmonary vascular remodelling (Figure 3.5). Representative resistance pulmonary arteries also appeared remodelled to a greater extent in these mice (Figure 3.6). This was apparent in the absence of RVH (Figure 3.7). Absolute RV, LV+S and body weight of these mice is summarized in Table 3.1, and haemodynamics summarized in Table 3.2. The increased RVSP and pulmonary vascular remodelling observed in female SERT+ mice was abolished following ovariectomy (OVX). We subsequently hypothesized that the pre-dominant female hormone 17 β estradiol was critical to the development of PAH in these mice. To examine, this, SERT+

OVX mice were subject to chronic 17β estradiol administration (1.5mg/kg/21 days). This successfully re-established increased RVSP and pulmonary vascular remodelling in these mice. RVH was similar in both wildtype and SERT+ mice, and ovariectomy had no further effect on this. However, ovariectomized SERT+ mice administered 17β estradiol exhibited a decrease in RVH. Following their exposure to chronic hypoxia, female SERT+ mice exhibited an exaggerated PAH phenotype, as assessed by a greater increase in both RVSP and pulmonary vascular remodelling compared to wildtype mice. This exaggerated hypoxia-induced PAH phenotype was attenuated in ovariectomized SERT+ mice, and increases in both RVSP and pulmonary vascular remodelling were re-established following 17β estradiol administration in these mice. The extent of RVH was also more pronounced in chronically hypoxic female SERT+ mice, however was unaffected following ovariectomy. We further observed that the administration of 17β estradiol decreased RVH in the hypoxic SERT+ mice. No differences in MAP (Figure 3.8) or HR (Figure 3.9) were reported. Of additional interest, we also observed that hypoxia-induced PAH was more established in male wildtype mice than female wildtype mice. This was confirmed by a marked elevation in both RVSP and pulmonary vascular remodelling in these males compared to females.

This evidence suggests a critical role for female hormones in the development of PAH in SERT+ mice. To further investigate this, we were also interested in assessing the effects of hormone depletion in WT mice. Ovariectomy was performed in WT mice and PAH was assessed in both normoxia and following exposure to chronic hypoxia.

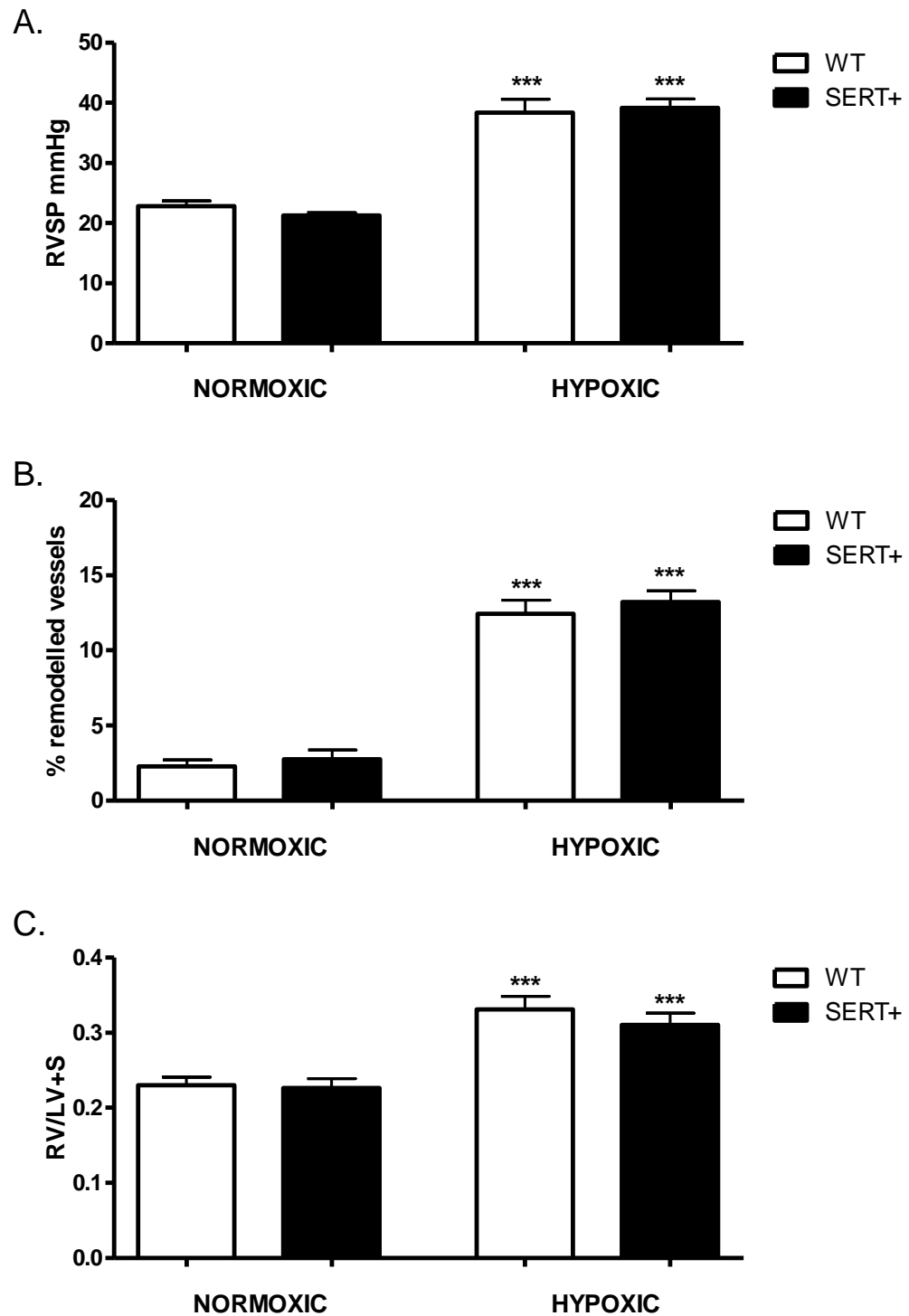


Figure 3.1 Male SERT⁺ mice do not exhibit spontaneous PAH or exaggerated hypoxia-induced PAH compared to male WT mice. Right ventricular systolic pressure (RVSP; A), pulmonary vascular remodelling (% remodelled vessels; B) and right ventricular hypertrophy (RVH; C) is similar in male wildtype and male SERT⁺ mice in both normoxia and following exposure to chronic hypoxia. Data are expressed as mean \pm SEM and analysed by two-way ANOVA followed by Bonferroni's post-hoc test. ***P<0.001 cf. normoxic mice. n=8-12.

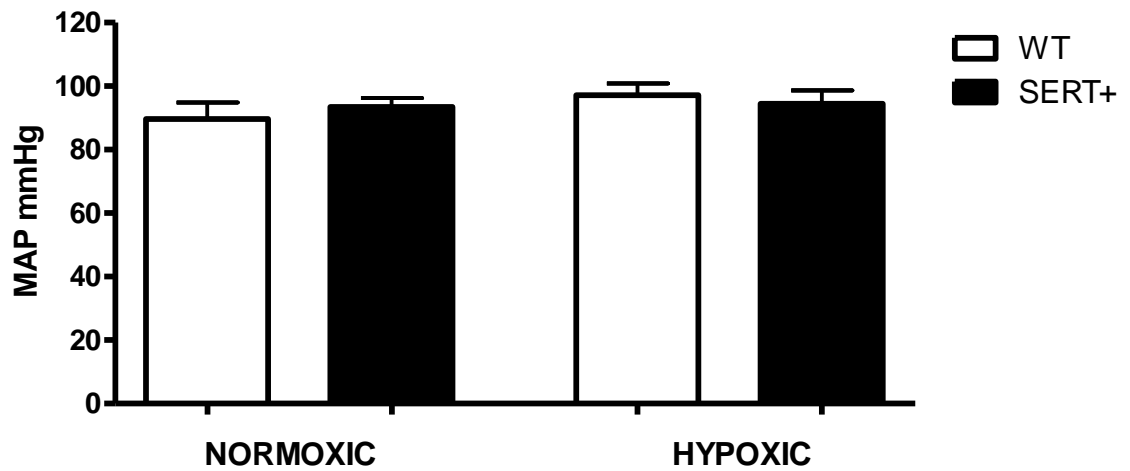


Figure 3.2 Male SERT+ mice exhibit similar systemic arterial pressure to male WT mice. Mean systemic arterial pressure (MAP) is unaffected in both normoxic and chronically hypoxic SERT+ mice compared to their respective wildtype controls. Data are expressed as mean \pm SEM; n=7-9.

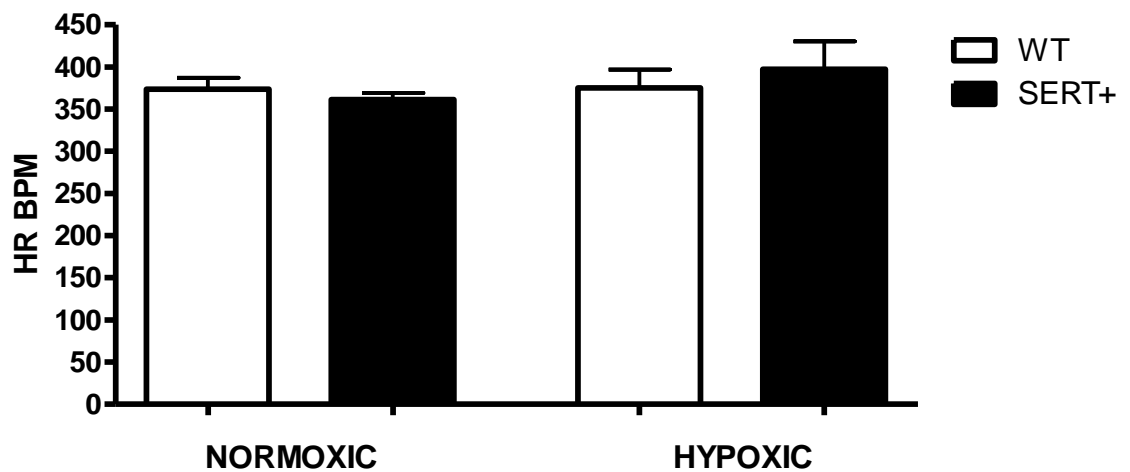


Figure 3.3 Male SERT+ mice exhibit a similar heart rate to male WT mice. Heart-rate (HR) is unaffected in both normoxic and chronically hypoxic SERT+ mice compared to their respective wildtype controls. Data are expressed as mean \pm SEM; n=7-9.

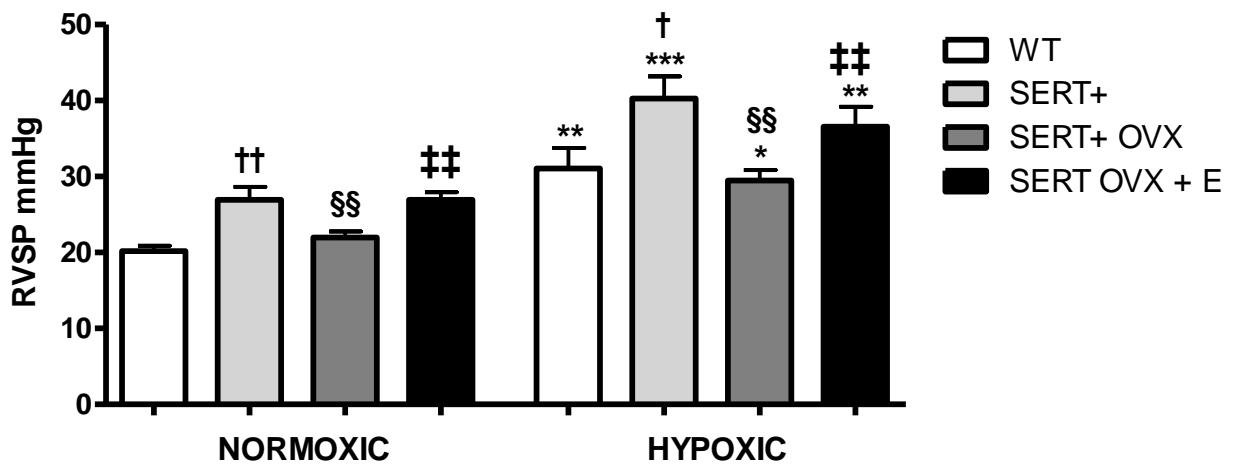


Figure 3.4 Female SERT+ mice exhibit increased RVSP in normoxia and chronic hypoxia, via the effects of 17 β estradiol. Sham-operated SERT+ mice (SERT+) exhibit increased RVSP compared to sham-operated wildtype (WT) mice. Ovariectomized SERT+ mice (SERT+ OVX) exhibit a decrease of RVSP, and this is fully re-established following the administration of 17 β estradiol (SERT+ OVX + E). In chronic hypoxia, SERT+ mice develop increased RVSP compared to WT mice. SERT+ OVX mice exhibit an attenuated hypoxia-induced elevation of RVSP and this is increased following the administration of 17 β estradiol. Data are expressed as mean \pm SEM and analysed by two-way ANOVA followed by Bonferroni's post-hoc test. * P <0.05, ** P <0.01, *** P <0.001 cf. normoxic mice; † P <0.05, †† P <0.01 cf. wildtype mice; §§ P <0.01 cf. sham-operated mice; ‡‡ P <0.01 cf. vehicle-dosed mice. n=6-9.

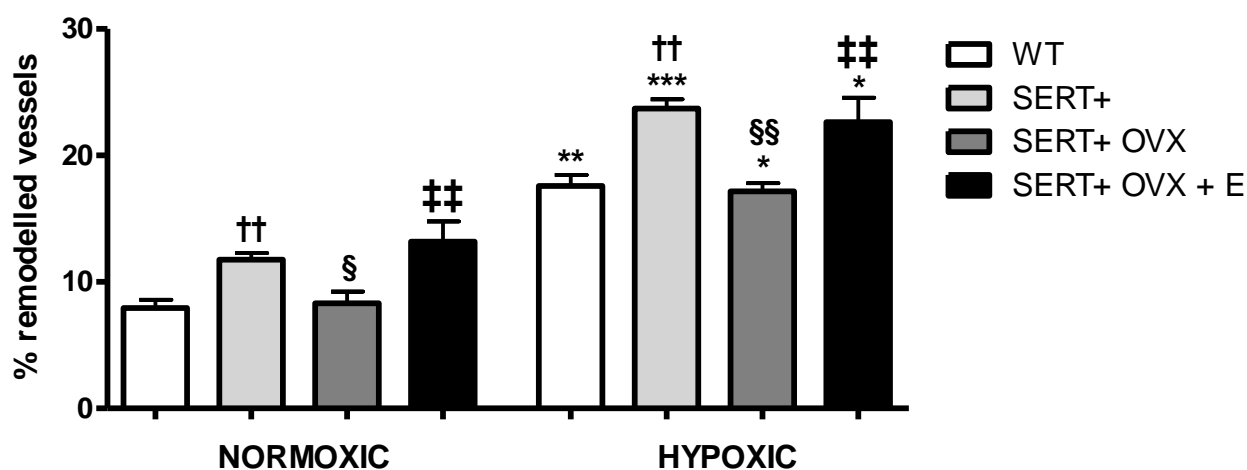


Figure 3.5 Female SERT+ mice exhibit increased pulmonary vascular remodelling in normoxia and chronic hypoxia, via the effects of 17 β estradiol. Sham-operated SERT+ mice (SERT+) exhibit increased pulmonary vascular remodelling compared to sham-operated wildtype (WT) mice. Ovariectomized SERT+ mice (SERT+ OVX) exhibit a reduction in pulmonary vascular remodelling, and this is fully re-established following the administration of 17 β estradiol in these mice (SERT+ OVX + E). In chronic hypoxia, SERT+ mice develop increased pulmonary vascular remodelling compared to WT mice. SERT+ OVX mice exhibit attenuated pulmonary vascular remodelling, and this is increased following the administration of 17 β estradiol. Data are expressed as mean \pm SEM and analysed by two-way ANOVA followed by Bonferroni's post-hoc test. *P<0.05, **P<0.01, ***P<0.001 cf. normoxic mice; ††P<0.01 cf. wildtype mice; §P<0.05, §§P<0.01 cf. sham-operated mice; ‡‡P<0.01 cf. vehicle-dosed mice. n=5.

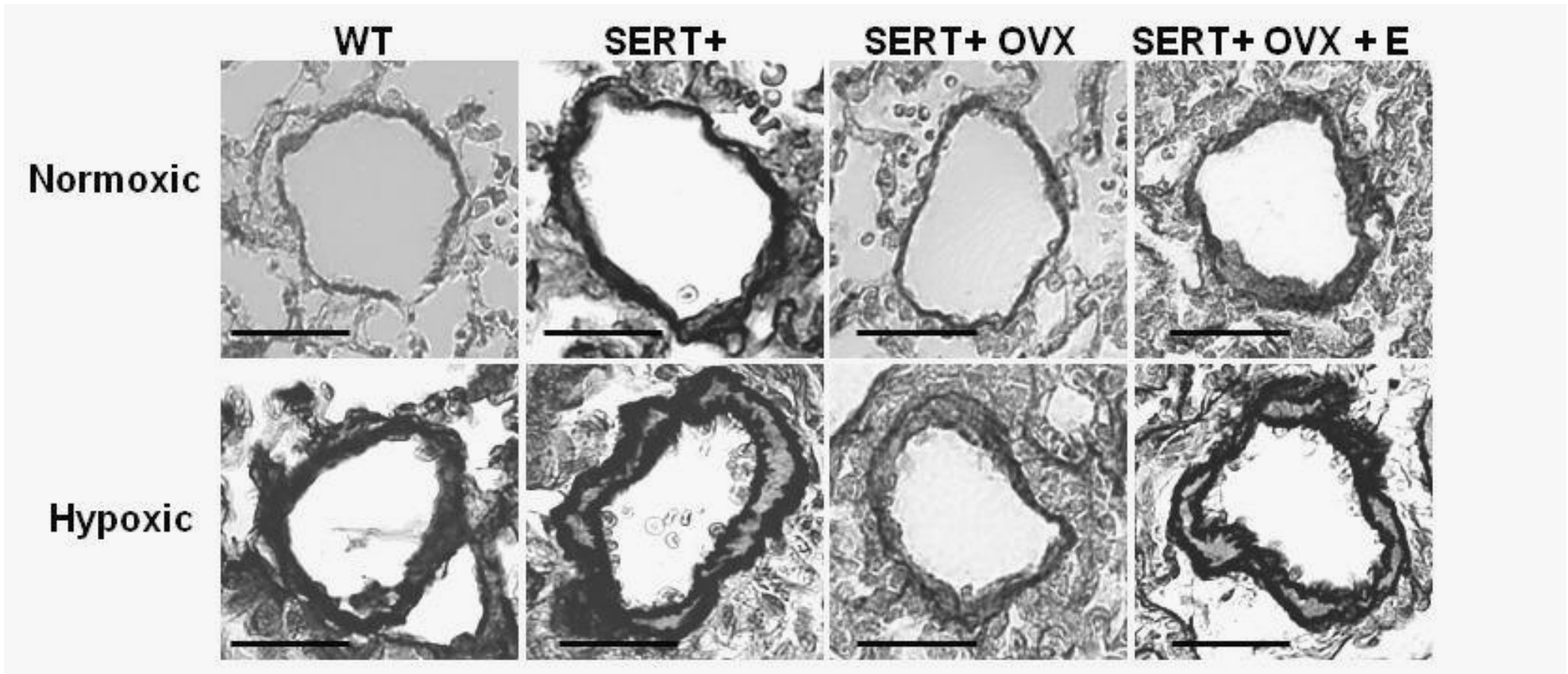


Figure 3.6 Photomicrographs of representative resistance pulmonary arteries in SERT+ mice. Pulmonary arteries are stained with elastica-Van Gieson from both normoxic and hypoxic female WT and female SERT+ mice (Scale bar 50 μ m). SERT+ mice exhibit remodelling to a greater extent than WT mice and this is attenuated following ovariectomy however can be re-established following the administration of 17 β estradiol (E).

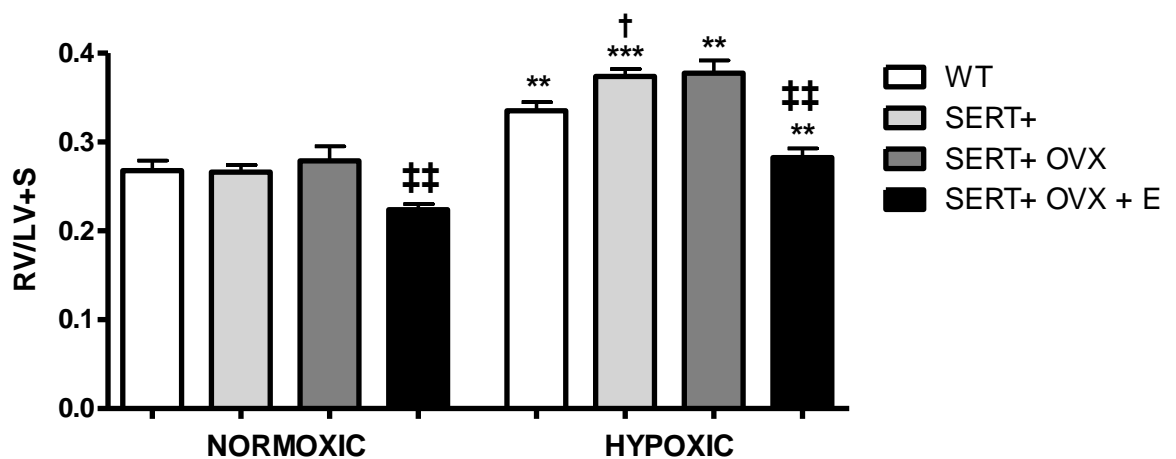


Figure 3.7 Female ovariectomized SERT+ mice exhibit reduced right ventricular hypertrophy in normoxia and chronic hypoxia, via the effects of 17 β estradiol. Right ventricular hypertrophy (RVH) is unaffected in sham-operated SERT+ mice compared to sham-operated wildtype mice (WT). Ovariectomized SERT+ mice (SERT+ OVX) also exhibit RVH to a similar extent. However, the administration of 17 β estradiol reduces RVH in these mice (SERT+ OVX + E). In chronic hypoxia, SERT+ mice develop increased RVH compared to WT mice. RVH is unchanged in SERT+ OVX mice, however is reduced following the administration of 17 β estradiol in these mice. Data are expressed as mean \pm SEM and analysed by two-way ANOVA followed by Bonferroni's post-hoc test. **P<0.01, ***P<0.001 cf. normoxic mice; †P<0.05 cf. wildtype mice; ††P<0.01 cf. vehicle-dosed mice. n=6-9.

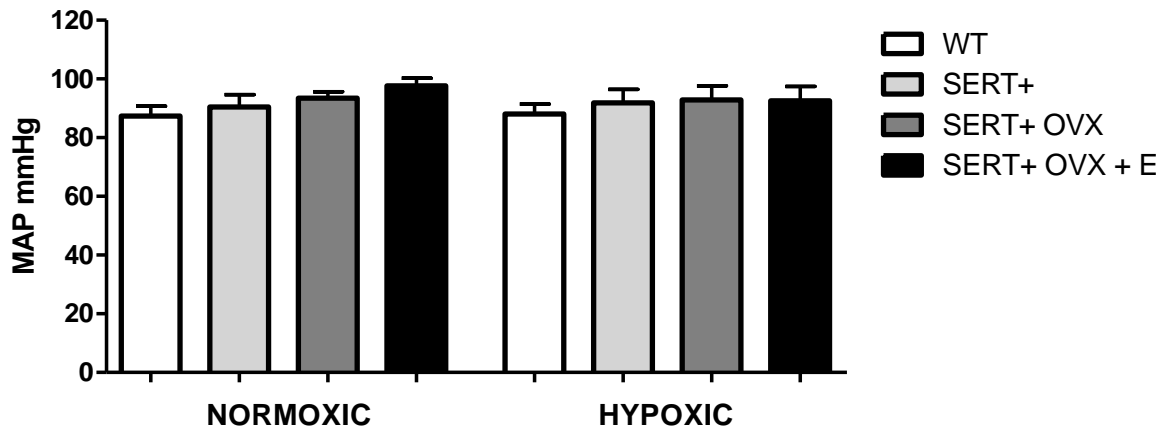


Figure 3.8 Female SERT+ mice exhibit no change in systemic arterial pressure compared to female wildtype mice, and this is further unaffected by ovariectomy or 17 β estradiol. Mean systemic arterial pressure (MAP) is unchanged in normoxic and chronically hypoxic SERT+ mice compared to their respective wildtype controls. Similarly, this is further unaffected following ovariectomy or 17 β estradiol administration. Data are expressed as mean \pm SEM; n=6-9.

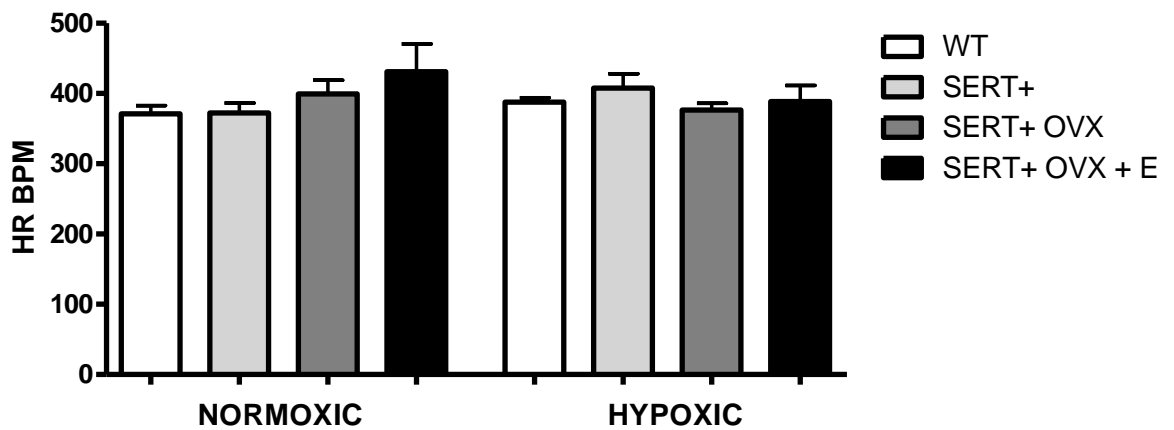


Figure 3.9 Female SERT+ mice exhibit no change in heart rate compared to female wildtype mice, and this is further unaffected by ovariectomy or 17 β estradiol. Heart rate (HR) is unchanged in both normoxic and chronically hypoxic SERT+ mice compared to their respective wildtype controls. Similarly, this is further unaffected following ovariectomy or 17 β estradiol administration. Data are expressed as mean \pm SEM; n=6-9.

<i>Group</i>	RV (mg)	LV+S (mg)	RV/LV+S	Body Weight (g)
<i>Normoxic</i>				
Wildtype				
Sham	19.34 ± 0.78	73.31 ± 1.19	0.26 ± 0.013	24.75 ± 0.99
Ovariectomy	20.84 ± 1.15	78.03 ± 3.54	0.26 ± 0.014	29.30 ± 0.94 ^{§§}
SERT+				
Sham	17.70 ± 0.66	67.94 ± 2.52	0.25 ± 0.009	21.34 ± 0.86
Ovariectomy	22.04 ± 0.88	78.08 ± 2.06	0.27 ± 0.009	22.62 ± 0.53
Ovariectomy + vehicle	23.92 ± 0.75	85.42 ± 3.10	0.28 ± 0.016	21.44 ± 0.80
Ovariectomy + estradiol	19.91 ± 0.58	90.50 ± 5.65	0.22 ± 0.008 ^{‡‡}	20.97 ± 0.73
<i>Hypoxic</i>				
Wildtype				
Sham	22.86 ± 0.92	70.77 ± 2.85	0.32 ± 0.014 ^{**}	21.23 ± 1.02
Ovariectomy	24.48 ± 1.09	66.31 ± 1.86	0.36 ± 0.012	21.36 ± 1.02
SERT+				
Sham	25.04 ± 0.97	73.30 ± 2.76	0.34 ± 0.015 ^{**}	20.12 ± 0.89
Ovariectomy	26.42 ± 1.17	67.67 ± 3.99	0.39 ± 0.018 ^{***}	20.77 ± 0.41
Ovariectomy + vehicle	28.11 ± 1.02	75.97 ± 4.11	0.38 ± 0.014 ^{**†}	21.83 ± 0.56
Ovariectomy + estradiol	26.96 ± 1.85	96.29 ± 5.98	0.28 ± 0.011 ^{**‡‡}	20.28 ± 0.71

Table 3.1 Ventricle and body weight in WT and SERT+ mice. Right ventricle (RV) weight, left ventricle plus septum (LV+S) weight, RV/LV+S ratio and body weight. **P<0.01, ***P<0.001 cf. normoxic mice; †P<0.05 cf. WT mice; ‡‡P<0.01 cf. vehicle mice; §§P<0.01 cf. sham mice. Data expressed as mean ± SEM. n=8-11.

<i>Parameter</i>	WT sham	SERT+ sham	SERT+ OVX	SERT+ OVX+ E₂
<i>Normoxic</i>				
RVSP, mmHg	20.19 ± 0.72	26.93 ± 1.73 ^{††}	21.99 ± 0.77 ^{§§}	26.95 ± 0.99 ^{‡‡}
RVMP, mmHg	7.59 ± 0.46	9.99 ± 0.70 [†]	8.07 ± 0.41 [§]	9.97 ± 0.53 [‡]
RVDP, mmHg	1.26 ± 0.29	1.39 ± 0.33	1.11 ± 0.24	1.44 ± 0.60
SAP, mmHg	109 ± 4.56	112 ± 6.46	116 ± 7.20	121 ± 9.48
MAP, mmHg	87.37 ± 3.34	90.50 ± 4.19	93.43 ± 4.24	97.62 ± 5.23
DAP, mmHg	76.2 ± 2.23	79.75 ± 2.99	87.14 ± 3.87	85.93 ± 2.11
Heart rate, bpm	370 ± 12	372 ± 14	399 ± 20	431 ± 40
<i>Hypoxic</i>				
RVSP, mmHg	31.07 ± 2.69 ^{**}	40.28 ± 2.91 ^{***†}	29.47 ± 1.36 ^{*§§}	36.55 ± 2.62 ^{**‡‡}
RVMP, mmHg	12.58 ± 1.32 ^{**}	16.16 ± 1.71 ^{***}	12.40 ± 0.99 ^{**§}	15.06 ± 1.44 ^{**‡}
RVDP, mmHg	3.34 ± 0.55 [*]	4.15 ± 0.59 ^{**}	3.87 ± 0.78 [*]	4.29 ± 0.95 [*]
SAP, mmHg	112 ± 6.69	117 ± 9.00	118 ± 9.54	114 ± 10.22
MAP, mmHg	88.01 ± 3.45	91.83 ± 4.58	92.83 ± 4.85	92.56 ± 4.90
DAP, mmHg	76.78 ± 1.79	73.50 ± 3.21	79.57 ± 2.88	81.84 ± 1.84
Heart rate, bpm	388 ± 12	408 ± 20	376 ± 9	388 ± 23

Table 3.2 Haemodynamics in WT and SERT+ mice. Right ventricular systolic pressure (RVSP), right ventricular mean pressure (RVMP), right ventricular diastolic pressure (RVDP), systemic systolic arterial pressure (SAP), mean arterial pressure (MAP), diastolic arterial pressure (DAP) and heart rate measurements in normoxic and chronically hypoxic female WT and SERT+ mice. ovariectomy, OVX; 17 β estradiol, E₂ *P<0.05, **P<0.01, ***P<0.001 cf. normoxic mice; †P<0.05, ††P<0.01 cf. WT mice; §P<0.05, §§P<0.01 cf. SERT+ mice; ‡P<0.05, ‡‡P<0.01 cf. SERT+ OVX mice. Data expressed as mean + SEM. n=6-9.

3.2.3 Ovariectomized Wildtype Mice Develop PAH

We also studied the effects of ovariectomy on the development of PAH in wildtype mice. In normoxia, we observed that ovariectomized mice developed increased RVSP and pulmonary vascular remodelling compared to sham-operated mice (Figure 3.10). Increases in both of these indices were observed in the absence of increased RVH. In chronic hypoxia, ovariectomized females did not develop exaggerated hypoxia-induced PAH, as assessed by no further elevation of RVSP, pulmonary vascular remodelling and RVH compared to sham-operated mice. No effect on MAP (Figure 3.11) or HR (Figure 3.12) was reported in ovariectomized mice.

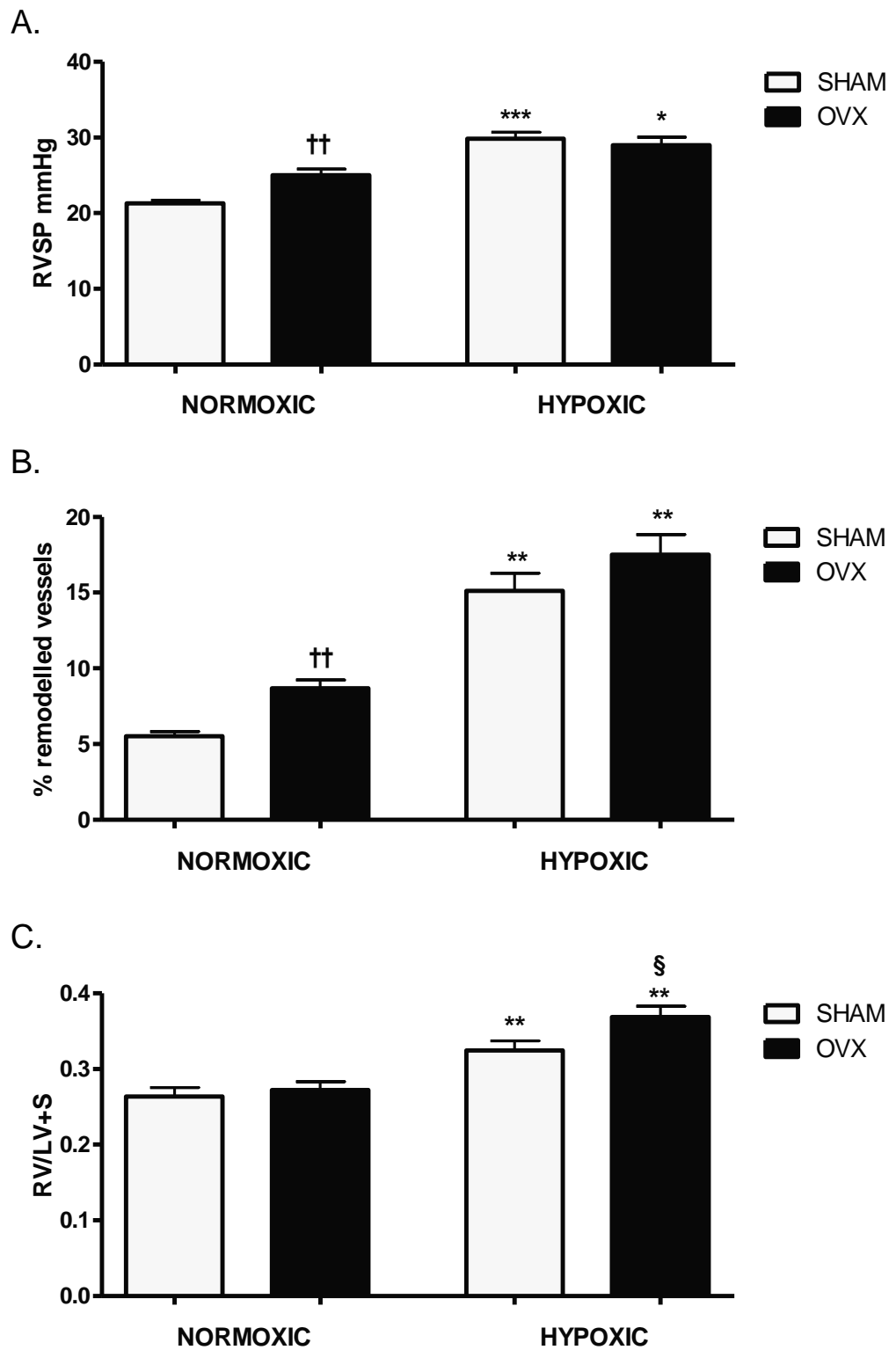


Figure 3.10 Ovariectomized wildtype mice exhibit PAH. OVX WT mice exhibit increased RVSP (A) and PVR (B). Increased RVH (C) is reported in chronically hypoxic OVX mice compared to chronically hypoxic sham mice. Data are expressed as mean \pm SEM and analysed by two-way ANOVA followed by Bonferroni's post-hoc test. * $P < 0.05$, ** $P < 0.01$, *** $P < 0.001$ cf. normoxic mice; †† $P < 0.01$ cf. normoxic sham mice; § $P < 0.05$ cf. hypoxic sham mice. $n = 8-10$.

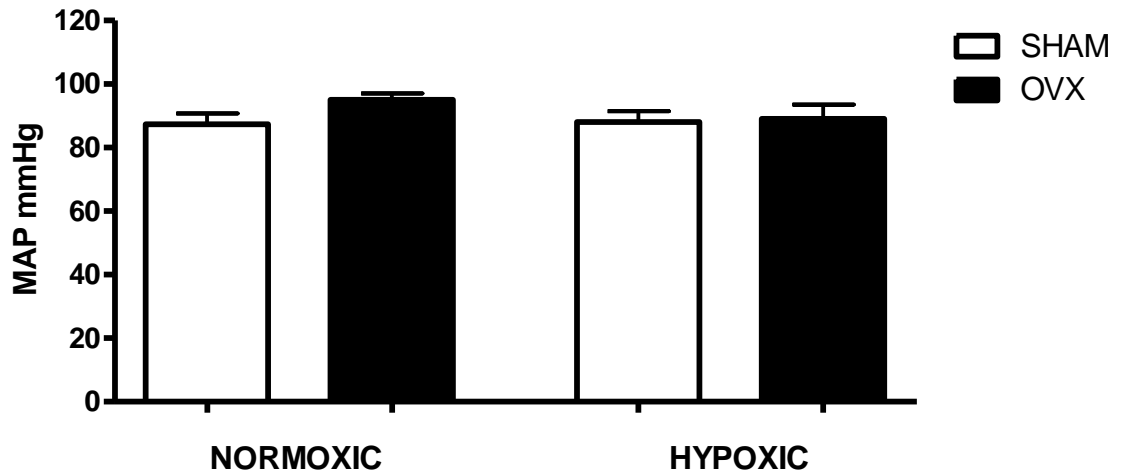


Figure 3.11 Ovariectomy has no effect on systemic arterial pressure in either normoxic or chronically hypoxic wildtype mice. Mean systemic arterial pressure (MAP) is unaffected in normoxic and chronically hypoxic mice following ovariectomy. Data are expressed as mean \pm SEM; n=7-8.

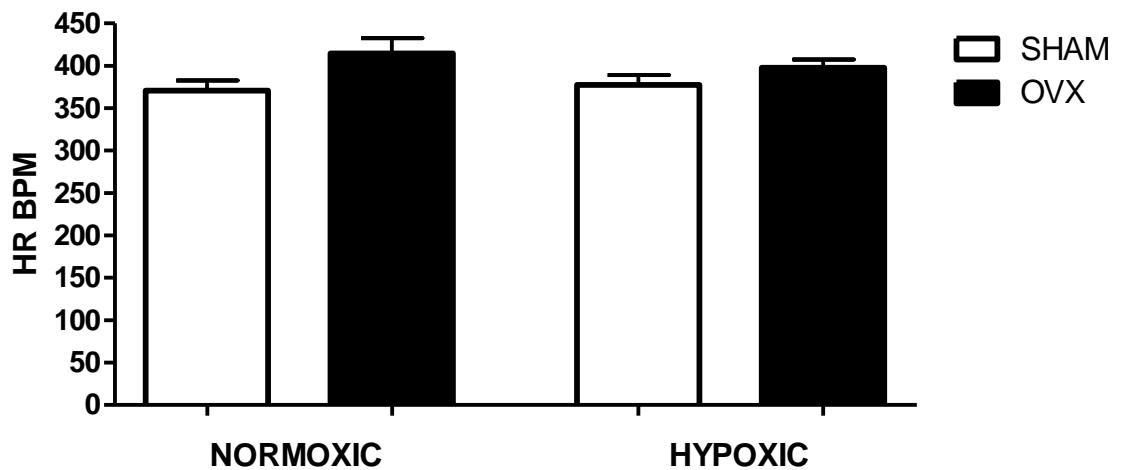


Figure 3.12 Ovariectomy has no effect on heart rate in either normoxic or chronically hypoxic wildtype mice. Heart rate (HR) is unaffected in normoxic and chronically hypoxic mice following ovariectomy. Data are expressed as mean \pm SEM; n=7-8.

3.2.4 Ovariectomy Increases Body Weight and Decreases Uterine Weight

To confirm that ovariectomy was successfully performed in mice, we assessed body weight and uterine weight. In ovariectomized WT mice, we observed a marked increase in body weight (Figure 3.13) whilst a decrease in uterine weight (Figure 3.14) was recorded in all ovariectomized groups, indicative of successful removal of the ovaries. Similar observations have been previously reported in mice following ovariectomy (Windahl et al., 2009). Further, increased uterine weight was observed in 17β estradiol-treated ovariectomized SERT+ mice, as a consequence of 17β estradiol-mediated uterine hypertrophy.

3.2.5 Male SERT+ Mice Do Not Develop PAH Following 17β Estradiol Administration

We previously observed that 17β estradiol is critical to the development of spontaneous PAH and exaggerated hypoxia-induced PAH in female SERT+ mice. To further investigate the role of this hormone in SERT+ mice *in vivo*, we administered male SERT+ mice with 17β estradiol (1.5mg/kg/21 days) to determine if this established a PAH phenotype. We observed that 17β estradiol did not uncover a PAH phenotype in these mice, as assessed by no change in RVSP, pulmonary vascular remodelling or RVH (Figure 3.15). Similarly, no changes in MAP (Figure 3.16) or HR (Figure 3.17) were reported in these mice.

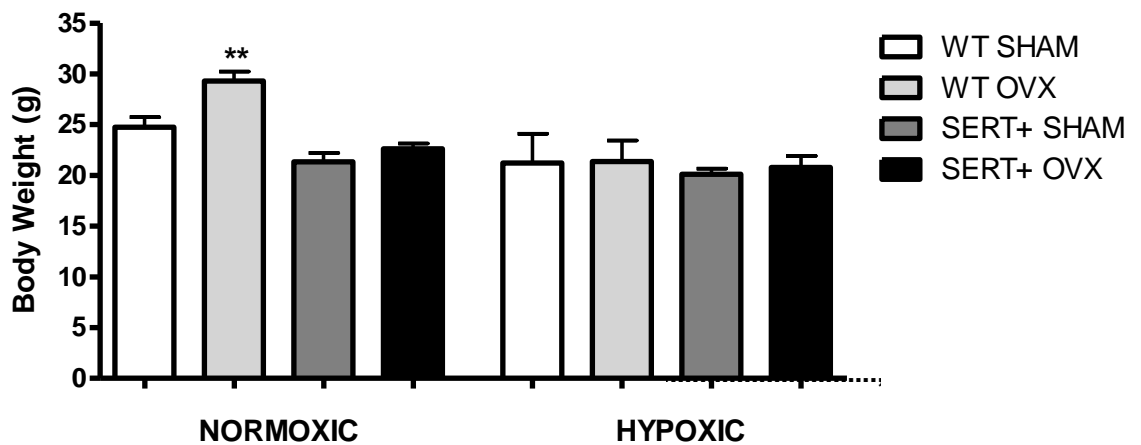


Figure 3.13 Body weight is increased in wildtype mice following ovariectomy. WT mice exhibit increased body weight following ovariectomy however SERT+ mice remain unaffected. Data are expressed as mean \pm SEM and analysed by two-way ANOVA followed by Bonferroni's post-hoc test; **P<0.01 cf. sham-operated controls. n=8-11.

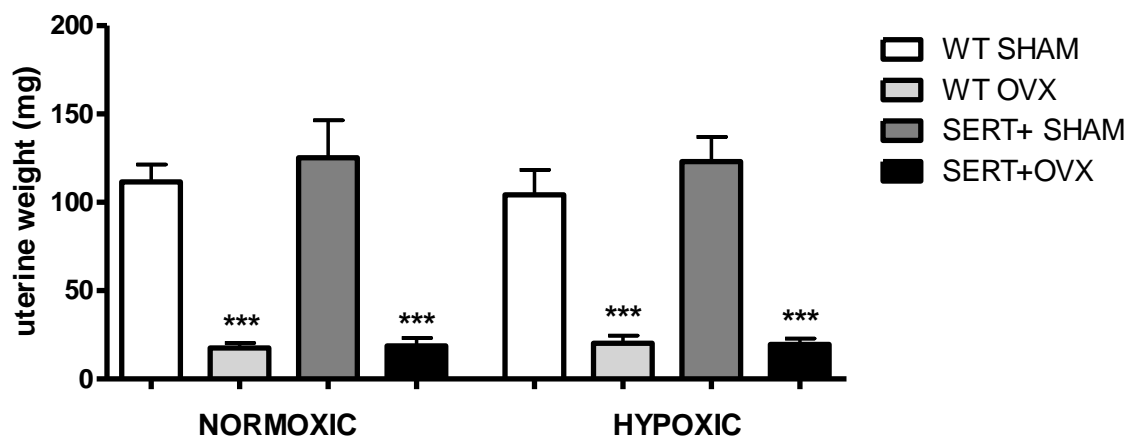


Figure 3.14 Uterine weight is decreased in normoxic and chronically hypoxic ovariectomized wildtype and SERT+ mice. Uterine weight is decreased in both wildtype and SERT+ mice following ovariectomy. Data are expressed as mean \pm SEM and analysed by two-way ANOVA followed by Bonferroni's post-hoc test; ***P<0.001 cf. sham-operated controls. n=10-11.

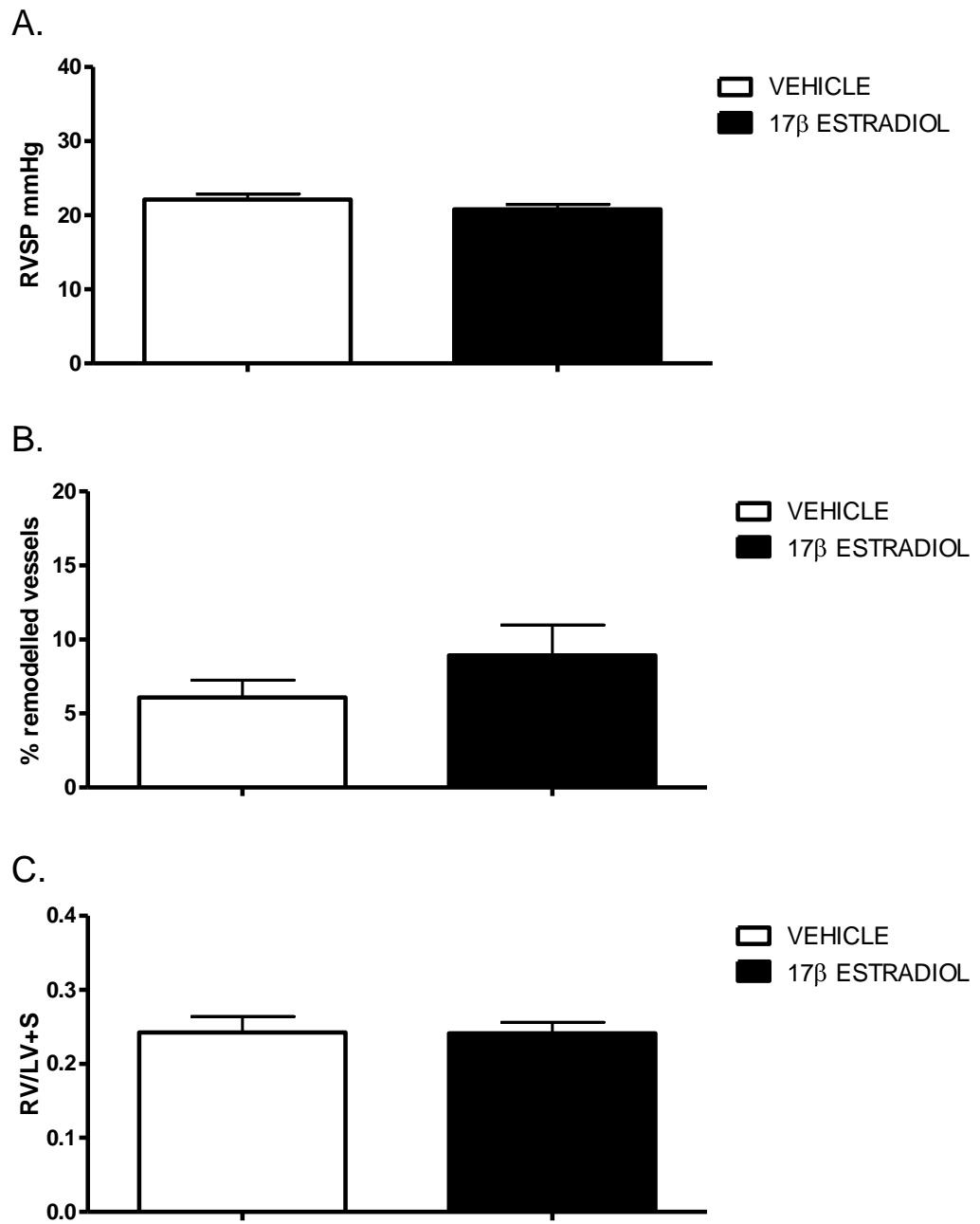


Figure 3.15 17β estradiol has no effect on PAH phenotype in male SERT+ mice. 17β estradiol administration does not increase RVSP (A), PVR (B) or RVH (C) in male SERT+ mice. Data are expressed as mean ± SEM. n=9-12.

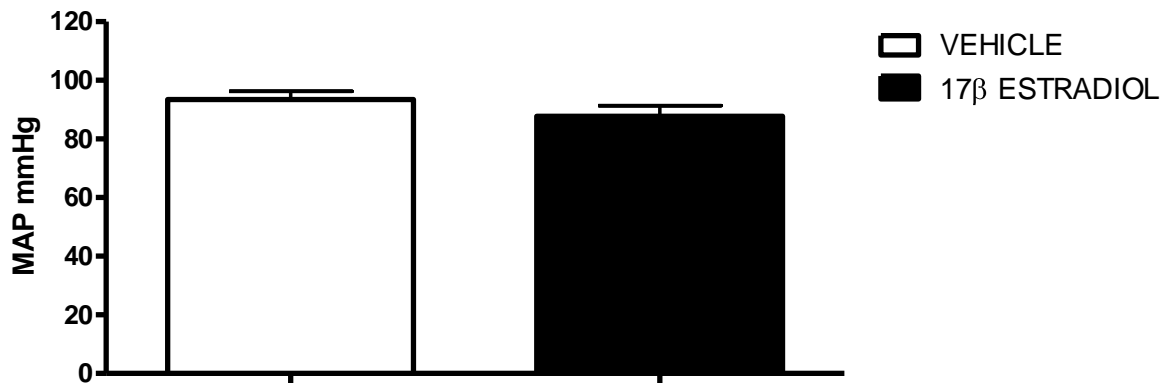


Figure 3.16 17β estradiol has no effect on systemic arterial pressure in male SERT+ mice. Mean systemic arterial pressure (MAP) is similar in normoxic and chronically hypoxic male SERT+ mice dosed with 17β estradiol when compared against their vehicle-dosed controls. Data are expressed as mean \pm SEM; n=8-9.



Figure 3.17 17β estradiol has no effect on heart rate in male SERT+ mice. Heart rate (HR) is similar in normoxic and chronically hypoxic male SERT+ mice dosed with 17β estradiol when compared against their vehicle-dosed controls. Data are expressed as mean \pm SEM; n=8-9.

3.2.6 17β Estradiol Prevents Hypoxia-Induced PAH in Male Wildtype Mice

Previously, we reported that ovariectomized WT mice develop moderate PAH. We were interested in further investigating the effects of 17β estradiol in the development of PAH in WT mice. In normoxia, the administration of 17β estradiol had no effect on RVSP, pulmonary vascular remodelling or RVH in male WT mice. In chronic hypoxia, 17β estradiol protected against the development of PAH via a reduction in RVSP, pulmonary vascular remodelling and RVH (Figure 3.18). We observed no effects on MAP (Figure 3.19) or HR (Figure 3.20) in 17β estradiol-dosed male WT mice compared to their vehicle-dosed WT controls.

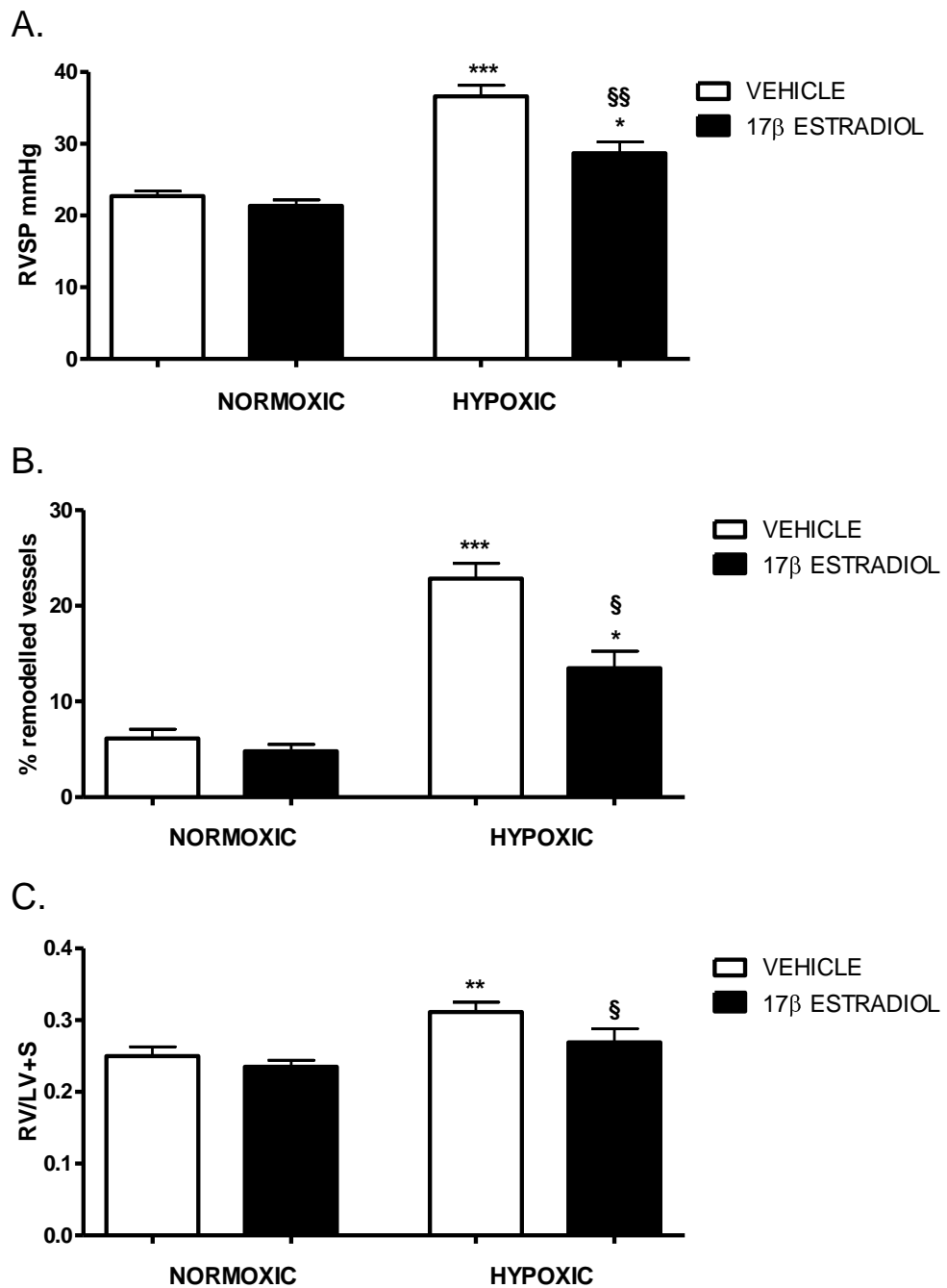


Figure 3.18 17 β estradiol attenuates hypoxia-induced PAH in male wildtype mice.

17 β estradiol attenuates RVSP (A), PVR (B) and RVH (C) in chronically hypoxic male wildtype mice. No effects are reported in normoxia. Data are expressed as mean \pm SEM and analysed by two-way ANOVA followed by Bonferroni's post-hoc test. *P<0.05, **P<0.01, ***P<0.001, cf. normoxic mice; §P<0.05, §§P<0.01 cf. vehicle-dosed mice. n=7-9.

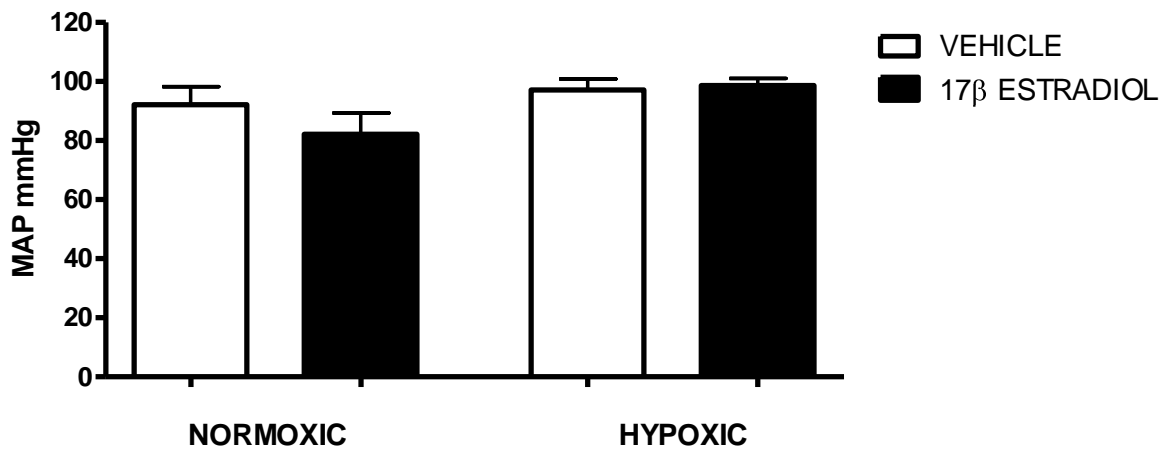


Figure 3.19 17 β estradiol has no effect on systemic arterial pressure in normoxic and chronically hypoxic male wildtype mice. Mean systemic arterial pressure (MAP) is similar in normoxic and chronically hypoxic male wildtype mice dosed with 17 β estradiol, when compared against their respective vehicle-dosed controls. Data are expressed as mean \pm SEM; n=8-9.

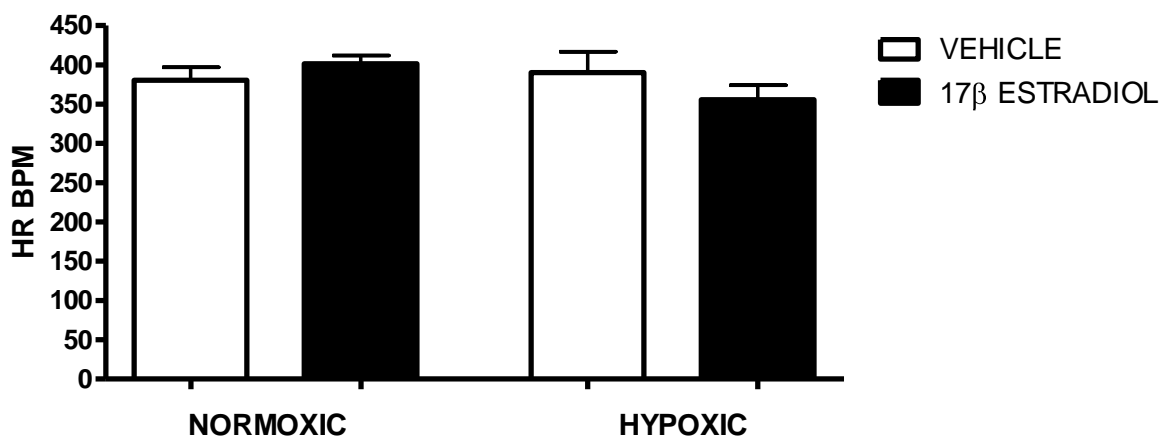


Figure 3.20 17 β estradiol has no effect on heart rate in normoxic and chronically hypoxic male wildtype mice. Heart rate (HR) is similar in normoxic and chronically hypoxic male wildtype mice dosed with 17 β estradiol, when compared against their respective vehicle-dosed controls. Data are expressed as mean \pm SEM; n=8-9.

3.2.7 Effects of Ovariectomy and 17 β Estradiol on Serotonin Induced Pulmonary Vascular Contraction

To determine if pulmonary vascular reactivity is affected in mice following ovariectomy or 17 β estradiol administration, we assessed serotonin-induced vasoconstriction in the pulmonary arteries. As previously reported, the potency of serotonin is decreased in SERT⁺ mice and this was not further affected following ovariectomy. Serotonin-induced vasoconstriction was also similar in both ovariectomized and sham-operated wildtype mice (Figure 3.21). Similarly, ovariectomy had no effect on serotonin-induced vasoconstriction in the pulmonary arteries of chronically hypoxic wildtype and SERT⁺ mice (Figure 3.22). As ovariectomized SERT⁺ mice develop PAH following the administration of 17 β estradiol, we were also interested in investigating any possible changes in pulmonary vascular reactivity. However, no changes in serotonin-induced vasoconstriction were apparent in either normoxic (Figure 3.23) or chronically hypoxic (Figure 3.24) 17 β estradiol-dosed SERT⁺ mice compared to vehicle-dosed SERT mice.

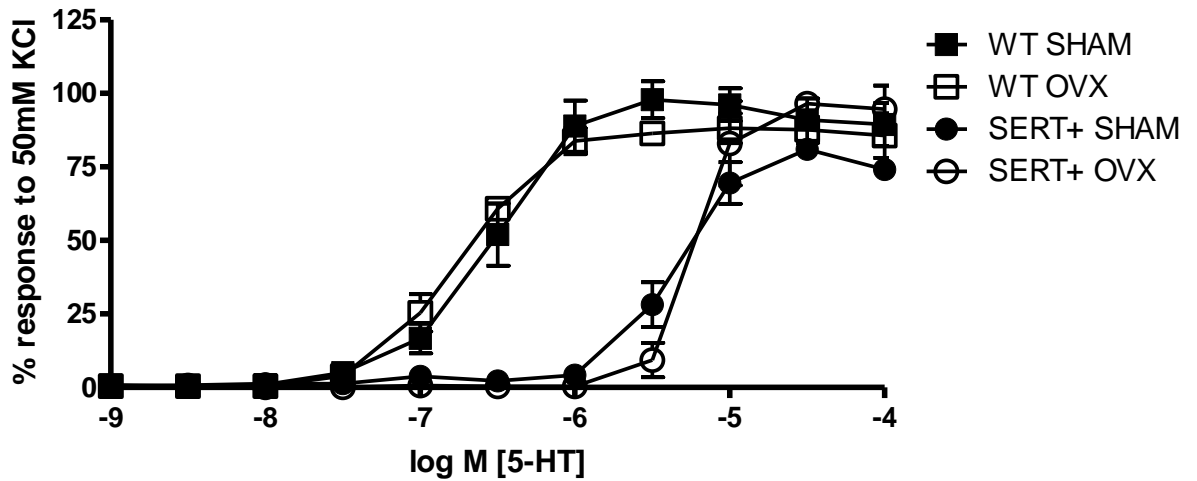


Figure 3.21 Serotonin-induced pulmonary arterial contraction is unaffected following ovariectomy in both normoxic wildtype and SERT+ mice. The potency of serotonin is decreased in the pulmonary arteries of SERT+ mice compared to wildtype mice, however is unaffected following ovariectomy. Data are expressed as mean \pm SEM. n=6-8.

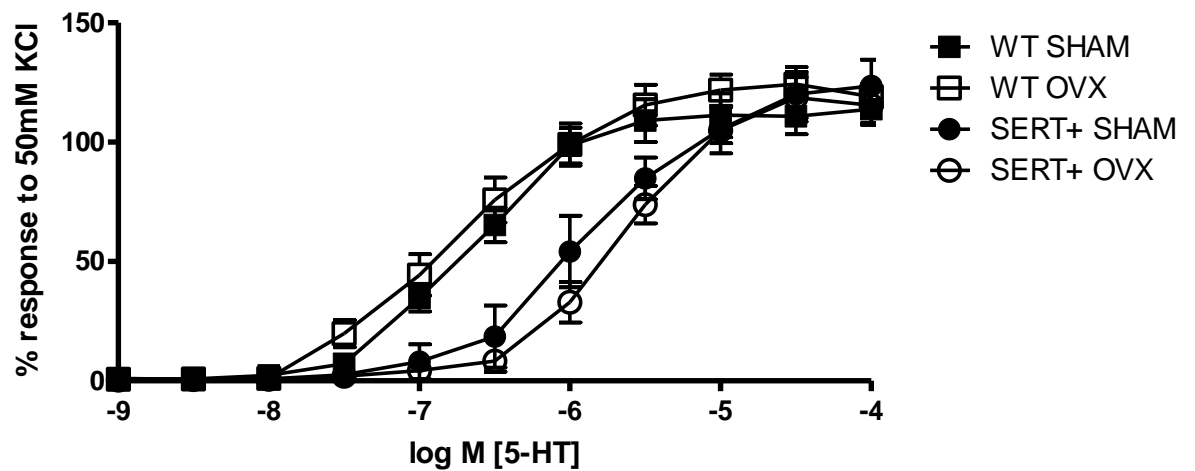


Figure 3.22 Serotonin-induced pulmonary arterial contraction is unaffected following ovariectomy in chronically hypoxic wildtype and SERT+ mice. The potency of serotonin is decreased in the pulmonary arteries of SERT+ mice compared to wildtype mice, however is unaffected following ovariectomy. Data are expressed as mean \pm SEM. n=6-7.

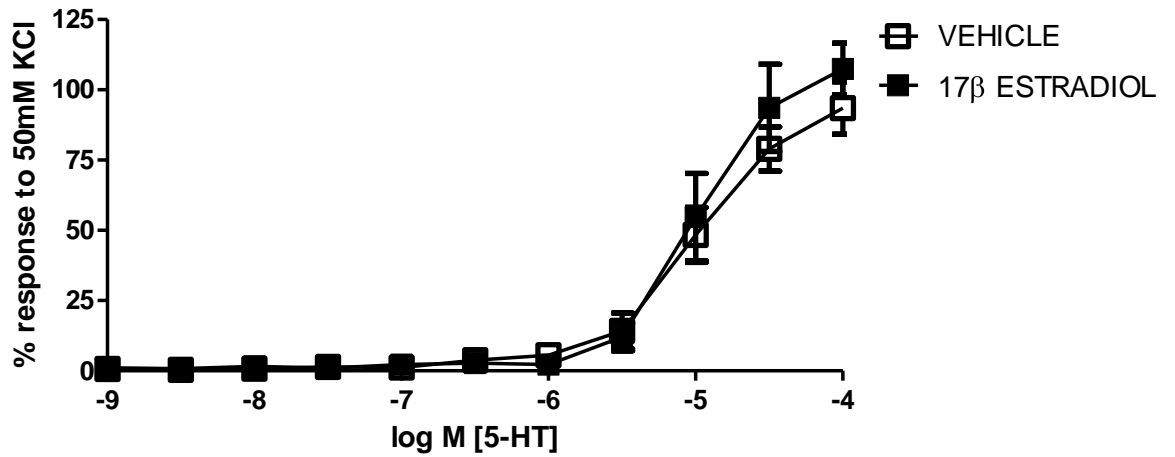


Figure 3.23 Serotonin-induced pulmonary arterial contraction is unaffected following 17β estradiol administration in ovariectomized SERT+ mice. Data are expressed as mean \pm SEM. n=6.

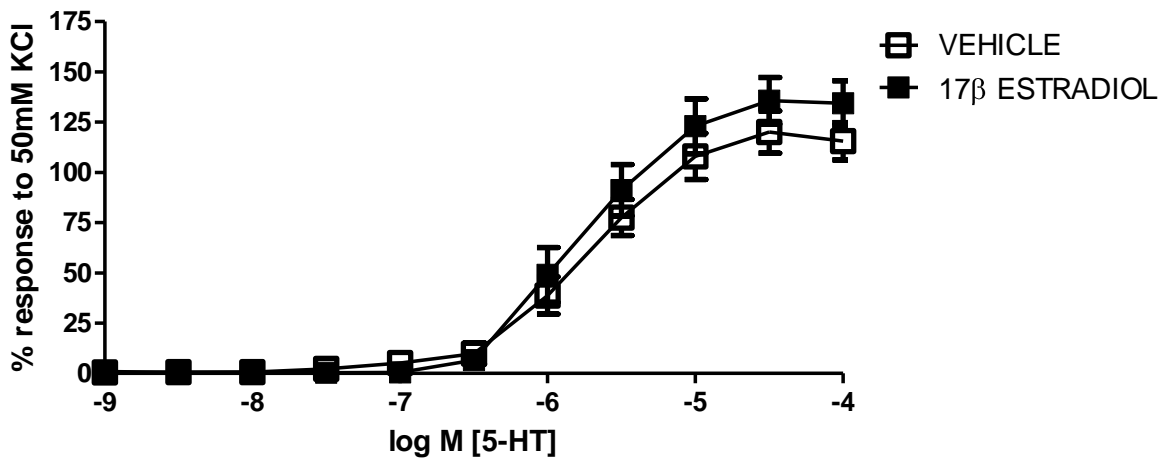


Figure 3.24 Serotonin-induced pulmonary arterial contraction is unaffected following 17β estradiol administration in chronically hypoxic ovariectomized SERT+ mice. Data are expressed as mean \pm SEM. n=6.

3.2.8 Effects of 17 β Estradiol, Estrone, Estriol and Progesterone in PSMCs

In summary of our *in vivo* findings, we identified that female SERT⁺ mice develop spontaneous PAH and exaggerated hypoxia-induced PAH whilst male SERT⁺ mice remain unaffected, compared to their respective WT controls. Through multiple intervention studies we confirmed that ovariectomy reversed PAH in SERT⁺ mice, and disease was successfully re-established following 17 β estradiol administration. Collectively, this evidence suggests a critical role for 17 β estradiol in the progression of PAH in SERT⁺ mice. To further test this hypothesis, male SERT⁺ mice were subjected to 17 β estradiol administration. However SERT⁺ males failed to develop PAH, confirming that 17 β estradiol effects are limited to SERT⁺ females. In WT mice, ovariectomy resulted in the development of PAH, whilst 17 β estradiol attenuated hypoxia-induced PAH in males, suggesting that female hormones and 17 β estradiol are protective against PAH in WT mice. To further delineate the role of female hormones in PAH, we assessed their effects in cultured pulmonary vascular cells.

We examined the effects of 17 β estradiol on human pulmonary artery smooth muscle cell (PASM) proliferation. This was investigated at physiological circulating concentrations (0.1-1nmol/L). For comparison, we also examined the effects of estrone, estriol and progesterone on PASM proliferation. At 1nmol/L, 17 β estradiol stimulated PASM proliferation (Figure 3.25) as assessed by increased cell number and DNA synthesis, whereas estrone (Figure 3.26), estriol (Figure 3.27) and progesterone (Figure 3.28) had no effect on PASM proliferation. These proliferative effects of 17 β estradiol are consistent with our *in vivo* findings.

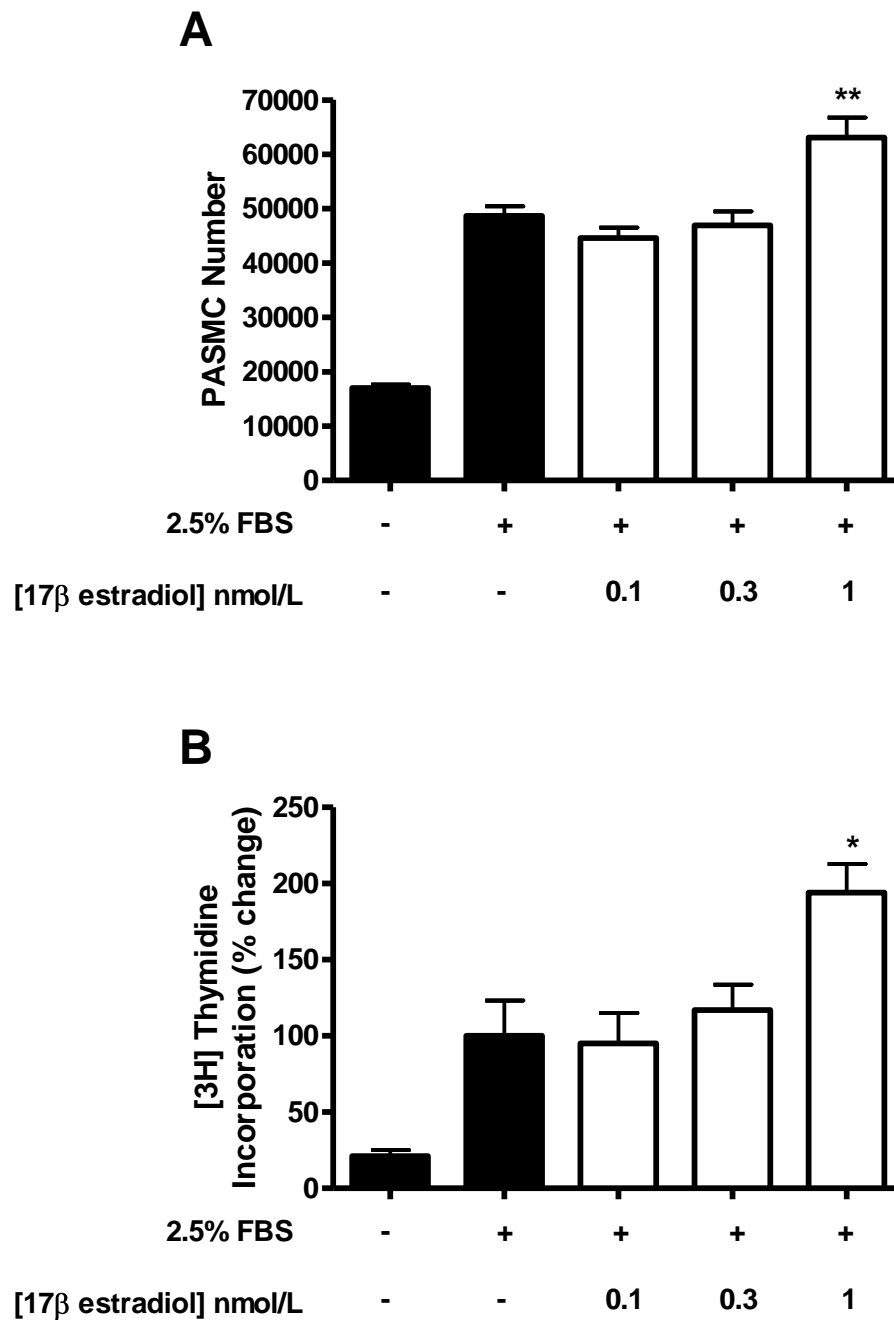


Figure 3.25 17β estradiol stimulates human pulmonary artery smooth muscle cell proliferation. 17β estradiol stimulates both cell number (A) and DNA synthesis (B) in PASMCs at 1nmol/L. *P<0.05, **P<0.01 increased proliferation cf. 2.5% FBS stimulation. Data are expressed as mean ± SEM and analysed by one-way ANOVA followed by Dunnett's post-hoc test. n=3 and performed in duplicate.

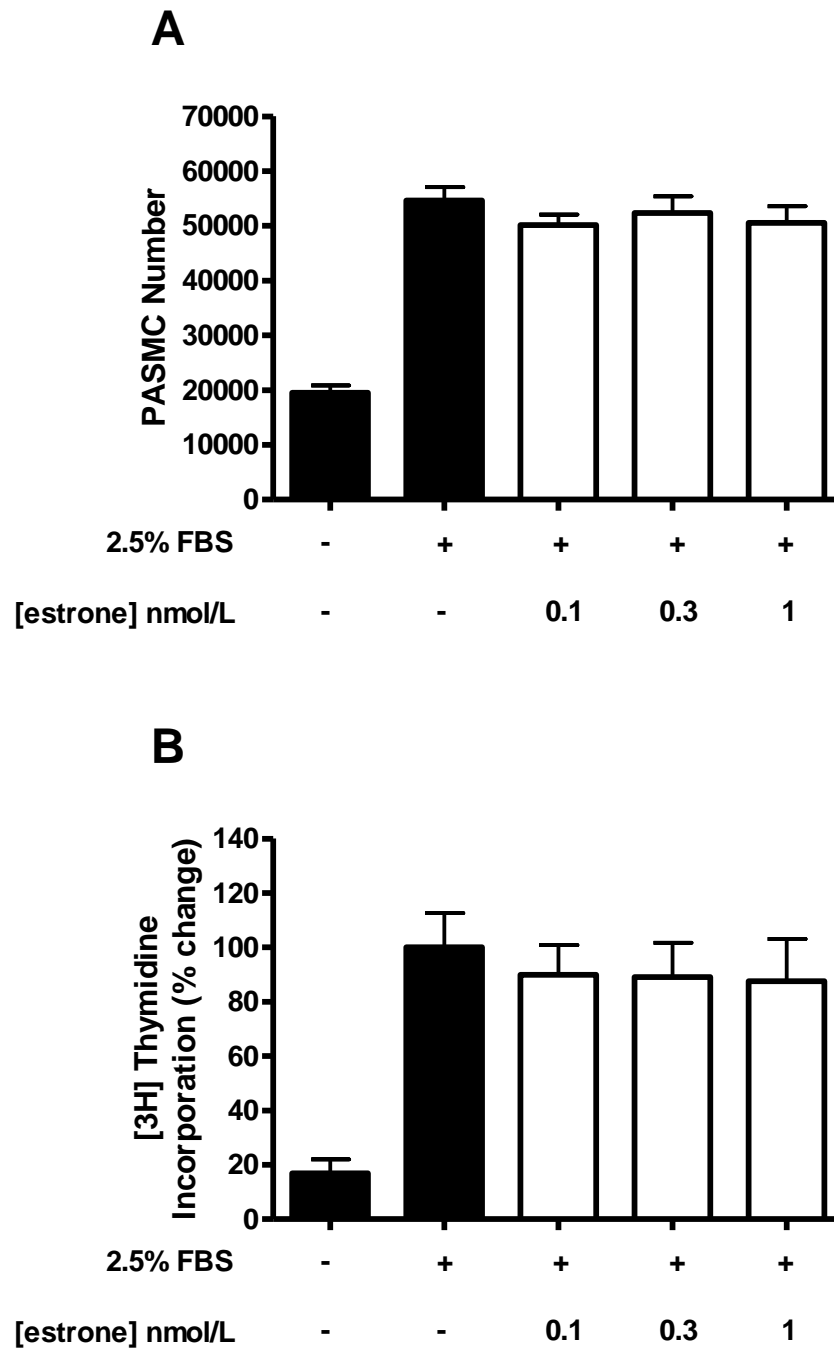


Figure 3.26 Estrone has no effect on human pulmonary artery smooth muscle cell proliferation. Estrone has no effect on cell number (A) or DNA synthesis (B) at a range of concentrations (0.1-1nmol/L). Data are expressed as mean \pm SEM. n=3 and performed in duplicate.

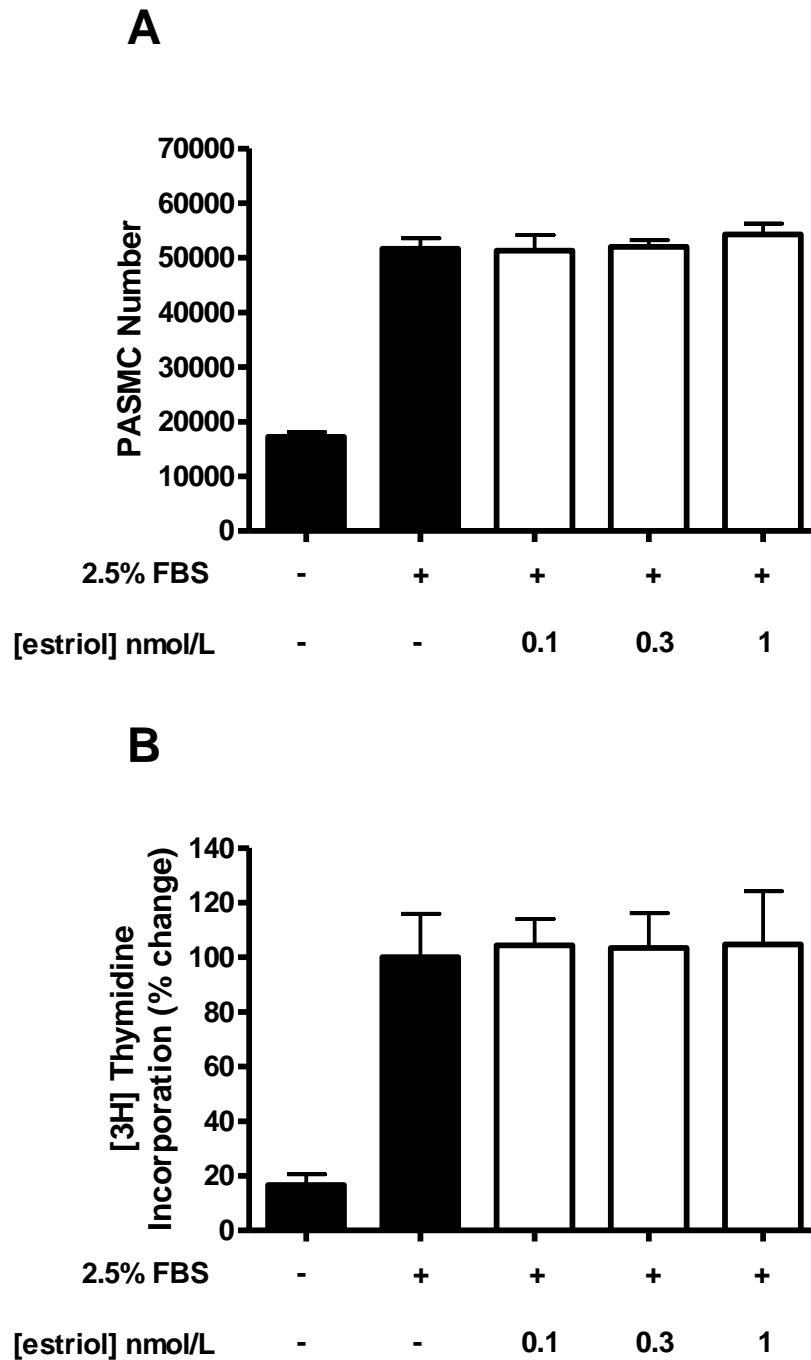


Figure 3.27 Estriol has no effect on human pulmonary artery smooth muscle cell proliferation. Estriol has no effect on cell number (A) or DNA synthesis (B) at a range of concentrations (0.1-1nmol/L). Data are expressed as mean \pm SEM. n=3 and performed in duplicate.

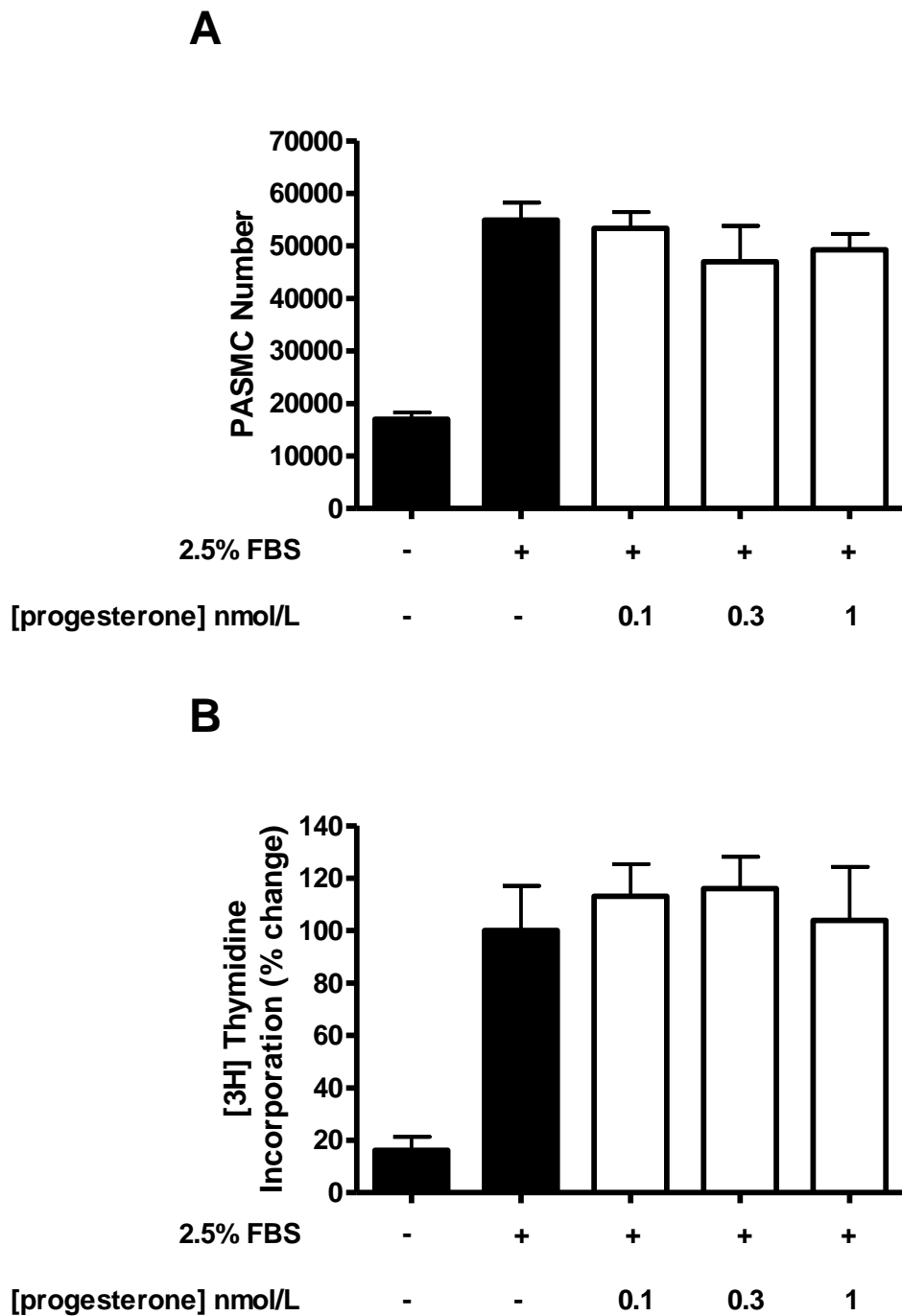


Figure 3.28 Progesterone has no effect on human pulmonary artery smooth muscle cell proliferation. Progesterone has no effect on cell number (A) or DNA synthesis (B) at a range of concentrations (0.1-1nmol/L). Data are expressed as mean \pm SEM. n=3 and performed in duplicate.

3.2.9 17β Estradiol Has No Effect on Serotonin Induced Proliferation in PASCs

Following our observation that 17β estradiol is critical to the development of PAH in a serotonin-dependent model of PAH (SERT⁺ mice), we investigated if this hormone potentiates serotonin-induced proliferation in cultured PASCs. We observed that, although both serotonin and 17β estradiol stimulate PASC proliferation, their cumulative effect does not stimulate proliferation to a greater extent (Figure 3.29).

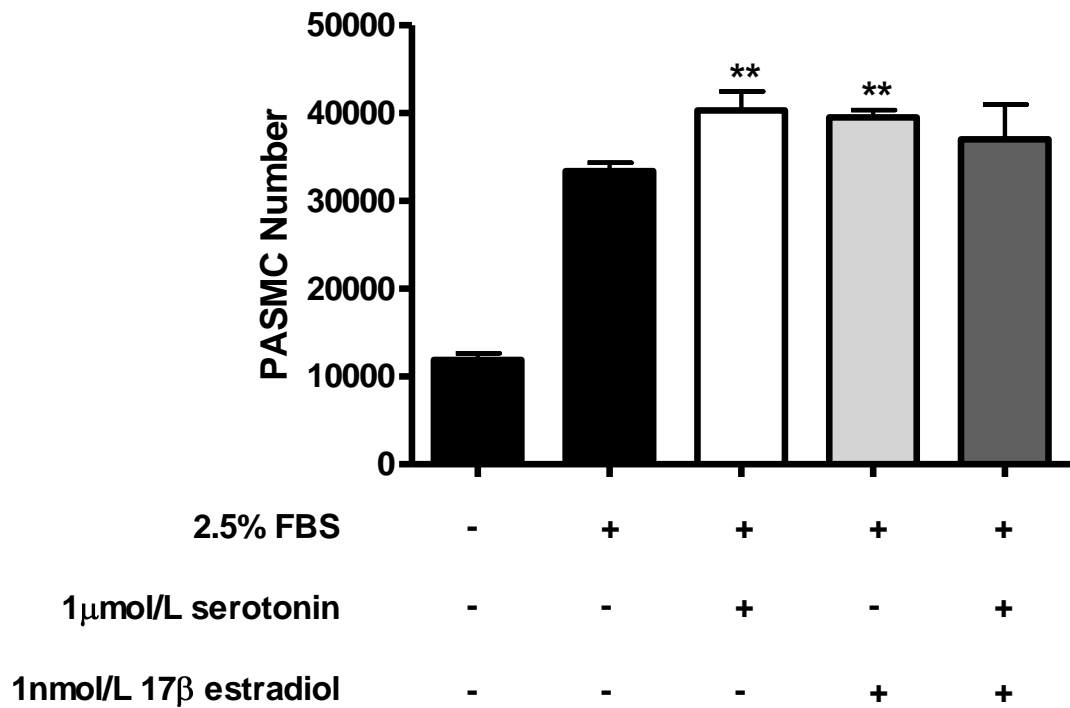


Figure 3.29 17β estradiol has no effect on serotonin-induced proliferation in human pulmonary artery smooth muscle cells. Both 1nmol/L 17β estradiol and 1µmol/L serotonin stimulate PASMC proliferation however their cumulative effect does not further stimulate proliferation. Data are expressed as mean ± SEM and analysed by one-way ANOVA followed by Dunnett’s post-hoc test. **P<0.01 cf. 2.5% FBS proliferation. n=4 and cell counts performed in duplicate.

3.2.10 *17 β Estradiol Increases Tryptophan Hydroxylase-1, 5-HT_{1B} Receptor and Serotonin Transporter Expression in PSMCs*

To determine if 17 β estradiol regulates the expression of key mediators in serotonin signalling we stimulated PSMCs with 1nmol/L 17 β estradiol at multiple time-points and investigated protein expression of TPH1, the 5-HT_{1B} receptors and SERT. Following exposure of PSMCs to 17 β estradiol for greater than 4 hours, we observed increased expression of TPH1 (Figure 3.30), the 5-HT_{1B} receptors (Figure 3.31) and SERT (Figure 3.32).

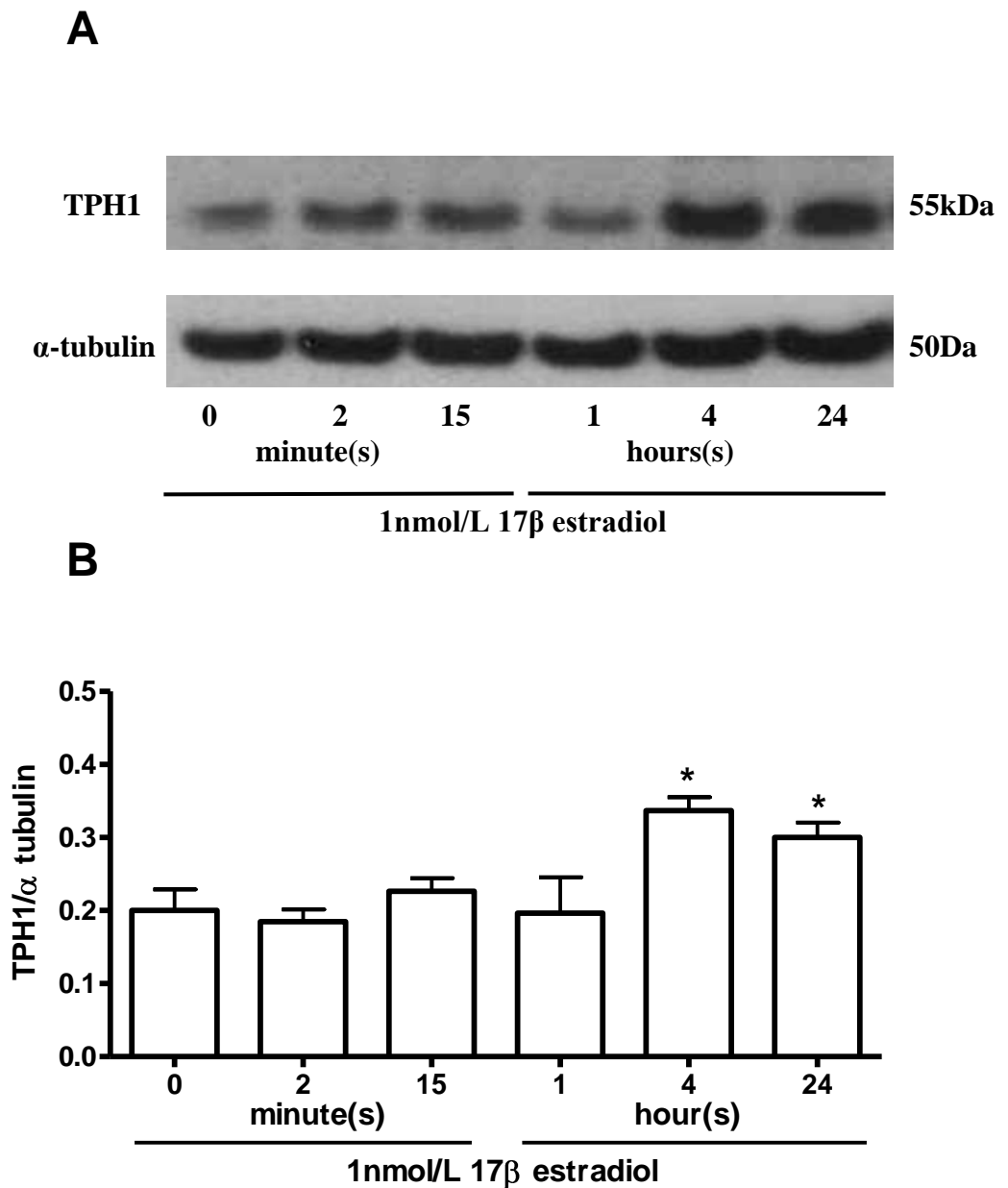


Figure 3.30 17 β estradiol increases tryptophan hydroxylase-1 expression in human pulmonary artery smooth muscle cells. Representative immunoblotting (A) and densitometrical analysis (B) showing that 1nmol/L 17 β estradiol increases TPH1 expression in PASM cells. Quantitative data is shown as mean \pm SEM and analysed using one-way ANOVA followed by Dunnett's post-hoc test. *P<0.05 cf. untreated PASM cells. n=3.

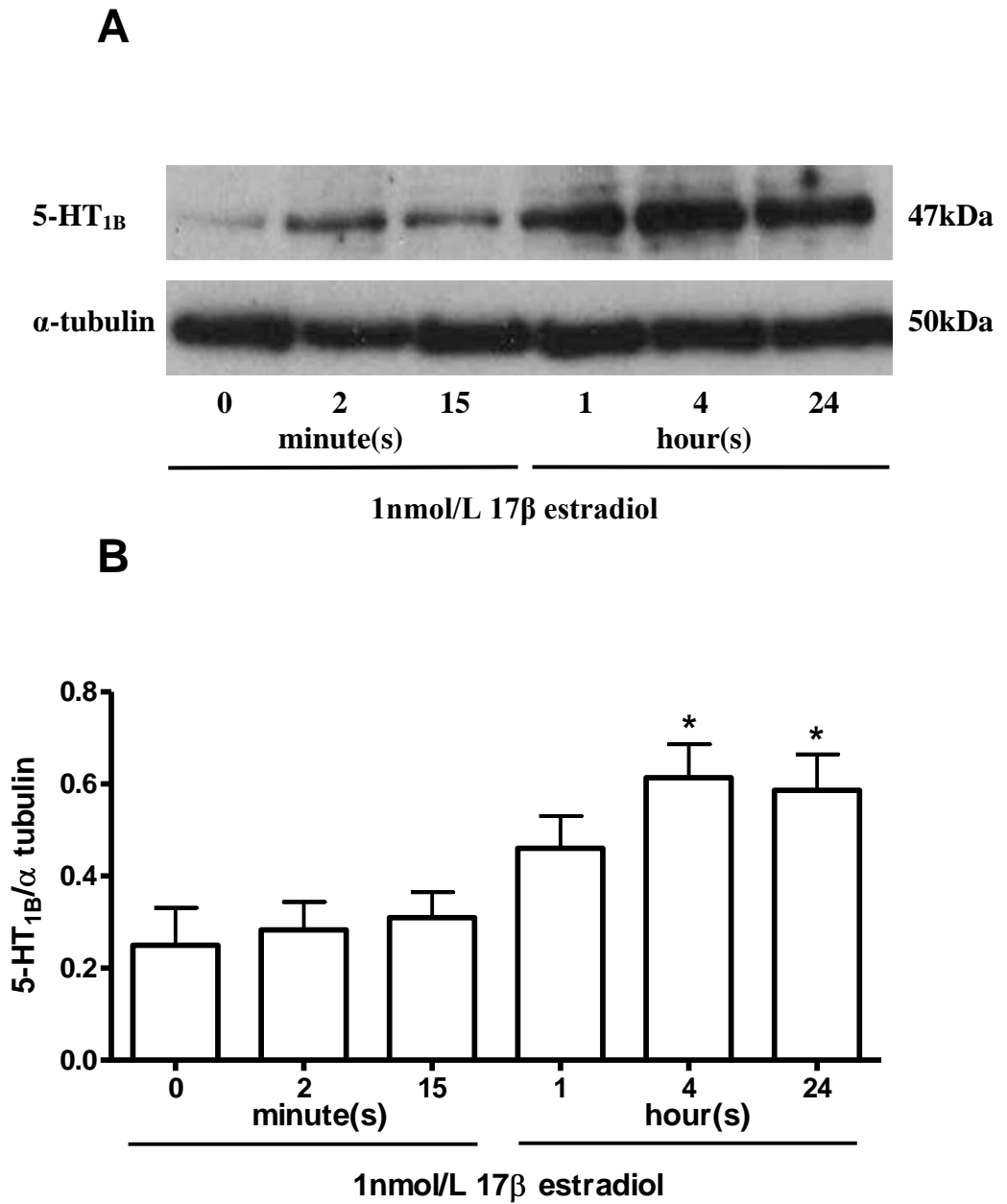


Figure 3.31 17 β estradiol increases 5-HT_{1B} receptor expression in human pulmonary artery smooth muscle cells. Representative immunoblotting (A) and densitometrical analysis (B) showing that 1nmol/L 17 β estradiol increases 5-HT_{1B} receptor expression in PSMCs. Quantitative data is shown as mean \pm SEM and analysed using one-way ANOVA followed by Dunnett's post-hoc test. *P<0.05 cf. untreated PSMCs. n=3.

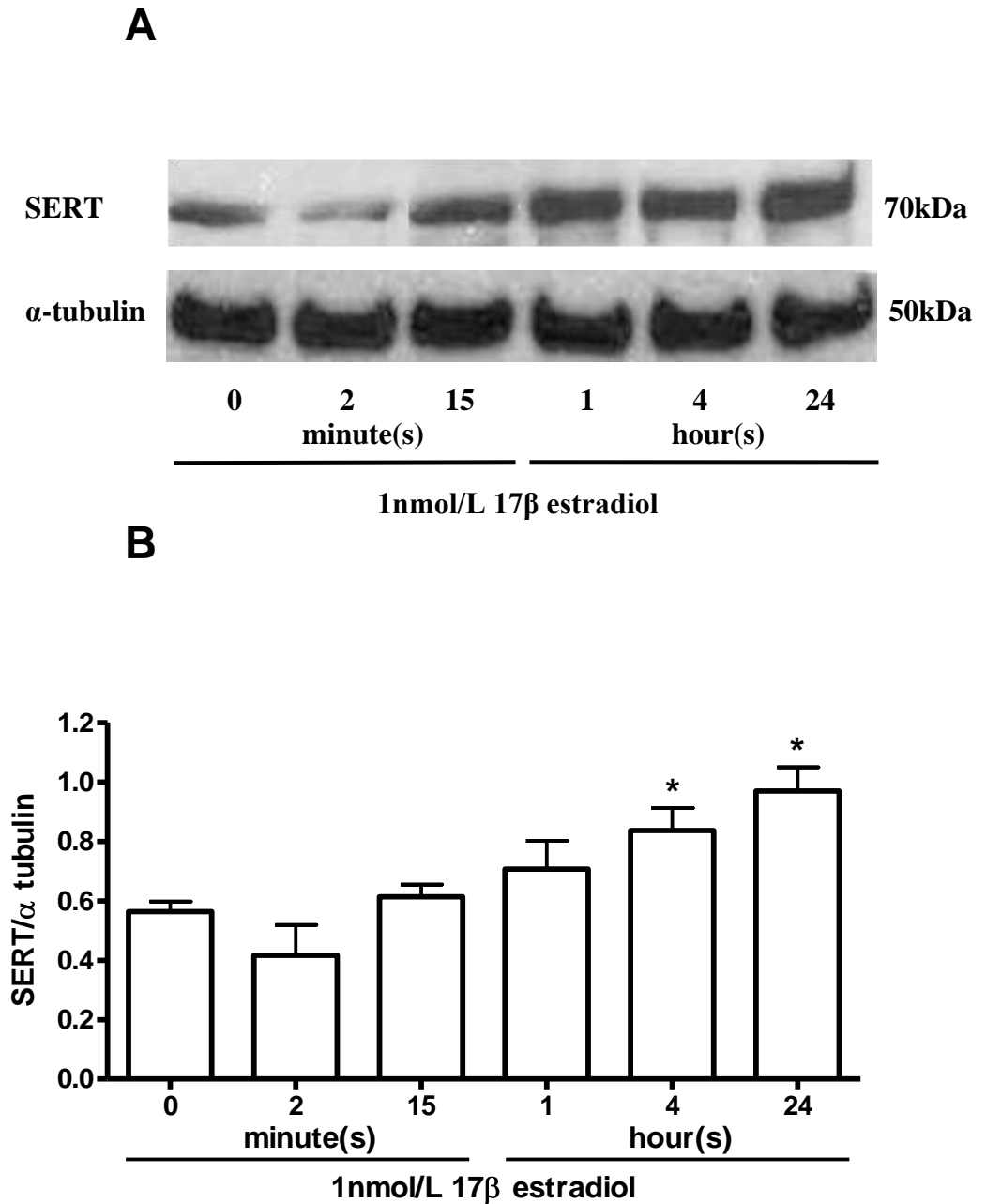


Figure 3.32 17 β estradiol increases serotonin transporter expression in human pulmonary artery smooth muscle cells. Representative immunoblotting (A) and densitometrical analysis (B) showing that 1nmol/L 17 β estradiol increases SERT expression in PASCs. Quantitative data is shown as mean \pm SEM and analysed using one-way ANOVA followed by Dunnett's post-hoc test. *P<0.05 cf. untreated PASCs. n=3.

3.2.11 Serotonin Pathway Inhibitors Prevent 17 β Estradiol

Induced Proliferation in PSMCs

Following the observation that 17 β estradiol increases expression of key serotonin pathway mediators (TPH1, 5-HT_{1B} receptors, SERT) critical to the development of PAH, we investigated if the serotonin system was also involved in 17 β estradiol-induced PSMC proliferation. To test this, we investigated the effects of inhibitors for TPH (p-chlorophenylalanine, PCPA 10 μ mol/L), the 5-HT receptors (5-HT_{1B} antagonist, SB224289 300nmol/L; 5-HT_{2A} antagonist, ketanserin 30nmol/L) and SERT (citalopram 1 μ mol/L) on 1nmol/L 17 β estradiol-mediated proliferation of PSMCs (Figure 3.33). Although none of the inhibitors had any effect on FBS-induced proliferation, both the TPH inhibitor PCPA and the 5-HT_{1B} receptor antagonist SB224289 successfully inhibited 17 β estradiol-stimulated proliferation. Of interest, the 5-HT_{2A} receptor antagonist ketanserin and the SERT inhibitor citalopram had no effect.

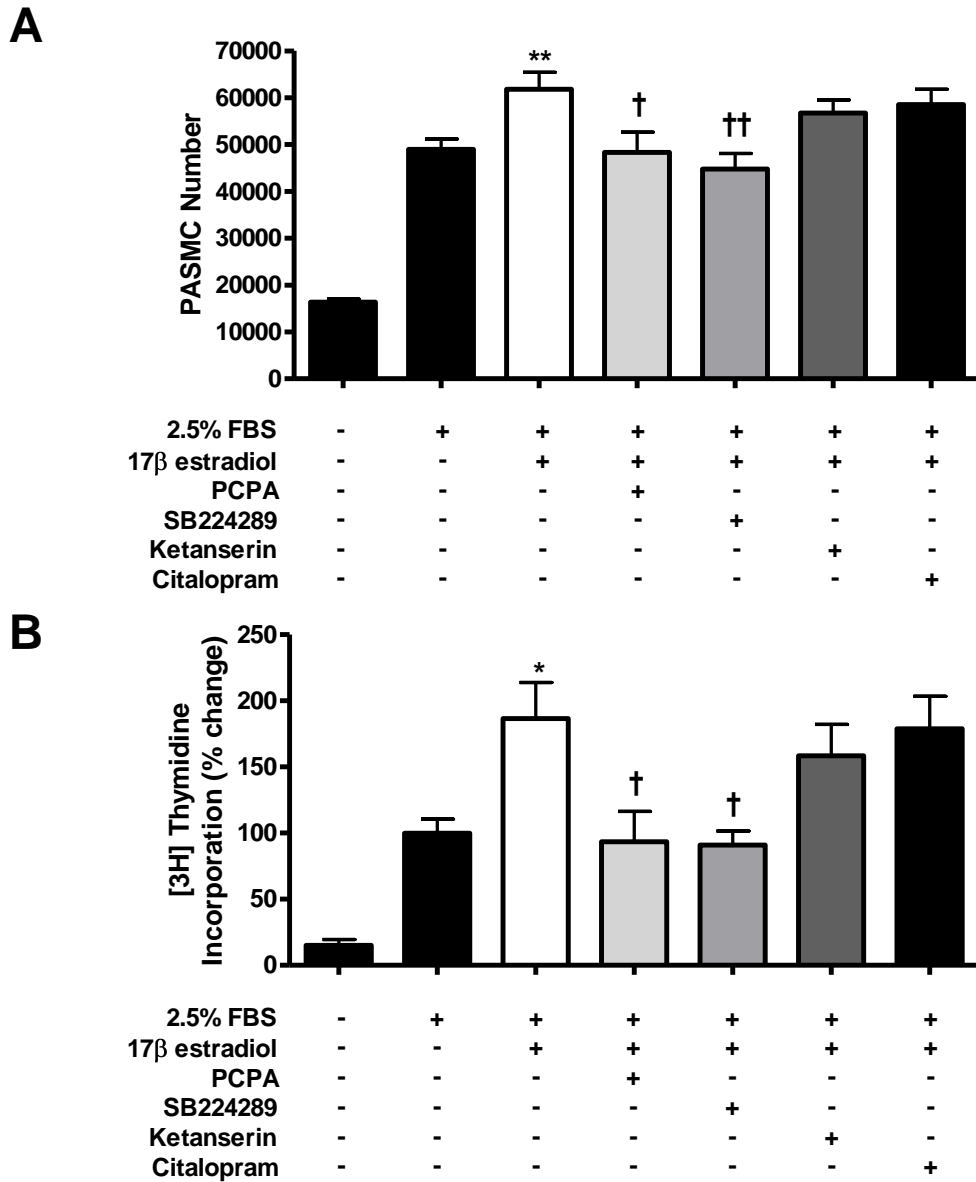


Figure 3.33 Effects of inhibitors for serotonin synthesis, 5-HT receptors and serotonin transporter on 17β estradiol-stimulated proliferation. 17β estradiol (1nmol/L) increases cell number (A) and DNA synthesis (B) in PASMCMs. This is inhibited by the tryptophan hydroxylase (TPH) inhibitor para-chlorophenylalanine (PCPA; 10μmol/L) and the 5-HT_{1B} receptor antagonist SB224289 (300nmol/L) but unaffected by the 5-HT_{2A} receptor antagonist ketanserin (30nmol/L) and the SERT inhibitor citalopram (1μmol/L). *P<0.05, **P<0.01 increased proliferation cf. 2.5% FBS; † P<0.05, †† P<0.01 decreased proliferation cf. 1nmol/L 17β estradiol. Data are expressed as mean ± SEM and analysed by one-way ANOVA followed by Dunnett's post-hoc test. n=3 and performed in duplicate.

3.3 Discussion

Both idiopathic PAH and heritable PAH occur more in females than in males. For example, in recent epidemiological studies carried out in Scotland, France and USA, 60%, 65% and 77% of patients studied respectively were female (Peacock et al., 2007; Humbert et al., 2006; Thenappan et al., 2007). The reasons for this increased frequency in females are unclear and under investigated. One reason for this under investigation is the absence of a suitable animal model. Paradoxically, it is observed that male rats exhibit severe hypoxia-induced PAH compared to female rats (Rabinovitch et al., 1981) and estrogens protect against monocrotaline-induced PAH (Farhat et al., 1993).

This is the first complete study to describe an animal model of PAH with female susceptibility. Preliminary evidence suggests that increased susceptibility in female mice may also be observed in dexfenfluramine-induced PAH (Dempsey et al., 2009; Dempsey et al., 2010) and VEGF receptor antagonist (SU 5416) + hypoxia-induced PAH (Tofovic and Rafikova, 2009). In the current study, only female SERT⁺ mice develop PAH and we provide experimental evidence that interactions between 17 β estradiol and the serotonin system may contribute towards this PAH pathogenesis. We demonstrate that female SERT⁺ mice develop PAH as indicated by elevated right ventricular pressure and pulmonary vascular remodelling, whereas male SERT⁺ mice remain unaffected. These results suggest that sex hormones are critical to the development of PAH in this model. To investigate this hypothesis, we ovariectomized these mice and assessed the PAH phenotype after twelve weeks. Ovariectomy completely prevented both the development of PAH and severe hypoxia-induced PAH in SERT⁺ mice. These results suggest a detrimental role for ovarian-derived hormones in SERT⁺ mice.

To determine if 17β estradiol is the hormone critical to the development of PAH *in vivo*, we assessed the effects of its re-introduction into ovariectomized SERT⁺ mice. As previously mentioned, ovariectomy protects SERT⁺ mice against the development of PAH, however 17β estradiol completely re-established a disease phenotype in these mice. Similarly, this hormone also re-established severe hypoxia-induced PAH in ovariectomized SERT⁺ mice. These results confirm that female gender, via the influence of ovarian-derived 17β estradiol, is critical to the development of PAH in SERT⁺ mice.

The potency of serotonin is decreased in the pulmonary arteries of SERT⁺ mice, as has been previously reported (MacLean et al., 2004). This is thought to occur via a reduction in extracellular serotonin concentration, arising as a consequence increased SERT-mediated serotonin uptake. Here, we investigated the effects of ovariectomy and 17β estradiol administration on serotonin-induced vasoconstriction in the pulmonary arteries of both normoxic and chronically hypoxic wildtype and SERT⁺ mice. However, we observed no changes in serotonin potency or efficacy in any of these mice. Similarly, serotonin-induced pulmonary vasoconstriction was also unchanged following 17β estradiol dosing in these mice.

We wished to establish a cellular model in order to investigate possible mechanisms of action of 17β estradiol and also examine the relevance of our *in vivo* study to human cells. We chose PASMCs as these have been extensively studied to investigate critical pathways in PAH. For example, PASMCs proliferate to serotonin via stimulation of the $5HT_{1B}$ receptors and SERT (Lawrie et al., 2005), and have also been studied to further investigate BMPR-II signalling in PAH (Yang et al., 2008). We observed that 17β estradiol stimulated proliferation, whereas estrone, estriol and progesterone had no effect. This is consistent with our observation that 17β estradiol re-established a PAH phenotype in ovariectomized SERT⁺ mice. 1nmol/L 17β estradiol was sufficient to promote PASMC proliferation and

similar growth effects have been previously reported in rat PSMCs (Farhat et al., 1992). This is physiologically relevant as 17β estradiol circulates at concentrations between 0.1-1nmol/L (Rosselli et al., 1994) and smooth muscle hyperplasia is a hallmark of PAH.

The suggestion that 17β estradiol is involved in the pathogenesis of experimental PAH is consistent with recent findings in human PAH. Decreased expression of the 17β estradiol-metabolising enzyme CYP1B1 has been reported in female PAH patients harbouring a BMPR-II mutation compared to unaffected female carriers⁸. Multiple factors modulate the levels of estrogen-metabolizing enzymes in the liver and target tissues, and the biological effects of an estrogen will therefore depend on the profile of metabolites formed and the biological activities of each of these metabolites (Zhu and Conney, 1998). 17β estradiol is metabolised to both pro- and anti-proliferative metabolites and its effects will depend on its metabolism. 17β estradiol can be converted to estrone and subsequently metabolized to 16α -hydroxyestrone (16-OHE1) via CYP3A4. Or alternatively, 17β estradiol is metabolized to 2-hydroxyestradiol (2-OHE) via the estrogen metabolizing enzymes CYP1A1/2 and to a lesser extent via CYP1B1 (Hanna et al., 2000; Tsuchiya et al., 2005). 2-OHE can itself be metabolized to 2-methoxyestradiol (2-ME) via catechol O-methyltransferase (COMT). Both 2-OHE and 2-ME have anti-proliferative effects on cells (Tofovic et al., 2006), whereas 16α -OHE1 stimulates proliferation by constitutively activating the estrogen receptor (Swanek and Fishman, 1988). Metabolism of 17β estradiol will therefore be species, gender and strain-dependent and differential disruption in the balance of metabolites may therefore account for the differential effects of female hormones in different models of PAH. Consistent with this, 17β estradiol did not promote PAH in male SERT⁺ mice suggesting gender differences in estrogen metabolism and/or its effects.

As discussed above, in other models of PAH it would appear that male gender predisposes to PAH and 17β estradiol may actually be protective in PAH. It has, for example, been shown to improve both right ventricular hypertrophy and pulmonary vascular remodeling in hypoxia-induced and monocrotaline-induced PAH (Farhat et al., 1993; Resta et al., 2001). Our studies are consistent with this as we show that male WT mice developed more severe hypoxia-induced PAH compared to female wildtype mice and 17β estradiol ablated hypoxia-induced PAH in these males. 17β estradiol also reduced RVH in ovariectomized SERT⁺ mice. In addition to the anti-proliferative effects of various 17β estradiol metabolites, it is also an established nitric oxide-dependent vasodilator in rat pulmonary arteries (Lahm et al., 2008), up-regulates endothelial nitric oxide synthase expression in pulmonary arterial endothelial cells (MacRitchie et al., 1997) and suppresses hypoxia-induced endothelin-1 gene expression (Earley and Resta, 2002). These effects may protect against the development of PAH in some species and/or strains. However, our results suggest that when SERT is up-regulated, 17β estradiol loses these protective effects and this may be via facilitating the mitogenic effects of serotonin. The implications of our study may translate clinically and help explain the inconsistency of the occurrence of PAH which may depend on multiple influences on 17β estradiol metabolism including age, early menopause, gender and various other factors that affect 17β estradiol metabolism.

There are multiple serotonin effects within the pulmonary circulation which promote PAH including microthrombosis, arterial vasoconstriction and proliferation. Indeed, it has been previously shown that TPH1, SERT and the 5-HT_{1B} receptors are all implicated in both human and experimental PAH. For example, the expression of TPH1, the rate-limiting enzyme involved in peripheral serotonin synthesis, is increased in the lungs of IPAH patients (Eddahibi et al., 2006). The exogenous administration of serotonin uncovers a PAH phenotype in BMPR-II^{+/-} mice (Long et al., 2006) and also increases the severity of hypoxia-induced PAH in rats (Eddahibi et al., 1997). In addition, mice deficient of

peripheral serotonin (tph1^{-/-} mice), achieved through deletion of the tph1 gene, do not develop hypoxia-induced PAH (Morecroft et al., 2007) or dexfenfluramine-induced PAH (Dempsie et al., 2008). Serotonin effects within the pulmonary vasculature are mediated in part via SERT. For example, PASMCs derived from IPAH patients proliferate to a greater extent than those from controls following serotonin stimulation and this is dependent on SERT activity (Eddahibi et al., 2001). A genetic polymorphism leading to increased activity/expression of SERT has been identified in a small cohort of PAH patients (Eddahibi et al., 2001). Subsequent studies in larger patient studies have failed to support these findings although patients with the SERT polymorphism may present at an earlier age than those without (Machado et al., 2006; Willers et al., 2006). As previously reported (MacLean et al., 2004) and further observed in the current study, mice over-expressing SERT develop PAH and severe hypoxia-induced PAH. Conversely, mice devoid of the SERT gene are less susceptible to the development of hypoxia-induced PAH (Eddahibi et al., 2000). Here, our findings demonstrate that female gender is also a risk factor in the development of PAH in SERT⁺ mice.

In the central nervous system, estrogens influence serotonin signalling via up-regulation of multiple pathway mediators including TPH and SERT (Pecins-Thompson et al., 1996; Lu et al., 2003). On this premise, we hypothesised that 17 β estradiol was similarly affecting the serotonin system within the pulmonary circulation and this was the mechanism through which serotonin and 17 β estradiol synergise to facilitate PAH. Thus, we investigated whether 17 β estradiol regulated expression of any serotonin pathway mediators in PASMCs. Here, we report for the first time that TPH1 is present in PASMCs, and this is markedly increased following stimulation with 17 β estradiol. In addition, 17 β estradiol also increased both 5-HT_{1B} receptor and SERT expression in PASMCs. This may be relevant, as both have previously been shown to interact to promote serotonin-induced PASMC proliferation (Lawrie et al., 2005). Based on these findings, we were interested in

determining if 17β estradiol mediated PASMCM proliferation via a serotonergic mechanism. Indeed, we report that 17β estradiol-induced proliferation is completely abolished in the presence of the TPH inhibitor PCPA and the 5-HT_{1B} receptor antagonist SB224289. This suggests that serotonin synthesis, and subsequent activation of the 5-HT_{1B} receptor, is essential in mediating the proliferative response of PASMCMs to 17β estradiol. It could be expected that the increased SERT expression may also increase the SERT-dependent serotonin activation of small GTPases within the cytoplasm ('serotonylation'), to further promote the mitogenic effects of serotonin. However, the observation that the SERT inhibitor citalopram was not sufficient to block proliferation suggests a minor role, although co-operation between the 5-HT_{1B} receptors and SERT have previously been shown to mediate serotonin-induced proliferation and therefore a role for SERT in 17β estradiol-induced proliferation cannot be ruled out. These findings are consistent with a role for serotonin in PAH as TPH1, the 5HT_{1B} receptors and SERT have all previously been implicated in the pathogenesis of both experimental and human PAH, as discussed above.

We have previously reported that un-dosed SERT⁺ mice develop elevated RVSP in the absence of RVH (MacLean et al., 2004). Conversely, chronically hypoxic *tph1*^{-/-} mice develop RVH in the absence of increased RVSP (Morecroft et al., 2007). The present study confirms dissociation of these indices in SERT⁺ mice. Further, we now show that ovariectomy decreased RVSP in SERT⁺ mice whilst having no effect on RVH, and the administration of 17β estradiol to ovariectomized SERT⁺ mice increased RVSP whilst decreasing RVH. One explanation for this dissociation is that both 17β estradiol and serotonin have direct effects on ventricular cardiomyocytes. 17β estradiol exerts both pro- and anti-hypertrophic effects on these cells (Kilic et al., 2009). Serotonin is considered a survival factor in cardiomyocytes (Nebigil et al., 2003) and apoptosis is a pre-dominant feature of ventricular remodelling (Williams, 1999).

In conclusion, here we have shown that female gender pre-disposes SERT⁺ mice to the development of PAH and 17 β estradiol is critical to this. 17 β estradiol appears to increase serotonin synthesis in PASMCs. This, in combination with 17 β estradiol-mediated upregulation of SERT and the 5-HT_{1B} receptor, may act to enhance serotonin-induced proliferation. The SERT and the 5-HT_{1B} receptor have previously been shown to mediate both serotonin-induced proliferation of PASMCs (Lawrie et al., 2005; Morecroft et al., 2010) and serotonin-induced constriction of pulmonary arteries (Morecroft et al., 2005). These findings may offer insight into the gender differences apparent in human PAH.

Chapter 4

The Serotonin Transporter, Gender and Hypoxia: Microarray Analysis in the Pulmonary Arteries of Mice Identifies Genes with Relevance to Human PAH

4.1 Introduction

Gender bias exists in both HPAH and IPAH, with women up to three-fold more likely to present with disease (Humbert et al., 2006; Peacock et al., 2007; Thenappan et al., 2007). The underlying reasons for these differences remain to be characterised. Estrogen is one risk factor in PAH (Lahm et al., 2008). Genotyping studies have revealed alterations in estrogen signalling in PAH. For example, female PAH patients exhibit increased expression levels of ESR1 (estrogen receptor-1), which is the gene encoding for estrogen receptor alpha, compared to unaffected females (Rajkumar et al., 2010), and decreased cytochrome P450 1B1 (CYP1B1) expression is reported in HPAH (Austin et al., 2009).

Multiple studies have implicated serotonin in the pathobiology of PAH, as previously discussed. For example, peripheral serotonin synthesis is required for the development of both hypoxia-induced PAH (Morecroft et al., 2007) and dexfenfluramine-induced PAH (Dempsie et al., 2008). Mice over-expressing the SERT (SERT⁺ mice) also develop PAH and exaggerated hypoxia-induced PAH (MacLean et al., 2004). Consistent with this, mice with targeted SERT over-expression in the PSMCs under the guidance of its own SM22 promoter develop PAH and severe hypoxia-induced PAH (Guignabert et al., 2006). SERT expression is increased in human pulmonary artery smooth muscle cells (PSMCs) derived from IPAH patients, and mediates enhanced serotonin-induced proliferation in these cells (Eddahibi et al., 2006). Taken together, this evidence highlights a critical role of smooth muscle-SERT in mediating serotonin effects in experimental and human PAH.

In this study, we characterised genotypic differences in the development of PAH in SERT⁺ mice. Female SERT⁺ mice develop PAH and exaggerated hypoxia-induced PAH whereas male SERT⁺ mice remain unaffected compared to their respective wildtype controls. This was only apparent at 5 months of age. This experimental model of PAH is the first to

exhibit female susceptibility, and may provide insight into the female bias observed in human PAH. To investigate genotypic changes associated with the development and progression of PAH, microarray analysis was performed in the pulmonary arteries of normoxic and hypoxic 2 month old SERT+ mice. A total of thirty two microarrays were performed (n=4 biological replicates each group). The dysregulation of biological pathways was observed to a much greater extent in female SERT+ mice compared to male SERT+ mice. Ingenuity Pathway Analysis (IPA) gene mapping identified three key genes of interest for further validation (CEBPB, CYP1B1, FOS). Genes of interest were further assessed via quantitative RT-PCR and immunoblotting. With relevance to human PAH, CEBPB, CYP1B1 and FOS expression was also investigated in PSMCs derived from IPAH patients.

4.2 Results

4.2.1 Female SERT+ Mice Exhibit Right Ventricular Hypertrophy in Chronic Hypoxia at 2 Months and PAH at 5 Months

In normoxia, right ventricular systolic pressure (RVSP), pulmonary vascular remodelling (PVR; % remodelled vessels) and right ventricular hypertrophy (RVH) were similar in 2 month old male (Figure 4.1-3) and female (Figure 4.4-6) wildtype and SERT+ mice. However, at 5 months of age female SERT+ mice exhibited PAH, as assessed by increased RVSP, PVR and RVP, whereas male SERT+ mice remained unaffected. Following exposure to chronic hypoxia, all groups developed hypoxia-induced PAH as indicated by significant increases in RVSP, PVR and RVH. However at 2 months of age, chronically hypoxic female SERT+ mice exhibited increased RVH compared to WT mice. Similarly, at 5 months of age these mice exhibited increased RVSP, PVR and RVH compared to 5 month WT mice. Exaggerated hypoxia-induced PAH was not apparent in male SERT+ mice at 2 or 5 months of age. There were no systemic effects reported in both female and male normoxic and chronically hypoxic SERT+ mice compared to WT mice, as assessed by no changes in systemic arterial pressure or heart rate (data not shown).

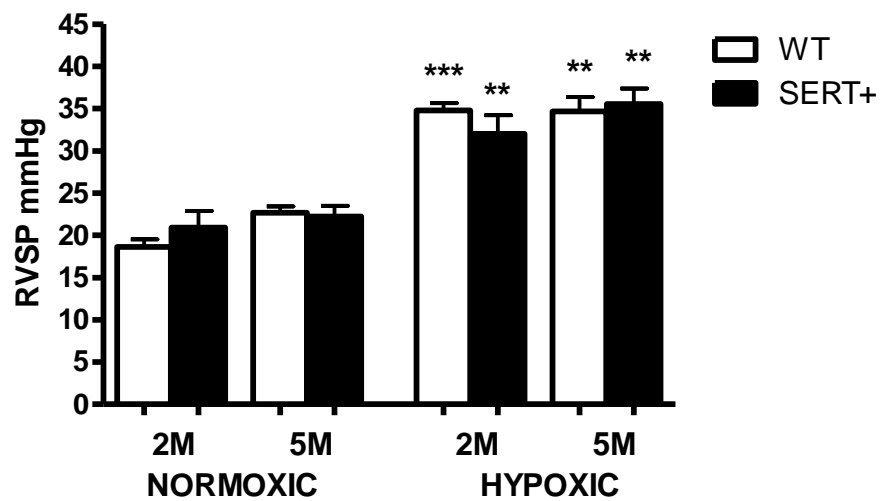


Figure 4.1 Male SERT+ mice do not exhibit increased right ventricular systolic pressure in normoxia or chronic hypoxia. RVSP is unaffected in normoxic male SERT+ mice at 2 and 5 months of age compared to their respective wildtype (WT) controls. Chronic hypoxia elevated RVSP in all groups. Chronically hypoxic 2 month SERT+ mice do not exhibit any change in RVSP compared to their respective WT controls. Data are expressed as mean \pm SEM and analysed by two-way ANOVA followed by Bonferroni's post-hoc test. **P<0.01, ***P<0.001 cf. normoxic controls; n=6-8.

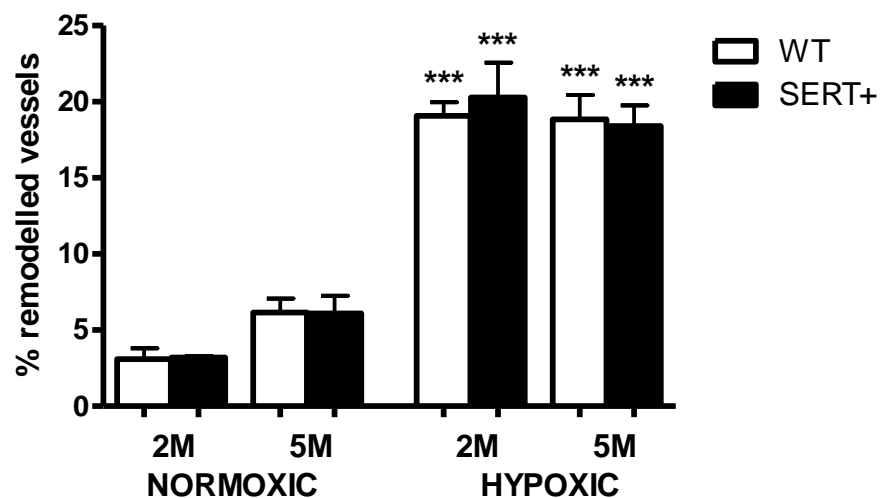


Figure 4.2 Male SERT+ mice do not exhibit increased pulmonary vascular remodelling. Pulmonary vascular remodelling is unaffected in normoxic male SERT+ mice compared to their respective wildtype (WT) controls. Chronic hypoxia elevated pulmonary vascular remodelling in all groups. Chronically hypoxic 2 month SERT+ mice do not exhibit any change in pulmonary vascular remodelling compared to their respective WT controls. Data are expressed as mean \pm SEM and analysed by two-way ANOVA followed by Bonferroni's post-hoc test. *** $P < 0.001$ cf. normoxic controls; $n = 5$.

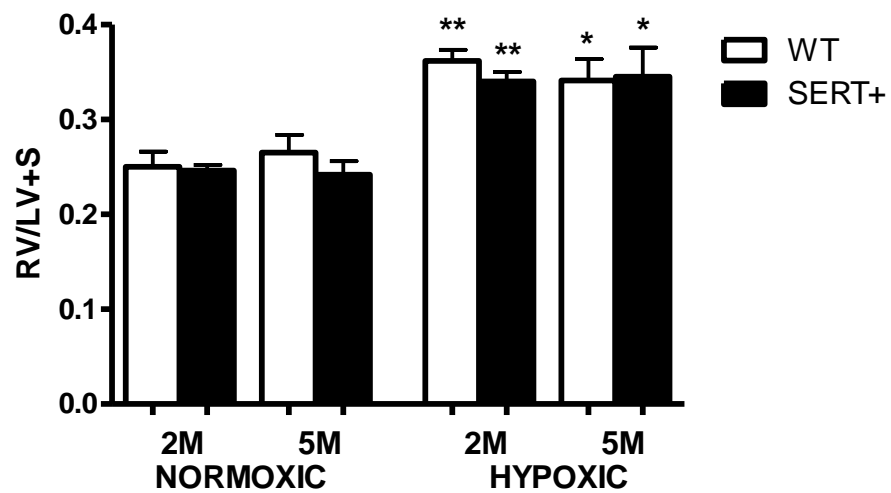


Figure 4.3 Male SERT+ mice do not exhibit increased right ventricular hypertrophy.

RVH is unaffected in normoxic male SERT+ mice compared to their respective wildtype (WT) controls. Chronic hypoxia increased RVH in all groups. Chronically hypoxic 2 month SERT+ mice do not exhibit any change in RVH compared to their respective WT controls. Data are expressed as mean \pm SEM and analysed by two-way ANOVA followed by Bonferroni's post-hoc test. * $P < 0.05$, ** $P < 0.01$ cf. normoxic controls. $n = 6-8$.

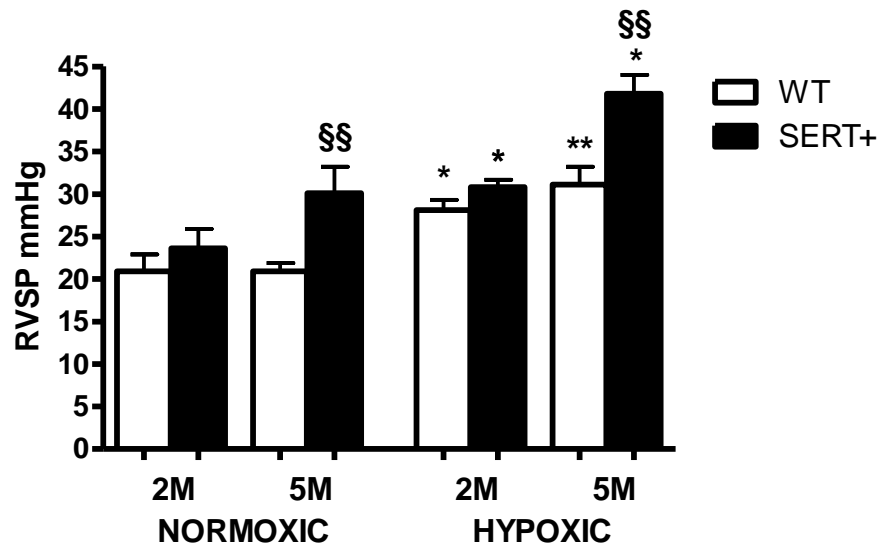


Figure 4.4 Female SERT+ mice exhibit increased right ventricular systolic pressure in normoxia and chronic hypoxia at 5 months of age. RVSP is increased in normoxic SERT+ mice at 5 months of age but unaffected at 2 months of age compared to their respective wildtype (WT) controls. Chronic hypoxia elevated RVSP in all groups. Chronically hypoxic 5 month SERT+ mice also exhibit increased RVSP. Data are expressed as mean \pm SEM and analysed by two-way ANOVA followed by Bonferroni's post-hoc test. * $P < 0.05$, ** $P < 0.01$ cf. normoxic controls; §§ $P > 0.01$ cf. WT mice. $n = 6-8$.

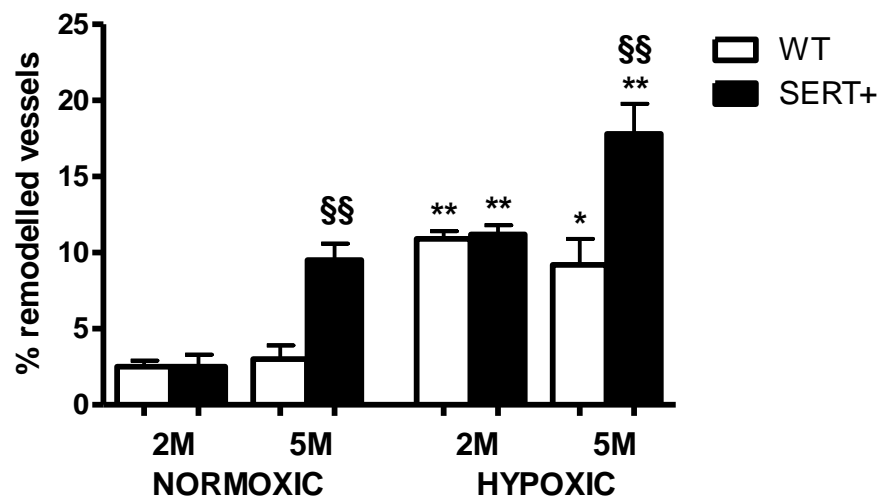


Figure 4.5 Female SERT+ mice exhibit increased pulmonary vascular remodelling in normoxia and chronic hypoxia at 5 months of age. Pulmonary vascular remodelling (PVR) is increased in normoxic SERT+ mice at 5 months of age but unaffected at 2 months of age compared to their respective wildtype (WT) controls. Chronic hypoxia elevated PVR in all groups. Chronically hypoxic 5 month SERT+ mice exhibit increased PVR. Data are expressed as mean \pm SEM and analysed by two-way ANOVA followed by Bonferroni's post-hoc test. * $P < 0.05$, ** $P < 0.01$ cf. normoxic controls; §§ $P < 0.01$ cf. WT mice. n=5.

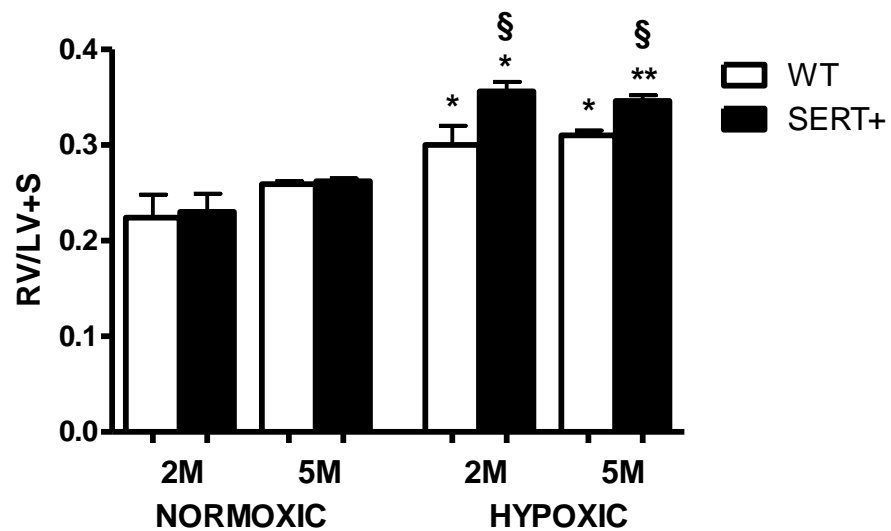


Figure 4.6 Female SERT+ mice exhibit increased right ventricular hypertrophy in chronic hypoxia at both 2 and 5 months of age. Right ventricular hypertrophy (RVH) is unaffected in normoxic SERT+ mice at both 2 and 5 months of age compared to their respective wildtype (WT) controls. Chronic hypoxia elevated RVH in all groups. Chronically hypoxic SERT+ mice exhibit increased RVH at both 2 and 5 months of age. Data are expressed as mean \pm SEM and analysed by two-way ANOVA followed by Bonferroni's post-hoc test. *P<0.05, **P<0.01 cf. normoxic controls §P<0.05 cf. WT mice. n=6-8.

4.2.2 Genotypic Differences in SERT+ Mice

We were interested in exploring the genotypic differences associated with the development and progression of PAH in female SERT+ mice. In total, we identified 155 genes that were significantly ($P < 0.05$) differentially expressed in female SERT+ mice compared to their wildtype controls. 71 genes show increased expression (Table 4.1), whilst the remaining 84 genes show reduced expression (Table 4.2). To determine their biological relevance, we functionally categorized these genes by biological processes. A considerable number of these genes (>40%) were assigned to one or more biological processes, of which 15 categories were present in total (Figure 4.7). Specifically, a large number of these genes were assigned to biological functions with relevance to PAH. These included oxidation-reduction, cell differentiation, regulation of transcription, apoptosis, muscle contraction, cellular calcium ion homeostasis and glycolysis.

In order to further investigate the genotypic changes underlying these gender differences in SERT+ mice, we also performed microarray analysis in the pulmonary arteries of male SERT+ mice. We observed that a total of 148 genes were significantly differentially expressed in male SERT+ mice compared to male WT mice. Of these, 110 genes were increased (table 4.5) whilst the remaining 38 genes were decreased (table 4.6). When categorised by biological processes, only 25% of these genes were assigned to biological function and 9 categories were represented in total.

Hierarchical cluster analysis between the 4 normoxic groups (258 genes in total) revealed distinct gene expression patterns between female SERT+ and female WT which were not apparent in the identical male SERT+ and WT comparison.

4.2.3 Genotypic Differences in Hypoxic SERT+ Mice

We were also interested in investigating the genotypic differences associated with exaggerated hypoxia-induced PAH in female SERT+ mice. Following exposure to chronic hypoxia, female SERT+ mice exhibited a greater than two-fold increase in the number of differentially expressed genes compared against the identical normoxic comparison. In total, 316 genes were differentially expressed. We observed that 254 genes were increased (Table 4.3), whilst the remaining 62 genes showed decreased expression (Table 4.4). When arranged by biological processes, 53% of genes were assigned to a total of 26 distinct pathways. Moreover, a significant number of these dysregulated pathways observed in chronically hypoxic female SERT+ mice have been previously associated with PAH including apoptosis, inflammation, transcription and metabolism (Figure 4.8).

In contrast, a large number of these changes were not apparent in hypoxic male SERT+ mice. A total of 145 genes were differentially expressed in male SERT+ mice, with 87 showing increased expression (Table 4.7) and 58 showing decreased expression (Table 4.8). When categorised by biological processes, 42% of these genes were assigned a biological function. 12 categories were represented in total.

Hierarchical cluster analysis of the differentially expressed genes between the 4 hypoxic groups revealed distinct gene expression patterns which were unique to female SERT+ mice. This may be critical to the exaggerated hypoxia-induced PAH phenotype observed in these mice.

Table 4.1 List of genes up-regulated in the pulmonary arteries of 2 month female SERT+ mice compared to 2 month female wildtype mice, arranged by biological process.

Gene Symbol	Gene Name	Accession No	Fold Change	False Discovery Rate
<i>Oxidation Reduction</i>				
CYP2S1	cytochrome P450, family 2, subfamily s, polypeptide 1	NM_028775.2	1.52	0.046
SCD1	stearoyl-Coenzyme A desaturase 1	scl52445.7_23	2.51	0.009
FASN	fatty acid synthase	scl014104.1_1	1.70	0.044
ALDH1A7	aldehyde dehydrogenase family 1, subfamily A7	scl52665.13.1_14	2.20	0.018
GPD1	glycerol-3-phosphate dehydrogenase 1	NM_010271.2	2.74	0.010
CYP1B1	cytochrome P450, family 1, subfamily b, polypeptide 1	scl49594.5.189_22	1.54	0.037
<i>Cell Differentiation</i>				
CEBPB	CCAAT/enhancer binding protein	NM_009883.1	1.50	0.049
LGALS3	lectin, galactose binding, soluble 3	NM_010705.1	1.76	0.022
DMKN	dermokine	scl32804.19.1_0	1.92	0.017
<i>Regulation of transcription</i>				
CEBPB	CCAAT/enhancer binding protein	NM_009883.1	1.50	0.049
FOS	FBJ osteosarcoma oncogene	NM_010234.2	2.79	0.017
Xbp1	X-box binding protein 1	NM_013842.2	1.56	0.029
HOXA4	homeo box A4	NM_008265.2	2.02	0.018
HOXB5	homeo box B5	NM_008268.1	1.90	0.015
AXUD1	AXIN1 up-regulated 1	scl35215.8_496	1.87	0.017
<i>Immune Response</i>				
CFD	complement factor D	NM_013459.1	1.86	0.045
SPON2	spondin 2, extracellular matrix protein	NM_133903.2	1.76	0.017
<i>Apoptosis</i>				
CIDEC	cell death-inducing DFFA-like effector c	NM_178373.2	2.91	0.014
SRGN	serglycin	scl019073.1_109	1.62	0.021
AXUD1	AXIN1 up-regulated 1	scl35215.8_496	1.87	0.017
<i>Metabolic Process</i>				
UGT1A10	UDP glycosyltransferase 1 family, polypeptide A10	scl0394435.7_126	1.66	0.046
ACLY	ATP citrate lyase	NM_134037.2	1.68	0.044
FASN	fatty acid synthase	scl014104.1_1	1.70	0.044
ALDH1A7	aldehyde dehydrogenase family 1, subfamily A7	scl52665.13.1_14	2.20	0.018
AACS	acetoacetyl-CoA synthetase	NM_030210.1	1.94	0.026
GPD1	glycerol-3-phosphate dehydrogenase 1	NM_010271.2	2.74	0.010
UAP1	UDP-N-acetylglucosamine pyrophosphorylase 1	NM_133806.2	1.74	0.026
<i>Lipid Metabolic Process</i>				
SCD1	stearoyl-Coenzyme A desaturase 1	NM_011182.2	2.51	0.009
AACS	acetoacetyl-CoA synthetase	NM_030210.1	1.94	0.026
<i>Lipid Biosynthetic Process</i>				
SCD1	stearoyl-Coenzyme A desaturase 1	scl52445.7_23	2.51	0.009
ACLY	ATP citrate lyase	NM_134037.2	1.68	0.044
FASN	fatty acid synthase	scl014104.1_1	1.70	0.044
ELOVL6	ELOVL family member 6	scl00170439.1_29	2.16	0.014
<i>Brown Fat Cell Differentiation</i>				
SCD1	stearoyl-Coenzyme A desaturase 1	scl52445.7_23	2.51	0.009
ADIPOQ	adiponectin, CIQ and collagen domain containing	scl49310.3_131	2.66	0.017
UCP1	uncoupling protein 1	NM_009463.2	15.14	0.000
CEBPB	CCAAT/enhancer binding protein	NM_009883.1	1.50	0.049
BC054059	cDNA sequence BC054059	scl19994.5.1_11	2.54	0.017
<i>Glycolysis</i>				
ENO2	enolase 2, gamma neuronal	NM_013509.2	1.61	0.045

Table 4.2 List of genes down-regulated in the pulmonary arteries of 2 month female SERT+ mice compared to 2 month female wildtype mice, arranged by biological process.

Gene Symbol	Gene Name	Accession No	Fold Change	False Discovery Rate
<i>Oxidation Reduction</i>				
SC4MOL	sterol-C4-methyl oxidase-like	NM_025436.1	2.09	0.034
PRDX2	peroxiredoxin 2	NM_011563.2	2.89	0.017
<i>Cell Differentiation</i>				
TRIM54	tripartite motif-containing 54	NM_021447.1	2.58	0.026
OBSCN	obscurin, cytoskeletal calmodulin and titin-interacting RhoGEF	scl40175.7.1_79	2.13	0.042
CSRP3	cysteine and glycine-rich protein 3	NM_013808.3	5.14	0.003
<i>Regulation of transcription</i>				
TBX20	T-box 20	NM_194263.1	2.06	0.041
<i>Immune Response</i>				
PRG4	proteoglycan 4	scl000882.1_25	2.57	0.019
<i>Apoptosis</i>				
ACTC1	actin, alpha, cardiac	NM_009608.1	2.17	0.037
COMP	cartilage oligomeric matrix protein	scl33728.21.1_0	4.73	0.011
<i>Metabolic Process</i>				
PGAM2	phosphoglycerate mutase 2	scl40555.3.1_120	8.59	0.003
<i>Lipid Metabolic Process</i>				
CPT1B	carnitine palmitoyltransferase 1b, muscle	NM_009948.1	2.81	0.022
LPL	lipoprotein lipase	scl0016956.1_234	1.92	0.047
<i>Heart Development</i>				
MB	myoglobin	NM_013593.2	22.71	0.000
TNNI3	troponin I, cardiac	NM_009406.2	6.86	0.003
MYL2	myosin, light polypeptide 2, regulatory, cardiac, slow	scl27267.9.1_12	70.40	0.000
TNNT2	troponin T2, cardiac	NM_011619.1	3.18	0.015
<i>Muscle Contraction</i>				
MYBPC3	myosin binding protein C, cardiac	NM_008653.1	3.34	0.014
ACTN2	actinin alpha 2	NM_016798.2	9.71	0.003
TBX20	T-box 20	NM_194263.1	2.06	0.041
MYOM2	myomesin 2	scl34033.37.1_91	2.40	0.028
TTN	titin	scl19104.8.1_3	6.48	0.003
TNNT2	troponin T2, cardiac	NM_011619.1	3.18	0.015
<i>Lipid Biosynthetic Process</i>				
SC4MOL	sterol-C4-methyl oxidase-like	NM_025436.1	2.09	0.034
<i>Cellular Calcium Ion Homeostasis</i>				
PLN	phospholamban	scl38924.3_494	6.93	0.003
TNNI3	troponin I, cardiac	NM_009406.2	6.86	0.003
CSRP3	cysteine and glycine-rich protein 3	NM_013808.3	5.14	0.003
<i>Brown Fat Cell Differentiation</i>				
MB	myoglobin	NM_013593.2	22.71	0.000
<i>Glycolysis</i>				
ENO3	enolase 3, beta muscle	NM_007933.2	3.82	0.010
PGAM2	phosphoglycerate mutase 2	scl40555.3.1_120	8.59	0.003
<i>Sarcomere Organization</i>				
MYBPC3	myosin binding protein C, cardiac	NM_008653.1	3.34	0.014
MYH6	myosin, heavy polypeptide 6, cardiac muscle, alpha	scl46291.1.1_325	2.60	0.018
TTN	titin	scl19104.8.1_3	6.48	0.003
TNNT2	troponin T2, cardiac	NM_011619.1	3.18	0.015

Table 4.2 Continued

Gene Symbol	Gene Name	Accession No	Fold Change	False Discovery Rate
<i>Regulation of Heart Contraction</i>				
MYBPC3	myosin binding protein C, cardiac	NM_008653.1	3.34	0.014
HRC	histidine rich calcium binding protein	NM_010473.1	3.71	0.011
MYH6	myosin, heavy polypeptide 6, cardiac muscle, alpha	scl46291.1.1_325	2.60	0.018
TNNT2	troponin T2, cardiac	NM_011619.1	3.18	0.015

Table 4.3 List of genes up-regulated in the pulmonary arteries of 2 month hypoxic female SERT+ mice compared to 2 month hypoxic female wildtype mice, arranged by biological process.

Gene Symbol	Gene Name	Accession No	Fold Change	False Discovery Rate
<i>apoptosis</i>				
PGLYRP1	peptidoglycan recognition protein 1	scl33021.4.288_87	3.30	0.000
CIDEC	cell death-inducing DFFA-like effector c	NM_178373.2	1.84	0.000
SRGN	serglycin	scl019073.1_109	1.32	0.048
KRT8	keratin 8	scl0016691.1_37	3.13	0.000
CIDEA	cell death-inducing DNA fragmentation factor, alpha subunit-like effector A	NM_007702.1	2.38	0.000
<i>induction of apoptosis</i>				
CEBPB	CCAAT/enhancer binding protein	NM_009883.1	1.67	0.004
CIDEC	cell death-inducing DFFA-like effector c	NM_178373.2	1.84	0.000
ERN2	endoplasmic reticulum	scl30713.22.1_242	2.08	0.003
<i>brown fat cell differentiation</i>				
SCD1	stearoyl-Coenzyme A desaturase 1	scl52445.7_23	1.97	0.000
ADIPOQ	adiponectin, C1Q and collagen domain containing	scl49310.3_131	1.87	0.025
UCP1	uncoupling protein 1	NM_009463.2	2.60	0.000
CEBPB	CCAAT/enhancer binding protein	NM_009883.1	1.67	0.004
BC054059	cDNA sequence BC054059	scl19994.5.1_11	1.86	0.004
NUDT7	nudix NM_024446.2 1.57			
MRAP	melanocortin 2 receptor accessory protein	NM_029844.1	1.96	0.001
ALDH6A1	aldehyde dehydrogenase family 6, subfamily A1	NM_134042.1	1.65	0.021
PPARG	peroxisome proliferator activated receptor gamma	NM_011146.1	1.75	0.000
<i>carbohydrate metabolic process</i>				
AMY1	amylase 1, salivary scl077379.3_13 1.66			
PDK4	pyruvate dehydrogenase kinase, isoenzyme 4	scl29310.11_209	2.95	0.005
PYGL	liver glycogen phosphorylase	NM_133198.1	1.86	0.000
GPD1	glycerol-3-phosphate dehydrogenase 1	NM_010271.2	2.00	0.001
CHST1	carbohydrate	NM_023850.1	1.42	0.031
PPP1R3C	protein phosphatase 1, regulatory	NM_016854.1	1.54	0.025
KLB	klotho beta	scl27771.5.1_89	1.87	0.005
<i>cell adhesion</i>				
MYBPC2	myosin binding protein C, fast-type	NM_146189.1	1.34	0.031
LGALS3BP	lectin, galactoside-binding, soluble, 3 binding protein	scl39273.6_263	1.66	0.011
1110049B09RIK	RIKEN cDNA 1110049B09 gene	scl42544.15.6_29	1.39	0.017
CDH5	cadherin 5	NM_009868.4	1.75	0.030
CD93	CD93 antigen	scl18542.4.1_65	1.99	0.034
<i>cell-cell adhesion</i>				
CDH5	cadherin 5	scl33446.12_65	1.75	0.030
CD93	CD93 antigen	scl18542.4.1_65	1.99	0.034
<i>chemotaxis</i>				
CYSLTR1	cysteinyl leukotriene receptor 1	NM_021476.2	1.33	0.041
CMTM8	CKLF-like MARVEL transmembrane domain containing 8	NM_027294.1	1.34	0.047
CXCL12	chemokine	scl0001073.1_120	1.77	0.007
<i>defense response to bacterium</i>				
PGLYRP1	peptidoglycan recognition protein 1	scl33021.4.288_87	3.30	0.000
HAMP2	hepcidin antimicrobial peptide 2	NM_183257.1	5.38	0.000
FCER1G	Fc receptor, IgE, high affinity I, gamma polypeptide	scl15940.5.1_15	2.29	0.016
H2-K1	histocompatibility 2, K1, K region	scl0014972.1_210	1.61	0.016
<i>DNA replication</i>				
POLN	DNA polymerase N	scl0272158.1_149	1.69	0.031
SUPT16H	suppressor of Ty 16 homolog	NM_033618.1	1.76	0.021
POLK	polymerase	scl43651.15_178	1.29	0.047
<i>immune response</i>				
PGLYRP1	peptidoglycan recognition protein 1	scl33021.4.288_87	3.30	0.000

Table 4.3 Continued

Gene Symbol	Gene Name	Accession No	Fold Change	False Discovery Rate
CXCL12	chemokine	sc10001073.1_120	1.77	0.007
CFD	complement factor D	NM_013459.1	1.68	0.007
CD300LG	CD300 antigen like family member G	sc140868.8_408	1.72	0.049
H2-T23	histocompatibility 2, T region locus 23	NM_010398.1	1.37	0.036
H2-K1	histocompatibility 2, K1, K region	sc10014972.1_210	1.61	0.016
<i>inflammatory response</i>				
REG3G	regenerating islet-derived 3 gamma	NM_011260.1	2.97	0.049
CHST1	carbohydrate	NM_023850.1	1.42	0.031
KNG1	kininogen 1	NM_023125.2	1.79	0.006
PPARG	peroxisome proliferator activated receptor gamma	NM_011146.1	1.75	0.000
<i>integrin-mediated signaling pathway</i>				
ADAM9	a disintegrin and metallopeptidase domain 9	NM_007404.1	1.39	0.018
<i>lipid biosynthetic process</i>				
SCD1	stearoyl-Coenzyme A desaturase 1	sc152445.7_23	1.97	0.000
PCX	pyruvate carboxylase	sc1000483.1_20	1.74	0.002
ACLY	ATP citrate lyase	NM_134037.2	1.81	0.009
FASN	fatty acid synthase	sc1014104.1_1	1.97	0.004
ELOVL6	ELOVL family member 6, elongation of long chain fatty acids	sc100170439.1_29	2.86	0.000
ELOVL5	ELOVL family member 5, elongation of long chain fatty acids	NM_134255.2	1.39	0.031
DGAT2	diacylglycerol O-acyltransferase 2	sc131009.10_67	2.20	0.000
<i>lipid metabolic process</i>				
HSD11B1	hydroxysteroid 11-beta dehydrogenase 1	sc1000857.1_11	1.55	0.054
SCD1	stearoyl-Coenzyme A desaturase 1	sc152445.7_23	1.97	0.000
HADHB	hydroxyacyl-Coenzyme A dehydrogenase/3-ketoacyl-Coenzyme A thiolase/enoyl-Coenzyme A hydratase	NM_145558.1	1.52	0.001
CPT1B	carnitine palmitoyltransferase 1b, muscle	NM_009948.1	1.94	0.013
AACS	acetoacetyl-CoA synthetase	NM_030210.1	1.47	0.028
CPT2	carnitine palmitoyltransferase 2	sc1000022.1_12	1.56	0.006
ACADVL	acyl-Coenzyme A dehydrogenase, very long chain	sc140004.19.1_140	1.41	0.042
ACAA2	acetyl-Coenzyme A acyltransferase 2	sc10002163.1_25	1.40	0.033
ACADL	acyl-Coenzyme A dehydrogenase, long-chain	NM_007381.2	2.12	0.000
ACSM3	acyl-CoA synthetase medium-chain family member 3	sc1000249.1_5	1.67	0.010
DGAT2	diacylglycerol O-acyltransferase 2	sc131009.10_67	2.20	0.000
PNPLA2	patatin-like phospholipase domain containing 2	sc18719.1.1_106	1.79	0.006
LPL	lipoprotein lipase	sc10016956.1_234	1.86	0.007
ADIPOR2	adiponectin receptor 2	sc128480.7_231	1.50	0.041
CIDEA	cell death-inducing DNA fragmentation factor, A alpha subunit-like effector	NM_007702.1	2.38	0.000
<i>metabolic process</i>				
HSD11B1	hydroxysteroid 11-beta dehydrogenase 1	sc1000857.1_11	1.55	0.005
PCX	pyruvate carboxylase	sc1000483.1_20	1.74	0.002
ACLY	ATP citrate lyase	NM_134037.2	1.81	0.009
FASN	fatty acid synthase	sc1014104.1_1	1.97	0.004
AMY1	amylase 1, salivary	sc1077379.3_13	1.66	0.005
AGPAT2	1-acylglycerol-3-phosphate O-acyltransferase 2	NM_026212.1	2.76	0.002
ALAS2	aminolevulinic acid synthase 2, erythroid	sc154562.12.1_64	1.29	0.034
HADHB	hydroxyacyl-Coenzyme A dehydrogenase/3-ketoacyl-Coenzyme A thiolase/enoyl-Coenzyme A hydratase	NM_145558.1	1.52	0.001
AACS	acetoacetyl-CoA synthetase	NM_030210.1	1.47	0.028
GPD1	glycerol-3-phosphate dehydrogenase 1	NM_010271.2	2.00	0.000
EPHX2	epoxide hydrolase 2, cytoplasmic	sc145408.20.1_29	1.48	0.021
ALDH3A1	aldehyde dehydrogenase family 3, subfamily A1	NM_007436.1	1.92	0.003
ACO2	aconitase 2, mitochondrial	NM_080633.1	1.89	0.000
UAP1	UDP-N-acetylglucosamine pyrophosphorylase 1	NM_133806.2	3.48	0.000
ACADVL	acyl-Coenzyme A dehydrogenase, very long chain	sc140004.19.1_140	1.41	0.042
GSTA3	glutathione S-transferase, alpha 3	sc118127.10.1_92	2.43	0.000
GSTO1	glutathione S-transferase omega 1	NM_010362.1	2.01	0.034

Table 4.3 Continued

Gene Symbol	Gene Name	Accession No	Fold Change	False Discovery Rate
ACAA2	acetyl-Coenzyme A acyltransferase 2	scl0002163.1_25	1.40	0.033
EYA3	eyes absent 3 homolog	NM_010166.2	2.10	0.002
NAT8L	N-acetyltransferase 8-like	scl27919.3_374	1.47	0.040
ALDH6A1	aldehyde dehydrogenase family 6, subfamily A1	NM_134042.1	1.65	0.021
ACADL	acyl-Coenzyme A dehydrogenase, long-chain	NM_007381.2	2.12	0.000
ACSM3	acyl-CoA synthetase medium-chain family member 3	scl000249.1_5	1.67	0.010
ACSS1	acyl-CoA synthetase short-chain family member 1	NM_080575.1	1.47	0.012
PNPLA2	patatin-like phospholipase domain containing 2	scl8719.1.1_106	1.79	0.006
GSTA4	glutathione S-transferase, alpha 4	NM_010357.1	2.61	0.000
<i>muscle contraction</i>				
MYBPC2	myosin binding protein C, fast-type	NM_146189.1	1.34	0.031
TBX20	T-box 20	NM_194263.1	1.57	0.034
PPARG	peroxisome proliferator activated receptor gamma	NM_011146.1	1.75	0.000
<i>oxidation reduction</i>				
CYP2S1	cytochrome P450, family 2, subfamily s, polypeptide 1	NM_028775.2	1.56	0.034
HSD11B1	hydroxysteroid 11-beta dehydrogenase 1	scl000857.1_11	1.55	0.005
SCD1	stearoyl-Coenzyme A desaturase 1	scl52445.7_23	1.97	0.000
GPX2	glutathione peroxidase 2	NM_030677.1	1.53	0.045
FASN	fatty acid synthase	scl014104.1_1	1.97	0.000
GPX3	glutathione peroxidase 3	NM_008161.1	1.55	0.007
CYP2E1	cytochrome P450, family 2, subfamily e, polypeptide 1	NM_021282.1	2.09	0.003
GPD2	glycerol phosphate dehydrogenase 2, mitochondrial	NM_010274.2	1.52	0.007
ETFHDH	electron transferring flavoprotein, dehydrogenase	NM_025794.1	1.64	0.047
DLD	dihydrolipoamide dehydrogenase	NM_007861.2	1.41	0.046
GPD1	glycerol-3-phosphate dehydrogenase 1	NM_010271.2	2.00	0.000
ALDH3A1	aldehyde dehydrogenase family 3, subfamily A1	NM_007436.1	1.92	0.003
ACADVL	acyl-Coenzyme A dehydrogenase, very long chain	scl40004.19.1_140	1.41	0.046
CYP2F2	cytochrome P450, family 2, subfamily f, polypeptide 2	scl32906.13.1_13	8.61	0.000
CYP2A5	cytochrome P450, family 2, subfamily a, polypeptide 5	NM_009997.1	1.85	0.022
CYP4A12B	cytochrome P450, family 4, subfamily a, polypeptide 12B	scl013118.12_302	3.42	0.000
ALDH6A1	aldehyde dehydrogenase family 6, subfamily A1	NM_134042.1	1.65	0.021
ACADL	acyl-Coenzyme A dehydrogenase, long-chain	NM_007381.2	2.12	0.000
PRDX2	peroxiredoxin 2	NM_011563.2	6.22	0.000
<i>response to toxin</i>				
EPHX2	epoxide hydrolase 2, cytoplasmic	scl45408.20.1_29	1.48	0.021
CES3	carboxylesterase 3	scl34490.14.1_30	2.18	0.002
CYP2F2	cytochrome P450, family 2, subfamily f, polypeptide 2	scl32906.13.1_13	8.61	0.000
PON1	paraoxonase 1	NM_011134.1	2.09	0.001
<i>signal transduction</i>				
RRG	RAS-like, estrogen-regulated, growth-inhibitor	NM_181988.1	2.02	0.001
GPR109A	G protein-coupled receptor 109A	NM_030701.1	1.61	0.009
CYSLTR1	cysteinyl leukotriene receptor 1	NM_021476.2	1.33	0.042
ELTD1	EGF, latrophilin seven transmembrane domain containing 1	NM_133222.1	2.08	0.001
FCER1G	Fc receptor, IgE, high affinity I, gamma polypeptide	scl15940.5.1_15	2.29	0.016
<i>small GTPase mediated signal transduction</i>				
KNDC1	kinase non-catalytic C-lobe domain	scl31927.18.1_9	2.41	0.002
RAB25	RAB25, member RAS oncogene family	scl21969.5.1_66	1.31	0.047
G3BP2	GTPase activating protein	scl0023881.1_86	1.33	0.021
<i>temperature homeostasis</i>				
GPX2	glutathione peroxidase 2	NM_030677.1	1.53	0.045
ACADVL	acyl-Coenzyme A dehydrogenase, very long chain	scl40004.19.1_140	1.41	0.042
ACADL	acyl-Coenzyme A dehydrogenase, long-chain	NM_007381.2	2.12	0.001
CIDEA	cell death-inducing DNA fragmentation factor, alpha subunit-like effector A	NM_007702.1	2.38	0.000

Table 4.3 Continued

Gene Symbol	Gene Name	Accession No	Fold Change	False Discovery Rate
<i>transcription</i>				
FOS	FBJ osteosarcoma oncogene	NM_010234.2	2.34	0.000
SUPT16H	suppressor of Ty 16 homolog	NM_033618.1	1.76	0.021
KLF5	Kruppel-like factor 5	scl45215.1.1_294	1.99	0.001
CEBPB	CCAAT/enhancer binding protein	NM_009883.1	1.67	0.002
TBX20	T-box 20	NM_194263.1	1.57	0.034
PPARG	peroxisome proliferator activated receptor gamma	NM_011146.1	1.75	0.000
ZFP367	zinc finger protein 367	NM_175494.2	1.22	0.031
EYA3	eyes absent 3 homolog	NM_010166.2	2.10	0.002
<i>transport</i>				
UCP1	uncoupling protein 1	NM_009463.2	2.60	0.000
SLC5A6	solute carrier family 5	scl26744.20.688_4	1.38	0.024
APOC1	apolipoprotein C-I	NM_007469.2	1.95	0.001
NDUFB4NADH	dehydrogenase (ubiquinone) 1 beta subcomplex 4	scl48493.1_0	1.34	0.028
ETFB	electron transferring flavoprotein, beta polypeptide	NM_026695.2	1.29	0.044
ETFFA	electron transferring flavoprotein, alpha polypeptide	NM_145615.2	1.42	0.043
ETFDH	electron transferring flavoprotein, dehydrogenase	NM_025794.1	1.64	0.047
CPT1B	carnitine palmitoyltransferase 1b, muscle	NM_009948.1	1.94	0.013
CPT2	carnitine palmitoyltransferase 2	scl000022.1_12	1.56	0.007
RAB25	RAB25, member RAS oncogene family	scl21969.5.1_66	1.31	0.047
FXYD3	FXYD domain-containing ion transport regulator 3	NM_008557.1	1.84	0.003
GABRP	gamma-aminobutyric acid	scl0001520.1_108	2.35	0.022
ATP5K	ATP synthase, H+ transporting, mitochondrial F1F0 complex, subunit e	scl011958.2_29	1.49	0.033
G3BP2	GTPase activating protein	scl0023881.1_86	1.33	0.021
MFI2	antigen p97	scl0001844.1_62	1.45	0.014
SLC25A1	solute carrier family 25	NM_153150.1	1.71	0.002
MTCH2	mitochondrial carrier homolog 2	NM_019758.2	1.41	0.033
<i>triglyceride metabolic process</i>				
APOC1	apolipoprotein C-I	NM_007469.2	1.95	0.001
<i>Other</i>				
CISH	cytokine inducible SH2-containing protein	scl012700.3_170	1.60	0.004
STMN2	stathmin-like 2	scl23400.7_310	1.65	0.000
SOCS3	suppressor of cytokine signaling 3	NM_007707.2	1.41	0.022
TUBA8	tubulin, alpha 8	scl29555.5_307	1.71	0.020
DNAHC2	dynein, axonemal, heavy chain 2	scl40034.27.1_30	1.57	0.004
SCGB1A1	secretoglobin, family 1A, member 1	NM_011681.1	9.55	0.000
HSPA5	heat shock 70kD protein 5	NM_022310.2	1.75	0.005
DUSP1	dual specificity phosphatase 1	NM_013642.1	1.64	0.021
DUSP23	dual specificity phosphatase 23	NM_026725.2	1.45	0.044
BMPER	BMP-binding endothelial regulator	NM_028472.1	1.95	0.004

Table 4.4 List of genes down-regulated in the pulmonary arteries of 2 month hypoxic female SERT+ mice compared to 2 month hypoxic female wildtype mice, arranged by biological process.

Gene Symbol	Gene Name	Accession No	Fold Change	False Discovery Rate
<i>brown fat cell differentiation</i>				
MB	myoglobin	NM_013593.2	1.89	0.003
<i>carbohydrate metabolic process</i>				
IGF2	insulin-like growth factor 2	sc130469.7_1	1.82	0.015
RPE	ribulose-5-phosphate-3-epimerase	sc10227227.1_0	2.13	0.019
<i>Cell adhesion</i>				
VCAN	versican	sc1013003.1_89	1.11	0.025
STAB1	stabilin 1	NM_138672.1	1.39	0.030
SELP	selectin, platelet	NM_011347.1	1.38	0.021
ITGA3	integrin alpha 3	NM_013565.2	1.25	0.017
ITGB1	integrin beta 1	NM_010578.1	1.72	0.008
<i>cell-cell adhesion</i>				
TNXB	tenascin XB	NM_031176.1	1.71	0.021
<i>cellular iron ion homeostasis</i>				
LTF	lactotransferrin	NM_008522.2	11.84	0.000
ALAS2	aminolevulinic acid synthase 2, erythroid	sc154562.12.1_64	1.29	0.033
HAMP2	hepcidin antimicrobial peptide 2	NM_183257.1	5.38	0.000
MFI2	antigen p97	sc10001844.1_62	1.45	0.014
<i>chemotaxis</i>				
CCL21B	chemokine	sc10018829.1_65	2.04	0.026
<i>DNA replication</i>				
NFIC	nuclear factor I/C	sc1068530.1_6	2.03	0.005
RBBP4	retinoblastoma binding protein 4	sc124919.4.1_260	2.09	0.021
<i>heart development</i>				
MB	myoglobin	NM_013593.2	1.89	0.004
MYL2	myosin, light polypeptide 2, regulatory, cardiac, slow	sc127267.9.1_12	6.36	0.001
VCAN	versican	sc1013003.1_89	1.11	0.025
OSR1	oxidative-stress responsive 1	sc135223.18_513	1.53	0.007
<i>immune response</i>				
H2-EA	histocompatibility 2, class II antigen E alpha	NM_010381.2	1.17	0.030
CCL21B	chemokine	sc10018829.1_65	2.04	0.026
<i>inflammatory response</i>				
STAB1	stabilin 1	NM_138672.1	1.39	0.030
CCL21B	chemokine	sc10018829.1_65	2.04	0.026
SELP	selectin, platelet	NM_011347.1	1.38	0.021
<i>integrin-mediated signaling pathway</i>				
ITGA3	integrin alpha 3	NM_013565.2	1.25	0.018
ITGB1	integrin beta 1	NM_010578.1	1.72	0.009
<i>lipid biosynthetic process</i>				
PRKAG2	protein kinase, AMP-activated, gamma 2 non-catalytic subunit	NM_145401.1	2.38	0.021
<i>lipid metabolic process</i>				
PTPN11	protein tyrosine phosphatase, non-receptor type 11	NM_011202.2	1.88	0.040
TNXB	tenascin XB	NM_031176.1	1.71	0.022
<i>metabolic process</i>				
RPE	ribulose-5-phosphate-3-epimerase	sc10227227.1_0	2.13	0.019
<i>muscle contraction</i>				
TTN	titin	sc119104.8.1_3	1.18	0.037

Table 4.4 Continued

Gene Symbol	Gene Name	Accession No	Fold Change	False Discovery Rate
ZBTB7A	zinc finger and BTB domain containing 7a	scl0016969.1_242	3.43	0.002
<i>oxidation reduction</i>				
4933406E20RIK	RIKEN cDNA 4933406E20 gene	NM_028944.2	1.24	0.009
<i>signal transduction</i>				
RAP2C	RAP2C, member of RAS oncogene family	scl54266.5_48	2.00	0.025
<i>transcription</i>				
CREBBP	CREB binding protein	scl48815.9.1_11	2.07	0.033
SKI	superkiller viralicidic activity 2-like (<i>S.cerevisiae</i>)	scl23441.8_64	1.98	0.003
RBBP4	retinoblastoma binding protein 4	scl24919.4.1_260	2.09	0.021
NFIC	nuclear factor I/C	scl068530.1_6	2.03	0.005
<i>transport</i>				
MB	myoglobin	NM_013593.2	1.89	0.004
LTF	lactotransferrin	NM_008522.2	11.84	0.000
TRAM1	translocating chain-associating membrane protein 1	NM_028173.1	1.72	0.036
RAMP1	receptor	scl17654.5.1_10	1.54	0.034
RAB17	RAB17, member RAS oncogene family	NM_008998.2	2.33	0.006
<i>triglyceride metabolic process</i>				
PTPN11	protein tyrosine phosphatase, non-receptor type 11	NM_011202.2	1.88	0.040
TNXB	tenascin XB	NM_031176.1	1.71	0.022
<i>Other</i>				
GUCY1A3	guanylate cyclase 1, soluble, alpha 3	scl0060596.1_205	1.03	0.011
BMX	BMX non-receptor tyrosine kinase	NM_009759.2	1.62	0.030
KIF1B	kinesin family member 1B	scl0002773.1_49	2.29	0.021
ZBTB7A	zinc finger and BTB domain containing 7a	scl0016969.1_242	3.43	0.002
PRRX1	paired related homeobox 1	scl018933.1_11	1.78	0.021

Table 4.5 List of genes up-regulated in the pulmonary arteries of 2 month male SERT+ mice compared to 2 month male wildtype mice, arranged by biological process.

Gene Symbol	Gene Name	Accession No	Fold Change	False Discovery Rate
<i>Transport</i>				
SCNN1G	sodium channel, nonvoltage-gated 1 gamma	scl32105.12.878_39	1.90	0.029
CLIC6	chloride intracellular channel 6	NM_172469.1	2.28	0.009
SLC39A4	solute carrier family 39	NM_028064.2	2.04	0.021
RAB25	RAB25, member RAS oncogene family	scl21969.5.1_66	2.04	0.021
GABRP	gamma-aminobutyric acid	scl0001520.1_108	2.83	0.002
Ltf	lactotransferrin	NM_008522.2	11.43	0.000
<i>Transport; oxygen transport</i>				
MB	myoglobin	NM_013593.2	2.74	0.000
HBB-B2	hemoglobin, beta adult minor chain	NM_016956.2	2.35	0.000
<i>Signal transduction</i>				
FCER1G	Fc receptor, IgE, high affinity I, gamma polypeptide	scl15940.5.1_15	2.68	0.002
GRB7	growth factor receptor bound protein 7	scl40936.14_9	1.86	0.021
<i>Cell adhesion</i>				
MUC4	mucin 4	scl0140474.33_123	1.82	0.031
WISP2	WNT1 inducible signaling pathway protein 2	NM_016873.1	1.92	0.010
SPON2	spondin 2, extracellular matrix protein	NM_133903.2	1.54	0.045
<i>Oxidation reduction</i>				
CYP2E1	cytochrome P450, family 2, subfamily e, polypeptide 1	NM_021282.1	1.98	0.008
CYP2F2	cytochrome P450, family 2, subfamily f, polypeptide 2	scl32906.13.1_13	12.08	0.000
CYP2A5	cytochrome P450, family 2, subfamily a, polypeptide 5	NM_009997.1	3.32	0.004
CYP4A12B	cytochrome P450, family 4, subfamily a, polypeptide 12B	scl013118.12_302	4.46	0.001
ABP1	amiloride binding protein 1	NM_029638.1	1.62	0.044
GPX2	glutathione peroxidase 2	NM_030677.1	2.20	0.004
ALDH3A1	aldehyde dehydrogenase family 3, subfamily A1	NM_007436.1	2.10	0.013
ALDH1A1	aldehyde dehydrogenase family 1, subfamily A1	scl011668.12_94	2.55	0.027
PRDX2	peroxiredoxin 2	NM_011563.2	2.25	0.012
<i>Immune response</i>				
PGLYRP1	peptidoglycan recognition protein 1	scl33021.4.288_87	2.08	0.035
CXCL15	chemokine	scl27600.3.1_4	5.76	0.000
SPON2	spondin 2, extracellular matrix protein	NM_133903.2	1.54	0.045
<i>Metabolic process</i>				
ALDH3A1	aldehyde dehydrogenase family 3, subfamily A1	NM_007436.1	2.10	0.013
ALDH1A1	aldehyde dehydrogenase family 1, subfamily A1	scl011668.12_94	2.55	0.027
GSTA3	glutathione S-transferase, alpha 3	scl18127.10.1_92	2.14	0.014
GSTO1	glutathione S-transferase omega 1	NM_010362.1	2.92	0.004
<i>Hemopoiesis</i>				
CXCL15	chemokine	scl27600.3.1_4	5.76	0.000
<i>Regulation of transcription</i>				
IRX5	Iroquois related homeobox 5	NM_018826.2	1.94	0.025
OTX1	orthodenticle homolog 1	scl40460.6_595	1.72	0.038
IRX3	Iroquois related homeobox 3	scl34499.5.1_0	1.69	0.024
FOXA1	forkhead box A1	scl42430.2_236	1.84	0.015

Table 4.6 List of genes down-regulated in the pulmonary arteries of 2 month male SERT+ mice compared to 2 month male wildtype mice, arranged by biological process.

Gene Symbol	Gene Name	Accession No	Fold Change	False Discovery Rate
<i>Transport: oxygen transport</i>				
HBB-B1	hemoglobin, beta adult major chain	NM_008220.2	2.41	0.019
<i>Signal transduction</i>				
LGR6	leucine-rich repeat-containing G protein-coupled receptor 6	sc100329252.1_132	1.86	0.011
<i>Oxidation reduction</i>				
JARID1B	lysine (K)-specific demethylase 5B	sc117448.26_107	1.65	0.032
SC4MOL	sterol-C4-methyl oxidase-like	NM_025436.1	2.25	0.003
<i>Hemopoiesis</i>				
PICALM	phosphatidylinositol binding clathrin assembly protein	sc132408.23_56	3.80	0.001
HBB-B1	hemoglobin, beta adult major chain	NM_008220.2	2.41	0.019
<i>Regulation of transcription</i>				
TEF	thyrotroph embryonic factor	sc10002562.1_0	1.82	0.022
DBP	D site albumin promoter binding protein	NM_016974.1	2.45	0.002
PER2	period homolog 2	NM_011066.1	1.89	0.013

Table 4.7 List of genes up-regulated in the pulmonary arteries of 2 month hypoxic male SERT+ mice compared to 2 month hypoxic male wildtype mice, arranged by biological process.

Gene Symbol	Gene Name	Accession No	Fold Change	False Discovery Rate
<i>transport</i>				
LBP	lipopolysaccharide binding protein	scl20002.16.7_10	1.92	0.019
LTF	lactotransferrin	NM_008522.2	6.63	0.000
APOC1	apolipoprotein C-I	NM_007469.2	1.95	0.020
SLC4A1	solute carrier family 4	NM_011403.1	2.28	0.004
HBB-B1	hemoglobin, beta adult major chain	NM_008220.2	3.05	0.032
ABCC9	ATP-binding cassette, sub-family C	scl0001165.1_35	2.25	0.015
SLC1A3	solute carrier family 1	NM_148938.2	1.85	0.011
LCN2	lipocalin 2	NM_008491.1	1.65	0.021
<i>signal transduction, protein binding</i>				
FGL1	fibrogen-like protein 1	scl34887.7.1_10	2.48	0.007
ANGPTL4	angiopoietin-like 4	scl50042.7_106	1.89	0.019
TNC	tenascin C	scl0002731.1_70	1.77	0.018
<i>immune response</i>				
CCL7	chemokine	scl41159.3.1_10	2.02	0.014
CFD	complement factor D	NM_013459.1	1.78	0.042
CCL2	chemokine	scl020296.2_11	2.03	0.014
CLEC4D	C-type lectin domain family 4, member d	scl017474.5_5	1.54	0.034
C3	complement component 3	scl49743.39.1_15	1.74	0.042
C1S	complement component 1, s subcomponent	NM_144938.1	3.34	0.003
PRG4	PREDICTED: proteoglycan 4	scl000882.1_25	2.34	0.003
SPON2	spondin 2, extracellular matrix protein	NM_133903.2	1.98	0.019
CXCL14	chemokine	scl43911.4.1_38	1.52	0.031
<i>proteolysis</i>				
DPEP2	dipeptidase 2	scl34381.6_178	1.40	0.047
CTSK	cathepsin K	NM_007802.2	1.56	0.014
CFD	complement factor D	NM_013459.1	1.78	0.042
CPXM1	carboxypeptidase X 1	NM_019696.1	1.25	0.020
CTSC	cathepsin C	NM_009982.2	1.75	0.020
C1S	complement component 1, s subcomponent	NM_144938.1	3.34	0.003
HP	haptoglobin	NM_017370.1	3.13	0.002
<i>cell adhesion</i>				
CNTN2	contactin 2	scl0021367.1_277	2.19	0.017
CPXM1	carboxypeptidase X 1	NM_019696.1	1.25	0.020
COL8A2	collagen, type VIII, alpha 2	scl24964.1.1958_52	1.98	0.018
CYR61	cysteine rich protein 61	NM_010516.1	1.66	0.039
TNC	tenascin C	scl0002731.1_70	1.77	0.018
SPP1	secreted phosphoprotein 1	NM_009263.1	2.51	0.006
SPON2	spondin 2, extracellular matrix protein	NM_133903.2	1.98	0.019
COMP	cartilage oligomeric matrix protein	scl33728.21.1_0	1.85	0.025
FN1	fibronectin 1	scl16639.44.189_5	1.57	0.013
<i>apoptosis</i>				
CIDEA	cell death-inducing DFFA-like effector c	NM_178373.2	1.90	0.046
COMP	cartilage oligomeric matrix protein	scl33728.21.1_0	1.85	0.025
<i>lipid metabolic process</i>				
SLC27A3	solute carrier family 27	scl21918.10.1_222	1.74	0.031
LPL	lipoprotein lipase	scl0016956.1_234	1.71	0.018
<i>innate immune response</i>				
LBP	lipopolysaccharide binding protein	scl20002.16.7_10	1.92	0.019
CFD	complement factor D	NM_013459.1	1.78	0.042
C3	complement component 3	scl49743.39.1_15	1.74	0.042
C1S	complement component 1, s subcomponent	NM_144938.1	3.34	0.003

Table 4.7 Continued

Gene Symbol	Gene Name	Accession No	Fold Change	False Discovery Rate
<i>brown fat cell differentiation</i>				
ADIPOQ	adiponectin, C1Q and collagen domain containing	scl49310.3_131	2.30	0.003
LRG1	leucine-rich alpha-2-glycoprotein 1	NM_029796.2	2.31	0.004
<i>skeletal system development</i>				
RUNX1	runt related transcription factor 1	scl48188.1.1_190	2.07	0.011
COL1A1	procollagen, type I, alpha 1	scl012842.26_28	2.15	0.007
<i>blood vessel development</i>				
COL3A1	procollagen, type III, alpha 1	NM_009930.1	1.57	0.039
COL1A1	procollagen, type I, alpha 1	scl012842.26_28	2.15	0.007

Table 4.8 List of genes down-regulated in the pulmonary arteries of 2 month hypoxic male SERT+ mice compared to 2 month hypoxic male wildtype mice, arranged by biological process.

Gene Symbol	Gene Name	Accession No	Fold Change	False Discovery Rate
<i>transport</i>				
UCP1	uncoupling protein 1	NM_009463.2	3.84	0.000
KCNAB1	potassium voltage-gated channel, shaker-related 1 subfamily, beta member	NM_010597.2	1.68	0.025
KCNH2	potassium voltage-gated channel, subfamily H	NM_013569.1	1.74	0.014
TOMM22	translocase of outer mitochondrial membrane 22 homolog	scl47742.5_273	3.76	0.000
RAMP1	receptor (calcitonin) activity modifying protein 1	scl17654.5.1_10	1.59	0.046
RAB17	RAB17, member RAS oncogene family	NM_008998.2	1.92	0.006
<i>proteolysis</i>				
MIPEP	mitochondrial intermediate peptidase	NM_027436.1	1.50	0.046
DPEP1	dipeptidase 1	NM_007876.1	1.70	0.031
CORIN	corin	NM_016869.1	1.84	0.014
<i>cell adhesion</i>				
MCAM	melanoma cell adhesion molecule	NM_023061.1	1.51	0.046
PKP4	plakophilin 4	scl0003206.1_31	1.70	0.025
<i>apoptosis</i>				
ACTC1	actin, alpha, cardiac	NM_009608.1	1.14	0.018
CIDEA	cell death-inducing DNA fragmentation factor, alpha subunit-like effector A	NM_007702.1	1.88	0.018
PAWR	PRKC, apoptosis, WT1, regulator	scl38461.7.1_1	1.67	0.031
<i>lipid metabolic process</i>				
TNXB	tenascin XB	NM_031176.1	1.91	0.013
CIDEA	cell death-inducing DNA fragmentation factor, alpha subunit-like effector A	NM_007702.1	1.88	0.018
<i>heart development</i>				
PDLIM3	PDZ and LIM domain 3	NM_016798.2	1.59	0.028
EDN1	endothelin 1	NM_010104.2	1.55	0.046
TNNT2	troponin T2, cardiac	NM_011619.1	1.62	0.004
<i>brown fat cell differentiation</i>				
UCP1	uncoupling protein 1	NM_009463.2	3.84	0.000
<i>skeletal system development</i>				
GJA5	gap junction membrane channel protein alpha 5	NM_008121.2	1.55	0.042
<i>blood vessel development</i>				
GJA5	gap junction membrane channel protein alpha 5	NM_008121.2	1.55	0.042
GJA4	gap junction membrane channel protein alpha 4	NM_008120.2	1.80	0.014

Table 4.9 Primer pairs used for PCR analysis

Gene Symbol	Accession No	Sense-primer	Anti-sense primer
Mouse			
HAMP2	NM_183257.2	5'-AGCAGAACAGGAGGCATGAT-3'	5'-GCAGATGGGAAGTTGATGT-3'
CEBPB	NM_009883.1	5'-CAAGCTGAGCGACGAGTACA-3'	5'-AGCTGCTCCACCTTCTTCTG-3'
CYP1B1	NM_009994.1	5'-GCGACGATTCTCCGGGCTG-3'	5'-CTCATGCAGGGCAGGCGGTC-3'
TNNC1	NM_009393.1	5'-GGAATTCATGAAGGGTGTGG-3'	5'-GGAATGGGGAGAGAAAAGTCC-3'
PLN	NM_023129	5'-ATCTTGCTGTGTTGGCTGTG-3'	5'-AGGGGACAACCACTTCCTCT-3'
MYL3	NM_010859	5'-GATGCTGACACCATGTCTGG-3'	5'-TAAGGCCACAGGGTGGATAC-3'
MB	NM_013593.3	5'-CCTGGGTACCATCCTGAAGA-3'	5'-GAGCATCTGCTCCAAAGTCC-3'
NPPA	NM_008725.2	5'-CCTAAGCCCTTGTGGTGTGT-3'	5'-CAGAGTGGGAGAGGCAAGAC-3'
FOS	NM_010234	5'-CTCCCGTGGTCACCTGTACT-3'	5'-TTGCCTTCTCTGACTGCTCA-3'
COX6A2	NM_009943.2	5'-CGGTTATGAGCACCTTGAT-3'	5'-CTGTTCCCAAAGAGCCAGAG-3'
β-ACTIN	NM_007393.2	5'-AGCCATGTACGTAGCCATCC-3'	5'-TCTCAGCTGTGGTGGTGAAG-3'
Human			
CEBPB	NM_005194	5'-GACAAGCACAGCGACGAGTA-3'	5'-AGCTGCTCCACCTTCTTCTG-3'
CYP1B1	NM_005252	5'-AACCGCAACTTCAGCAACTT-3'	5'-GAGGATAAAGGCGTCCATCA-3'
FOS	NM_000104.3	5'-AGCAATGAGCCTTCCTCTGA-3'	5'-TGAGTCCACACATGGATGCT-3'
β-ACTIN	NM_001101	5'-TCCCTGGAGAAGAGCTACGA-3'	5'-AGCACTGTGTTGGCGTACAG-3'

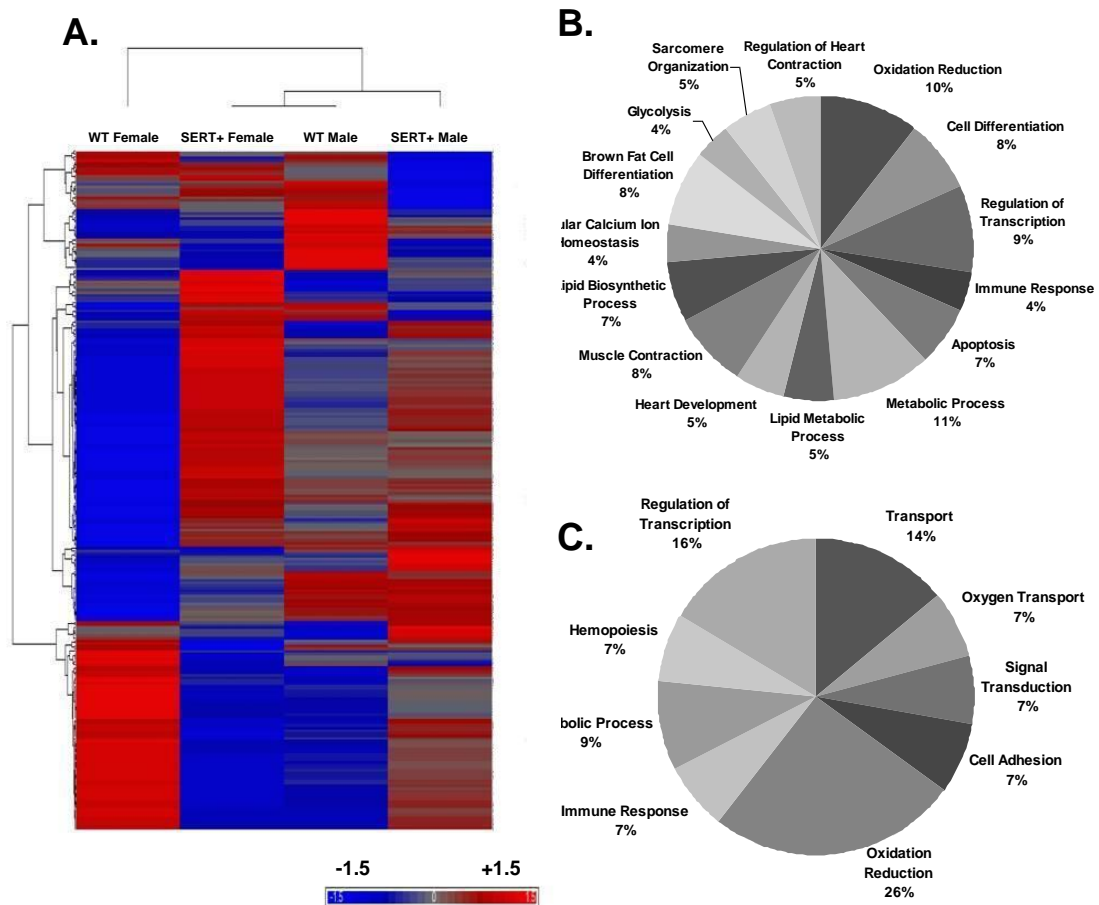


Figure 4.7 Representation of differentially expressed genes in normoxic female and male wildtype and SERT+ mice by hierarchical cluster analysis and gene ontology. Hierarchical cluster analysis of the differentially expressed genes in normoxic female and male WT and SERT+ mice (A). Representation of the differentially expressed genes in female SERT+ mice (B) and male SERT+ mice (C), arranged by biological processes. n=4.

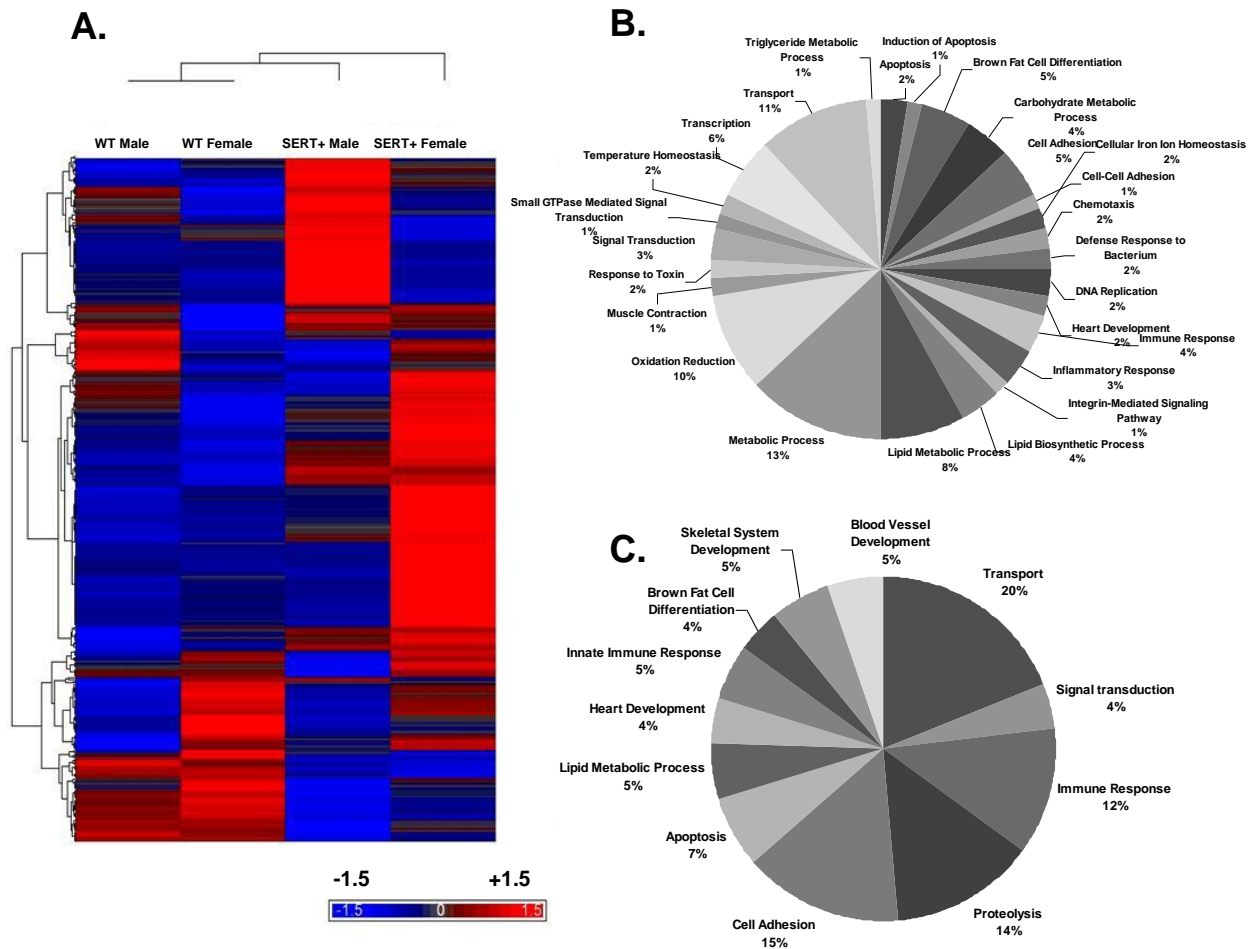


Figure 4.8 Representation of differentially expressed genes in chronically hypoxic female and male wildtype and SERT+ mice by hierarchical cluster analysis and gene ontology. Hierarchical cluster analysis of the differentially expressed genes in chronically hypoxic female and male WT and SERT+ mice (A). Representation of the differentially expressed genes in female SERT+ mice (B) and male SERT+ mice (C), arranged by biological processes. n=4.

4.2.4 qRT-PCR Analysis in the Pulmonary Arteries of SERT+ Mice

For validation of the microarray study, we employed qRT-PCR. To perform this, we selected three differentially expressed genes for each of the 4 group comparisons (Table 4.9). Our genes of interest were FOS, CEBPB, CYP1B1, MYL3, HAMP2, LTF, PLN, NPPA, UCP1 and C1S. In concordance with our microarray data, expression of these genes was significantly altered in relevant groups (Figure 4.9-12). Of particular interest, qRT-PCR analysis confirmed that FOS, CEBPB and CYP1B1 were considerably up-regulated (4-fold, 20-fold and 8-fold respectively) in female SERT+ mice.

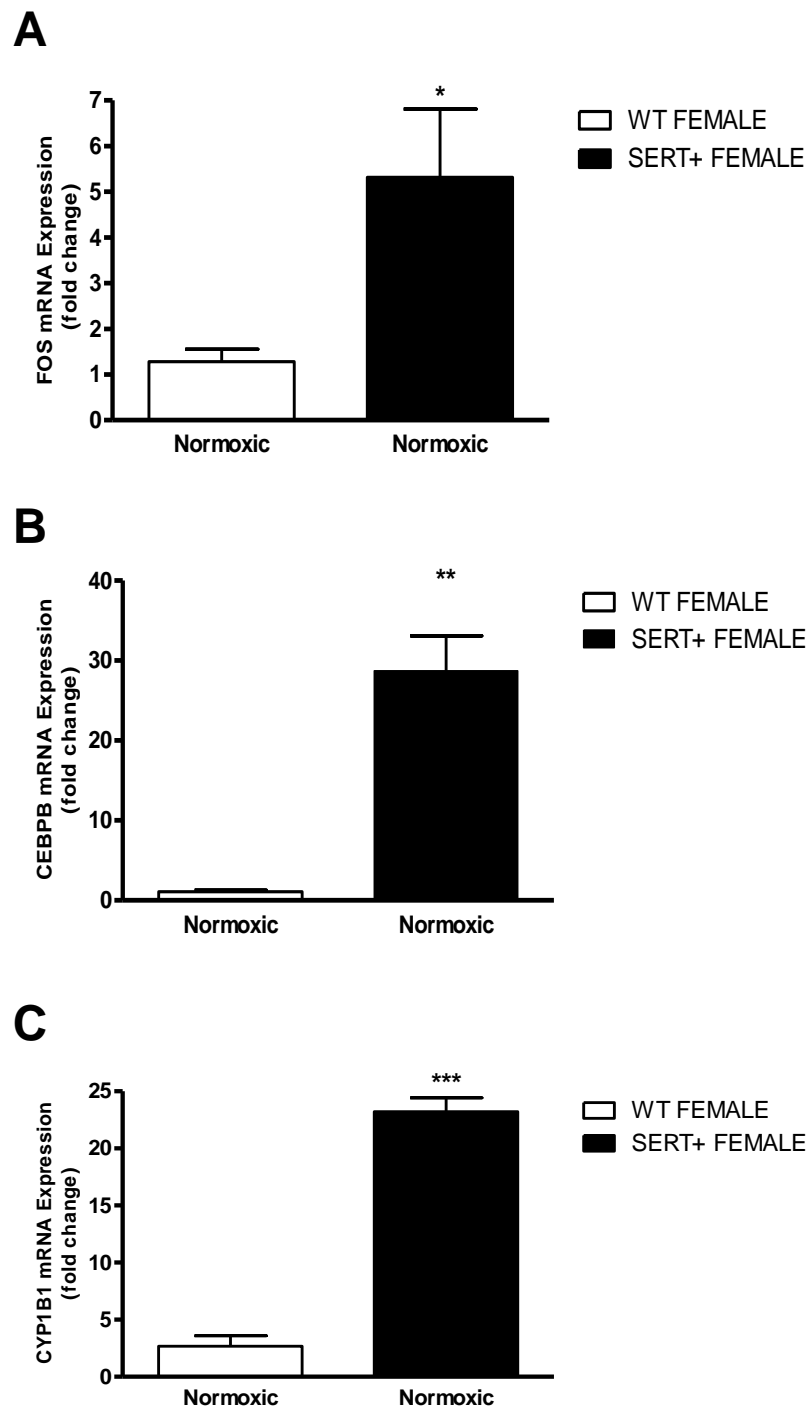


Figure 4.9 FOS, CEBPB and CYP1B1 mRNA expression in the pulmonary arteries of normoxic female wildtype and SERT+ mice. FOS (A), CEBPB (B) and CYP1B1 (C) mRNA expression is increased in normoxic female SERT+ mice, concordant with microarray analysis. Data are expressed as mean \pm SEM and analysed by Students t-test; * $P < 0.05$, ** $P < 0.01$, *** $P < 0.001$ cf. normoxic female WT mice. $n = 4$ and performed in triplicate.

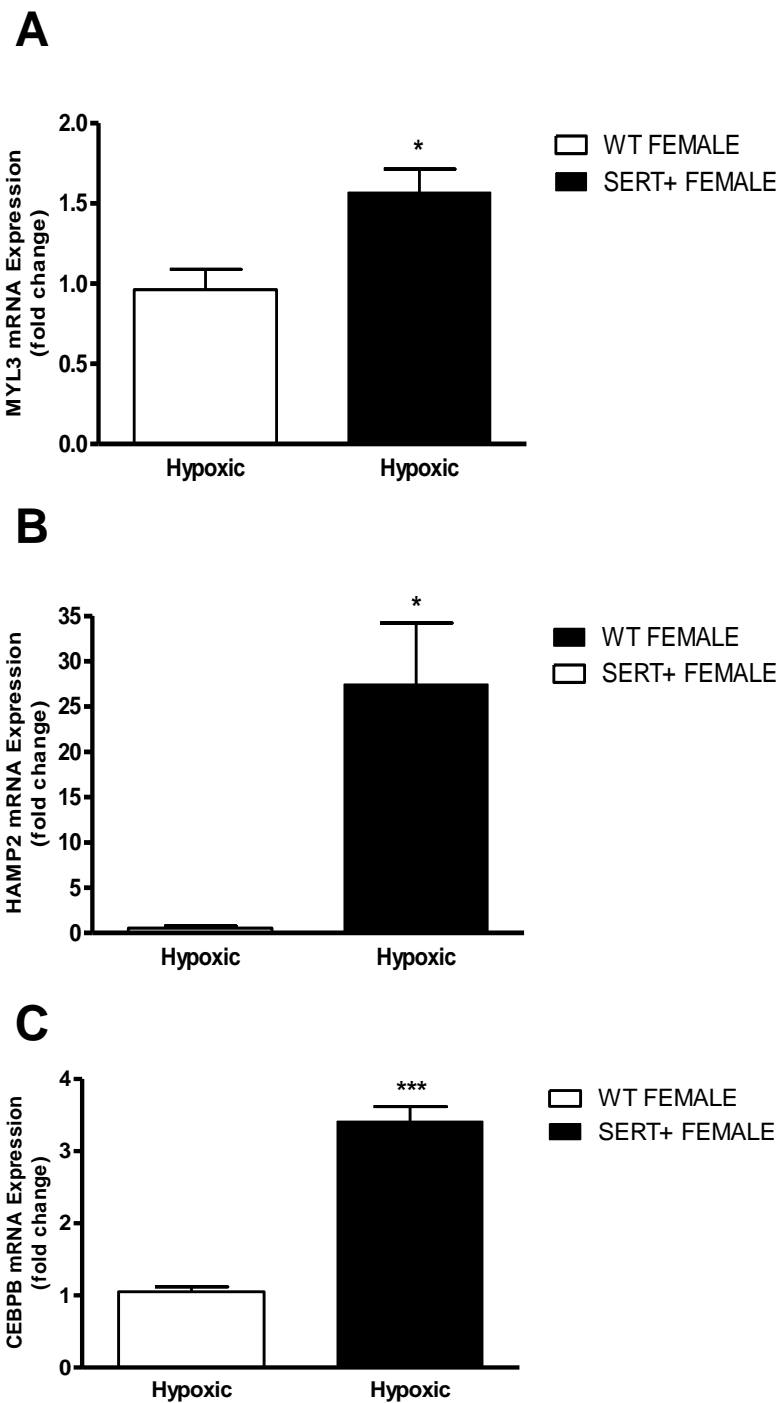


Figure 4.10 MYL3, HAMP2 and CEBPB mRNA expression in the pulmonary arteries of chronically hypoxic female wildtype and SERT+ mice. MYL3 (A), HAMP2 (B) and CEBPB (C) mRNA expression is increased in chronically hypoxic female SERT+ mice, concordant with microarray analysis. Data are expressed as mean \pm SEM and analysed by Students t-test; * $P < 0.05$, *** $P < 0.001$ cf. chronically hypoxic female WT mice. $n = 4$ and performed in triplicate.

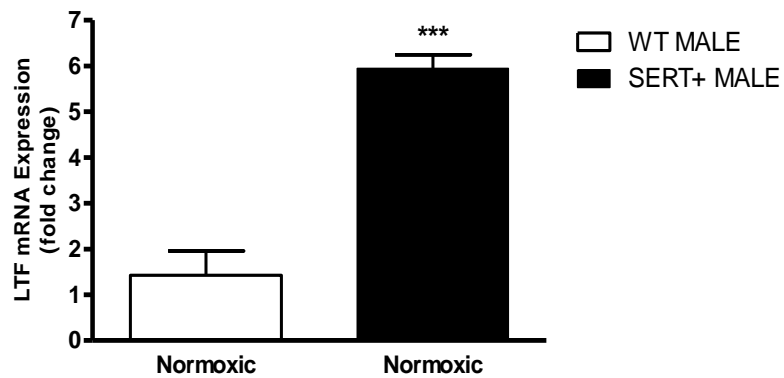
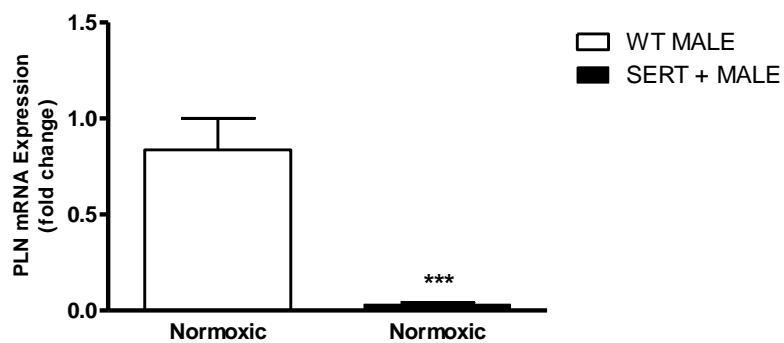
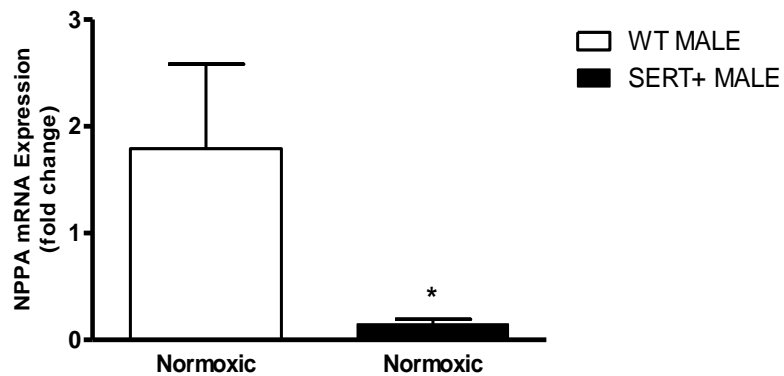
A**B****C**

Figure 4.11 LTF, PLN and NPPA mRNA expression in the pulmonary arteries of normoxic male wildtype and SERT+ mice. LTF (A) mRNA expression is increased and PLN (B) and NPPA (C) mRNA expression is decreased in normoxic male SERT+ mice, concordant with microarray analysis. Data are expressed as mean \pm SEM and analysed by Students t-test; * $P < 0.05$, *** $P < 0.001$ cf. normoxic male WT mice. $n = 4$ and performed in triplicate.

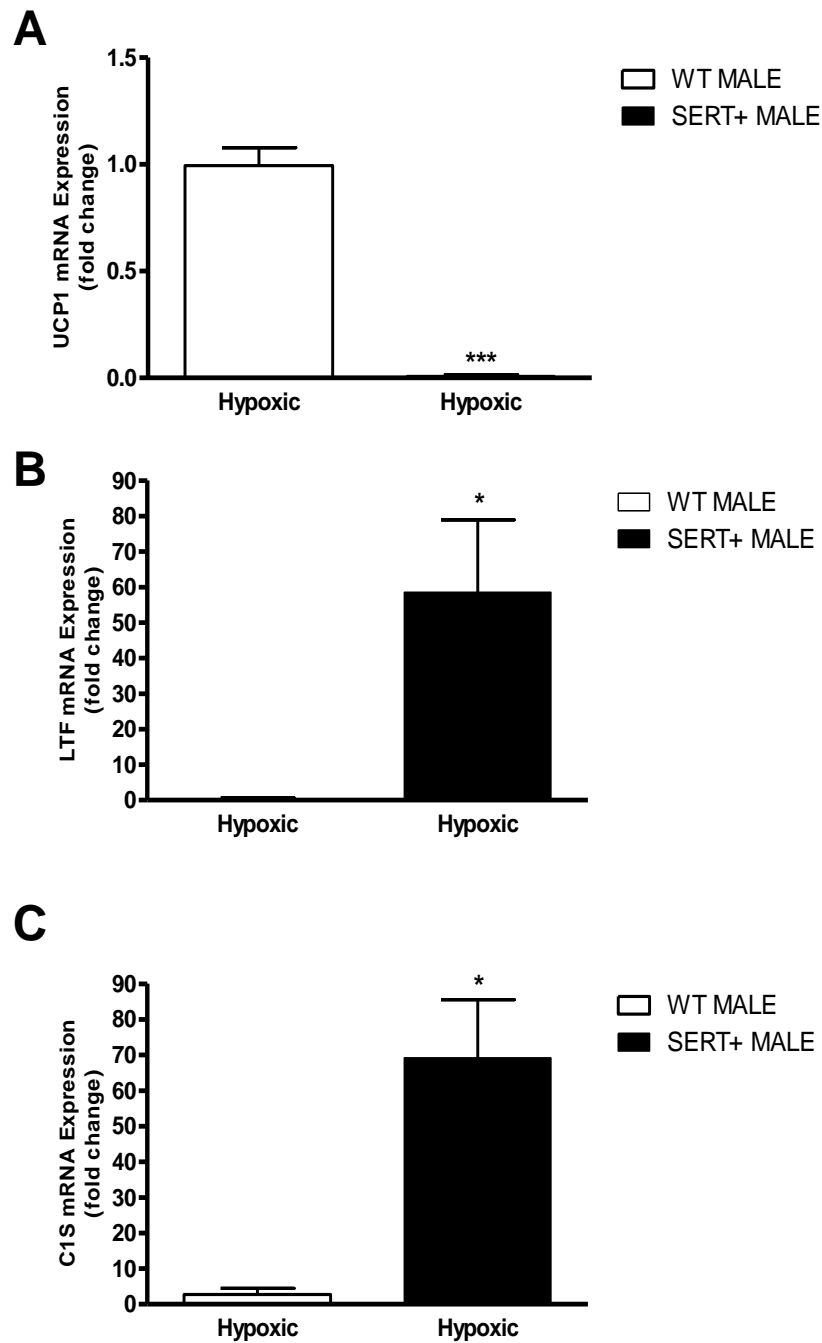


Figure 4.12 UCP1, LTF and C1S mRNA expression in the pulmonary arteries of chronically hypoxic male wildtype and SERT+ mice. UCP1 (A) mRNA expression is increased and LTF (B) and C1S (C) mRNA expression is decreased in chronically hypoxic male SERT+ mice, concordant with microarray analysis. Data are expressed as mean \pm SEM and analysed by Students t-test; * $P < 0.05$, *** $P < 0.001$ cf. chronically hypoxic male WT mice. $n = 4$ and performed in triplicate.

4.2.5 *C/EBP β , CYP1B1 and c-FOS Protein Expression is Increased in Female SERT+ Mice*

To further investigate interesting gene expression differences observed in female SERT+ mice, we assessed expression of CEBPB, CYP1B1 and FOS at protein level. In agreement with our qRT-PCR findings, protein expression of C/EBP β (Figure 4.13), CYP1B1 (Figure 4.14) and c-FOS (Figure 4.15) were also up-regulated in the pulmonary arteries of female SERT+ mice.

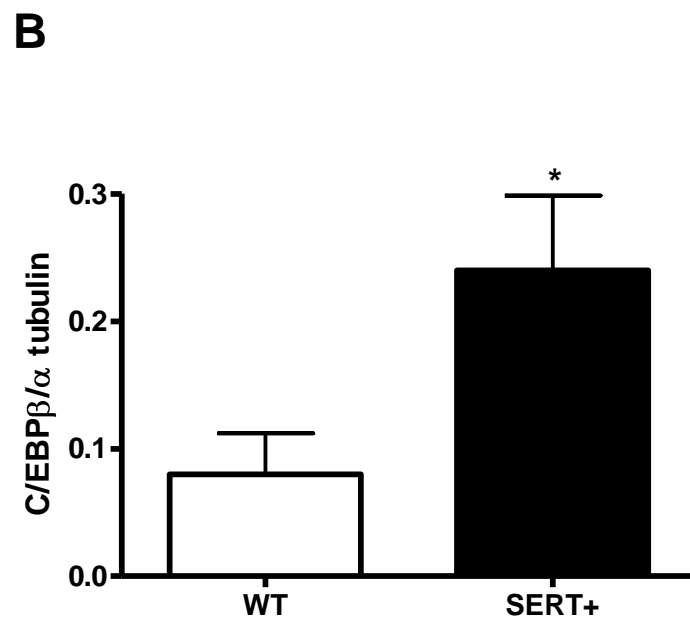
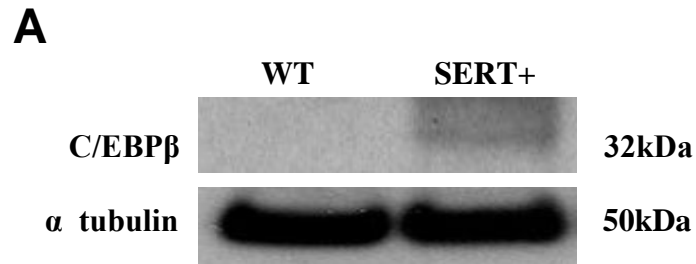


Figure 4.13 C/EBP β expression in the pulmonary arteries of female wildtype and SERT+ mice. Representative immunoblotting (A) and densitometrical analysis (B) confirming that C/EBP β expression is increased in the pulmonary arteries of female SERT+ mice compared to female WT mice. Data are expressed as mean \pm SEM and analysed by Students t-test; *P<0.05 cf. WT mice. n=4 and performed in triplicate.

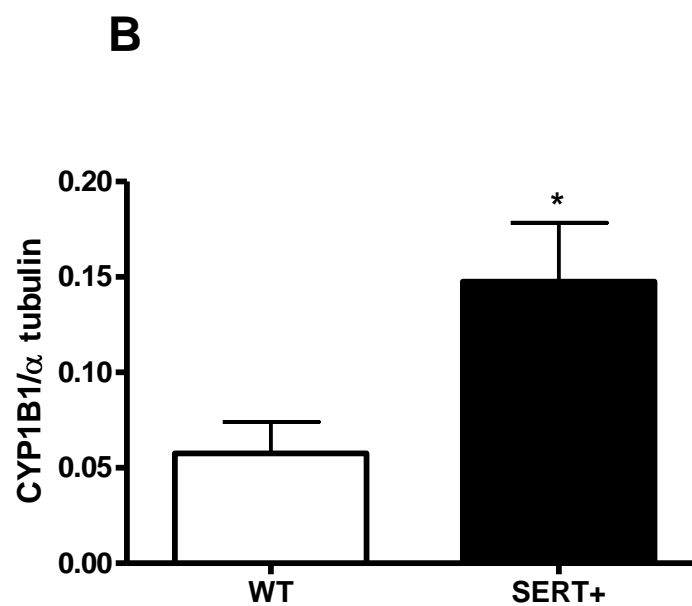
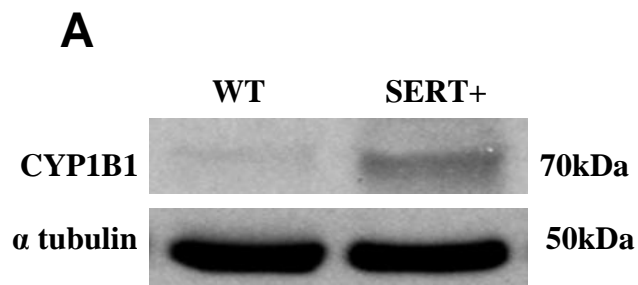
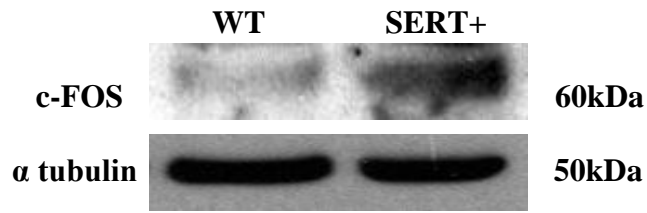


Figure 4.14 CYP1B1 expression in the pulmonary arteries of female wildtype and SERT+ mice. Representative immunoblotting (A) and densitometrical analysis (B) confirming that CYP1B1 expression is increased in the pulmonary arteries of female SERT+ mice compared to female WT mice. Data are expressed as mean \pm SEM and analysed by Students t-test; *P<0.05 cf. WT mice. n=4 and performed in triplicate.

A



B

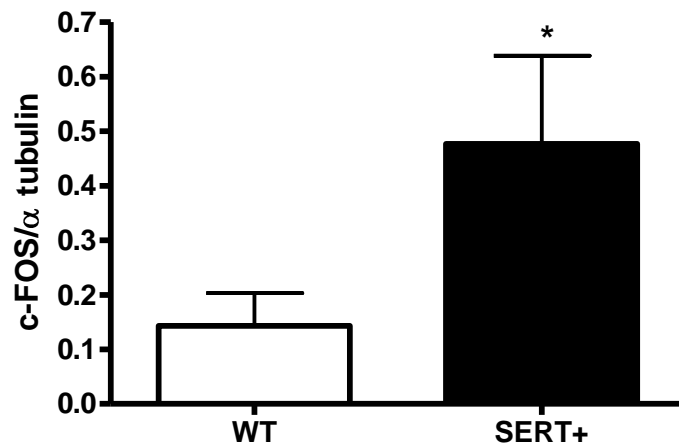


Figure 4.15 c-FOS expression in the pulmonary arteries of female wildtype and SERT+ mice. Representative immunoblotting (A) and densitometrical analysis (B) confirming that c-FOS expression is increased in the pulmonary arteries of female SERT+ mice compared to female WT mice. Data are expressed as mean \pm SEM and analysed by Students t-test; *P<0.05 cf. WT mice. n=4 and performed in triplicate.

4.2.6 Serotonin and 17 β Estradiol Stimulate C/EBP β , CYP1B1 and c-FOS Expression in PASMCs

To determine if serotonin and 17 β estradiol stimulate expression of C/EBP β , CYP1B1 and c-FOS, we investigated expression of these in PASMCs following 24 hour stimulation with serotonin and 17 β estradiol. Stimulation with serotonin or 17 β estradiol for 24 hours was sufficient to increase C/EBP β (Figure 4.16), CYP1B1 (Figure 4.17) and c-FOS (Figure 4.18) expression in PASMCs.

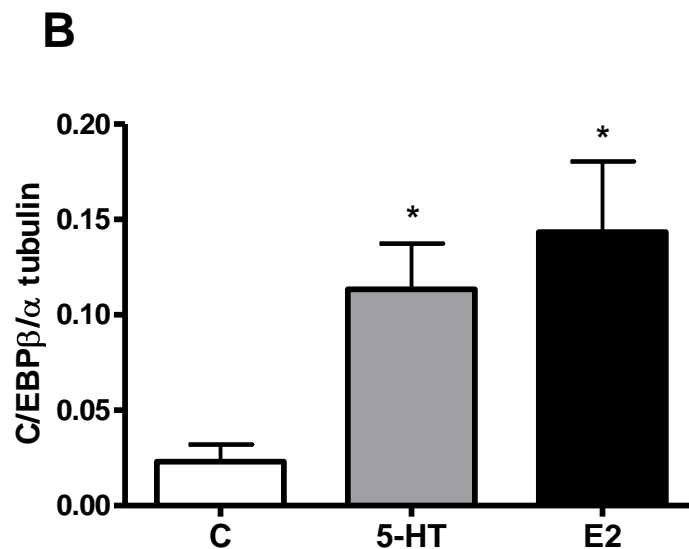
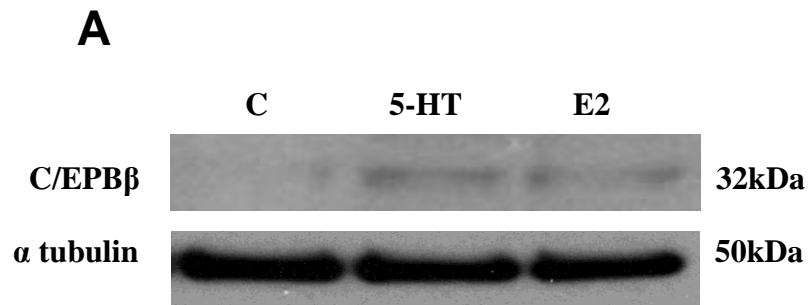


Figure 4.16 C/EBP β expression in human PSMCs following serotonin and 17 β estradiol stimulation. Representative immunoblotting (A) and densitometric analysis (B) confirming increased protein expression of C/EBP β in human PSMCs following 24 hours stimulation with 1 μ mol/L serotonin (5-HT) or 1nmol/L 17 β estradiol (E2). Data are expressed as mean \pm SEM and analysed by one-way ANOVA followed by Dunnetts post-hoc test; *P<0.05 cf. control PSMCs. n=3 and performed in triplicate.

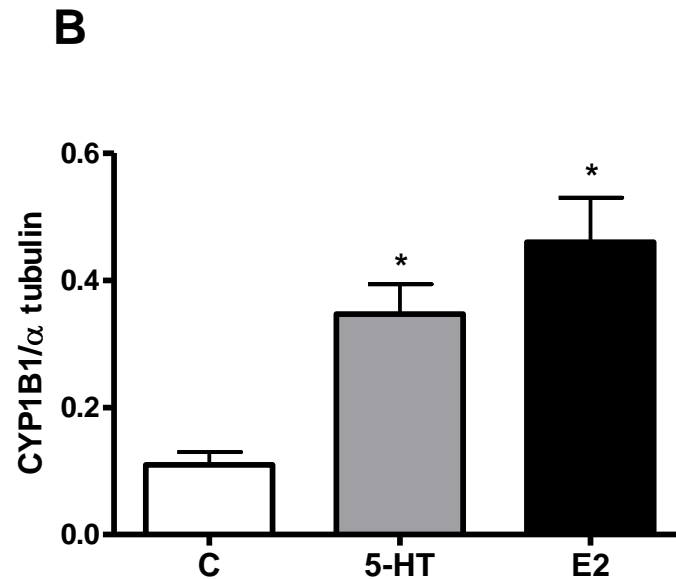
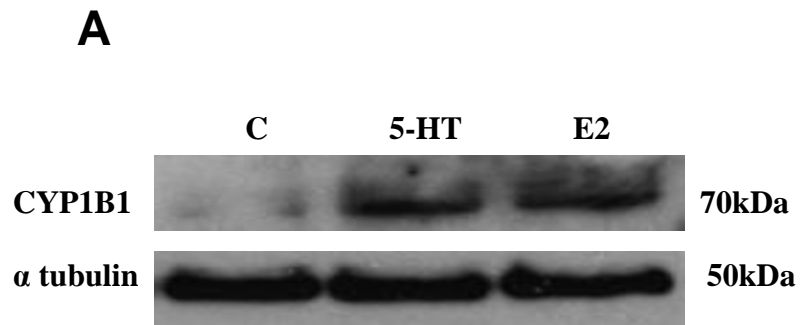


Figure 4.17 CYP1B1 expression in human PSMCs following serotonin and 17 β estradiol stimulation. Representative immunoblotting (A) and densitometric analysis (B) confirming increased protein expression of CYP1B1 in human PSMCs following 24 hours stimulation with 1 μ mol/L serotonin (5-HT) or 1nmol/L 17 β estradiol (E2). Data are expressed as mean \pm SEM and analysed by one-way ANOVA followed by Dunnetts post-hoc test. *P<0.05 cf. control PSMCs. n=3 and performed in triplicate.

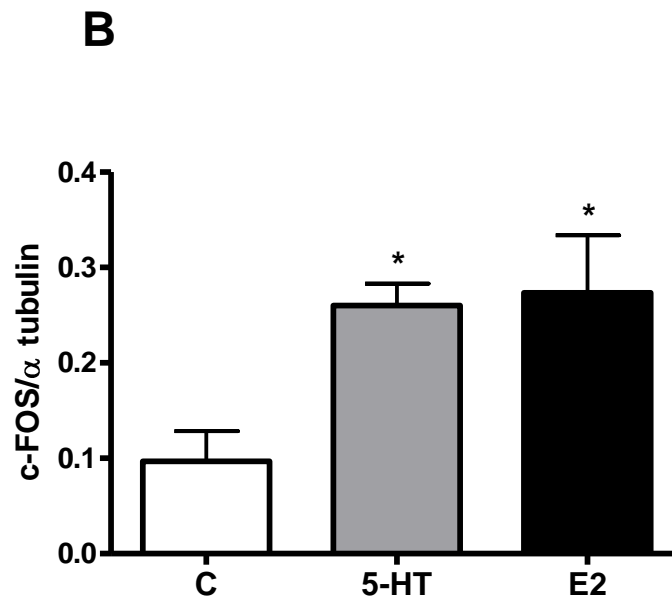
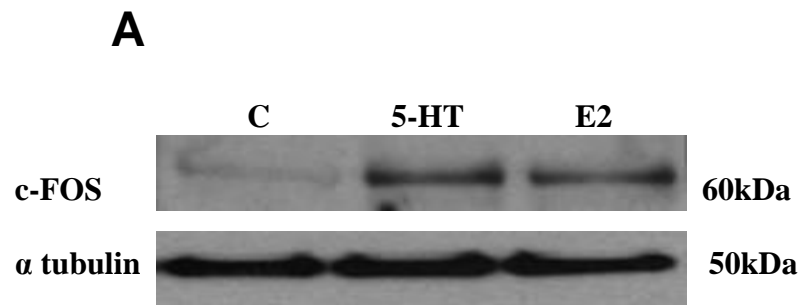


Figure 4.18 c-FOS expression in human PASMCs following serotonin and 17 β estradiol stimulation. Representative immunoblotting (A) and densitometric analysis (B) confirming increased protein expression of c-FOS in human PASMCs following 24 hours stimulation with 1 μ mol/L serotonin (5-HT) or 1nmol/L 17 β estradiol (E2). Data are expressed as mean \pm SEM and analysed by one-way ANOVA followed by Dunnetts post-hoc test. *P<0.05 cf. control PASMCs. n=3 and performed in triplicate.

4.2.7 C/EBP β , CYP1B1 and c-FOS mRNA and Protein Expression is Increased in PSMCs Derived From IPAH Patients

To identify if these findings translate with relevance to human PAH, we investigated the expression of CEBPB, CYP1B1 and FOS in PSMCs derived from IPAH patients. PSMCs from non-PAH donors were studied as controls. Interestingly, CEBPB, CYP1B1 and FOS expression appeared significantly increased in mRNA extracted from IPAH PSMCs (Figure 4.19). Similarly, Western blot analysis confirmed that protein expression of C/EBP β (Figure 4.20), CYP1B1 (Figure 4.21) and c-FOS (Figure 4.22) is also increased in IPAH PSMCs compared to control PSMCs.

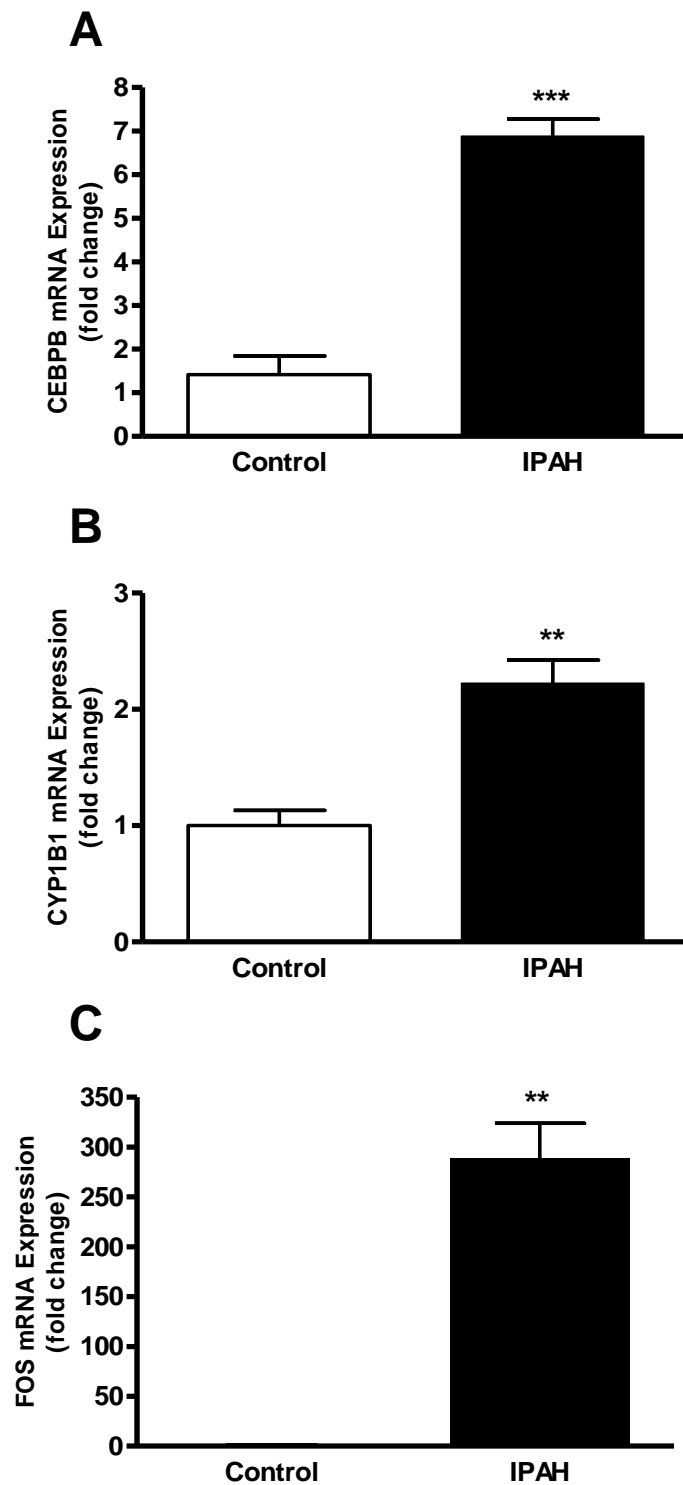


Figure 4.19 CEBPB, CYP1B1 and FOS mRNA expression in PASMCs derived from control and IPAH patients. Expression of CEBPB (A), CYP1B1 (B) and FOS (C) is increased in PASMCs derived from IPAH patients. Data are expressed as mean \pm SEM and analysed by Students t-test; ** $P < 0.01$, *** $P < 0.001$ cf. control. $n = 3$ and performed in triplicate.

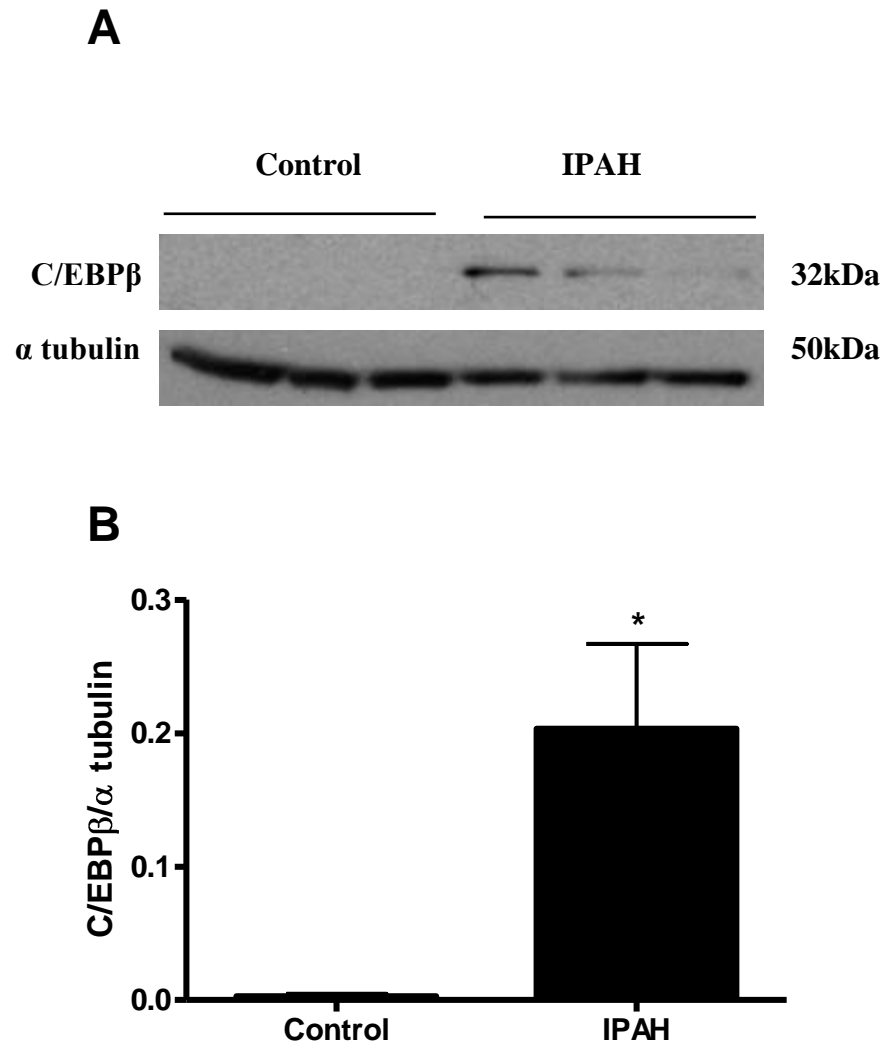


Figure 4.20 C/EBP β expression is increased in PASMCs derived from IPAH patients.

Representative immunoblotting (A) and densitometrical analysis (B) confirming that C/EBP β is increased in PASMCs derived from IPAH patients. Data are expressed as mean \pm SEM and analysed by Students t-test; *P<0.05 cf. control. n=3 and performed in triplicate.

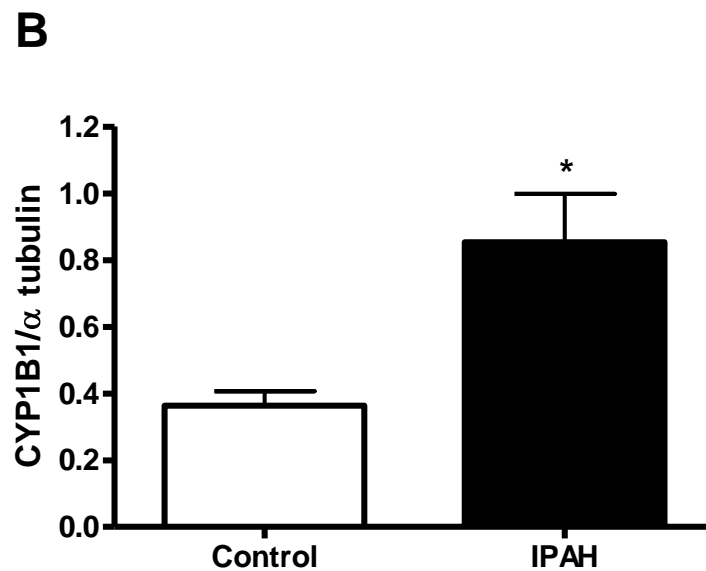
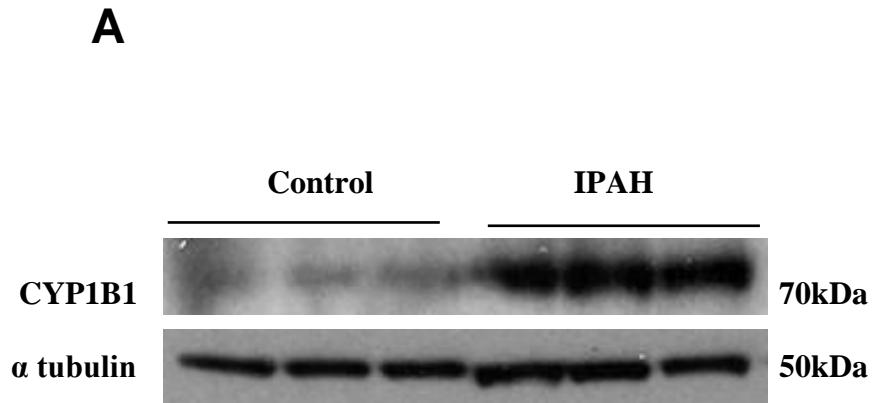


Figure 4.21 CYP1B1 expression is increased in PSMCs derived from IPAH patients.

Representative immunoblotting (A) and densitometrical analysis (B) confirming that CYP1B1 is increased in PSMCs derived from IPAH patients. Data are expressed as mean \pm SEM and analysed by Students t-test; *P<0.05 cf. control. n=3 and performed in triplicate.

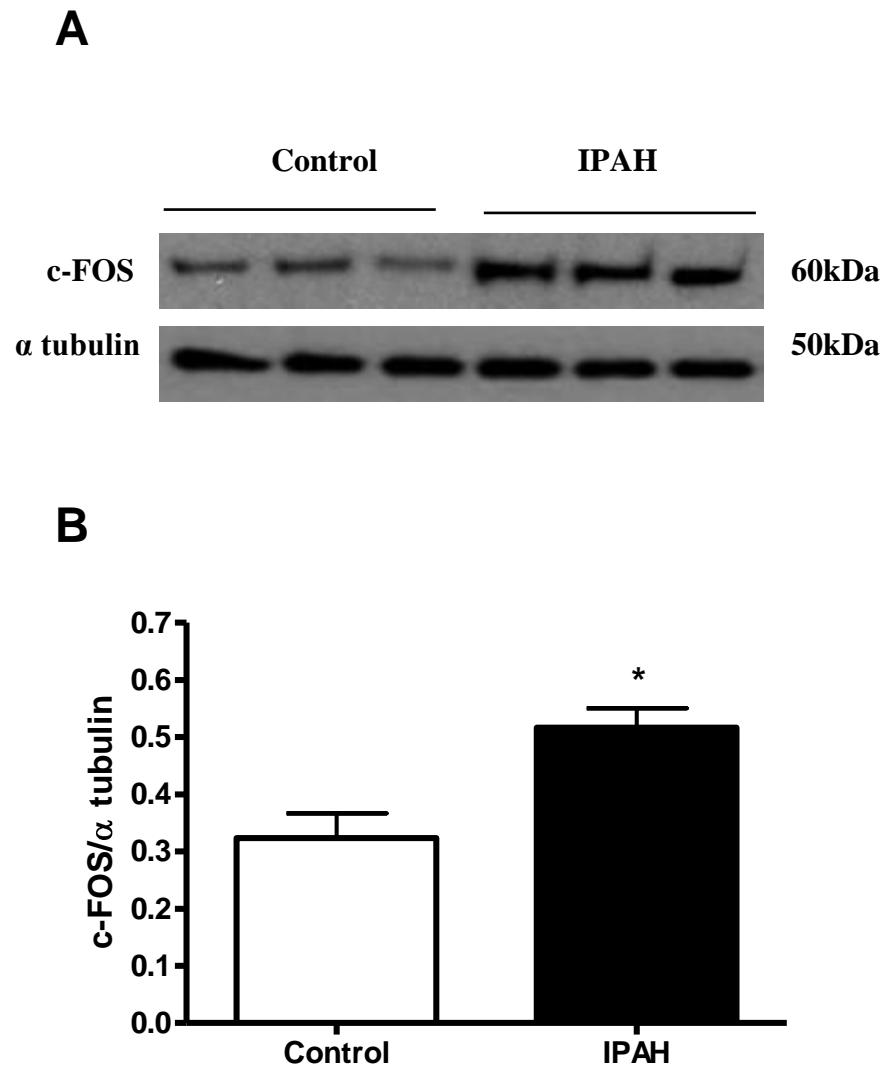


Figure 4.22 c-FOS expression is increased in PSMCs derived from IPAH patients. Representative immunoblotting (A) and densitometrical analysis (B) confirming that c-FOS is increased in PSMCs derived from IPAH patients. Data are expressed as mean \pm SEM and analysed by Students t-test; *P<0.05 cf. control. n=3 and performed in triplicate.

4.3 Discussion

Despite increased mortality reported in men (Humbert et al., 2010), the incidence of both IPAH and HPAH remains up to three-fold more common in women. This is highlighted in recent epidemiological studies carried out in Scotland, France and USA, where 60%, 65% and 77% of the patients studied respectively were female (Peacock et al., 2007; Humbert et al., 2006; Thenappan et al., 2007). Established experimental models of PAH have failed to provide insight into this increased occurrence. Paradoxically, several experimental models of PAH exhibit male susceptibility compared to their female counterparts (Rabinovitch et al., 1981; Hansmann et al., 2007; Said et al., 2007; Miller et al., 2005). Here, we describe an experimental model of PAH which exhibits female susceptibility. Female SERT⁺ mice develop PAH and exaggerated hypoxia-induced PAH whereas male SERT⁺ mice remain unaffected, when compared against their respective WT controls. We were interested in determining the genotypic differences associated with the development and progression of PAH in SERT⁺ mice. To investigate this, microarray analysis was performed in the pulmonary arteries of SERT⁺ mice at 2 months of age, where no PAH phenotype is reported.

Through microarray analysis we have identified a large number of differentially expressed genes in the pulmonary arteries of SERT⁺ mice. In total, we identified 155 genes changed in female SERT⁺ mice whilst 148 genes were changed in male SERT⁺ mice. Heat map analysis identified gene expression changes in females which were not apparent in males. When assigned to biological processes, we also identified that over 40% of the differentially expressed genes in female SERT⁺ mice were directly involved in biological pathways. In total, fifteen known biological pathways were dysregulated in female SERT⁺ mice and included oxidation-reduction, cell differentiation, regulation of transcription, apoptosis, muscle contraction, cellular calcium ion homeostasis and glycolysis. This may

be relevant to the development of PAH in SERT⁺ mice, as dysregulation of these pathways has been previously implicated in the pathogenesis of PAH (Rehman and Archer, 2010; Sakao et al., 2009). Indeed, similar pathway changes have also been described in the lungs of VIP^{-/-} mice (Hamidi et al., 2008) and BMPR-II mutant mice (Tada et al., 2007). In contrast to female SERT⁺ mice, only 25% of altered genes in male SERT⁺ mice were associated with biological function and as a consequence resulted in the dysregulation of pathways to a much lesser extent.

In chronic hypoxia, there were also a large number of differentially expressed genes in SERT⁺ mice compared to their respective WT controls. We observed a total of 316 genes altered in females whilst less than half (154) of these were altered in males. In hypoxic female SERT⁺ mice, 53% of genes were associated with biological function. Similar to the normoxic female comparison, altered genes were related to apoptotic, inflammatory, transcription and metabolic processes, all of which are well-described in PAH (Hassoun et al., 2009). In total, 26 biological pathways were identified as dysregulated. As expected, fewer genes were reported as changed in male SERT⁺ mice. These differences may help explain the exaggerated hypoxia-induced PAH phenotype in female SERT⁺ mice.

The female hormone 17 β estradiol is one risk factor in PAH. Decreased expression of the 17 β estradiol metabolising enzyme cytochrome P450 1B1 (CYP1B1), resulting in altered estrogen metabolism, has been identified in female PAH patients harbouring a BMPR-II mutation compared to unaffected female carriers (Austin et al., 2009). Multiple factors modulate the levels of estrogen-metabolizing enzymes in the liver and target tissues, and the biological effects of an estrogen will depend on the profile of metabolites formed and the biological activities of each of these metabolites (Zhu and Conney, 1998). 17 β estradiol is metabolised to both pro- and anti-proliferative metabolites and its effects will depend on its metabolism. 17 β estradiol can be converted to estrone and subsequently

metabolized to 16 α -hydroxyestrone (16-OHE1) via CYP3A4. Or alternatively, 17 β estradiol is metabolized to 2-hydroxyestradiol (2-OHE) via the estrogen metabolizing enzymes CYP1A1/2 and to a lesser extent via CYP1B1 (Hanna et al., 2000; Tsuchiya et al., 2005). 2-OHE can itself be metabolized to 2-methoxyestradiol (2-ME) via catechol O-methyltransferase (COMT). Both 2-OHE and 2-ME have anti-proliferative effects on cells (Tofovic et al., 2006), whereas 16 α -OHE1 stimulates proliferation by constitutively activating the estrogen receptor (Swanek and Fishman, 1988). Metabolism of 17 β estradiol will therefore be species, gender and strain-dependent and differential disruption in the balance of metabolites may therefore account for the differential effects of female hormones in different models of PAH. Consistent with this, our microarray findings show that CYP1B1 mRNA expression is increased in female SERT⁺ mice. In further support of this, immunoblotting confirmed that CYP1B1 protein expression is also increased in the pulmonary arteries of female SERT⁺ mice. Of further interest, both serotonin and 17 β estradiol stimulation increased CYP1B1 expression in PSMCs. Indeed, similar 17 β estradiol effects have been previously described in cancer cells (Tsuchiya et al., 2004). On this evidence, serotonin and 17 β estradiol may be accountable for increased CYP1B1 expression in female SERT⁺ mice.

CCAAT/enhancer-binding protein beta (C/EBP β) is a transcription factor encoded by the CEBPB gene. C/EBP β has been previously shown to regulate inflammation, cell differentiation and cell proliferation (Ramji and Foka, 2002). For example, C/EBP β is essential in the pathogenesis of multiple proliferative disorders including skin, breast and ovarian cancer (Zhu et al., 2002; Raught et al., 1996; Sundfeldt et al., 1999). In line with this, C/EBP β deficient mice appear resistant to tumorigenesis (Sterneck et al., 2006). The role of C/EBP β in the development of PAH is poorly defined. Increased C/EBP β expression has been reported in the lungs of chronically hypoxic rats (Teng et al., 2002), where it appears to stimulate inducible nitric oxide synthase expression. Reduced CEBPB

expression has also been previously reported in the lungs of SERT knockout mice (Crona et al., 2009). Conversely, our microarray data shows the up-regulation CEBPB in female SERT+ mice. Increased CEBPB mRNA expression was confirmed by qRT-PCR analysis. We also identified that C/EBP β protein expression was increased in the pulmonary arteries of female SERT+ mice. In support of this, we observed that serotonin and 17 β estradiol increased C/EBP β expression in human PASMCs. These findings suggest that serotonin and 17 β estradiol may stimulate C/EBP β expression *in vivo*, and this contributes to the pathogenesis of PAH in female SERT+ mice.

We observed increased FOS expression in the pulmonary arteries of female SERT+ mice. FOS is a proto-oncogene which exists as an immediate early gene transcription factor, and is transactivated in response to various stimuli (Herschman, 1991). For example, FOS expression is increased in the heart following exposure to hypoxia (Deindl et al., 2003). In bovine PASMCs, serotonin is also a potent inducer of FOS expression via a MAPK-dependent pathway (Simon et al., 2005). In agreement with this, we observed that serotonin stimulation also increased c-FOS expression in human PASMCs. Of interest, expression was also increased in 17 β estradiol stimulated cells. Similar effects have also been described in rat hepatocytes (Lee and Edwards, 2001). *In vivo*, c-FOS expression is increased in the pulmonary arteries of female SERT+ mice. Here, our evidence suggests serotonin and 17 β estradiol stimulate c-FOS expression, and this may be relevant to the pathogenesis of PAH in female SERT+ mice.

With relevance to human PAH we further examined CEBPB, CYP1B1 and FOS expression in PASMCs derived from IPAH patients. We observed that expression of these three genes (CEBPB, CYP1B1 and FOS) was increased in IPAH PASMCs. We observed at least five-fold increases in CEBPB and FOS mRNA expression compared to control PASMCs. Immunoblotting confirmed that the upregulation of C/EBP β and c-FOS was

also apparent at protein level. Since these genes are involved in inflammation and proliferation, both of which are essential components in disease pathogenesis (Tuder et al., 2009), our findings suggest their importance in human PAH. Their role in the pathobiology of experimental and human PAH is of particular interest. We also observed increased CYP1B1 mRNA and protein expression in IPAH PSMCs, suggesting the importance of CYP1B1-mediated estrogen metabolism in PAH. However, these findings are inconsistent with previous studies in Epstein Barr virus immortalized B cells derived from female BMPR-II PAH patients (West et al., 2008), where decreased CYP1B1 mRNA expression was described. Most likely, this is attributable to the differences in cell type investigated. This study focuses on changes in PSMCs, which represent a more physiologically relevant cell type in PAH. The dysfunction in estrogen metabolism, and particularly CYP1B1, appears a causative factor in human PAH and merits further investigation.

We have previously reported that SERT⁺ mice develop elevated RVSP in the absence of RVH (MacLean et al., 2004). This phenomenon is particular to normoxic mice as we, like others, have shown that mice develop RVH following exposure to hypoxia (MacLean et al., 2004; Keegan et al., 2001). We are not alone in observing this phenomenon as other studies have similarly demonstrated elevated RVSP in transgenic mice in the absence of RVH. For example, mice that express BMPR-II^{R899X} in smooth muscle or molecular loss of BMPR-II signaling in smooth muscle demonstrate elevated RVSP with no change in RVH (Tada et al., 2007; West et al., 2004). The observation that this only occurs in normoxic mice suggests that hypoxia induces an effect on RVH that may indeed be independent of RVSP.

The distal arteries are typically those most susceptible to pulmonary vascular remodelling in PAH, however microarray analysis was performed in the proximal pulmonary arteries of

mice as these were the smallest that could be practically dissected out from whole lung. Therefore, these gene changes may not be entirely representative of gene expression changes in smaller resistance arteries. For example, our microarray results show that hypoxic female SERT⁺ mice exhibit increased PPAR- γ expression relative to hypoxic female WT mice. However, previous observations confirm that PPAR- γ expression is reduced in the distal pulmonary arteries of PAH patients (Ameshima et al., 2003), and its targeted deletion in pulmonary artery smooth muscle or endothelial cells is sufficient to cause PAH in mice (Hansmann et al., 2008; Guignabert et al., 2009). This contrast in findings may well result from the effect of hypoxia *per se* or an indirect compensatory change in response to PAH in SERT⁺ mice.

Additional bioinformatics analysis may help further identify ‘gene networks’ which are dysfunctional in SERT⁺ mice. Additionally, it would be relevant to further investigate any dysregulated genes/pathways also present in alternative models of PAH and human PAH. Specific to this study, dysregulation of associated genes ‘upstream’ or ‘downstream’ of CEBPB, CYP1B1 and FOS would be of particular interest.

In conclusion, through microarray analysis we have identified a large number of differentially expressed genes in the pulmonary arteries of SERT⁺ mice. These findings offer further insight into the gender differences observed in this serotonin-dependent model of PAH. At least three of these genes (CEBPB, CYP1B1 and FOS) are also up-regulated at protein level in these mice. With relevance to human PAH, we identified that mRNA and protein expression of CEBPB, CYP1B1 and FOS was also increased in PASMCs derived from IPAH patients. This study has described genotypic differences in a serotonin-dependent model of PAH and these findings at least in part, may be relevant to the pathogenesis observed in human PAH.

Chapter 5

General Discussion

General Discussion

Serotonin is a monoamine synthesized from dietary tryptophan. In the pulmonary vasculature, it is a potent mitogen and vasoconstrictor (MacLean and Dempsie, 2009). These effects are well established in the pathogenesis of both experimental and human PAH. The exogenous administration of serotonin exaggerates hypoxia-induced PAH in rats (Eddahibi et al., 1997), and uncovers a PAH phenotype in BMPR-II mutant mice (Long et al., 2006). Also, mice devoid of peripheral serotonin are resistant to the development of both hypoxia-induced (Morecroft et al., 2007) and dexfenfluramine-induced PAH (Dempsie et al., 2008). TPH1, which is the rate-limiting enzyme involved in serotonin synthesis, is increased in the lungs and PAECs derived from IPAH patients (Eddahibi et al., 2006). Serotonin is thought to mediate its effects via SERT. For example, serotonin-induced proliferation of PASMCs is abolished by the SERT inhibitor citalopram (Welsh et al., 2004). Indeed, SERT⁺ mice develop PAH and exaggerated hypoxia-induced PAH (MacLean et al., 2004) whilst mice devoid of the SERT gene are resistant to hypoxia-induced PAH (Eddahibi et al., 2000). Targeted over-expression of SERT in PASMCs is also sufficient for the development of PAH in mice (Guignabert et al., 2006).

Increased female susceptibility in human PAH is well-described. This is highlighted in recent epidemiological studies carried out in Scotland, USA and France, where a female bias of up to three-fold is observed (Peacock et al., 2007; Thenappan et al., 2007; Humbert et al., 2006). Currently, no animal model of PAH has recapitulated this female susceptibility. Paradoxical to this, male susceptibility is reported in several experimental models (Said et al., 2007; Rabinovitch et al., 1981). This absence of a suitable experimental model has limited research to date. In the central nervous system, estrogen regulates expression of several key serotonin signalling components including TPH, SERT and the 5-HT receptors. Most likely, this results in enhanced serotonin signalling. On this

evidence, we hypothesized that similar observations were apparent in the pulmonary circulation, and that this may be responsible for increased female susceptibility in PAH. We investigated this in a serotonin-dependent model of PAH (SERT⁺ mice).

Here, we provide evidence that females are at an increased risk to the development of PAH, via the effects of 17 β estradiol (Chapter 3). Involvement of the serotonin pathway appears critical to this. We observed that female SERT⁺ mice exhibit PAH and exaggerated hypoxia-induced PAH whilst male SERT⁺ mice remained unaffected compared to their respective WT controls. Ovariectomy abolished this PAH phenotype in SERT⁺ mice confirming the involvement of ovarian-derived female hormones in disease pathogenesis. The administration of 17 β estradiol, which is the pre-dominant circulating hormone in pre-menopausal females, in ovariectomized SERT⁺ mice fully re-established PAH and exaggerated hypoxia-induced PAH. These findings highlight the critical role of 17 β estradiol in the development of PAH in SERT⁺ mice. Surprisingly, male SERT⁺ mice subjected to 17 β estradiol did not develop an exaggerated PAH phenotype. This observation must be further investigated, but one hypothesis to explain this is via the differential effects of 17 β estradiol and its metabolism in males compared to females. For example, altered estrogen metabolism arising from polymorphisms in the estrogen-metabolising enzyme CYP1B1 has been associated with the development of PAH in women (West et al., 2008). Here, we propose that dysfunctional estrogen metabolism, likely via altered expression of key estrogen metabolising enzymes, is essential in 'switching' estrogen effects from disease-preventing to disease-promoting. For example, SERT⁺ PAH is unique to female mice suggesting involvement of the serotonin pathway in this, and requires further investigation. In humans, the *SERTLPR* polymorphism results in increased transcription, translation and function of SERT. Therefore, it would be of interest to determine the precise gender bias in PAH patients who carry the *SERTLPR*

polymorphism. Based on this evidence, we propose that female carriers are at a much greater risk to the development of PAH than male carriers.

To translate clinical relevance to our findings, we further investigated the effects of female hormones in human PASMCs. Consistent with our *in vivo* findings, we observed that physiological concentrations of 17β estradiol stimulate proliferation as assessed by increased DNA synthesis and cell number, whereas estrone, estriol and progesterone had no effect. The proliferation of pulmonary vascular cells is essential for pulmonary vascular remodelling and currently considered an irreversible component in PAH (Humbert et al., 2004). These 17β estradiol effects may be relevant to the increased female susceptibility observed in PAH. We also observed that activation and utilisation of the serotonin pathway is essential for 17β estradiol-induced proliferation. This was apparent as presence of the TPH inhibitor PCPA or the 5-HT_{1B} receptor antagonist SB224289 was sufficient to completely inhibit 17β estradiol stimulated proliferation. On this evidence, it would be of interest to establish if inhibition of TPH1 or the 5-HT_{1B} receptors is sufficient to abolish PAH in female SERT⁺ mice *in vivo*. In contrast, the 5-HT_{2A} receptor antagonist ketanserin had no effect on proliferation suggesting a minor role of this receptor, and is consistent with previous reports in human PASMCs (Morecroft et al., 2010). Immunoblotting performed in PASMC lysates treated with 17β estradiol also confirmed that TPH1, SERT and 5-HT_{1B} receptor expression was increased. These findings are the first to describe the expression of TPH1 in PASMCs and suggest the possible existence of autocrine serotonin signalling in pulmonary vascular cells. Increased SERT and 5-HT_{1B} receptor expression in PASMCs are also sufficiently important, as both have been previously implicated in serotonin-induced PASMC proliferation (Morecroft et al., 2010). Along these lines, it would be of interest to investigate if TPH1, SERT and 5-HT_{1B} receptor expression is similarly altered in the lungs of ovariectomized and estrogen-dosed SERT⁺ mice. In conclusion of these findings, we have described the first experimental model of PAH

which exhibits female susceptibility. Specifically, female mice appear at increased risk to the development of PAH via the proliferative effects of 17β estradiol. This is likely achieved via 17β estradiol-mediated increased expression of TPH1, SERT and the 5-HT_{1B} receptors to enhance PASMC proliferation and pulmonary vascular remodelling.

Given the gender differences we observed in the development of PAH in SERT⁺ mice, we further investigated possible underlying genotypic differences which may help explain this (Chapter 4). Through microarray analysis in the pulmonary arteries, we identified a large number of differentially expressed genes which were apparent in SERT⁺ mice compared to their respective WT controls. When assigned to biological function, 43% of these genes were important in females whilst only 27% were important in males. Similarly, these dysregulated genes in female SERT⁺ mice were associated with a large number (>15) of biological pathways whereas this was apparent to a much lesser extent in male SERT⁺ mice. Moreover, a large number of altered pathways in females were associated with inflammation, metabolism and contraction, all of which have been previously implicated in the pathogenesis of PAH (Tuder and Voelkel, 1998; Rehman and Archer, 2010). This suggests that dysregulation of these pathways is sufficient in promoting the development of PAH, and this is unique to female SERT⁺ mice. Hierarchical cluster analysis also revealed gene expression patterns in female SERT⁺ mice which were not apparent in male SERT⁺ mice. We also repeated microarray analysis in the pulmonary arteries of chronically hypoxic SERT⁺ mice to investigate the genotypic differences associated with exaggerated hypoxia-induced PAH. We observed a total of 316 differentially expressed genes in females whilst less than half of this number (145) was altered in males. Similar to the normoxic comparison, when assigned to biological function over half (53%) were important in females whereas significantly less (42%) appeared important in males. As expected, the dysregulation of multiple pathways with relevance to PAH was observed in chronically hypoxic females.

For validation of the microarray study, we performed RT-PCR analysis in three differentially expressed genes across each group comparison. These results were concordant with the microarray data. Specifically, following interim Ingenuity Pathway Analysis (IPA) analysis, we focused our interest on three genes which were up-regulated in female SERT⁺ mice (CEBPB, CYP1B1 and FOS).

The CEBPB gene encodes for CCAAT-enhancer binding protein beta (C/EBP β). It is important in inflammation and proliferation, both of which are essential in the pathogenesis of PAH (Rehman and Archer, 2010; Humbert et al., 2004). CEBPB mRNA is intronless and is usually translated into three distinct isoforms termed full-length liver-activating protein (LAP), medium-length LAP and short-length liver-inhibitory protein (LIP). The translated C/EBP β isoform is determined by the inherent translation start codon site. Although LIP is a dominant-negative isoform with no biological function, the opposing effects of medium and full-length LAP are thought to determine function. For example, in mouse embryonic fibroblasts (MEFs) full-length LAP is a transcriptional activator whereas medium-length LAP is a transcriptional repressor (Qiu et al., 2008). *In vivo*, we observed increased CEBPB mRNA and protein expression in the pulmonary arteries of female SERT⁺ mice compared to female WT mice. In agreement with this, CEBPB is decreased in the lungs of SERT knockout mice (Crona et al., 2009), whilst expression is increased in the lungs of rats following exposure to chronic hypoxia (Teng et al., 2002). Serotonin and 17 β estradiol increased C/EBP β expression in PASMCs, which may be relevant to these *in vivo* findings. In relation to human PAH, both mRNA and protein expression is increased in PASMCs derived from IPAH patients, suggesting its importance in human PAH. On this evidence, we propose that C/EBP β is a key inflammatory component in the progression of PAH.

Estrogen is one risk factor in PAH. Decreased expression of the estrogen-metabolising enzyme cytochrome P450 1B1 (CYP1B1) has been previously described in PAH (West et al., 2008). Here, we also observed alterations in CYP1B1 expression. However, in contrast we reported increased CYP1B1 mRNA and protein expression in the pulmonary arteries of female SERT⁺ mice. One explanation for this disparity in findings may be the different cell types investigated. Here, we focused on pulmonary vascular cells, which may be more relevant cell type to study. Serotonin and 17 β estradiol may be important regulators of this, as stimulation with these increase CYP1B1 expression in PSMCs. With respect to human PAH, we similarly observed increased CYP1B1 mRNA and protein in PSMCs derived from IPAH patients compared against control PSMCs. Our evidence suggests a role for CYP1B1 in the pathogenesis of experimental and human PAH. It would also be of interest to further investigate C/EBP β expression in PAECs and PAFs. Relevant to this, CYP1B1 is also over-expressed in pro-proliferative tumour cells (Murray et al., 2001; Murray et al., 1997), and polymorphisms in this gene are associated with increased incidence of tumorigenesis (Sasaki et al., 2004; Sasaki et al., 2003; Tanaka et al., 2002; Van Emburgh et al., 2008; Cussenot et al., 2007). One hypothesis we propose is that CYP1B1-derived estrogen metabolites are pro-proliferative in pulmonary vascular cells, and this alteration in estrogen metabolism is promoting the development of PAH in females. Therefore, it would be of interest to assess the proliferative effects of CYP1B1-derived estrogen metabolites in PSMCs. Recently, vaccine-based CYP1B1 immunotherapy successfully completed phase I clinical trial and appears a promising preventative treatment for cancer (Luby, 2008). CYP1B1 appears an important mediator of estrogen signalling in PAH via regulation of its metabolism, and merits further investigation.

We also investigated c-FOS expression in SERT⁺ PAH and human PAH. FOS is a proto-oncogene which exists as an immediate early gene transcription factor, and is

transactivated in response to various stimuli. It is also involved in cellular proliferation (Herschman, 1991). In bovine PSMCs, serotonin is a potent inducer of c-FOS expression via the ERK pathway (Simon et al., 2005). Here, we observed increased expression of both FOS mRNA and c-FOS protein in the pulmonary arteries of female SERT⁺ mice. With relevance, stimulation of human PSMCs with either serotonin or 17 β estradiol was sufficient to increase c-FOS expression. Of further interest, FOS mRNA and c-FOS protein was also up-regulated in IPAH PSMCs. Given this increased expression in both experimental and human PAH, c-FOS may be an important signalling regulator in pulmonary vascular mitogenesis, however requires further investigation.

Through microarray analysis we identified a large number of novel genes which appear to be promoting the development of PAH in a serotonin-dependent model of female PAH. Moreover, at least three of these genes (CEBPB, CYP1B1 and FOS) are up-regulated at protein level in mice and also up-regulated in PSMCs derived from IPAH patients, further suggesting their importance in human PAH. These novel genes may be essential in promoting a PAH phenotype in females.

In summary of these findings, through a translational approach we have provided evidence which greatly advances our understanding as to why increased female susceptibility exists in PAH. This includes the upregulation of key genes which appear to be promoting a PAH phenotype in females. Both serotonin and estrogen are critical to this. In future perspective, the therapeutic target of these dysregulated pathways may be one potential treatment strategy in women with PAH.

Future Perspective

Therapeutic target of the estrogen pathway appears a promising candidate in PAH. From findings previously discussed, the therapeutic potential of CYP1B1 inhibition in the prevention and reversal of experimental PAH is of particular interest. To test this, effects of the CYP1B1 inhibitor TMS in hypoxia-induced PAH should be considered. Along these lines, the characterisation of PAH in CYP1B1 deficient mice is also of interest. In translational perspective to human PAH, CYP1B1 inhibition via immunotherapy is one approach currently in phase I development for the treatment of cancer (Luby, 2008), and may be of potential clinical interest in the treatment of PAH if pre-clinical studies appear promising.

In addition, those signalling pathways activated by estrogen and/or its metabolites must be further delineated. It is likely that one or more ER isoforms (ER α , ER β and GPR30) are directly involved in PAH, or at least indirectly via regulating expression of key estrogen metabolizing enzymes including CYP1B1, as previously reported (Tsuchiya et al., 2004). Therefore, inhibition of ERs via selective antagonists and/or SERMs is also of interest. Indeed, SERMs are already an effective therapeutic approach in the treatment of multiple other estrogen-dependent diseases including breast cancer (Veronesi et al., 2005). C/EBP β and FOS may also play an important role in the pathogenesis of PAH. Here, our data suggests that C/EBP β and FOS act downstream of estrogen-dependent pathways, as 17 β estradiol increase their expression in PSMCs. In support of this, C/EBP β and FOS are increased in both experimental PAH and human PAH and further highlights their potential importance in PAH progression.

In future perspective, this evidence implicates estrogen in the pathogenesis of PAH, and highlights the estrogen pathway as one novel therapeutic target in the treatment of PAH.

Reference List

1. Aaronson PI, Robertson TP, Knock GA, Becker S, Lewis TH, Snetkov V, and Ward JP. Hypoxic pulmonary vasoconstriction: mechanisms and controversies. *J Physiol* 570: 53-58, 2006.
2. Aaronson PI, Robertson TP, and Ward JP. Endothelium-derived mediators and hypoxic pulmonary vasoconstriction. *Respir Physiol Neurobiol* 132: 107-120, 2002.
3. Abe K, Toba M, Alzoubi A, Ito M, Fagan KA, Cool CD, Voelkel NF, McMurtry IF, and Oka M. Formation of plexiform lesions in experimental severe pulmonary arterial hypertension. *Circulation* 121: 2747-2754, 2010.
4. Abenhaim L, Rich S, Moride Y, and Brenot F. Anorexic drugs and the development of primary pulmonary hypertension: Results of the international primary pulmonary hypertension study. *Circulation* 94: 1240, 1996.
5. Alexander SP, Mathie A, and Peters JA. Guide to receptors and channels, 2nd edition. *Br J Pharmacol* 147 Suppl 3: S1-168, 2006.
6. Ameshima S, Golpon H, Cool CD, Chan D, Vandivier RW, Gardai SJ, Wick M, Nemenoff RA, Geraci MW, and Voelkel NF. Peroxisome proliferator-activated receptor gamma (PPARgamma) expression is decreased in pulmonary hypertension and affects endothelial cell growth. *Circ Res* 92: 1162-1169, 2003.
7. Ameshima S, Golpon H, Cool CD, Chan D, Vandivier RW, Gardai SJ, Wick M, Nemenoff RA, Geraci MW, and Voelkel NF. Peroxisome proliferator-activated

receptor gamma (PPARgamma) expression is decreased in pulmonary hypertension and affects endothelial cell growth. *Circ Res* 92: 1162-1169, 2003.

8. Anderson GL, Limacher M, Assaf AR, Bassford T, Beresford SA, Black H, Bonds D, Brunner R, Brzyski R, Caan B, Chlebowski R, Curb D, Gass M, Hays J, Heiss G, Hendrix S, Howard BV, Hsia J, Hubbell A, Jackson R, Johnson KC, Judd H, Kotchen JM, Kuller L, Lacroix AZ, Lane D, Langer RD, Lasser N, Lewis CE, Manson J, Margolis K, Ockene J, O'Sullivan MJ, Phillips L, Prentice RL, Ritenbaugh C, Robbins J, Rossouw JE, Sarto G, Stefanick ML, Van HL, Wactawski-Wende J, Wallace R, and Wassertheil-Smoller S. Effects of conjugated equine estrogen in postmenopausal women with hysterectomy: the Women's Health Initiative randomized controlled trial. *JAMA* 291: 1701-1712, 2004.
9. Anter E, Chen K, Shapira OM, Karas RH, and Keaney JF, Jr. p38 mitogen-activated protein kinase activates eNOS in endothelial cells by an estrogen receptor alpha-dependent pathway in response to black tea polyphenols. *Circ Res* 96: 1072-1078, 2005.
10. Archer SL, Nelson DP, and Weir EK. Detection of activated O₂ species in vitro and in rat lungs by chemiluminescence. *J Appl Physiol* 67: 1912-1921, 1989.
11. Archer SL, Peterson D, Nelson DP, DeMaster EG, Kelly B, Eaton JW, and Weir EK. Oxygen radicals and antioxidant enzymes alter pulmonary vascular reactivity in the rat lung. *J Appl Physiol* 66: 102-111, 1989.
12. Archer SL, Wu XC, Thebaud B, Nsair A, Bonnet S, Tyrrell B, McMurtry MS, Hashimoto K, Harry G, and Michelakis ED. Preferential expression and function of

voltage-gated, O₂-sensitive K⁺ channels in resistance pulmonary arteries explains regional heterogeneity in hypoxic pulmonary vasoconstriction: ionic diversity in smooth muscle cells. *Circ Res* 95: 308-318, 2004.

13. Aronica SM, Kraus WL, and Katzenellenbogen BS. Estrogen action via the cAMP signaling pathway: stimulation of adenylate cyclase and cAMP-regulated gene transcription. *Proc Natl Acad Sci U S A* 91: 8517-8521, 1994.
14. Austin ED, Cogan JD, West JD, Hedges LK, Hamid R, Dawson EP, Wheeler LA, Parl FF, Loyd JE, and Phillips JA, III. Alterations in oestrogen metabolism: implications for higher penetrance of familial pulmonary arterial hypertension in females. *Eur Respir J* 34: 1093-1099, 2009.
15. Badesch DB, Tapson VF, McGoon MD, Brundage BH, Rubin LJ, Wigley FM, Rich S, Barst RJ, Barrett PS, Kral KM, Jobsis MM, Loyd JE, Murali S, Frost A, Girgis R, Bourge RC, Ralph DD, Elliott CG, Hill NS, Langleben D, Schilz RJ, McLaughlin VV, Robbins IM, Groves BM, Shapiro S, and Medsger TA, Jr. Continuous intravenous epoprostenol for pulmonary hypertension due to the scleroderma spectrum of disease. A randomized, controlled trial. *Ann Intern Med* 132: 425-434, 2000.
16. Barnes PJ and Liu SF. Regulation of pulmonary vascular tone. *Pharmacol Rev* 47: 87-131, 1995.
17. Barst RJ, McGoon M, Torbicki A, Sitbon O, Krowka MJ, Olschewski H, and Gaine S. Diagnosis and differential assessment of pulmonary arterial hypertension. *J Am Coll Cardiol* 43: 40S-47S, 2004.

18. Barst RJ, Rubin LJ, Long WA, McGoon MD, Rich S, Badesch DB, Groves BM, Tapson VF, Bourge RC, Brundage BH, and . A comparison of continuous intravenous epoprostenol (prostacyclin) with conventional therapy for primary pulmonary hypertension. The Primary Pulmonary Hypertension Study Group. *N Engl J Med* 334: 296-302, 1996.
19. Benza RL, Barst RJ, Galie N, Frost A, Girgis RE, Highland KB, Strange C, Black CM, Badesch DB, Rubin L, Fleming TR, and Naeije R. Sitaxsentan for the treatment of pulmonary arterial hypertension: a 1-year, prospective, open-label observation of outcome and survival. *Chest* 134: 775-782, 2008.
20. Benza RL, Mehta S, Keogh A, Lawrence EC, Oudiz RJ, and Barst RJ. Sitaxsentan treatment for patients with pulmonary arterial hypertension discontinuing bosentan. *J Heart Lung Transplant* 26: 63-69, 2007.
21. Benza RL, Park MH, Keogh A, and Girgis RE. Management of pulmonary arterial hypertension with a focus on combination therapies. *J Heart Lung Transplant* 26: 437-446, 2007.
22. Benza RL, Rayburn BK, Tallaj JA, Pamboukian SV, and Bourge RC. Treprostinil-based therapy in the treatment of moderate-to-severe pulmonary arterial hypertension: long-term efficacy and combination with bosentan. *Chest* 134: 139-145, 2008.
23. Berger M, Gray JA, and Roth BL. The expanded biology of serotonin. *Annu Rev Med* 60: 355-366, 2009.

24. Bertrand PP, Parnavitane UT, Chavez C, Gogos A, Jones M, and van den BM. The effect of low estrogen state on serotonin transporter function in mouse hippocampus: a behavioral and electrochemical study. *Brain Res* 1064: 10-20, 2005.
25. Black SM, Sanchez LS, Mata-Greenwood E, Bekker JM, Steinhorn RH, and Fineman JR. sGC and PDE5 are elevated in lambs with increased pulmonary blood flow and pulmonary hypertension. *Am J Physiol Lung Cell Mol Physiol* 281: L1051-L1057, 2001.
26. Blanpain C, Le Poul E, Parma J, Knoop C, Detheux M, Parmentier M, Vassart G, and Abramowicz MJ. Serotonin 5-HT_{2B} receptor loss of function mutation in a patient with fenfluramine-associated primary pulmonary hypertension. *Cardiovasc Res* 60: 518-528, 2003.
27. Bourassa PA, Milos PM, Gaynor BJ, Breslow JL, and Aiello RJ. Estrogen reduces atherosclerotic lesion development in apolipoprotein E-deficient mice. *Proc Natl Acad Sci U S A* 93: 10022-10027, 1996.
28. Brouchet L, Krust A, Dupont S, Chambon P, Bayard F, and Arnal JF. Estradiol accelerates reendothelialization in mouse carotid artery through estrogen receptor-alpha but not estrogen receptor-beta. *Circulation* 103: 423-428, 2001.
29. Broughton BR, Miller AA, and Sobey CG. Endothelium-dependent relaxation by G protein-coupled receptor 30 agonists in rat carotid arteries. *Am J Physiol Heart Circ Physiol* 298: H1055-H1061, 2010.

30. Bush TL, Barrett-Connor E, Cowan LD, Criqui MH, Wallace RB, Suchindran CM, Tyroler HA, and Rifkind BM. Cardiovascular mortality and noncontraceptive use of estrogen in women: results from the Lipid Research Clinics Program Follow-up Study. *Circulation* 75: 1102-1109, 1987.
31. Callebert J, Esteve JM, Herve P, Peoc'h K, Tournois C, Drouet L, Launay JM, and Maroteaux L. Evidence for a control of plasma serotonin levels by 5-hydroxytryptamine(2B) receptors in mice. *J Pharmacol Exp Ther* 317: 724-731, 2006.
32. Caulin-Glaser T, Garcia-Cardena G, Sarrel P, Sessa WC, and Bender JR. 17 beta-estradiol regulation of human endothelial cell basal nitric oxide release, independent of cytosolic Ca²⁺ mobilization. *Circ Res* 81: 885-892, 1997.
33. Channick R, Badesch DB, Tapson VF, Simonneau G, Robbins I, Frost A, Roux S, Rainisio M, Bodin F, and Rubin LJ. Effects of the dual endothelin receptor antagonist bosentan in patients with pulmonary hypertension: a placebo-controlled study. *J Heart Lung Transplant* 20: 262-263, 2001.
34. Channick RN, Simonneau G, Sitbon O, Robbins IM, Frost A, Tapson VF, Badesch DB, Roux S, Rainisio M, Bodin F, and Rubin LJ. Effects of the dual endothelin-receptor antagonist bosentan in patients with pulmonary hypertension: a randomised placebo-controlled study. *Lancet* 358: 1119-1123, 2001.
35. Chavez C, Hollaus M, Scarr E, Pavey G, Gogos A, and van den Buuse M. The effect of estrogen on dopamine and serotonin receptor and transporter levels in the brain: an autoradiography study. *Brain Res* 1321: 51-59, 2010.

36. Christman BW, McPherson CD, Newman JH, King GA, Bernard GR, Groves BM, and Loyd JE. An imbalance between the excretion of thromboxane and prostacyclin metabolites in pulmonary hypertension. *N Engl J Med* 327: 70-75, 1992.
37. Comroe JH, Jr. The main functions of the pulmonary circulation. *Circulation* 33: 146-158, 1966.
38. Comroe JH, Jr. The main functions of the pulmonary circulation. *Circulation* 33: 146-158, 1966.
39. Cool CD, Groshong SD, Oakey J, and Voelkel NF. Pulmonary hypertension: cellular and molecular mechanisms. *Chest* 128: 565S-571S, 2005.
40. Cool CD, Groshong SD, Oakey J, and Voelkel NF. Pulmonary hypertension: cellular and molecular mechanisms. *Chest* 128: 565S-571S, 2005.
41. Crona D, Harral J, Adnot S, Eddahibi S, and West J. Gene expression in lungs of mice lacking the 5-hydroxytryptamine transporter gene. *BMC Pulm Med* 9: 19, 2009.
42. Crosby A, Jones FM, Southwood M, Stewart S, Schermuly R, Butrous G, Dunne DW, and Morrell NW. Pulmonary vascular remodeling correlates with lung eggs and cytokines in murine schistosomiasis. *Am J Respir Crit Care Med* 181: 279-288, 2010.
43. Cussenot O, Azzouzi AR, Nicolaiew N, Fromont G, Mangin P, Cormier L, Fournier G, Valeri A, Larre S, Thibault F, Giordanella JP, Pouchard M, Zheng Y, Hamdy FC, Cox A, and Cancel-Tassin G. Combination of polymorphisms from

genes related to estrogen metabolism and risk of prostate cancers: the hidden face of estrogens. *J Clin Oncol* 25: 3596-3602, 2007.

44. Cutrer FM, Yu XJ, Ayata G, Moskowitz MA, and Waeber C. Effects of PNU-109,291, a selective 5-HT_{1D} receptor agonist, on electrically induced dural plasma extravasation and capsaicin-evoked c-fos immunoreactivity within trigeminal nucleus caudalis. *Neuropharmacology* 38: 1043-1053, 1999.
45. Darblade B, Pendaries C, Krust A, Dupont S, Fouque MJ, Rami J, Chambon P, Bayard F, and Arnal JF. Estradiol alters nitric oxide production in the mouse aorta through the alpha-, but not beta-, estrogen receptor. *Circ Res* 90: 413-419, 2002.
46. Dawson CA. Role of pulmonary vasomotion in physiology of the lung. *Physiol Rev* 64: 544-616, 1984.
47. Deindl E, Kolar F, Neubauer E, Vogel S, Schaper W, and Ostadal B. Effect of intermittent high altitude hypoxia on gene expression in rat heart and lung. *Physiol Res* 52: 147-157, 2003.
48. deMello DE, Sawyer D, Galvin N, and Reid LM. Early fetal development of lung vasculature. *Am J Respir Cell Mol Biol* 16: 568-581, 1997.
49. Dempsie Y and MacLean MR. Pulmonary hypertension: therapeutic targets within the serotonin system. *Br J Pharmacol* 155: 455-462, 2008.
50. Dempsie Y, Macritchie NA, Morecroft I, Nilsen M, Loughlin L, and MacLean MR. The Effects of Gender on the Development of Dexfenfluramine-Induced

- Pulmonary Arterial Hypertension in Mice. *Am J Respir Crit Care Med* 179: A1808, 2009.
51. Dempsie Y, Morecroft I, Welsh DJ, Macritchie NA, Herold N, Loughlin L, Nilsen M, Peacock AJ, Harmar A, Bader M, and MacLean MR. Converging evidence in support of the serotonin hypothesis of dexfenfluramine-induced pulmonary hypertension with novel transgenic mice. *Circulation* 117: 2928-2937, 2008.
 52. Dempsie Y, White K, Nilsen M, Loughlin L, and MacLean MR. The Effects Of Endogenous Female Sex Hormones On Dexfenfluramine-Induced Pulmonary Arterial Hypertension In Mice. *Am J Respir Crit Care Med* 181: A6314, 2010.
 53. Dewachter L, Adnot S, Fadel E, Humbert M, Maitre B, Barlier-Mur AM, Simonneau G, Hamon M, Naeije R, and Eddahibi S. Angiotensin/Tie2 pathway influences smooth muscle hyperplasia in idiopathic pulmonary hypertension. *Am J Respir Crit Care Med* 174: 1025-1033, 2006.
 54. Ding Q, Gros R, Limbird LE, Chorazyczewski J, and Feldman RD. Estradiol-mediated ERK phosphorylation and apoptosis in vascular smooth muscle cells requires GPR 30. *Am J Physiol Cell Physiol* 297: C1178-C1187, 2009.
 55. Domenighetti G, Leuenberger P, and Feihl F. Haemodynamic effects of ketanserin either alone or with oxygen in COPD patients with secondary pulmonary hypertension. *Monaldi Arch Chest Dis* 52: 429-433, 1997.
 56. Downing SE and Lee JC. Nervous control of the pulmonary circulation. *Annu Rev Physiol* 42: 199-210, 1980.

57. Druce M, Rockall A, and Grossman AB. Fibrosis and carcinoid syndrome: from causation to future therapy. *Nat Rev Endocrinol* 5: 276-283, 2009.
58. Dubey RK, Jackson EK, Gillespie DG, Rosselli M, Barchiesi F, Krust A, Keller H, Zacharia LC, and Imthurn B. Cytochromes 1A1/1B1- and catechol-O-methyltransferase-derived metabolites mediate estradiol-induced antimitogenesis in human cardiac fibroblast. *J Clin Endocrinol Metab* 90: 247-255, 2005.
59. Dubey RK, Jackson EK, Gillespie DG, Rosselli M, Barchiesi F, Krust A, Keller H, Zacharia LC, and Imthurn B. Cytochromes 1A1/1B1- and catechol-O-methyltransferase-derived metabolites mediate estradiol-induced antimitogenesis in human cardiac fibroblast. *J Clin Endocrinol Metab* 90: 247-255, 2005.
60. Dunning AM, Healey CS, Baynes C, Maia AT, Scollen S, Vega A, Rodriguez R, Barbosa-Morais NL, Ponder BA, Low YL, Bingham S, Haiman CA, Le ML, Broeks A, Schmidt MK, Hopper J, Southey M, Beckmann MW, Fasching PA, Peto J, Johnson N, Bojesen SE, Nordestgaard B, Milne RL, Benitez J, Hamann U, Ko Y, Schmutzler RK, Burwinkel B, Schurmann P, Dork T, Heikkinen T, Nevanlinna H, Lindblom A, Margolin S, Mannermaa A, Kosma VM, Chen X, Spurdle A, Change-Claude J, Flesch-Janys D, Couch FJ, Olson JE, Severi G, Baglietto L, Borresen-Dale AL, Kristensen V, Hunter DJ, Hankinson SE, Devilee P, Vreeswijk M, Lissowska J, Brinton L, Liu J, Hall P, Kang D, Yoo KY, Shen CY, Yu JC, Anton-Culver H, Ziogas A, Sigurdson A, Struewing J, Easton DF, Garcia-Closas M, Humphreys MK, Morrison J, Pharoah PD, Pooley KA, and Chenevix-Trench G. Association of ESR1 gene tagging SNPs with breast cancer risk. *Hum Mol Genet* 18: 1131-1139, 2009.

61. Earley S and Resta TC. Estradiol attenuates hypoxia-induced pulmonary endothelin-1 gene expression. *Am J Physiol Lung Cell Mol Physiol* 283: L86-L93, 2002.
62. Eddahibi S, Guignabert C, Barlier-Mur AM, Dewachter L, Fadel E, Darteville P, Humbert M, Simonneau G, Hanoun N, Saurini F, Hamon M, and Adnot S. Cross talk between endothelial and smooth muscle cells in pulmonary hypertension - Critical role for serotonin-induced smooth muscle hyperplasia. *Circulation* 113: 1857-1864, 2006.
63. Eddahibi S, Hanoun N, Lanfumey L, Lesch KP, Raffestin B, Hamon M, and Adnot S. Attenuated hypoxic pulmonary hypertension in mice lacking the 5-hydroxytryptamine transporter gene. *J Clin Invest* 105: 1555-1562, 2000.
64. Eddahibi S, Humbert M, Fadel E, Raffestin B, Darmon M, Capron F, Simonneau G, Darteville P, Hamon M, and Adnot S. Serotonin transporter overexpression is responsible for pulmonary artery smooth muscle hyperplasia in primary pulmonary hypertension. *J Clin Invest* 108: 1141-1150, 2001.
65. Eddahibi S, Raffestin B, Launay JM, Sitbon M, and Adnot S. Effect of dexfenfluramine treatment in rats exposed to acute and chronic hypoxia. *Am J Respir Crit Care Med* 157: 1111-1119, 1998.
66. Eddahibi S, Raffestin B, Pham I, Launay JM, Aegerter P, Sitbon M, and Adnot S. Treatment with 5-HT potentiates development of pulmonary hypertension in chronically hypoxic rats. *Am J Physiol Heart Circ Physiol* 41: H1173-H1181, 1997.

67. Farhat MY, Chen MF, Bhatti T, Iqbal A, Cathapermal S, and Ramwell PW. Protection by oestradiol against the development of cardiovascular changes associated with monocrotaline pulmonary hypertension in rats. *Br J Pharmacol* 110: 719-723, 1993.
68. Farhat MY, Vargas R, Dingaam B, and Ramwell PW. In vitro effect of oestradiol on thymidine uptake in pulmonary vascular smooth muscle cell: role of the endothelium. *Br J Pharmacol* 107: 679-683, 1992.
69. Filardo E, Quinn J, Pang Y, Graeber C, Shaw S, Dong J, and Thomas P. Activation of the novel estrogen receptor G protein-coupled receptor 30 (GPR30) at the plasma membrane. *Endocrinology* 148: 3236-3245, 2007.
70. Fishman AP. Respiratory gases in the regulation of the pulmonary circulation. *Physiol Rev* 41: 214-280, 1961.
71. Fitzgerald LW, Burn TC, Brown BS, Patterson JP, Corjay MH, Valentine PA, Sun JH, Link JR, Abbaszade I, Hollis JM, Largent BL, Hartig PR, Hollis GF, Meunier PC, Robichaud AJ, and Robertson DW. ACCELERATED COMMUNICATION: Possible Role of Valvular Serotonin 5-HT_{2B} Receptors in the Cardiopathy Associated with Fenfluramine. *Mol Pharmacol* 57: 75-81, 2000.
72. Frid MG, Dempsey EC, Durmowicz AG, and Stenmark KR. Smooth muscle cell heterogeneity in pulmonary and systemic vessels. Importance in vascular disease. *Arterioscler Thromb Vasc Biol* 17: 1203-1209, 1997.

73. Fukuroda T, Nishikibe M, Ohta Y, Ihara M, Yano M, Ishikawa K, Fukami T, and Ikemoto F. Analysis of responses to endothelins in isolated porcine blood vessels by using a novel endothelin antagonist, BQ-153. *Life Sci* 50: L107-L112, 1992.
74. Gaine SP and Rubin LJ. Primary pulmonary hypertension. *Lancet* 352: 719-725, 1998.
75. Galie N, Badesch D, Oudiz R, Simonneau G, McGoon MD, Keogh AM, Frost AE, Zwicke D, Naeije R, Shapiro S, Olschewski H, and Rubin LJ. Ambrisentan therapy for pulmonary arterial hypertension. *J Am Coll Cardiol* 46: 529-535, 2005.
76. Galie N, Ghofrani HA, Torbicki A, Barst RJ, Rubin LJ, Badesch D, Fleming T, Parpia T, Burgess G, Branzi A, Grimminger F, Kurzyna M, and Simonneau G. Sildenafil citrate therapy for pulmonary arterial hypertension. *N Engl J Med* 353: 2148-2157, 2005.
77. Galie N, Manes A, and Branzi A. The endothelin system in pulmonary arterial hypertension. *Cardiovasc Res* 61: 227-237, 2004.
78. Galie N, Olschewski H, Oudiz RJ, Torres F, Frost A, Ghofrani HA, Badesch DB, McGoon MD, McLaughlin VV, Roecker EB, Gerber MJ, Dufton C, Wiens BL, and Rubin LJ. Ambrisentan for the treatment of pulmonary arterial hypertension: results of the ambrisentan in pulmonary arterial hypertension, randomized, double-blind, placebo-controlled, multicenter, efficacy (ARIES) study 1 and 2. *Circulation* 117: 3010-3019, 2008.
79. Geraci MW, Gao B, Shepherd DC, Moore MD, Westcott JY, Fagan KA, Alger LA, Tuder RM, and Voelkel NF. Pulmonary prostacyclin synthase overexpression in

transgenic mice protects against development of hypoxic pulmonary hypertension.
J Clin Invest 103: 1509-1515, 1999.

80. Ghofrani HA, Morrell NW, Hoeper MM, Olschewski H, Peacock AJ, Barst RJ, Shapiro S, Golpon H, Toshner M, Grimminger F, and Pascoe S. Imatinib in pulmonary arterial hypertension patients with inadequate response to established therapy. *Am J Respir Crit Care Med* 182: 1171-1177, 2010.
81. Ghofrani HA, Seeger W, and Grimminger F. Imatinib for the treatment of pulmonary arterial hypertension. *N Engl J Med* 353: 1412-1413, 2005.
82. Giaid A, Yanagisawa M, Langleben D, Michel RP, Levy R, Shennib H, Kimura S, Masaki T, Duguid WP, and Stewart DJ. Expression of endothelin-1 in the lungs of patients with pulmonary hypertension. *N Engl J Med* 328: 1732-1739, 1993.
83. Girerd B, Montani D, Eyries M, Yaici A, Sztrymf B, Coulet F, Sitbon O, Simonneau G, Soubrier F, and Humbert M. Absence of influence of gender and BMPR2 mutation type on clinical phenotypes of pulmonary arterial hypertension. *Respir Res* 11: 73, 2010.
84. Girgis RE, Li D, Zhan X, Garcia JG, Tuder RM, Hassoun PM, and Johns RA. Attenuation of chronic hypoxic pulmonary hypertension by simvastatin. *Am J Physiol Heart Circ Physiol* 285: H938-H945, 2003.
85. Girgis RE, Mozammel S, Champion HC, Li D, Peng X, Shimoda L, Tuder RM, Johns RA, and Hassoun PM. Regression of chronic hypoxic pulmonary hypertension by simvastatin. *Am J Physiol Lung Cell Mol Physiol* 292: L1105-L1110, 2007.

86. Goldstein JL and Brown MS. Regulation of the mevalonate pathway. *Nature* 343: 425-430, 1990.
87. Gonzales RJ, Walker BR, and Kanagy NL. 17beta-estradiol increases nitric oxide-dependent dilation in rat pulmonary arteries and thoracic aorta. *Am J Physiol Lung Cell Mol Physiol* 280: L555-L564, 2001.
88. Goodwin TM. A role for estriol in human labor, term and preterm. *Am J Obstet Gynecol* 180: S208-S213, 1999.
89. Greenberg B, Rhoden K, and Barnes PJ. Endothelium-dependent relaxation of human pulmonary arteries. *Am J Physiol* 252: H434-H438, 1987.
90. Greenway S, van Suylen RJ, Sarvaas GD, Kwan E, Ambartsumian N, Lukanidin E, and Rabinovitch M. S100A4/Mts1 produces murine pulmonary artery changes resembling plexogenic arteriopathy and is increased in human plexogenic arteriopathy. *Am J Pathol* 164: 253-262, 2004.
91. Gregor M and Janig. Effects of systemic hypoxia and hypercapnia on cutaneous and muscle vasoconstrictor neurones to the cat's hindlimb. *Pflugers Arch* 368: 71-81, 1977.
92. Grimminger F and Schermuly RT. PDGF receptor and its antagonists: role in treatment of PAH. *Adv Exp Med Biol* 661: 435-446, 2010.
93. Gryglewski RJ, Botting RM, and Vane JR. Mediators produced by the endothelial cell. *Hypertension* 12: 530-548, 1988.

94. Guignabert C, Alvira CM, Alastalo TP, Sawada H, Hansmann G, Zhao M, Wang L, El-Bizri N, and Rabinovitch M. Tie2-mediated loss of peroxisome proliferator-activated receptor-gamma in mice causes PDGF receptor-beta-dependent pulmonary arterial muscularization. *Am J Physiol Lung Cell Mol Physiol* 297: L1082-L1090, 2009.
95. Guignabert C, Izikki M, Tu LI, Li ZL, Zadigue P, Barlier-Mur AM, Hanoun N, Rodman D, Hamon M, Adnot S, and Eddahibi S. Transgenic mice overexpressing the 5-hydroxytryptamine transporter gene in smooth muscle develop pulmonary hypertension. *Circ Res* 98: 1323-1330, 2006.
96. Gunst SJ and Fredberg JJ. The first three minutes: smooth muscle contraction, cytoskeletal events, and soft glasses. *J Appl Physiol* 95: 413-425, 2003.
97. Haas E, Bhattacharya I, Brailoiu E, Damjanovic M, Brailoiu GC, Gao X, Mueller-Guerre L, Marjon NA, Gut A, Minotti R, Meyer MR, Amann K, Ammann E, Perez-Dominguez A, Genoni M, Clegg DJ, Dun NJ, Resta TC, Prossnitz ER, and Barton M. Regulatory role of G protein-coupled estrogen receptor for vascular function and obesity. *Circ Res* 104: 288-291, 2009.
98. Hamidi SA, Prabhakar S, and Said SI. Enhancement of pulmonary vascular remodelling and inflammatory genes with VIP gene deletion. *Eur Respir J* 31: 135-139, 2008.
99. Hamm HE. The many faces of G protein signaling. *J Biol Chem* 273: 669-672, 1998.

100. Hanna IH, Dawling S, Roodi N, Guengerich FP, and Parl FF. Cytochrome P450 1B1 (CYP1B1) Pharmacogenetics: Association of Polymorphisms with Functional Differences in Estrogen Hydroxylation Activity. *Cancer Res* 60: 3440-3444, 2000.
101. Hansmann G, de Jesus Perez VA, Alastalo TP, Alvira CM, Guignabert C, Bekker JM, Schellong S, Urashima T, Wang L, Morrell NW, and Rabinovitch M. An antiproliferative BMP-2/PPARgamma/apoE axis in human and murine SMCs and its role in pulmonary hypertension. *J Clin Invest* 118: 1846-1857, 2008.
102. Hansmann G, de JP, V, Alastalo TP, Alvira CM, Guignabert C, Bekker JM, Schellong S, Urashima T, Wang L, Morrell NW, and Rabinovitch M. An antiproliferative BMP-2/PPARgamma/apoE axis in human and murine SMCs and its role in pulmonary hypertension 4. *J Clin Invest* 118: 1846-1857, 2008.
103. Hansmann G, Wagner RA, Schellong S, Perez VA, Urashima T, Wang L, Sheikh AY, Suen RS, Stewart DJ, and Rabinovitch M. Pulmonary arterial hypertension is linked to insulin resistance and reversed by peroxisome proliferator-activated receptor-gamma activation. *Circulation* 115: 1275-1284, 2007.
104. Hansmann G, Wagner RA, Schellong S, Perez VA, Urashima T, Wang L, Sheikh AY, Suen RS, Stewart DJ, and Rabinovitch M. Pulmonary arterial hypertension is linked to insulin resistance and reversed by peroxisome proliferator-activated receptor-gamma activation. *Circulation* 115: 1275-1284, 2007.
105. Hansmann G, Wagner RA, Schellong S, Perez VA, Urashima T, Wang L, Sheikh AY, Suen RS, Stewart DJ, and Rabinovitch M. Pulmonary arterial hypertension is linked to insulin resistance and reversed by peroxisome proliferator-activated receptor-gamma activation. *Circulation* 115: 1275-1284, 2007.

106. Harf A, Pratt T, and Hughes JM. Regional distribution of VA/Q in man at rest and with exercise measured with krypton-81m. *J Appl Physiol* 44: 115-123, 1978.
107. Harrison RE, Flanagan JA, Sankelo M, Abdalla SA, Rowell J, Machado RD, Elliott CG, Robbins IM, Olschewski H, McLaughlin V, Gruenig E, Kermeen F, Halme M, Raisanen-Sokolowski A, Laitinen T, Morrell NW, and Trembath RC. Molecular and functional analysis identifies ALK-1 as the predominant cause of pulmonary hypertension related to hereditary haemorrhagic telangiectasia. *J Med Genet* 40: 865-871, 2003.
108. Hart CM and Block ER. Lung serotonin metabolism. *Clin Chest Med* 10: 59-70, 1989.
109. Hassoun PM, Mouthon L, Barbera JA, Eddahibi S, Flores SC, Grimminger F, Jones PL, Maitland ML, Michelakis ED, Morrell NW, Newman JH, Rabinovitch M, Schermuly R, Stenmark KR, Voelkel NF, Yuan JX, and Humbert M. Inflammation, growth factors, and pulmonary vascular remodeling. *J Am Coll Cardiol* 54: S10-S19, 2009.
110. Hassoun PM, Mouthon L, Barbera JA, Eddahibi S, Flores SC, Grimminger F, Jones PL, Maitland ML, Michelakis ED, Morrell NW, Newman JH, Rabinovitch M, Schermuly R, Stenmark KR, Voelkel NF, Yuan JX, and Humbert M. Inflammation, growth factors, and pulmonary vascular remodeling. *J Am Coll Cardiol* 54: S10-S19, 2009.
111. Heath D and Edwards JE. The pathology of hypertensive pulmonary vascular disease; a description of six grades of structural changes in the pulmonary arteries

with special reference to congenital cardiac septal defects. *Circulation* 18: 533-547, 1958.

112. Heldring N, Pike A, Andersson S, Matthews J, Cheng G, Hartman J, Tujague M, Strom A, Treuter E, Warner M, and Gustafsson JA. Estrogen receptors: how do they signal and what are their targets. *Physiol Rev* 87: 905-931, 2007.
113. Herschman HR. Primary response genes induced by growth factors and tumor promoters. *Annu Rev Biochem* 60: 281-319, 1991.
114. Herve P, Drouet L, Dosquet C, Launay JM, Rain B, Simonneau G, Caen J, and Duroux P. Primary pulmonary hypertension in a patient with a familial platelet storage pool disease: role of serotonin. *Am J Med* 89: 117-120, 1990.
115. Herve P, Launay JM, Scrobahaci ML, Brenot F, Simonneau G, Petitpretz P, Poubeau P, Cerrina J, Duroux P, and Drouet L. Increased Plasma Serotonin in Primary Pulmonary-Hypertension. *Am J Med* 99: 249-254, 1995.
116. Holden WE and McCall E. Hypoxia-induced contractions of porcine pulmonary artery strips depend on intact endothelium. *Exp Lung Res* 7: 101-112, 1984.
117. Hong ZG, Olschewski A, Reeve HL, Nelson DP, Hong FX, and Weir EK. Nordexfenfluramine causes more severe pulmonary vasoconstriction than dexfenfluramine. *Am J Physiol Lung Cell Mol Physiol* 286: L531-L538, 2004.
118. Hori S, Komatsu Y, Shigemoto R, Mizuno N, and Nakanishi S. Distinct tissue distribution and cellular localization of two messenger ribonucleic acids encoding

different subtypes of rat endothelin receptors. *Endocrinology* 130: 1885-1895, 1992.

119. Hoshikawa Y, Voelkel NF, Gesell TL, Moore MD, Morris KG, Alger LA, Narumiya S, and Geraci MW. Prostacyclin receptor-dependent modulation of pulmonary vascular remodeling. *Am J Respir Crit Care Med* 164: 314-318, 2001.
120. Hoyer D, Hannon JP, and Martin GR. Molecular, pharmacological and functional diversity of 5-HT receptors. *Pharmacol Biochem Behav* 71: 533-554, 2002.
121. Hoyer D, Hannon JP, and Martin GR. Molecular, pharmacological and functional diversity of 5-HT receptors. *Pharmacol Biochem Behav* 71: 533-554, 2002.
122. Huang W, Yen RT, McLaurine M, and Bledsoe G. Morphometry of the human pulmonary vasculature. *J Appl Physiol* 81: 2123-2133, 1996.
123. Hughes JM. Lung gas tensions and active regulation of ventilation/perfusion ratios in health and disease. *Br J Dis Chest* 69: 153-170, 1975.
124. Humbert M, Morrell NW, Archer SL, Stenmark KR, MacLean MR, Lang IM, Christman BW, Weir EK, Eickelberg O, Voelkel NF, and Rabinovitch M. Cellular and molecular pathobiology of pulmonary arterial hypertension. *J Am Coll Cardiol* 43: 13S-24S, 2004.
125. Humbert M, Sitbon O, Chaouat A, Bertocchi M, Habib G, Gressin V, Yaici A, Weitzenblum E, Cordier JF, Chabot F, Dromer C, Pison C, Reynaud-Gaubert M, Haloun A, Laurent M, Hachulla E, Cottin V, Degano B, Jais X, Montani D, Souza R, and Simonneau G. Survival in patients with idiopathic, familial, and anorexigen-

associated pulmonary arterial hypertension in the modern management era.

Circulation 122: 156-163, 2010.

126. Humbert M, Sitbon O, Chaouat A, Bertocchi M, Habib G, Gressin V, Yaici A, Weitzenblum E, Cordier JF, Chabot F, Dromer C, Pison C, Reynaud-Gaubert M, Haloun A, Laurent M, Hachulla E, and Simonneau G. Pulmonary arterial hypertension in France: results from a national registry. *Am J Respir Crit Care Med* 173: 1023-1030, 2006.
127. Hussain MB and Marshall I. Characterization of alpha1-adrenoceptor subtypes mediating contractions to phenylephrine in rat thoracic aorta, mesenteric artery and pulmonary artery. *Br J Pharmacol* 122: 849-858, 1997.
128. Hyman AL, Lipton HL, and Kadowitz PJ. Nature of alpha 1 and postjunctional alpha 2 adrenoceptors in the pulmonary vascular bed. *Fed Proc* 45: 2336-2340, 1986.
129. Hyman AL, Lipton HL, and Kadowitz PJ. Analysis of pulmonary vascular responses in cats to sympathetic nerve stimulation under elevated tone conditions. Evidence that neuronally released norepinephrine acts on alpha 1-, alpha 2-, and beta 2-adrenoceptors. *Circ Res* 67: 862-870, 1990.
130. Hyman AL, Nandiwada P, Knight DS, and Kadowitz PJ. Pulmonary vasodilator responses to catecholamines and sympathetic nerve stimulation in the cat. Evidence that vascular beta-2 adrenoreceptors are innervated. *Circ Res* 48: 407-415, 1981.
131. Imamov O, Shim GJ, Warner M, and Gustafsson JA. Estrogen receptor beta in health and disease. *Biol Reprod* 73: 866-871, 2005.

132. Jayachandran M, Mukherjee R, Steinkamp T, Labreche P, Bracamonte MP, Okano H, Owen WG, and Miller VM. Differential effects of 17beta-estradiol, conjugated equine estrogen, and raloxifene on mRNA expression, aggregation, and secretion in platelets. *Am J Physiol Heart Circ Physiol* 288: H2355-H2362, 2005.
133. Jayachandran M, Preston CC, Hunter LW, Jahangir A, Owen WG, Korach KS, and Miller VM. Loss of estrogen receptor beta decreases mitochondrial energetic potential and increases thrombogenicity of platelets in aged female mice. *Age (Dordr)* 32: 109-121, 2010.
134. Jiang C, Ting AT, and Seed B. PPAR-gamma agonists inhibit production of monocyte inflammatory cytokines. *Nature* 391: 82-86, 1998.
135. Jordan VC and O'Malley BW. Selective estrogen-receptor modulators and antihormonal resistance in breast cancer. *J Clin Oncol* 25: 5815-5824, 2007.
136. Kadowitz PJ, Joiner PD, and Hyman AL. Effect of sympathetic nerve stimulation on pulmonary vascular resistance in the intact spontaneously breathing dog. *Proc Soc Exp Biol Med* 147: 68-71, 1974.
137. Karas RH, Schulten H, Pare G, Aronovitz MJ, Ohlsson C, Gustafsson JA, and Mendelsohn ME. Effects of estrogen on the vascular injury response in estrogen receptor alpha, beta (double) knockout mice. *Circ Res* 89: 534-539, 2001.
138. Katzenellenbogen BS, Choi I, Delage-Mourroux R, Ediger TR, Martini PG, Montano M, Sun J, Weis K, and Katzenellenbogen JA. Molecular mechanisms of estrogen action: selective ligands and receptor pharmacology. *J Steroid Biochem Mol Biol* 74: 279-285, 2000.

139. Katzenellenbogen BS, Montano MM, Ediger TR, Sun J, Ekena K, Lazennec G, Martini PG, McInerney EM, Delage-Mourroux R, Weis K, and Katzenellenbogen JA. Estrogen receptors: selective ligands, partners, and distinctive pharmacology. *Recent Prog Horm Res* 55: 163-193, 2000.
140. Kawut SM, Horn EM, Berekashvili KK, Lederer DJ, Widlitz AC, Rosenzweig EB, and Barst RJ. Selective serotonin reuptake inhibitor use and outcomes in pulmonary arterial hypertension. *Pulm Pharmacol Ther* 19: 370-374, 2006.
141. Keegan A, Morecroft I, Smillie D, Hicks MN, and MacLean MR. Contribution of the 5-HT1B receptor to hypoxia-induced pulmonary hypertension - Converging evidence using 5-HT1B-receptor knockout mice and the 5-HT1B/1D-receptor antagonist GR127935. *Circ Res* 89: 1231-1239, 2001.
142. Keegan A, Morecroft I, Smillie D, Hicks MN, and MacLean MR. Contribution of the 5-HT1B receptor to hypoxia-induced pulmonary hypertension - Converging evidence using 5-HT1B-receptor knockout mice and the 5-HT1B/1D-receptor antagonist GR127935. *Circ Res* 89: 1231-1239, 2001.
143. Kilic A, Javadov S, and Karmazyn M. Estrogen exerts concentration-dependent pro-and anti-hypertrophic effects on adult cultured ventricular myocytes. Role of NHE-1 in estrogen-induced hypertrophy. *J Mol Cell Cardiol* 46: 360-369, 2009.
144. Killilea DW, Hester R, Balczon R, Babal P, and Gillespie MN. Free radical production in hypoxic pulmonary artery smooth muscle cells. *Am J Physiol Lung Cell Mol Physiol* 279: L408-L412, 2000.

145. Kilner PJ. Pulmonary resistance in cardiovascular context. *Int J Cardiol* 97 Suppl 1: 3-6, 2004.
146. Klepetko W, Mayer E, Sandoval J, Trulock EP, Vachiery JL, Dartevielle P, Pepke-Zaba J, Jamieson SW, Lang I, and Corris P. Interventional and surgical modalities of treatment for pulmonary arterial hypertension. *J Am Coll Cardiol* 43: 73S-80S, 2004.
147. Kobayashi Y and Amenta F. Neurotransmitter receptors in the pulmonary circulation with particular emphasis on pulmonary endothelium. *J Auton Pharmacol* 14: 137-164, 1994.
148. Kramer MS and Lane DA. Aminorex, dexfenfluramine, and primary pulmonary hypertension. *J Clin Epidemiol* 51: 361-364, 1998.
149. Krenz GS, Lin J, Dawson CA, and Linehan JH. Impact of parallel heterogeneity on a continuum model of the pulmonary arterial tree. *J Appl Physiol* 77: 660-670, 1994.
150. Kubota E, Hamasaki Y, Sata T, Saga T, and Said SI. Autonomic innervation of pulmonary artery: evidence for a nonadrenergic noncholinergic inhibitory system. *Exp Lung Res* 14: 349-358, 1988.
151. Kuiper GG, Enmark E, Pelto-Huikko M, Nilsson S, and Gustafsson JA. Cloning of a novel receptor expressed in rat prostate and ovary. *Proc Natl Acad Sci U S A* 93: 5925-5930, 1996.

152. Kuriyama H, Ito Y, Suzuki H, Kitamura K, and Itoh T. Factors modifying contraction-relaxation cycle in vascular smooth muscles. *Am J Physiol* 243: H641-H662, 1982.
153. Kushner PJ, Agard D, Feng WJ, Lopez G, Schiau A, Uht R, Webb P, and Greene G. Oestrogen receptor function at classical and alternative response elements. *Novartis Found Symp* 230: 20-26, 2000.
154. Kushner PJ, Agard DA, Greene GL, Scanlan TS, Shiau AK, Uht RM, and Webb P. Estrogen receptor pathways to AP-1. *J Steroid Biochem Mol Biol* 74: 311-317, 2000.
155. Lahm T, Crisostomo PR, Markel TA, Wang M, Wang Y, Weil B, and Meldrum DR. Exogenous estrogen rapidly attenuates pulmonary artery vasoreactivity and acute hypoxic pulmonary vasoconstriction. *Shock* 30: 660-667, 2008.
156. Lahm T, Crisostomo PR, Markel TA, Wang M, Weil BR, Novotny NM, and Meldrum DR. The effects of estrogen on pulmonary artery vasoreactivity and hypoxic pulmonary vasoconstriction: potential new clinical implications for an old hormone. *Crit Care Med* 36: 2174-2183, 2008.
157. Lahm T, Patel KM, Crisostomo PR, Markel TA, Wang M, Herring C, and Meldrum DR. Endogenous estrogen attenuates pulmonary artery vasoreactivity and acute hypoxic pulmonary vasoconstriction: the effects of sex and menstrual cycle. *Am J Physiol Endocrinol Metab* 293: E865-E871, 2007.
158. Lane KB, Machado RD, Pauciulo MW, Thomson JR, Phillips JA, Loyd JE, Nichols WC, and Trembath RC. Heterozygous germline mutations in BMPR2, encoding a

- TGF-beta receptor, cause familial primary pulmonary hypertension. *Nat Genet* 26: 81-84, 2000.
159. Laufs U, La F, V, Plutzky J, and Liao JK. Upregulation of endothelial nitric oxide synthase by HMG CoA reductase inhibitors. *Circulation* 97: 1129-1135, 1998.
160. Launay JM, Herve P, Peoc'h K, Tournois C, Callebert J, Nebigil CG, Etienne N, Drouet L, Humbert M, Simonneau G, and Maroteaux L. Function of the serotonin 5-hydroxytryptamine 2B receptor in pulmonary hypertension. *Nat Med* 8: 1129-1135, 2002.
161. Lawrie A, Spiekerkoetter E, Martinez EC, Ambartsumian N, Sheward WJ, MacLean MR, Harmar AJ, Schmidt AM, Lukanidin E, and Rabinovitch M. Interdependent serotonin transporter and receptor pathways regulate S100A4/Mts1, a gene associated with pulmonary vascular disease. *Circ Res* 97: 227-235, 2005.
162. Lee CH and Edwards AM. Stimulation of DNA synthesis and c-fos mRNA expression in primary rat hepatocytes by estrogens. *Carcinogenesis* 22: 1473-1481, 2001.
163. Lee GJ. Regulation of the pulmonary circulation. *Br Heart J* 33: Suppl-26, 1971.
164. Lesch KP, Bengel D, Heils A, Sabol SZ, Greenberg BD, Petri S, Benjamin J, Muller CR, Hamer DH, and Murphy DL. Association of anxiety-related traits with a polymorphism in the serotonin transporter gene regulatory region. *Science* 274: 1527-1531, 1996.

165. Liu S, Kuo HP, Sheppard MN, Barnes PJ, and Evans TW. Vagal stimulation induces increased pulmonary vascular permeability in guinea pig. *Am J Respir Crit Care Med* 149: 744-750, 1994.
166. Liu Y and Fanburg BL. Serotonin-induced growth of pulmonary artery smooth muscle requires activation of phosphatidylinositol 3-kinase/serine-threonine protein kinase B/mammalian target of rapamycin/p70 ribosomal S6 kinase 1. *Am J Respir Cell Mol Biol* 34: 182-191, 2006.
167. Liu Y, Li M, Warburton RR, Hill NS, and Fanburg BL. The 5-HT transporter transactivates the PDGFbeta receptor in pulmonary artery smooth muscle cells. *FASEB J* 21: 2725-2734, 2007.
168. Liu Y, Wei L, Laskin DL, and Fanburg BL. Role of Protein Transamidation in Serotonin-induced Proliferation and Migration of Pulmonary Artery Smooth Muscle Cells. *Am J Respir Cell Mol Biol* 2010.
169. Liu YL and Fanburg BL. Serotonin-induced growth of pulmonary artery smooth muscle requires activation of phosphatidylinositol 3-kinase/serine-threonine protein kinase B/mammalian target of rapamycin/p70 ribosomal S6 kinase 1. *Am J Respir Cell Mol Biol* 34: 182-191, 2006.
170. Liu YL, Suzuki YJ, Day RM, and Fanburg BL. Rho kinase-induced nuclear translocation of ERK1/ERK2 in smooth muscle cell mitogenesis caused by serotonin. *Circ Res* 95: 579-586, 2004.
171. Long L, MacLean MR, Jeffery TK, Morecroft I, Yang XD, Rudarakanjana N, Southwood M, James V, Trembath RC, and Morrell NW. Serotonin increases

- susceptibility to pulmonary hypertension in BMPR2-deficient mice. *Circ Res* 98: 818-827, 2006.
172. Lu H, Higashikata T, Inazu A, Nohara A, Yu W, Shimizu M, and Mabuchi H. Association of estrogen receptor-alpha gene polymorphisms with coronary artery disease in patients with familial hypercholesterolemia. *Arterioscler Thromb Vasc Biol* 22: 817-823, 2002.
173. Lu NZ, Eshleman AJ, Janowsky A, and Bethea CL. Ovarian steroid regulation of serotonin reuptake transporter (SERT) binding, distribution, and function in female macaques. *Mol Psychiatry* 8: 353-360, 2003.
174. Luby TM. Targeting cytochrome P450 CYP1B1 with a therapeutic cancer vaccine. *Expert Rev Vaccines* 7: 995-1003, 2008.
175. Machado RD, Koehler R, Glissmeyer E, Veal C, Suntharalingam J, Kim M, Carlquist J, Town M, Elliott CG, Hoeper M, Fijalkowska A, Kurzyna M, Thomson JR, Gibbs SR, Wilkins MR, Seeger W, Morrell NW, Gruenig E, Trembath RC, and Janssen B. Genetic association of the serotonin transporter in pulmonary arterial hypertension. *Am J Respir Crit Care Med* 173: 793-797, 2006.
176. MacLean MR, Clayton RA, Hillis SW, McIntyre PD, Peacock AJ, and Templeton AG. 5-HT1-receptor-mediated vasoconstriction in bovine isolated pulmonary arteries: influences of vascular endothelium and tone. *Pulm Pharmacol* 7: 65-72, 1994.

177. MacLean MR, Clayton RA, Templeton AGB, and Morecroft I. Evidence for 5-HT₁-like receptor-mediated vasoconstriction in human pulmonary artery. *Br J Pharmacol* 119: 277-282, 1996.
178. MacLean MR and Dempsie Y. Serotonin and pulmonary hypertension--from bench to bedside? *Curr Opin Pharmacol* 9: 281-286, 2009.
179. MacLean MR and Dempsie Y. The serotonin hypothesis of pulmonary hypertension revisited. *Adv Exp Med Biol* 661: 309-322, 2010.
180. MacLean MR, Deuchar GA, Hicks MN, Morecroft I, Shen SB, Sheward J, Colston J, Loughlin L, Nilsen M, Dempsie Y, and Harmar A. Overexpression of the 5-hydroxytryptamine transporter gene - Effect on pulmonary hemodynamics and hypoxia-induced pulmonary hypertension. *Circulation* 109: 2150-2155, 2004.
181. MacLean MR, Deuchar GA, Hicks MN, Morecroft I, Shen SB, Sheward J, Colston J, Loughlin L, Nilsen M, Dempsie Y, and Harmar A. Overexpression of the 5-hydroxytryptamine transporter gene - Effect on pulmonary hemodynamics and hypoxia-induced pulmonary hypertension. *Circulation* 109: 2150-2155, 2004.
182. MacLean MR, Herve P, Eddahibi S, and Adnot S. 5-hydroxytryptamine and the pulmonary circulation: receptors, transporters and relevance to pulmonary arterial hypertension. *Br J Pharmacol* 131: 161-168, 2000.
183. MacRitchie AN, Jun SS, Chen Z, German Z, Yuhanna IS, Sherman TS, and Shaul PW. Estrogen upregulates endothelial nitric oxide synthase gene expression in fetal pulmonary artery endothelium. *Circ Res* 81: 355-362, 1997.

184. MacRitchie AN, Jun SS, Chen Z, German Z, Yuhanna IS, Sherman TS, and Shaul PW. Estrogen upregulates endothelial nitric oxide synthase gene expression in fetal pulmonary artery endothelium. *Circ Res* 81: 355-362, 1997.
185. Madden JA, Vadula MS, and Kurup VP. Effects of hypoxia and other vasoactive agents on pulmonary and cerebral artery smooth muscle cells. *Am J Physiol* 263: L384-L393, 1992.
186. Mahmoodzadeh S, Eder S, Nordmeyer J, Ehler E, Huber O, Martus P, Weiske J, Pregla R, Hetzer R, and Regitz-Zagrosek V. Estrogen receptor alpha up-regulation and redistribution in human heart failure. *FASEB J* 20: 926-934, 2006.
187. Mandegar M, Fung YC, Huang W, Remillard CV, Rubin LJ, and Yuan JX. Cellular and molecular mechanisms of pulmonary vascular remodeling: role in the development of pulmonary hypertension. *Microvasc Res* 68: 75-103, 2004.
188. Marcos E, Adnot S, Pham MH, Nosjean A, Raffestin B, Hamon M, and Eddahibi S. Serotonin transporter inhibitors protect against hypoxic pulmonary hypertension. *Am J Respir Crit Care Med* 168: 487-493, 2003.
189. Mark CJ, Tatchum-Talom R, Martin DS, and Eyster KM. Effects of estrogens and selective estrogen receptor modulators on vascular reactivity in the perfused mesenteric vascular bed. *Am J Physiol Regul Integr Comp Physiol* 293: R1969-R1975, 2007.
190. Marshall C and Marshall BE. Hypoxic pulmonary vasoconstriction is not endothelium dependent. *Proc Soc Exp Biol Med* 201: 267-270, 1992.

191. Martucci CP and Fishman J. P450 enzymes of estrogen metabolism. *Pharmacol Ther* 57: 237-257, 1993.
192. Masi AT. Editorial: Pulmonary hypertension and oral contraceptive usage. *Chest* 69: 451-453, 1976.
193. McCormack DG, Mak JC, Minette P, and Barnes PJ. Muscarinic receptor subtypes mediating vasodilation in the pulmonary artery. *Eur J Pharmacol* 158: 293-297, 1988.
194. McCulloch KM, Docherty C, and MacLean MR. Endothelin receptors mediating contraction of rat and human pulmonary resistance arteries: effect of chronic hypoxia in the rat. *British Journal of Pharmacology* 123: 1621-1630, 1998.
195. McCulloch KM, Kempshall FE, Buchanan KJ, and Gurney AM. Regional distribution of potassium currents in the rabbit pulmonary arterial circulation. *Exp Physiol* 85: 487-496, 2000.
196. McLaughlin VV, Shillington A, and Rich S. Survival in primary pulmonary hypertension: the impact of epoprostenol therapy. *Circulation* 106: 1477-1482, 2002.
197. McQueen JK, Wilson H, and Fink G. Estradiol-17 beta increases serotonin transporter (SERT) mRNA levels and the density of SERT-binding sites in female rat brain. *Mol Brain Res* 45: 13-23, 1997.
198. Mendelsohn ME. Genomic and nongenomic effects of estrogen in the vasculature. *Am J Cardiol* 90: 3F-6F, 2002.

199. Mendelsohn ME and Karas RH. The protective effects of estrogen on the cardiovascular system. *N Engl J Med* 340: 1801-1811, 1999.
200. Mendelsohn ME and Karas RH. Rapid progress for non-nuclear estrogen receptor signaling. *J Clin Invest* 120: 2277-2279, 2010.
201. Meyrick B and Reid L. Pulmonary hypertension. Anatomic and physiologic correlates. *Clin Chest Med* 4: 199-217, 1983.
202. Michelakis ED, Rebeyka I, Wu X, Nsair A, Thebaud B, Hashimoto K, Dyck JR, Haromy A, Harry G, Barr A, and Archer SL. O₂ sensing in the human ductus arteriosus: regulation of voltage-gated K⁺ channels in smooth muscle cells by a mitochondrial redox sensor. *Circ Res* 91: 478-486, 2002.
203. Mikkola T, Turunen P, Avela K, Orpana A, Viinikka L, and Ylikorkala O. 17 beta-estradiol stimulates prostacyclin, but not endothelin-1, production in human vascular endothelial cells. *J Clin Endocrinol Metab* 80: 1832-1836, 1995.
204. Miller AA, Hislop AA, Vallance PJ, and Haworth SG. Deletion of the eNOS gene has a greater impact on the pulmonary circulation of male than female mice. *Am J Physiol Lung Cell Mol Physiol* 289: L299-L306, 2005.
205. Milligan G and Kostenis E. Heterotrimeric G-proteins: a short history. *Br J Pharmacol* 147 Suppl 1: S46-S55, 2006.
206. Mitani Y, Mutlu A, Russell JC, Brindley DN, DeAlmeida J, and Rabinovitch M. Dexfenfluramine protects against pulmonary hypertension in rats. *Journal of Applied Physiology* 93: 1770-1778, 2002.

207. Molderings GJ, Bruss M, and Gothert M. Functional and molecular identification of 5-hydroxytryptamine receptors in rabbit pulmonary artery: involvement in complex regulation of noradrenaline release. *Pharmacol Rep* 58: 188-199, 2006.
208. Morani A, Barros RP, Imamov O, Hultenby K, Arner A, Warner M, and Gustafsson JA. Lung dysfunction causes systemic hypoxia in estrogen receptor beta knockout (ERbeta^{-/-}) mice. *Proc Natl Acad Sci U S A* 103: 7165-7169, 2006.
209. Morecroft I, Heeley RP, Prentice HM, Kirk A, and MacLean MR. 5-hydroxytryptamine receptors mediating contraction in human small muscular pulmonary arteries: importance of the 5-HT_{1B} receptor. *Br J Pharmacol* 128: 730-734, 1999.
210. Morecroft I, Loughlin L, Nilsen M, Colston J, Dempsie Y, Sheward J, Harmar A, and MacLean MR. Functional interactions between 5-hydroxytryptamine receptors and the serotonin transporter in pulmonary arteries. *J Pharmacol Exp Ther* 313: 539-548, 2005.
211. Morecroft I, Pang L, Baranowska M, Nilsen M, Loughlin L, Dempsie Y, Millet C, and MacLean MR. In vivo effects of a combined 5-HT_{1B} receptor/SERT antagonist in experimental pulmonary hypertension. *Cardiovasc Res* 85: 593-603, 2010.
212. Morecroft I, Dempsie Y, Bader M, Walther DJ, Kotnik K, Loughlin L, Nilsen M, and MacLean MR. Effect of Tryptophan Hydroxylase 1 Deficiency on the Development of Hypoxia-Induced Pulmonary Hypertension. *Hypertension* 49: 232-236, 2007.

213. Morgan T, Lauri J, Bertram D, and Anderson A. Effect of different antihypertensive drug classes on central aortic pressure. *Am J Hypertens* 17: 118-123, 2004.
214. Moro L, Reineri S, Piranda D, Pietrapiana D, Lova P, Bertoni A, Graziani A, Defilippi P, Canobbio I, Torti M, and Sinigaglia F. Nongenomic effects of 17beta-estradiol in human platelets: potentiation of thrombin-induced aggregation through estrogen receptor beta and Src kinase. *Blood* 105: 115-121, 2005.
215. Morrell NW. Role of bone morphogenetic protein receptors in the development of pulmonary arterial hypertension. *Adv Exp Med Biol* 661: 251-264, 2010.
216. Morse JH, Horn EM, and Barst RJ. Hormone replacement therapy: a possible risk factor in carriers of familial primary pulmonary hypertension. *Chest* 116: 847, 1999.
217. Morse JH, Jones AC, Barst RJ, Hodge SE, Wilhelmsen KC, and Nygaard TG. Familial primary pulmonary hypertension locus mapped to chromosome 2q31-q32. *Chest* 114: 57S-58S, 1998.
218. Murray GI, Melvin WT, Greenlee WF, and Burke MD. Regulation, function, and tissue-specific expression of cytochrome P450 CYP1B1. *Annu Rev Pharmacol Toxicol* 41: 297-316, 2001.
219. Murray GI, Taylor MC, McFadyen MC, McKay JA, Greenlee WF, Burke MD, and Melvin WT. Tumor-specific expression of cytochrome P450 CYP1B1. *Cancer Res* 57: 3026-3031, 1997.

220. Murray PA, Lodato RF, and Michael JR. Neural antagonists modulate pulmonary vascular pressure-flow plots in conscious dogs. *J Appl Physiol* 60: 1900-1907, 1986.
221. Nagatomo T, Rashid M, Abul MH, and Komiyama T. Functions of 5-HT_{2A} receptor and its antagonists in the cardiovascular system. *Pharmacol Ther* 104: 59-81, 2004.
222. Nebigil CG, Choi DS, Dierich A, Hickel P, Le MM, Messaddeq N, Launay JM, and Maroteaux L. Serotonin 2B receptor is required for heart development. *Proc Natl Acad Sci U S A* 97: 9508-9513, 2000.
223. Nebigil CG, Etienne N, Messaddeq N, and Maroteaux L. Serotonin is a novel survival factor of cardiomyocytes: mitochondria as a target of 5-HT_{2B}-receptor signaling. *Faseb Journal* 17: 1373-+, 2003.
224. Nelson JC. Synergistic benefits of serotonin and noradrenaline reuptake inhibition. *Depress Anxiety* 7 Suppl 1: 5-6, 1998.
225. Newman JH, Trembath RC, Morse JA, Grunig E, Loyd JE, Adnot S, Coccolo F, Ventura C, Phillips JA, III, Knowles JA, Janssen B, Eickelberg O, Eddahibi S, Herve P, Nichols WC, and Elliott G. Genetic basis of pulmonary arterial hypertension: current understanding and future directions. *J Am Coll Cardiol* 43: 33S-39S, 2004.
226. Ni W, Li MW, Thakali K, Fink GD, and Watts SW. The fenfluramine metabolite (+)-norfenfluramine is vasoactive. *Journal of Pharmacology and Experimental Therapeutics* 309: 845-852, 2004.

227. Nishimura T, Faul JL, Berry GJ, Vaszar LT, Qiu D, Pearl RG, and Kao PN. Simvastatin attenuates smooth muscle neointimal proliferation and pulmonary hypertension in rats. *Am J Respir Crit Care Med* 166: 1403-1408, 2002.
228. Nishimura T, Vaszar LT, Faul JL, Zhao G, Berry GJ, Shi L, Qiu D, Benson G, Pearl RG, and Kao PN. Simvastatin rescues rats from fatal pulmonary hypertension by inducing apoptosis of neointimal smooth muscle cells. *Circulation* 108: 1640-1645, 2003.
229. Nong Z, Hoylaerts M, Van PN, Collen D, and Janssens S. Nitric oxide inhalation inhibits platelet aggregation and platelet-mediated pulmonary thrombosis in rats. *Circ Res* 81: 865-869, 1997.
230. Nordmeyer J, Eder S, Mahmoodzadeh S, Martus P, Fielitz J, Bass J, Bethke N, Zurbrugg HR, Pregla R, Hetzer R, and Regitz-Zagrosek V. Upregulation of myocardial estrogen receptors in human aortic stenosis. *Circulation* 110: 3270-3275, 2004.
231. Ohlstein EH, Horohonich S, Shebuski RJ, and Ruffolo RR, Jr. Localization and characterization of alpha-2 adrenoceptors in the isolated canine pulmonary vein. *J Pharmacol Exp Ther* 248: 233-239, 1989.
232. Olde B and Leeb-Lundberg LM. GPR30/GPER1: searching for a role in estrogen physiology. *Trends Endocrinol Metab* 20: 409-416, 2009.
233. Oudiz RJ. Pulmonary hypertension associated with left-sided heart disease. *Clin Chest Med* 28: 233-41, x, 2007.

234. Pan J, Copland I, Post M, Yeger H, and Cutz E. Mechanical stretch-induced serotonin release from pulmonary neuroendocrine cells: implications for lung development. *American Journal of Physiology-Lung Cellular and Molecular Physiology* 290: L185-L193, 2006.
235. Payne AH and Hales DB. Overview of steroidogenic enzymes in the pathway from cholesterol to active steroid hormones. *Endocr Rev* 25: 947-970, 2004.
236. Peacock AJ, Murphy NF, McMurray JJ, Caballero L, and Stewart S. An epidemiological study of pulmonary arterial hypertension. *Eur Respir J* 30: 104-109, 2007.
237. Pecins-Thompson M, Brown NA, Kohama SG, and Bethea CL. Ovarian steroid regulation of tryptophan hydroxylase mRNA expression in rhesus macaques. *J Neurosci* 16: 7021-7029, 1996.
238. Pendaries C, Darblade B, Rochaix P, Krust A, Chambon P, Korach KS, Bayard F, and Arnal JF. The AF-1 activation-function of ERalpha may be dispensable to mediate the effect of estradiol on endothelial NO production in mice. *Proc Natl Acad Sci U S A* 99: 2205-2210, 2002.
239. Perros F, Montani D, Dorfmueller P, Durand-Gasselini I, Tcherakian C, Le PJ, Mazmanian M, Fadel E, Mussot S, Mercier O, Herve P, Emilie D, Eddahibi S, Simonneau G, Souza R, and Humbert M. Platelet-derived growth factor expression and function in idiopathic pulmonary arterial hypertension. *Am J Respir Crit Care Med* 178: 81-88, 2008.

240. Pietras RJ and Szego CM. Specific binding sites for oestrogen at the outer surfaces of isolated endometrial cells. *Nature* 265: 69-72, 1977.
241. Platoshyn O, Yu Y, Ko EA, Remillard CV, and Yuan JX. Heterogeneity of hypoxia-mediated decrease in I(K(V)) and increase in [Ca²⁺]_(cyt) in pulmonary artery smooth muscle cells. *Am J Physiol Lung Cell Mol Physiol* 293: L402-L416, 2007.
242. Qiu X, Aiken KJ, Chokas AL, Beachy DE, and Nick HS. Distinct functions of CCAAT enhancer-binding protein isoforms in the regulation of manganese superoxide dismutase during interleukin-1 β stimulation. *J Biol Chem* 283: 25774-25785, 2008.
243. Rabinovitch M, Gamble WJ, Miettinen OS, and Reid L. Age and Sex Influence on Pulmonary-Hypertension of Chronic Hypoxia and on Recovery. *American Journal of Physiology* 240: H62-H72, 1981.
244. Rajkumar R, Konishi K, Richards T, Ishizawar D, Wiechert A, Kaminski N, and Ahmad F. Genome-Wide RNA Expression Profiling in Lung Identifies Distinct Signatures in Idiopathic Pulmonary Arterial Hypertension and Secondary Pulmonary Hypertension. *Am J Physiol Heart Circ Physiol* 2010.
245. Rajkumar R, Konishi K, Richards TJ, Ishizawar DC, Wiechert AC, Kaminski N, and Ahmad F. Genomewide RNA expression profiling in lung identifies distinct signatures in idiopathic pulmonary arterial hypertension and secondary pulmonary hypertension. *Am J Physiol Heart Circ Physiol* 298: H1235-H1248, 2010.

246. Ramamoorthy S, Bauman AL, Moore KR, Han H, Yang-Feng T, Chang AS, Ganapathy V, and Blakely RD. Antidepressant- and cocaine-sensitive human serotonin transporter: molecular cloning, expression, and chromosomal localization. *Proc Natl Acad Sci U S A* 90: 2542-2546, 1993.
247. Ramamoorthy S, Giovanetti E, Qian Y, and Blakely RD. Phosphorylation and regulation of antidepressant-sensitive serotonin transporters. *J Biol Chem* 273: 2458-2466, 1998.
248. Ramji DP and Foka P. CCAAT/enhancer-binding proteins: structure, function and regulation. *Biochem J* 365: 561-575, 2002.
249. Rapport MM, Green AA, and Page IH. Serum vasoconstrictor, serotonin; isolation and characterization. *J Biol Chem* 176: 1243-1251, 1948.
250. Raught B, Gingras AC, James A, Medina D, Sonenberg N, and Rosen JM. Expression of a translationally regulated, dominant-negative CCAAT/enhancer-binding protein beta isoform and up-regulation of the eukaryotic translation initiation factor 2alpha are correlated with neoplastic transformation of mammary epithelial cells. *Cancer Res* 56: 4382-4386, 1996.
251. Rehman J and Archer SL. A proposed mitochondrial-metabolic mechanism for initiation and maintenance of pulmonary arterial hypertension in fawn-hooded rats: the Warburg model of pulmonary arterial hypertension. *Adv Exp Med Biol* 661: 171-185, 2010.

252. Resta TC, Kanagy NL, and Walker BR. Estradiol-induced attenuation of pulmonary hypertension is not associated with altered eNOS expression. *Am J Physiol Lung Cell Mol Physiol* 280: L88-L97, 2001.
253. Rexrode KM, Ridker PM, Hegener HH, Buring JE, Manson JE, and Zee RY. Polymorphisms and haplotypes of the estrogen receptor-beta gene (ESR2) and cardiovascular disease in men and women. *Clin Chem* 53: 1749-1756, 2007.
254. Rich S, Kaufmann E, and Levy PS. The effect of high doses of calcium-channel blockers on survival in primary pulmonary hypertension. *N Engl J Med* 327: 76-81, 1992.
255. Rivera HM, Oberbeck DR, Kwon B, Houpt TA, and Eckel LA. Estradiol increases Pet-1 and serotonin transporter mRNA in the midbrain raphe nuclei of ovariectomized rats. *Brain Res* 1259: 51-58, 2009.
256. Robertson TP, Dipp M, Ward JP, Aaronson PI, and Evans AM. Inhibition of sustained hypoxic vasoconstriction by Y-27632 in isolated intrapulmonary arteries and perfused lung of the rat. *Br J Pharmacol* 131: 5-9, 2000.
257. Rochefort GY, Lemaire MC, Eder V, Hanton G, Hyvelin JM, Bonnet P, and Antier D. Dexfenfluramine does not worsen but moderates progression of chronic hypoxia-induced pulmonary hypertension. *European Journal of Pharmacology* 550: 149-154, 2006.
258. Rondelet B, Van Beneden R, Kerbaul F, Motte S, Fesler P, McEntee K, Brimioulle S, Ketelslegers JM, and Naeije R. Expression of the serotonin 1b receptor in

- experimental pulmonary hypertension. *European Respiratory Journal* 22: 408-412, 2003.
259. Rosano GM, Vitale C, Silvestri A, and Fini M. Hormone replacement therapy and cardioprotection: the end of the tale? *Ann N Y Acad Sci* 997: 351-357, 2003.
260. Rosenkranz S and Erdmann E. [World Conference 2008 in Dana Point: important developments in the field of pulmonary hypertension]. *Dtsch Med Wochenschr* 133 Suppl 6: S165-S166, 2008.
261. Rosselli M, Imthurm B, Macas E, Keller PJ, and Dubey RK. Circulating Nitrite/Nitrate Levels Increase with Follicular Development: Indirect Evidence for Estradiol-Mediated NO Release. *Biochemical and Biophysical Research Communications* 202: 1543-1552, 1994.
262. Rothman RB, Ayestas MA, Dersch CM, and Baumann MH. Aminorex, fenfluramine, and chlorphentermine are serotonin transporter substrates - Implications for primary pulmonary hypertension. *Circulation* 100: 869-875, 1999.
263. Rothman RB and Baumann MH. Methamphetamine and idiopathic pulmonary arterial hypertension: role of the serotonin transporter. *Chest* 132: 1412-1413, 2007.
264. Sabbah M, Courilleau D, Mester J, and Redeuilh G. Estrogen induction of the cyclin D1 promoter: involvement of a cAMP response-like element. *Proc Natl Acad Sci U S A* 96: 11217-11222, 1999.
265. Said SI, Hamidi SA, Dickman KG, Szema AM, Lyubsky S, Lin RZ, Jiang YP, Chen JJ, Waschek JA, and Kort S. Moderate pulmonary arterial hypertension in

- male mice lacking the vasoactive intestinal peptide gene. *Circulation* 115: 1260-1268, 2007.
266. Said SI, Hamidi SA, Dickman KG, Szema AM, Lyubsky S, Lin RZ, Jiang YP, Chen JJ, Waschek JA, and Kort S. Moderate pulmonary arterial hypertension in male mice lacking the vasoactive intestinal peptide gene. *Circulation* 115: 1260-1268, 2007.
267. Sakao S, Tatsumi K, and Voelkel NF. Endothelial cells and pulmonary arterial hypertension: apoptosis, proliferation, interaction and transdifferentiation. *Respir Res* 10: 95, 2009.
268. Samuvel DJ, Jayanthi LD, Bhat NR, and Ramamoorthy S. A role for p38 mitogen-activated protein kinase in the regulation of the serotonin transporter: Evidence for distinct cellular mechanisms involved in transporter surface expression 4. *J Neurosci* 25: 29-41, 2005.
269. Sasaki M, Kaneuchi M, Fujimoto S, Tanaka Y, and Dahiya R. CYP1B1 gene in endometrial cancer. *Mol Cell Endocrinol* 202: 171-176, 2003.
270. Sasaki M, Tanaka Y, Okino ST, Nomoto M, Yonezawa S, Nakagawa M, Fujimoto S, Sakuragi N, and Dahiya R. Polymorphisms of the CYP1B1 gene as risk factors for human renal cell cancer. *Clin Cancer Res* 10: 2015-2019, 2004.
271. Schermuly RT, Dony E, Ghofrani HA, Pullamsetti S, Savai R, Roth M, Sydykov A, Lai YJ, Weissmann N, Seeger W, and Grimminger F. Reversal of experimental pulmonary hypertension by PDGF inhibition. *J Clin Invest* 115: 2811-2821, 2005.

272. Scott JA and McCormack DG. Nonadrenergic noncholinergic vasodilation of guinea pig pulmonary arteries is mediated by nitric oxide. *Can J Physiol Pharmacol* 77: 89-95, 1999.
273. Sealy WC, Connally SR, and Dalton ML. Naming the bronchopulmonary segments and the development of pulmonary surgery. *Ann Thorac Surg* 55: 184-188, 1993.
274. Sherman TS, Chambliss KL, Gibson LL, Pace MC, Mendelsohn ME, Pfister SL, and Shaul PW. Estrogen acutely activates prostacyclin synthesis in ovine fetal pulmonary artery endothelium. *Am J Respir Cell Mol Biol* 26: 610-616, 2002.
275. Shoemaker WC. Pattern of pulmonary hemodynamic and functional changes in shock. *Crit Care Med* 2: 200-210, 1974.
276. Simon AR, Severgnini M, Takahashi S, Rozo L, Andrahbi B, Agyeman A, Cochran BH, Day RM, and Fanburg BL. 5-HT induction of c-fos gene expression requires reactive oxygen species and Rac1 and Ras GTPases. *Cell Biochem Biophys* 42: 263-276, 2005.
277. Simon AR, Severgnini M, Takahashi S, Rozo L, Andrahbi B, Agyeman A, Cochran BH, Day RM, and Fanburg BL. 5-HT induction of c-fos gene expression requires reactive oxygen species and Rac1 and Ras GTPases. *Cell Biochem Biophys* 42: 263-276, 2005.
278. Simonneau G, Robbins IM, Beghetti M, Channick RN, Delcroix M, Denton CP, Elliott CG, Gaine SP, Gladwin MT, Jing ZC, Krowka MJ, Langleben D, Nakanishi N, and Souza R. Updated clinical classification of pulmonary hypertension. *J Am Coll Cardiol* 54: S43-S54, 2009.

279. Sitbon O, Badesch DB, Channick RN, Frost A, Robbins IM, Simonneau G, Tapson VF, and Rubin LJ. Effects of the dual endothelin receptor antagonist bosentan in patients with pulmonary arterial hypertension: a 1-year follow-up study. *Chest* 124: 247-254, 2003.
280. Sitbon O, Humbert M, Jais X, Ioos V, Hamid AM, Provencher S, Garcia G, Parent F, Herve P, and Simonneau G. Long-term response to calcium channel blockers in idiopathic pulmonary arterial hypertension. *Circulation* 111: 3105-3111, 2005.
281. Sitbon O, Humbert M, Nunes H, Parent F, Garcia G, Herve P, Rainisio M, and Simonneau G. Long-term intravenous epoprostenol infusion in primary pulmonary hypertension: prognostic factors and survival. *J Am Coll Cardiol* 40: 780-788, 2002.
282. Smith LJ, Henderson JA, Abell CW, and Bethea CL. Effects of ovarian steroids and raloxifene on proteins that synthesize, transport, and degrade serotonin in the raphe region of macaques. *Neuropsychopharmacology* 29: 2035-2045, 2004.
283. Spiekerkoetter E, Alvira CM, Kim YM, Bruneau A, Pricola KL, Wang L, Ambartsumian N, and Rabinovitch M. Reactivation of gamma HV68 induces neointimal lesions in pulmonary arteries of S100A4/Mts1-overexpressing mice in association with degradation of elastin 1. *American Journal of Physiology-Lung Cellular and Molecular Physiology* 294: L276-L289, 2008.
284. Spiekerkoetter E, Lawrie A, Merklinger S, Ambartsumian N, Lukanidin E, Schmidt AM, and Rabinovitch M. Mts1/S100A4 stimulates human pulmonary artery smooth muscle cell migration through multiple signaling pathways. *Chest* 128: 577S, 2005.

285. Stampfer MJ, Colditz GA, Willett WC, Manson JE, Rosner B, Speizer FE, and Hennekens CH. Postmenopausal estrogen therapy and cardiovascular disease. Ten-year follow-up from the nurses' health study. *N Engl J Med* 325: 756-762, 1991.
286. Stenmark KR, Davie N, Frid M, Gerasimovskaya E, and Das M. Role of the adventitia in pulmonary vascular remodeling. *Physiology (Bethesda)* 21: 134-145, 2006.
287. Stenmark KR and Frid MG. Smooth muscle cell heterogeneity: role of specific smooth muscle cell subpopulations in pulmonary vascular disease. *Chest* 114: 82S-90S, 1998.
288. Sterneck E, Zhu S, Ramirez A, Jorcano JL, and Smart RC. Conditional ablation of C/EBP beta demonstrates its keratinocyte-specific requirement for cell survival and mouse skin tumorigenesis. *Oncogene* 25: 1272-1276, 2006.
289. Stubbs EG, Budden SS, Jackson RH, Terdal LG, and Ritvo ER. Effects of fenfluramine on eight outpatients with the syndrome of autism. *Dev Med Child Neurol* 28: 229-235, 1986.
290. Stupfel M, Pesce VH, Gourlet V, Bouley G, Elabed A, and Lemercerre C. Sex-related factors in acute hypoxia survival in one strain of mice. *Aviat Space Environ Med* 55: 136-140, 1984.
291. Styrkarsdottir U, Halldorsson BV, Gretarsdottir S, Gudbjartsson DF, Walters GB, Ingvarsson T, Jonsdottir T, Saemundsdottir J, Center JR, Nguyen TV, Bagger Y, Gulcher JR, Eisman JA, Christiansen C, Sigurdsson G, Kong A, Thorsteinsdottir U,

- and Stefansson K. Multiple genetic loci for bone mineral density and fractures. *N Engl J Med* 358: 2355-2365, 2008.
292. Sumner BEH, Grant KE, Rosie R, Hegele-Hartung C, Fritzscheier KH, and Fink G. Raloxifene blocks estradiol induction of the serotonin transporter and 5-hydroxytryptamine(2A) receptor in female rat brain 11. *Neuroscience Letters* 417: 95-99, 2007.
293. Sundfeldt K, Ivarsson K, Carlsson M, Enerback S, Janson PO, Brannstrom M, and Hedin L. The expression of CCAAT/enhancer binding protein (C/EBP) in the human ovary in vivo: specific increase in C/EBPbeta during epithelial tumour progression. *Br J Cancer* 79: 1240-1248, 1999.
294. Swaneck GE and Fishman J. Covalent binding of the endogenous estrogen 16 alpha-hydroxyestrone to estradiol receptor in human breast cancer cells: characterization and intranuclear localization. *Proc Natl Acad Sci U S A* 85: 7831-7835, 1988.
295. Tada Y, Majka S, Carr M, Harral J, Crona D, Kuriyama T, and West J. Molecular effects of loss of BMPR2 signaling in smooth muscle in a transgenic mouse model of PAH. *Am J Physiol Lung Cell Mol Physiol* 292: L1556-L1563, 2007.
296. Tada Y, Majka S, Carr M, Harral J, Crona D, Kuriyama T, and West J. Molecular effects of loss of BMPR2 signaling in smooth muscle in a transgenic mouse model of PAH. *Am J Physiol Lung Cell Mol Physiol* 292: L1556-L1563, 2007.
297. Talvenheimo J and Rudnick G. Solubilization of the platelet plasma membrane serotonin transporter in an active form. *J Biol Chem* 255: 8606-8611, 1980.

298. Tanaka Y, Sasaki M, Kaneuchi M, Shiina H, Igawa M, and Dahiya R. Polymorphisms of the CYP1B1 gene have higher risk for prostate cancer. *Biochem Biophys Res Commun* 296: 820-826, 2002.
299. Tanaka Y, Sasaki M, Kaneuchi M, Shiina H, Igawa M, and Dahiya R. Polymorphisms of estrogen receptor alpha in prostate cancer. *Mol Carcinog* 37: 202-208, 2003.
300. Teichert-Kuliszewska K, Kutryk MJB, Kuliszewski MA, Karoubi G, Courtman DW, Zucco L, Granton J, and Stewart DJ. Bone Morphogenetic Protein Receptor-2 Signaling Promotes Pulmonary Arterial Endothelial Cell Survival: Implications for Loss-of-Function Mutations in the Pathogenesis of Pulmonary Hypertension. *Circulation Research* 98: 209-217, 2006.
301. Teng X, Li D, Catravas JD, and Johns RA. C/EBP-beta mediates iNOS induction by hypoxia in rat pulmonary microvascular smooth muscle cells. *Circ Res* 90: 125-127, 2002.
302. Thenappan T, Shah SJ, Rich S, and Gomberg-Maitland M. A USA-based registry for pulmonary arterial hypertension: 1982-2006. *Eur Respir J* 30: 1103-1110, 2007.
303. Thompson P and McRae C. Familial pulmonary hypertension. Evidence of autosomal dominant inheritance. *Br Heart J* 32: 758-760, 1970.
304. Tofovic SP, Jackson EK, and Zhang XC. 2-methoxyestradiol mediates protective effects of estradiol in monocrotaline-induced pulmonary hypertension. *Circulation* 110: 18, 2004.

305. Tofovic SP and Rafikova O. Preventive and Therapeutic Effects of 2-Methoxyestradiol, but Not Estradiol, in Severe Occlusive Pulmonary Arterial Hypertension in Female Rats. *Am J Respir Crit Care Med* 179: A1802, 2009.
306. Tofovic SP, Salah EM, Dubey RK, Melhem MF, and Jackson EK. Estradiol metabolites attenuate renal and cardiovascular injury induced by chronic nitric oxide synthase inhibition. *J Cardiovasc Pharmacol* 46: 25-35, 2005.
307. Tofovic SP, Salah EM, Mady HH, Jackson EK, and Melhem ME. Estradiol metabolites attenuate monocrotaline-induced pulmonary hypertension in rats. *Journal of Cardiovascular Pharmacology* 46: 430-437, 2005.
308. Tofovic SP, Zhang X, Zhu H, Jackson EK, Rafikova O, and Petrussevska G. 2-Ethoxyestradiol is antimitogenic and attenuates monocrotaline-induced pulmonary hypertension and vascular remodeling. *Vascul Pharmacol* 48: 174-183, 2008.
309. Tofovic SP, Zhang XC, Jackson EK, Dacic S, and Petrussevska G. 2-Methoxyestradiol mediates the protective effects of estradiol in monocrotaline-induced pulmonary hypertension. *Vascular Pharmacology* 45: 358-367, 2006.
310. Tong EY, Mathe AA, and Tisher PW. Release of norepinephrine by sympathetic nerve stimulation from rabbit lungs. *Am J Physiol* 235: H803-H808, 1978.
311. Torres GE, Gainetdinov RR, and Caron MG. Plasma membrane monoamine transporters: Structure, regulation and function 1. *Nature Reviews Neuroscience* 4: 13-25, 2003.

312. Trembath RC, Thomson JR, Machado RD, Morgan NV, Atkinson C, Winship I, Simonneau G, Galie N, Loyd JE, Humbert M, Nichols WC, Morrell NW, Berg J, Manes A, McGaughran J, Pauciulo M, and Wheeler L. Clinical and molecular genetic features of pulmonary hypertension in patients with hereditary hemorrhagic telangiectasia. *N Engl J Med* 345: 325-334, 2001.
313. Tsuchiya Y, Nakajima M, Kyo S, Kanaya T, Inoue M, and Yokoi T. Human CYP1B1 is regulated by estradiol via estrogen receptor. *Cancer Res* 64: 3119-3125, 2004.
314. Tsuchiya Y, Nakajima M, Kyo S, Kanaya T, Inoue M, and Yokoi T. Human CYP1B1 is regulated by estradiol via estrogen receptor. *Cancer Res* 64: 3119-3125, 2004.
315. Tsuchiya Y, Nakajima M, and Yokoi T. Cytochrome P450-mediated metabolism of estrogens and its regulation in human. *Cancer Lett* 227: 115-124, 2005.
316. Tsuchiya Y, Nakajima M, and Yokoi T. Cytochrome P450-mediated metabolism of estrogens and its regulation in human. *Cancer Lett* 227: 115-124, 2005.
317. Tuder RM, Abman SH, Braun T, Capron F, Stevens T, Thistlethwaite PA, and Haworth SG. Development and pathology of pulmonary hypertension. *J Am Coll Cardiol* 54: S3-S9, 2009.
318. Tuder RM, Abman SH, Braun T, Capron F, Stevens T, Thistlethwaite PA, and Haworth SG. Development and pathology of pulmonary hypertension. *J Am Coll Cardiol* 54: S3-S9, 2009.

319. Tudor RM, Groves B, Badesch DB, and Voelkel NF. Exuberant endothelial cell growth and elements of inflammation are present in plexiform lesions of pulmonary hypertension. *Am J Pathol* 144: 275-285, 1994.
320. Tudor RM and Voelkel NF. Pulmonary hypertension and inflammation. *Journal of Laboratory and Clinical Medicine* 132: 16-24, 1998.
321. Ullmer C, Schmuck K, Kalkman HO, and Lubbert H. Expression of serotonin receptor mRNAs in blood vessels. *FEBS Lett* 370: 215-221, 1995.
322. van den Broek RW, Bhalla P, VanDenBrink AM, de VR, Sharma HS, and Saxena PR. Characterization of sumatriptan-induced contractions in human isolated blood vessels using selective 5-HT(1B) and 5-HT(1D) receptor antagonists and in situ hybridization. *Cephalalgia* 22: 83-93, 2002.
323. Van Emburgh BO, Hu JJ, Levine EA, Mosley LJ, Perrier ND, Freimanis RI, Allen GO, Rubin P, Sherrill GB, Shaw CS, Carey LA, Sawyer LR, and Miller MS. Polymorphisms in CYP1B1, GSTM1, GSTT1 and GSTP1, and susceptibility to breast cancer. *Oncol Rep* 19: 1311-1321, 2008.
324. Varghese A, Hong Z, and Weir EK. Serotonin-induced inhibition of KV current: a supporting role in pulmonary vasoconstriction? *Circ Res* 98: 860-862, 2006.
325. Veronesi U, Boyle P, Goldhirsch A, Orecchia R, and Viale G. Breast cancer. *Lancet* 365: 1727-1741, 2005.
326. Vitale C, Mendelsohn ME, and Rosano GM. Gender differences in the cardiovascular effect of sex hormones. *Nat Rev Cardiol* 6: 532-542, 2009.

327. Voelkel NF and Cool C. Pathology of pulmonary hypertension. *Cardiol Clin* 22: 343-51, v, 2004.
328. Walther DJ, Peter JU, Bashammakh S, Hortnagl H, Voits M, Fink H, and Bader M. Synthesis of serotonin by a second tryptophan hydroxylase isoform. *Science* 299: 76, 2003.
329. Wang J, Juhaszova M, Rubin LJ, and Yuan XJ. Hypoxia inhibits gene expression of voltage-gated K⁺ channel alpha subunits in pulmonary artery smooth muscle cells. *J Clin Invest* 100: 2347-2353, 1997.
330. Wang J, Weigand L, Wang W, Sylvester JT, and Shimoda LA. Chronic hypoxia inhibits Kv channel gene expression in rat distal pulmonary artery. *Am J Physiol Lung Cell Mol Physiol* 288: L1049-L1058, 2005.
331. Weir EK, Reeve HL, Huang JMC, Michelakis E, Nelson DP, Hampl V, and Archer SL. Anorexic agents aminorex, fenfluramine, and dexfenfluramine inhibit potassium current in rat pulmonary vascular smooth muscle and cause pulmonary vasoconstriction. *Circulation* 94: 2216-2220, 1996.
332. Welsh DJ, Harnett M, MacLean M, and Peacock AJ. Proliferation and signaling in fibroblasts - Role of 5-hydroxytryptamine(2A) receptor and transporter. *Am J Respir Crit Care Med* 170: 252-259, 2004.
333. Welsh DJ, Peacock AJ, MacLean M, and Harnett M. Chronic hypoxia induces constitutive p38 mitogen-activated protein kinase activity that correlates with enhanced cellular proliferation in fibroblasts from rat pulmonary but not systemic arteries. *Am J Respir Crit Care Med* 164: 282-289, 2001.

334. West J, Cogan J, Geraci M, Robinson L, Newman J, Phillips JA, Lane K, Meyrick B, and Loyd J. Gene expression in BMPR2 mutation carriers with and without evidence of Pulmonary Arterial Hypertension suggests pathways relevant to disease penetrance. *BMC Med Genomics* 1: 45, 2008.
335. West J, Fagan K, Steudel W, Fouty B, Lane K, Harral J, Hoedt-Miller M, Tada Y, Ozimek J, Tuder R, and Rodman DM. Pulmonary hypertension in transgenic mice expressing a dominant-negative BMPRII gene in smooth muscle. *Circ Res* 94: 1109-1114, 2004.
336. Wharton J, Strange JW, Moller GM, Growcott EJ, Ren X, Franklyn AP, Phillips SC, and Wilkins MR. Antiproliferative effects of phosphodiesterase type 5 inhibition in human pulmonary artery cells. *Am J Respir Crit Care Med* 172: 105-113, 2005.
337. Wilkins MR, Ali O, Bradlow W, Wharton J, Taegtmeyer A, Rhodes CJ, Ghofrani HA, Howard L, Nihoyannopoulos P, Mohiaddin RH, and Gibbs JS. Simvastatin as a treatment for pulmonary hypertension trial. *Am J Respir Crit Care Med* 181: 1106-1113, 2010.
338. Willers ED, Newman JH, Loyd JE, Robbins IM, Wheeler LA, Prince MA, Stanton KC, Cogan JA, Runo JR, Byrne D, Humbert M, Simonneau G, Sztrymf B, Morse JA, Knowles JA, Roberts KE, McElroy JJ, Barst RJ, and Phillips JA. Serotonin transporter polymorphisms in familial and idiopathic pulmonary arterial hypertension. *Am J Respir Crit Care Med* 173: 798-802, 2006.

339. Williams RS. Apoptosis and heart failure 2. *New England Journal of Medicine* 341: 759-760, 1999.
340. Windahl SH, Andersson N, Chagin AS, Martensson UE, Carlsten H, Olde B, Swanson C, Moverare-Skrtic S, Savendahl L, Lagerquist MK, Leeb-Lundberg LM, and Ohlsson C. The role of the G protein-coupled receptor GPR30 in the effects of estrogen in ovariectomized mice. *Am J Physiol Endocrinol Metab* 296: E490-E496, 2009.
341. Xu KM, Tang F, and Han C. Alterations of mRNA levels of alpha 1-adrenoceptor subtypes with maturation and ageing in different rat blood vessels. *Clin Exp Pharmacol Physiol* 24: 415-417, 1997.
342. Yang J, Davies RJ, Southwood M, Long L, Yang X, Sobolewski A, Upton PD, Trembath RC, and Morrell NW. Mutations in bone morphogenetic protein type II receptor cause dysregulation of Id gene expression in pulmonary artery smooth muscle cells: implications for familial pulmonary arterial hypertension 3. *Circ Res* 102: 1212-1221, 2008.
343. Yu Y, Keller SH, Remillard CV, Safrina O, Nicholson A, Zhang SL, Jiang W, Vangala N, Landsberg JW, Wang JY, Thistlethwaite PA, Channick RN, Robbins IM, Loyd JE, Ghofrani HA, Grimminger F, Schermuly RT, Cahalan MD, Rubin LJ, and Yuan JX. A functional single-nucleotide polymorphism in the TRPC6 gene promoter associated with idiopathic pulmonary arterial hypertension. *Circulation* 119: 2313-2322, 2009.

344. Yu Y, Sweeney M, Zhang S, Platoshyn O, Landsberg J, Rothman A, and Yuan JX. PDGF stimulates pulmonary vascular smooth muscle cell proliferation by upregulating TRPC6 expression. *Am J Physiol Cell Physiol* 284: C316-C330, 2003.
345. Zamora MA, Dempsey EC, Walchak SJ, and Stelzner TJ. BQ123, an ETA receptor antagonist, inhibits endothelin-1-mediated proliferation of human pulmonary artery smooth muscle cells. *Am J Respir Cell Mol Biol* 9: 429-433, 1993.
346. Zhang F, Carson RC, Zhang H, Gibson G, and Thomas HM, III. Pulmonary artery smooth muscle cell $[Ca^{2+}]_i$ and contraction: responses to diphenylethylideneiodonium and hypoxia. *Am J Physiol* 273: L603-L611, 1997.
347. Zhang XC, Jones T, Jackson EK, Petrusevska G, and Tofovic SP. 2-methoxyestradiol attenuates the development and retards the progression of chronic hypoxia-induced pulmonary hypertension in rats 21. *Circulation* 112: U152-U153, 2005.
348. Zhao L, Mason NA, Morrell NW, Kojonazarov B, Sadykov A, Maripov A, Mirrakhimov MM, Aldashev A, and Wilkins MR. Sildenafil inhibits hypoxia-induced pulmonary hypertension. *Circulation* 104: 424-428, 2001.
349. Zhu BT and Conney AH. Functional role of estrogen metabolism in target cells: review and perspectives. *Carcinogenesis* 19: 1-27, 1998.
350. Zhu BT and Conney AH. Functional role of estrogen metabolism in target cells: review and perspectives. *Carcinogenesis* 19: 1-27, 1998.

351. Zhu CB, Carneiro AM, Dostmann WR, Hewlett WA, and Blakely RD. p38 MAPK activation elevates serotonin transport activity via a trafficking-independent, protein phosphatase 2A-dependent process 5. *J Biol Chem* 280: 15649-15658, 2005.
352. Zhu S, Yoon K, Sterneck E, Johnson PF, and Smart RC. CCAAT/enhancer binding protein-beta is a mediator of keratinocyte survival and skin tumorigenesis involving oncogenic Ras signaling. *Proc Natl Acad Sci U S A* 99: 207-212, 2002.
353. Zhu Y, Bian Z, Lu P, Karas RH, Bao L, Cox D, Hodgins J, Shaul PW, Thoren P, Smithies O, Gustafsson JA, and Mendelsohn ME. Abnormal vascular function and hypertension in mice deficient in estrogen receptor beta. *Science* 295: 505-508, 2002.
354. Zolkowska D, Rothman RB, and Baumann MH. Amphetamine analogs increase plasma serotonin: implications for cardiac and pulmonary disease. *J Pharmacol Exp Ther* 318: 604-610, 2006.

Appendices

Appendix 1:

K. White, Y. Dempsie, M. Nilsen, A.F. Wright; L. Loughlin & M.R. MacLean. The Serotonin Transporter, Gender and 17 β Estradiol in the Development of Pulmonary Arterial Hypertension. *Cardiovascular Research* 1;90(2):373-382, 2011.

Appendix 2:

K. White, L. Loughlin, Z. Maqbool, M. Nilsen, J. McClure, Y. Dempsie, A.H. Baker & M.R. MacLean. The Serotonin Transporter, Gender and Hypoxia: Microarray Analysis in the Pulmonary Arteries of Mice Identifies Genes with Relevance to Human PAH. *Physiological Genomics* 43: 417–437, 2011.